Lymphocyte Migration and The Regulation of Brain Endothelial Cell Junctions

By

David John Wateridge

Thesis submitted for the degree of Doctor of Philosophy
Faculty of Biochemistry (Life Sciences)

Department of Cell Biology
Institute of Ophthalmology
University College London

ProQuest LLC
789 East Eisenhower Parkway
P.O. Box 1346
Ann Arbor, MI 48106-1346

Abstract

Through *bona fide* tight junctions and regulated transcytosis, brain endothelial cells (ECs) are able to establish a blood-brain barrier (BBB) that regulates access of leucocytes and solutes to the central nervous system (CNS). Occludin was the first transmembrane tight junction protein identified and it has been demonstrated that expression of mutant occludin proteins in epithelial cells dramatically affects neutrophil transmigration and monolayer permeability. To determine if similar strategies could influence transendothelial lymphocyte migration and other endothelial barrier properties, a brain EC line (GPNT) was transfected with a range of occludin proteins and characterised by functional assays. Expression of wild-type occludin reduced T cell migration and, as in epithelial cells, this was shown to be dependent on an unmodified N-terminal domain. The mechanism(s) by which lymphocytes physically cross the endothelial barrier remains a poorly described stage of lymphocyte extravasation. The possibility remains, however, that modulation of endothelial cell-cell junctions is a necessary pre-requisite to physically allow the passage of a leucocyte through the EC wall. i.e the paracellular pathway. The firm adhesion of circulating T cells to BBB ECs is predominantly via ICAM-1, a cell adhesion molecule of the immunoglobulin superfamily expressed on the EC and previously demonstrated to be capable of signal transduction. A hypothesis was generated that ICAM-1 engagement facilitates diapedesis by activating signalling pathways that regulate cell-cell junctions. Using GPNT EC, the role of ICAM-1 in regulating junctional proteins and integrity was assessed. Following crosslinking of ICAM-1, both VE-cadherin and PECAM showed increased tyrosine phosphorylation with identical experiments showing that ICAM-1 crosslinking correlated with an increase in transmonolayer permeability to molecular tracers. Immunoprecipitated VE-cadherin showed no change in its association with β- or γ-catenin following ICAM-1 crosslinking, however, there was increased association of both catenins with PECAM via a rho-dependent/ROCK-independent pathway. The existence of such pathways suggests that pharmacological targeting of ICAM-1-mediated signalling may be advantageous in the therapeutic management of neuroinflammatory diseases.

Acknowledgements

I would like to thank my PhD supervisors, Prof. John Greenwood and Dr Peter Adamson, not only for giving me the opportunity to undertake this studentship but also for the faith and trust they showed by allowing and encouraging me to explore my own ideas whilst always being around when things were not clear. I would also like to thank them for the understanding and support they gave my decisions not only during my time in the lab but also during the writing of this thesis. I am grateful also for the willingness and speed with which they reviewed my work and their many helpful suggestions about data presentation and format.

During my studentship many people passed through our lab and all contributed to an atmosphere I always found friendly and relaxing. A list of everyone who helped me during these three years is too long to include but for all their help and encouragement in the lab I would like to thank Claire Amos, Maria Balda, Robert Blaber, Vivien Chen, Rebecca Crawford, Matthew Gegg, Yadvinder Gill, Rachel Harry, Naheed Kanuga, Parminder Mann, Karl Matter, Peter Munro, Karen Noble, Zoe Ockrim, Jignesh Patel, Kelli Portbury, Katrina Radewicz, Julie Sathia, Raffaella Spagnuolo, Anne Tindale, Patric Turowski, Anthony Vugler and Claire Walters. I am extremely grateful to Patric and Rebecca for their efforts to optimise the immunofluorescence protocol following adhesion molecule crosslinking and they made a huge contribution to those studies within this thesis.

This thesis is dedicated entirely to my parents without whose continual unconditional support I could neither have started or finished the project.

This project was funded by the Medical Research Council of the United Kingdom.

Contents

List of Abbreviations

APC	Adenomatous polyposis coli
aPKC	Atypical protein kinase C
ASIP	Atypical protein kinase C-specific interacting protein
ATP	Adenosine triphosphate
BBB	Blood-brain barrier
BSA	Bovine serum albumin
C3-transferase	*Clostridium Botulinum* C3-transferase toxin
cAMP	Cyclic adenosine monophosphate
CD	Cluster of differentiation
cDNA	Complementary deoxyribonucleic acid
CEACAM-1	Carcinoembryonic antigen-related cell adhesion molecule-1
CHO	Chinese hamster ovary
CNS	Central nervous system
CSF	Cerebrospinal fluid
C-terminal	Carboxyl-terminal
CTL	Cytotoxic T lymphocyte
DEAE	Diethylaminoethyl
DMEM	Dulbeccos minimal essential medium
DMSO	Dimethyl sulphoxide
DNA	Deoxyribonucleic acid
dNTP	Deoxynucleotide triphosphate
DTT	Dithiothreitol
EAE	Experimental autoimmune encephalomyelitis
EC	Endothelial cell
E-cadherin	Epithelial-cadherin
E.Coli	*Escherichia Coli*
ECL	Enhanced chemiluminescence
EDTA	Ethylenediaminetetraacetic acid
E face	Extracytoplasmic face
ERM	Ezrin/radixin/moesin family of proteins

ERK	Extracellular signal-regulated kinase
ESAM	Endothelial cell-selective adhesion molecule
E-selectin	Endothelial-selectin
FACS	Fluorescence-activated cell sorting (flow cytometry)
F-actin	Filamentous actin
FAK	Focal adhesion kinase
FCS	Foetal calf serum
FITC	Fluorescein isothiocyanate
GAPDH	Glyceraldehyde-3-phosphate dehydrogenase
GAM	Goat anti-mouse immunoglobulin G
GDP	Guanosine diphosphate
GK	Guanylate kinase
GlyCAM	Gylcosylation-dependent cell adhesion molecule
GMP	Guanosine monophosphate
GSK	Glycogen synthase kinase 3β
GTPase	Guanosine triphosphatase
HA	Haemagluttinin epitope
HBSS	Hanks buffered salt solution
HEPES	N-[2-hydroxyethyl]piperazine-N'-[2-ethanesulphonic acid]
HLA	Human leucocyte antigen
HRP	Horseradish peroxidase
HUVEC	Human umbilical vein endothelial cell
IB	Immunoblot
ICAM	Intercellular adhesion molecule
IF	Immunofluorescence
IFN	Interferon
Ig	Immunoglobulin
IGF	Insulin-like growth factor
IL	Interleukin
IP	Immunoprecipitate
IQGAP	IQ motif-containing GTPase activating protein
ITAM	Immunoreceptor tyrosine-based activation motif
JNK	c-jun N-terminal kinase (a.k.a Stress-activated protein kinase, SAPK)
KD	Kilo Dalton

L Broth	Lennox broth
LEF/TCF	Lymphoid enhancing factor/ T cell factor
LFA	Lymphocyte function antigen
LPA	Lysophosphatidic acid
LPS	Lipopolysaccharide
L-selectin	Leucocyte-selectin
mAb	Monoclonal antibody
MAdCAM	Mucosal addressin cell adhesion molecule
MAGUK	Membrane-associated guanylate kinase
MAP	Mitogen-activated protein
MBP	Myelin basic protein
M-cadherin	Muscle-cadherin
MDCK	Madin-Darby canine kidney
MEM	Minimal essential medium
MHC	Major histocompatability complex
MMP	Matrix metalloproteinase
MOPS	3-[N-morpholino]propanesulphonic acid
mRNA	Messenger ribonucleic acid
MRP	Multi-drug resistance protein
MS	Multiple sclerosis
N-cadherin	Neural cadherin
NK	Natural killer
NO	Nitric oxide
NOS	Reactive nitrogen species
NP-40	Nonidet®-P40
N-terminal	Amino-terminal
CAS	p130 Crk-associated substrate
PAF	Platelet-activating factor
PAR	Partitioning defective protein
PBS	Phosphate-buffered saline
PBST	Phosphate buffered saline solution containing 0.1% Tween 20
PCR	Polymerase chain reaction
PDZ	Postsynaptic density protein 95/ discs large/zonula occludens-1

PECAM	Platelet-endothelial cell adhesion molecule
PI3K	Phosphatidylinositol 3-kinase
PKC	Protein kinase C
P-cadherin	Placental cadherin
P face	Protoplasmic face
PLC	Phospholipase C
PLNC	Peripheral lymph node cells
PMNs	Polymorphonuclear cells
PMSF	Phenylmethylsulphonyl fluoride
P-selectin	Platelet-selectin
PSGL	Platelet-selectin glycoprotein ligand
RANTES	Regulation upon activation, normal T-cell expressed and secreted
R-cadherin	Retinal-cadherin
ROCK	P160 Rho-associated coiled-coil-containing protein kinase (a.k.a Rho associated kinase (ROK))
ROS	Reactive oxygen species
SDS	Sodium dodecylsulphate
SDS-PAGE	Sodium dodecylsulphate polyacrylamide gel electrophoresis
SEM	Standard error of the mean
SFM	Serum free medium
SH3	Src homology 3 domain
SHP	Src-homology-2 protein tyrosine phosphatase
TAE	Tris-acetate buffer
Taq	*Thermus aquaticus*
TBS	Tris-buffered saline
TBST	0.1% v/v Tween/Tris-buffered saline
TBSTM	5% w/v milk/0.1% v/v Tween/Tris-buffered saline
TEMED	N,N,N',N'-tetramethylethylenediamine
TER	Transepi/endothelial electrical resistance
TGF	Transforming growth factor
TNF	Tumour necrosis factor
v/v	Volume per volume
VAMP	Vesicle-associated membrane protein

VAP	VAMP-associated protein
VCAM	Vascular cell adhesion molecule
VE-cadherin	Vascular endothelial cadherin
VEGF	Vascular endothelial growth factor
VLA-4	Very late antigen 4
w/v	Weight per volume
ZAK	ZO-1-associated kinase
ZO	Zonula occludens
ZONAB	ZO-1 associated nucleic acid binding protein

List of Figures, Tables and Appendices

Chapter 1:

Introduction

1.1 Microvasculature of the Brain

1.1.1 The Origin and Development of Endothelial Cells

The outer surfaces of the body and the lining of most internal cavities are covered by epithelial cells that associate in close-packed sheets that may be several layers in thickness. Exceptions to this distribution are the lining of the peritoneal cavity that is lined by a single layer of mesothelial cells, the blood vessels and the heart that are lined by a single layer of endothelial cells (ECs). All three cell types associate laterally with neighbouring cells and with any underlying basal lamina that couples the cells mechanically, providing anchorage and integrity and also allowing signalling between cells within a monolayer and between the cells and the substrate to which they are attached. The paracellular sealing caused by such close association between adjacent cells allows multicellular organisms to not only produce a barrier between themselves and their surroundings but also to separate tissues into distinct microenvironments. By regulating the integrity of these seals, cells are able to control solute concentration differences and host cell migration between tissues as well as establishing barriers that prevent invasion by potentially pathogenic microbes. Indeed, virulent forms of enteropathogenic *Escherichia Coli* (*E.Coli*) and *Vibrio Cholerae* have been demonstrated to disrupt or modify epithelial barrier function as a means of facilitating infection (Simonovic et al., 2000; Wu et al., 2000). Junctional abnormalities and dysregulation of EC junctions are known to occur in various pathological states including diabetes, ischaemic stroke and in ECs of the central nervous system (CNS) during neuroinflammatatory episodes, toxic shock and microbial infection (Huang and Ambrose, 2001).

It has been recognised for approximately 100 years that ECs develop from 'blood islands' that appear, in mouse embryos, within the yolk sac at day 7.5 of gestation. Such blood islands are derived from the embryonic mesoderm and contain two distinct cell populations believed to arise from a common precursor termed the haemangioblast (Cleaver & Melton, 2003; Fehling et al., 2003). Conclusive demonstration of the existence in vivo of

haemoangioblasts is lacking but a transient population of cells derived from embryonic stem cells and capable of generating cells of both endothelial and haematopoietic lineages has been isolated following in vitro culture (Lacaud et al., 2002). The two cell populations within blood islands are primitive erythroid cells and angioblasts that eventually form the vasculature. All arteries and veins develop from small vessels in the embryo, composed of ECs and basal lamina, by processes termed neovasculogenesis and angiogenesis, when new vessels are formed in previously unvascularised sites or from pre-existing vessels respectively. These two processes must occur rapidly enough to be capable of supporting growth and development in the embryo and to support the repair of damaged tissue in adults. Under pathologic conditions in mice, ECs can be stimulated to divide every few days whereas under steady-state conditions the endothelial turnover rate is very slow, being 1-2 months in the lung and liver and up to 1-2 years in the microvessels of the brain (Shima and Mailhos, 2000). The development of brain microvasculature begins when angioblasts invade the head region to form the perineural vascular plexus that in a 10-day rodent embryo covers the surface of the neural tube (Risau and Wolburg, 1990). None of the precursors that form the perineural vascular plexus or the intraneural vessels originate from the neuroectoderm, thus the brain microvasculature does not develop by vasculogenesis but rather vascular sprouts from the perineural plexus penetrate the neuroectoderm at E11 in rats by angiogenesis. The onset of angiogenesis at E11 is precisely reproducible and in mammals occurs via a predetermined pattern of development (Bär, 1980; Risau and Wolburg, 1990). The earliest known cell-surface marker of brain ECs appears at day E10.5 in mice, before the appearance of astrocytes, and is the multidrug resistance 1a/3 protein (Qin and Sato, 1995). Until approximately E13, the cerebral vessels of rats are fenestrated (see below) but these disappear and tight junction particles and a functional barrier is established. The paracellular flux of Horseradish peroxidase (HRP) across the cerebral vessels is already prevented at E14 even though the ECs continue to proliferate (Butt et al., 1990). However, the early embryonic capillaries are permeable to some molecules that are excluded from the adult brain (Johanson, 1980).

The development of this barrier does not occur simultaneously along the length of the cerebral vascular but rather in a step-wise process starting with the vasculature of the spinal cord and finishing with the telencephalon (Risau et al., 1986). Schulze and Firth (1992) describe the maturation of the barrier between E12-15 as an increase in the ratio of 'narrow zones' to 'wide zones' with regard to interendothelial clefts and the tight junction domains of the ECs increasingly give the appearance of fusion during this time (Cassella et al., 1997). At E13 there are few tight junction particles between brain ECs but these increase in number through to E18. At this stage, when viewed using freeze-fracture electron microscopy, the tight junction particles predominantly associate with the extracytoplasmic (E) face of the membrane whereas in postnatal and adult animals there is a switch to a predominantly protoplasmic (P) face distribution. Increasing P face association correlates with increasing transepi/endothelial resistance of cultured monolayers and this is in agreement with the rapid increase in transendothelial resistance (TER) of pial vessels of the rat measured at E21 (Butt et al., 1990). There is no direct method for measuring TER of capillaries within the brain parenchyma so instead direct measurements are usually taken from the capillaries within the pia mater on the surface on the brain. Up to and including E20, these measurements are low at around 10 $\Omega.cm^2$ and are similar to measurements taken from peripheral blood vessels showing that the junctions of the brain microvessels are not fully developed at this stage. Following birth and in the adult, these resistance values are typically between 1000-2000 $\Omega.cm^2$ (Butt et al., 1990).

1.1.2 Brain Endothelial Cells Contribute to the Formation of a Blood-brain Barrier

The impermeability of brain microvessels to certain protein-based tracers was first recognised over a century ago by the German microbiologist Paul Ehrlich and led to the concept of a blood-brain barrier (BBB). The ECs lining the capillaries of the brain form a continuous layer of non-fenestrated cells possessing well-developed tight junctions that exclude the passage of electron-dense tracers (Reese and Karnovsky, 1967). The molecular structure and regulation

of endothelial cell-cell junctions are described in greater detail in sections 1.2 and 1.4 respectively. Fenestrations are structures present in varying concentrations depending on the tissue site along the vascular endothelium. They are regions of endothelial cells where the luminal and abluminal membranes are brought into close proximity and form circular diaphragm-like structures that vary in a tissue-specific manner between 5-100 nm in diameter (Montesano and Orci, 1988; Braet and Wisse, 2002). They are differentiated from the rest of the cell with respect to cell-surface charge, membrane protein distribution and membrane fluidity. The association of caveolae and vesicles with these structures, in addition to their high concentration in the endothelia associated with tissues of high transport activity such as hepatic sinusoidal endothelium and the choriocapillaris in the eye has led to the speculation that these are sites of intensive fluid exchange between differing fluid compartments, e.g the blood and tissue interstitial fluid. Brain ECs also contain very few pinocytotic vesicles and exhibit a low rate of fluid-phase transcytosis compared to peripheral ECs (Joo, 1996; Stewart, 2000). Due to the effective sealing of the paracellular and transcellular pathways to the flux of solutes, most molecules except those that are very small and lipophilic are unable to easily diffuse across the brain capillary endothelium. Nutrients such as glucose and essential amino acids cross the barrier by carrier-facilitated diffusion whereas other groups of hydrophilic molecules are transported by receptor-mediated active transport mechanisms some of which, such as the transferrin receptor, are relatively highly abundant in brain ECs (Banks, 1999). Brain ECs also contain high numbers of mitochondria suggesting they are more metabolically active than peripheral endothelial cells. They express a range of catabolic enzymes such as monoamino oxidase, dihydroxyphenylalanine (l-dopa) decarboxylase and cholinesterases that block entry of neuroactive compounds into the brain (Öztas, 1998). Brain ECs also express several efflux pumps that actively translocate certain classes of molecules either out of the endothelial cytosol back into the circulation or out of the cerebrospinal fluid (CSF) back into the EC (Terasaki and Hosoya, 1999). Transporters of anionic and cationic organic compounds have both been described but detailed knowledge of their distribution and function remains to be

fully determined (Golden and Pollack, 2003). The most well characterised efflux pump present in brain ECs is p-glycoprotein, a 170 kD transmembrane glycoprotein that is capable of transporting a wide range of lipophilic and cationic molecules out of the cytosol and into the circulation (Cordon-Cardo et al., 1989; Seelig, 1998; Demeule et al., 2002). Mice lacking p-glycoprotein show an increased susceptibility to low concentrations of certain drugs that tend to accumulate within the brain (Schinkel et al., 1994; Schinkel et al., 1996). Another protein termed multi-drug resistance protein (MRP) has also recently been identified and displays some substrate similarity to p-glycoprotein although tending to bind more anionic than cationic compounds (Leier et al., 1996). The significance of MRP to the BBB in vivo is as yet undetermined. The brain capillary endothelium also acts as an immunological barrier due to the low basal level of cell adhesion molecule expression upon its surface (Hickey, 2001; Pachter et al., 2003). Acting in concert, these mechanisms constitute the BBB, the functions of which are to regulate the entry and removal of substances required by and excreted from the brain and to protect the CNS against potentially toxic compounds within the circulation.

There are exceptional areas of the brain microvasculature where the endothelium is fenestrated and the BBB is attenuated to the passage of certain molecules. These areas along the midline of the ventricle system of the brain are specialised tissues termed circumventricular organs and are sites of neuroendocrine feedback in the brain (Gross and Wiendl, 1987). Within these areas, neurons expressing specific receptors monitor the levels of various substances in the blood milieu. The circumventricular organs include the pineal body, the median eminence, the organum vasculosum of the lamina terminalis, the neurohypophysis and the area postrema (Prescott and Brightman, 1998). There is also an exception to this with the endothelium supplying the subcommisural organ displaying full BBB characteristics. Another exceptional site in the brain where endothelium display fenestrations is within highly vascularised leaf-like structures found in the third and fourth cerebral ventricle called choroid plexuses (Strazielle and Ghersi-Egea, 2000). The external covering of the choroid plexuses is the site of the barrier between

blood and cerebrospinal fluid (CSF, termed the blood-CSF barrier) and this is anatomically continuous with the ependymal barrier of the ventricles. The epithelial cells covering the external surfaces of the choroid plexuses express tight junctions as well as microvilli, abundant mitochondria and display the morphology of a transporting epithelium (Segal, 2000). The choroid plexuses actively produce and secrete the CSF, in addition to some trophic factors, that acts as a fluid 'cushion' for the brain and by providing part of a barrier, the other part being contributed by the ependyma of the ventricles, they maintain the sensitive composition of the fluid microenvironment of the brain. Due to there being a slow turnover of interstitial fluid from the brain into the CSF (Cserr et al., 1977 and 1981) and the CSFs' rapid turnover time of approximately six hours, it is believed that the CSF acts as a 'sink' for the brain by removing waste products and toxins. CSF circulates through the ventricles into the subarachnoid space located between the arachnoid and pial membranes and is mainly resorbed into venous blood through 'outpouchings' of the arachnoid membrane termed arachnoid villi that extend into the venous sinuses of the cerebral hemispheres (Ransahoff et al, 2003). Studies in murine and ovine models have indicated there there is a drainage of CSF into cervical lymph nodes (Cserr and Knopf, 1992; Widner et al., 1988). Whilst there are no identified lymphatic vessels in CNS tissue there has been the discovery of anatomical connections between the subarachnoid space and olfactory bulbs; that drain across the paper-thin cribrioform plate in the base of the ethmoid bone into lymphatics of the nasal submucosa (Weller et al., 1992). Studies measuring the contribution of extracranial lymphatics to the drainage of CSF estimate this may be as large as 50% of CSF volume (Boulton et al., 1999). These pathways have yet to be confirmed in human studies although anatomically similar relationships exist and in non-human primate models of experimental autoimmune encephalomyelitis myelin antgens have been detected in cervical lymph nodes where they are associated with dendritic-like cells (de Vos et al., 2002). The passage of CNS-derived antigens through the cervical lymphatics provides a mechanism whereby the antigenic content of the CNS and brain may be sampled by the immune system

without extensive leucocyte trafficking through the tissue (Ransohoff et al., 2003).

The cells that associate anatomically with brain capillary endothelial cells are believed to have a major role in the development and maintainance of the functional BBB (Miller, 1999; Wolburg and Lippoldt, 2002). Brain ECs are ensheathed by outgrowths of astrocytes termed astrocytic foot processes that are capable of producing a variety of soluble factors that modulate the endothelium although they do not form any physical barrier as they do in invertebrates (Abbott and Pichon, 1987; Abbott et al., 2002). Along the length of brain capillaries, but occurring less frequently than astrocytes, are smooth muscle-like cells termed pericytes that are believed to have an immunomodulatory role and potentially allow the vessels to contract (Allt and Lawrenson, 2001; Williams et al., 2001). There are other perivascular cells present that are phagocytic and capable of antigen presentation and so may represent an in situ population of macrophages (Prat et al., 2001). The anatomy of the BBB and associated cells is depicted in Fig. 1.1.

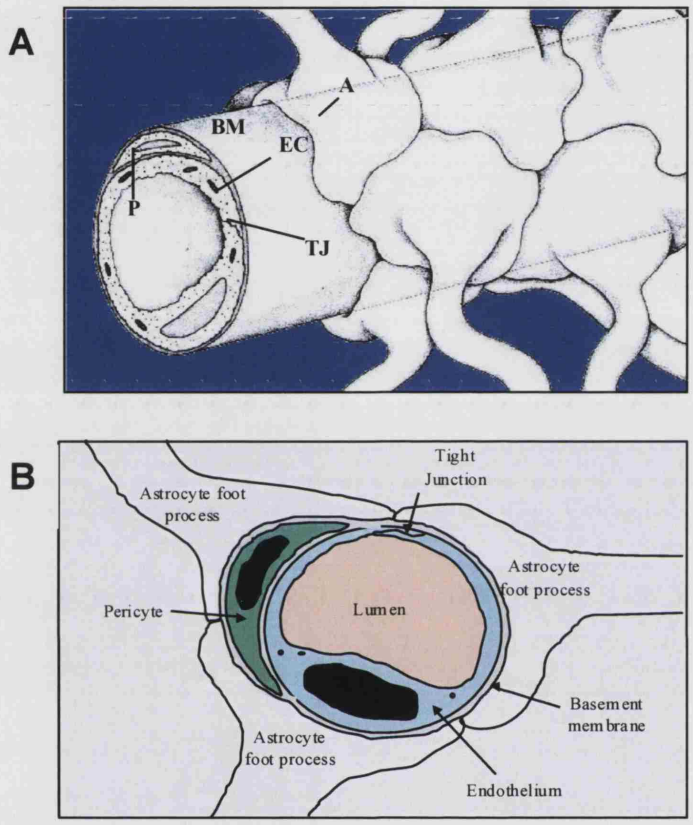

Fig. 1.1 Anatomy of brain capillary microvessels
Capillaries of the brain microvessels are lined by specialised endothelial cells whose properties are largely responsible for the formation of a blood-brain barrier. Brain endothelial cells are surrounded by an extracellular matrix, embedded within which are pericytes and that in turn is ensheathed by astrocytic foot processes (Panel A). Tight junctions between brain endothelial cells give brain microvessels an unfenestrated appearance when viewed in cross-section (Panel B). Abbreviations: P, pericyte; BM, basement membrane; TJ, tight junction; A, astrocyte (Taken from Bradbury, 1985).

1.1.3 Modelling the Blood-brain Barrier In Vitro

Establishing in vitro BBB models that are abundantly available, reproducible, easily manipulated and extensively characterised as exhibiting both cell and BBB-specific properties has great medical potential. These models allow not only the study of this specialised endothelium but also the permeability and transport characteristics of drug candidates across the BBB (Gumbleton and Audus, 2001). Various techniques have been used to isolate and culture ECs in models of the BBB that differ in the species from which they are derived, the isolation procedure and the subsequent culture conditions used. Such diversity makes comparison and transference of results difficult and uncertain. Primary ECs freshly isolated from brain microvessels or used within the first couple of subpassages are closest to retaining the in vivo phenotype and functional characteristics but have the disadvantage of only being available in small quantities that are inappropriate for many biochemical assays. Frequent or large-scale production of primary brain endothelial cultures can also be very labour intensive and raises ethical issues. Whilst bovine and porcine sources provide more material they have the disadvantage of a lack of species-specific diagnostic tools such as antibodies. Due to these restrictions, immortalised brain endothelial cell lines have been developed (Couraud et al., 2003) and these, in addition to ECs derived from peripheral vascular beds, have been tested in various model systems that try to produce cultures that are most 'brain-like' based on a number of functional criteria. These cells, whilst retaining expression of brain EC markers, some functional transport systems and in general producing cultures with a lower transendothelial permeability than those of peripheral ECs such as human umbilical vein endothelial cells (HUVECs), are unable to generate the very high transendothelial electrical resistance (TER) measurements recorded in pial vessels in vivo (Butt et al., 1990). The absence in vitro of seemingly crucial stimuli provided by the CNS microenvironment has led to much work on manipulating the conditions to try to produce cultures that exhibit higher TER values. Much attention has been focused on the role of astrocytes in inducing a BBB phenotype due to their intimate association in vivo. Early experiments reported the induction of BBB characteristics in

peripheral ECs by co-cultured astrocytes (Janzer and Raff, 1987). Subsequent research into the influence of such astrocyte co-culture on brain EC function has been inconsistent and although many groups report increased TER the observed effect appears to vary significantly and so the precise contribution of astrocytes remains unclear (de Boer and Breimer, 1996; Rubin and Staddon, 1999; Bauer and Bauer, 2000; Schiera et al., 2003). Much of this variability may be explained by the technical difficulty involved in synchronising the culture of the two cell types in these models. A disadvantage of all primary cultures is some degree of batch variability and with co-culture systems using two primary cell types the impact of such variability on any functional data is increased. This effect is increased even further if a third cell type such as pericytes is also included in the co-culture system (de Boer et al., 1999). In some models, astrocyte cell lines derived from glioma cells have been utilised but as the BBB in individuals with glioma is often compromised this would seem an inappropriate source of cells to study the healthy BBB (Hurst and Fritz, 1996). Astrocyte-conditioned medium has also been tested but has only demonstrated modest ability to increase monolayer TER although the source of the astrocytes may again be relevant when interpreting these data (Persidsky et al., 1999). Inclusion of compounds that raise intracellular levels of cyclic adenosine monophosphate (cAMP) within the brain endothelial culture medium has been shown to increase the TER of the culture (Rubin et al., 1991). Although high-resistance, low-permeability junctions are a hallmark of the BBB they are not the sole defining feature and such biochemical manipulation may prevent such cells responding normally during experiments due to dysregulated metabolism. This same line of argument can be applied to other models of the BBB that utilise either epithelial cell lines such as ECV304 or that use peripheral ECs such as HUVECs and then induce 'brain-like' characteristics by increasing their TER. Other factors that must be considered in the development of in vitro models include the presence of flow (Stanness et al., 1996) and the type of extracellular matrix upon which the cells are cultured (Domotor et al., 1999). As understanding of the various factors that are important for providing the conditions for brain ECs to retain their in vivo phenotype increases, then it would seem inevitable that research in this field will

diverge into at least two groups with differing goals. One group will aim to reproduce the CNS environment in vitro and so produce the most complete in vitro model of the BBB possible, although it may be that upon reaching this level of sophistication the experimental system becomes too complex to be used as a large-scale experimental tool. Other groups will instead strive to produce acceptable, representative models that are relevant to their own particular research interests and that can be investigated quickly and reliably whilst acknowledging their limitations. It should also be stated that whilst no in vitro model is a perfect representation, they have the advantage of being isolated from the many regulatory feedback systems that may exist within the CNS in vivo.

1.2 Endothelial Cell-cell Junctions

1.2.1 Adherens Junctions

Encircling both epithelial and endothelial cells are characteristic adhesion belts that are believed to provide the initial adhesive interactions between adjacent cells (Steinberg and McNutt, 1999). Such adherens junctions (sometimes refered to as zonula adherens) are also present between other cell types although these usually appear more punctate in distribution (Dejana et al., 2001). The adherens junctions of epithelia appear physically distinct from the more apical tight junction complexes (see below) whereas in endothelia the two types of junction complex may be more closely associated with apparent mixing of components (Schulze and Firth, 1993).

The molecular basis of the adhesive interactions at adherens junctions is the homophilic interaction of proteins of the cadherin family (Steinberg and McNutt, 1999; Dejana, 2004). Cadherins are transmembrane glycoproteins that associate, in a Ca^{2+}-dependent manner, into *cis* dimers and then in *trans* across the paracellular cleft with another dimer (Ahrens et al., 2003). Over 50 different cadherins have currently been identified and these have been divided into four groups based on protein sequence homology and genomic structure. Incorporated into adherens junctions are so-called 'classical'

cadherins that again have been subdivided into type I and type II based respectively on whether they do or do not contain a characteristic HAV amino acid motif in their most membrane-distal extracellular cadherin domain (Steinberg and McNutt, 1999). Aside from the classical cadherins, the other cadherin groups are the protocadherins, desmocollins and desmogleins. Due to their central role in cell-cell adhesion only classical cadherins will be discussed in detail here. Single classical cadherin molecules vary in molecular weight depending on their type but are all approximately 130 kD and composed of five extracellular cadherin motif domains, a transmembrane region and a cytoplasmic tail that interacts with several intracellular signalling proteins. The cytoplasmic tail also indirectly links the adherens junction complex to the cytoskeleton. Classical cadherin types include epithelial (E-cadherin), muscle (M-cadherin), neural (N-cadherin), placental (P-cadherin), retinal (R-cadherin) and vascular endothelial (VE-) cadherin -1 and -2 named after the tissue within which they are predominantly, although not exclusively, expressed. Predominant in ECs are VE-cadherin (a type II classical cadherin) and N-cadherin (Lampugnani et al., 1995) with VE-cadherin-2 also being expressed (Telò et al., 1998). VE-cadherin and N-cadherin are present in equal quantities but N-cadherin is not incorporated into adherens junctions but rather distributed across the cell surface (Navarro et al., 1998). VE-cadherin and VE-cadherin-2 have similar extracellular and transmembrane domains but their intracellular tails share no homology suggesting different cellular interactions for these two proteins. In addition to its structural role in cell-cell adhesion, VE-cadherin also functions in endothelial cell survival, migration, proliferation and vascular modelling during angiogenesis (Dejana et al., 1999; Dejana et al., 2001; Nelson and Chen, 2003). The importance of VE-cadherin in a wide range of developmental processes is demonstrated by the findings that VE-cadherin gene knockout mice die at E9.5 due to vascular deficiencies and that cultured ECs with targeted disruption of the VE-cadherin gene are unable to form vessel-like structures in vitro (Carmeliet et al., 1999).

As stated above, the intracellular domain of VE-cadherin (and other classical cadherins) is able to bind several different intracellular

proteins and the majority of these belong to the catenin protein family and are orthologous to the Armadillo (Arm) protein in *Drosophila*. The catenins are responsible for regulating many of the pathways of cadherin-mediated signalling (Zhurinsky et al., 2000). VE-cadherin directly associates with β-catenin (96 kD) and a homologue of β-catenin termed γ-catenin (86 kD, sometimes called plakoglobin) via the membrane-distal region of its intracellular tail, sometimes referred to as the catenin-binding domain (Steinberg and McNutt, 1999; Kaplan et al., 2001). It also binds p120-catenin ($p120^{CTN}$, hereafter p120) via the juxtamembrane region of the intracellular tail (Ferber et al., 2002). Both β- and γ-catenin are multifunctional and are capable of interacting with a variety of other proteins often through a common central domain that contains 13 repeats of the Arm binding domain motif (Zhurinsky et al., 2000). The similarity of this domain between the two proteins allows these two catenins to interact with many common partners. Despite this similarity and observations that they are sometimes able to functionally compensate for the absence of the other, neither is able to substitute entirely for the other as genetic knockout in mice of either gene is lethal at the embryonic stage due to developmental abnormalities (Ben-Ze'ev et al., 2000). The N- and C-termini of β- and γ-catenin are quite different and this influences their differing affinities for and selective recruitment into various protein complexes. Via their Arm repeat domains and their N- and C-termini being able to interact with different proteins, β- and γ-catenin act as scaffold molecules to bring interacting molecules into close proximity. Over 20 proteins have currently been identified as being able to bind these two catenins although the majority of cellular β- and γ-catenin is associated with adherens junction complexes. A single cadherin molecule can bind to the Arm repeat domain of one β- or γ-catenin molecule. These two catenins, via their N-terminus and first Arm repeat, in turn interact with α-catenin (102 kD) that is a structural homologue of the actin-bundling protein vinculin (Herrenknecht et al., 1991; Aberle et al., 1996). α-catenin associates either directly or indirectly via α-actinin or vinculin itself with filamentous (F)-actin thereby linking the adherens junction complex to the cytoskeleton (Tsukita et al., 1992; Bek and Kemler, 2002). The

tight junction associated proteins zonula occludens-1 and –2 (ZO-1, -2, described in greater detail below) are also able to bind α-catenin, potentially supporting interjunctional interactions between the different structural complexes (Itoh et al., 1999; Gonzalez-Mariscal, 2000). In addition to their structural role in adherens junctions, β- and γ-catenin are also both able to translocate to the nucleus and function as coactivators of transcription by interacting with members of the lymphoid enhancing factor (LEF)/T cell factor (TCF) transcription factor families (Simcha et al., 1998). Within such heterodimers, LEF/TCF proteins contribute the DNA-binding domain and catenins provide the transcriptional activation domain. β-catenin translocates to the nucleus following activation of the signalling pathway initiated by the binding of members of the wnt family of secreted glycoproteins to the cell-surface receptor frizzled that in turn 'activates' the scaffold protein dishevelled that negatively regulates the protein complex responsible for targeting cytoplasmic β-catenin for degradation. Cytoplasmic β- and γ-catenin not associated with junctions is quickly degraded by a well-characterised mechanism (Aberle et al., 1997; Saloman et al, 1997). Cytoplasmic 'free' catenin is bound by a molecular complex composed of axin, adenomatous polyposis coli (APC) and glycogen synthase kinase 3β (GSK) the latter of which phosphorylates N-terminal serine residues of both catenins. This phosphoserine motif is then recognised by the ubiquitin ligase β-transducin repeat containing protein (β-TrCP) that catalyses their ubiquitination that then targets them for degradation in the proteasome. The accumulation of cytoplasmic β-catenin (and perhaps γ-catenin) caused by wnt signalling inhibiting its degradation, allows it to then translocate to the nucleus and initiate LEF/TCF-targetted transcription (Ben-Ze'ev et al., 2000). The role of γ-catenin in wnt signalling in vivo is not entirely proven but evidence suggests that it may be involved although in a different function to that of β-catenin (Simcha et al., 1998; Zhurinsky et al., 2000). The different roles of β- and γ-catenin within the cell have been demonstrated to be modulated by phosphorylation events and this is discussed in greater detail below (see section 1.4).

As briefly stated above, VE-cadherin is also able to directly bind another Arm-repeat domain-containing protein called p120 that is the prototypic member of another subgroup of catenins (Anastasiadis and Reynolds, 2000). The p120 subgroup can itself be divided into two subgroups based on the degree of similarity of their Arm-repeat domains to that of p120. One group displays greater than 45% homology and interact with cadherins in adherens junctions. The other group are termed plakophilins and share approximately 30% homology with p120 but localise with the complexus adhaerentes (described in section 1.2.3) or to desmosomes in epithelia. All members of both groups can also be located within cell nuclei (van Hengel et al., 1999) where they may interact with the transcription factor Kaiso (Daniel and Reynolds, 1999); the transcriptional and biological significance of which is unknown. p120 and related proteins, that were first identified as substrates of the tyrosine kinase Src, contain 10 Arm repeats in their central domain, do not interact with γ- or α-catenin and are not degraded by the axin-APC-GSK machinery (Daniel and Reynolds, 1995). Cells express multiple isoforms of p120 and of other members of the subgroup generated from alternative splicing of a single gene. The splicing usually only affects the N- and C-termini and so the Arm repeat domains are preserved for binding to cadherins. The cell-type specific expression of different isoforms suggests a functional difference between isoforms and this may be one potential mechanism by which the specific properties of cell-cell junctions within different tissues are modulated. VE-cadherin (and classical cadherins in general) binds p120 and related proteins within their juxtamembrane domain, a ten amino acid sequence that represents the most highly conserved region of cadherin molecules and further demonstrates the importance of these interactions (Ohkubo and Ozawa, 1999; Thoresan et al., 2000). The role(s) of p120 in cell adhesion is not clear with evidence suggesting that its modulation can have both a pro- and anti-adhesive influence on adherens junctions. It has also been reported that p120 can regulate members of the rho guanine nucleotide triphosphatase (GTPase) family that regulate a wide range of cell processes including cytoskeletal rearrangement (Anastasiadis and Reynolds, 2001). Whether p120 regulates the adhesive properties of cadherins or whether cadherins act to buffer the level of

cytoplasmic p120 available for morphogenetic signalling is unclear and may be a complex combination of both (Anastasiadis and Reynolds, 2000).

1.2.2 Tight Junctions

Tight junctions (also known as zonula occludens) appear under thin-slice transmission electron microscopy as an electron-dense region in which the plasma membranes of adjacent cells are brought so close together as to give the appearance of fusion between the outer leaflets of the membrane (Balda and Matter, 1998; Zahraoui et al., 2000; Mitic et al., 2000, Lapierre, 2000, Tsukita et al., 2001; Wolburg and Lippoldt, 2002). When viewed by freeze-fracture electron microscopy, tight junctions appear as a series of continuous, branching strands that surround the apical end of the cell and that connect with complementary strands present on a neighbouring cell. Tight junctions fulfil two structural functions at the cell-cell junction referred to as the barrier and fence functions. The fence function contributes to cell polarisation by dividing epithelial and endothelial cell membranes into distinct apical and basolateral domains (Dragsten et al., 1981). The differing composition of these two membrane domains is maintained, at least in part, by the membrane-spanning tight junctions providing a physical barrier to the lateral diffusion of phospholipids and transmembrane proteins within the plane of the membrane thus preventing the intermixing of components. In this role as an intramembrane fence, there is evidence that the restriction of diffusion is more stringent within the outer leaflet of the membrane compared to the inner leaflet (Dragsten et al., 1981; van Meer and Simon, 1986). Tight junction complexes also restrict the paracellular diffusion of ions and solutes as well as the migration of cells across the cell sheet; forming a semi-permeable barrier that shows both size and charge selectivity (Mitic et al., 2000; Tsukita and Furuse, 2001). The amount of restriction through paracellular channels ('tightness') of tight junctions is most frequently assayed by TER measurements and this can vary between tissues by two orders of magnitude (Tsukita et al., 2001). The relationship between the structure of tight junctions formed by particular cell types and their functional characteristics is not fully understood. In general, the more tight

junction strands present between cells then the higher the TER of the tissue although exceptions to this are known indicating that the composition of these strands is also relevant. The complexity of the network of tight junction strands also varies between cell types from almost parallel, unconnected strands to those with frequent crossovers and branching points and this complexity may also contribute to the properties of the tight junctions. The association of tight junction particles with either the protoplasmic (P, the inner leaflet of the membrane viewed from the outside) or extracytoplasmic (E, the outer leaflet viewed from the inside) face in freeze-fracture electron microscopy samples is also an indicator of the integrity of the junctions formed (Wolburg and Lippoldt, 2002). The tight junction particles of epithelia and high-resistance endothelia, such as brain endothelia, are predominantly associated with the P face whereas in cells with low-resistance junctions they are found mainly associated with the E face (Simionescu et al., 1976; Wolburg et al., 1994). The distribution of tight junction particles between the two leaflets is influenced by the connectivity of junctions to, and the integrity of, the cytoskeleton to which the junctions are anchored (Nag, 1995). The molecular composition of tight junction strands has only been revealed in the past ten years and just how the interactions of tight junction proteins influence functional properties is slowly being unravelled. The identification of protein-based tight junction complexes suggests that earlier models proposing them to be composed of lipid-based structures (Kachar and Reese, 1982) may be of lesser importance although the existence of such domains and the role of membrane phospholipids in tight junction formation cannot be entirely discounted (Hein et al., 1992; Grebenkämper and Galla, 1994).

The first protein identified as a component of tight junctions was ZO-1 (220 kD) that shares homology with the *Drosophila* protein discs-large and was identified using antibodies raised against epithelial cell membrane fractions (Stevenson et al., 1986). The expression of ZO-1 by endothelial cells was confirmed several years later (Itoh et al., 1991; Itoh et al., 1993). ZO-1 is a cytoplasmic protein and a member of the membrane-associated guanylate kinase homologue (MAGUK) family (Gonzalez-Mariscal, 2000). It contains

three postsynaptic density protein-95/discs-large/ZO-1 (PDZ) domains, a Src-homology-3 (SH3) domain and a guanylate kinase (GK) domain. PDZ domains are 80-90 amino acid motifs that mediate protein-protein interactions and are found in mammals, flies, worms, yeast, bacteria and plants (Ponting, 1997). They are divided into two groups based on their recognition sequences (Songyang et al., 1997). Class I PDZ domains recognise the usually C-terminal peptide sequence S/TXV whereas class II recognises the C-termini of transmembrane proteins with a hydrophobic residue at position –2. The majority of PDZ domain-containing proteins are associated with membranes. The SH3 domain is another protein-protein binding domain that is 55-70 amino acids in size and that, in ZO-1, binds a serine kinase that phosphorylates ZO-1 on its C-terminal domain (Balda et al, 1996). The GK domain is homologous to the enzyme that catalyses the formation of guanosine diphosphate (GDP) from guanosine monophosphate (GMP) using adenosine triphosphate (ATP) as the phosphate donor. MAGUKs are, however, not able to bind either GMP or ATP and so the domain is enzymatically inactive although still able to support protein-protein interactions (Haskins et al., 1998). The C-terminal domain of tight junction MAGUKs differs considerably from that of other MAGUK proteins suggesting that this domain may be important for their function within cell junctions. Within this domain of ZO-1, there are three alternative splice sites; the first, α, contains an 80 amino acid domain whose expression tends to be higher in higher-resistance junctions (Balda and Anderson, 1993). ECs express both α^+ and α^- isoforms with the α^- isoform predominating. The relative levels of each within brain ECs are currently not known. The other splice sites, β_1, β_2 and γ comprise 7, 20 and 45 amino acid domains respectively whose influences on ZO-1 function are unknown (Gonzalez-Mariscal et al, 2000). Through these many domains, ZO-1 is able to act as an adaptor protein recruiting and acting as a scaffold for different structural and signalling molecules. Two related MAGUKs, ZO-2 (160 kD; Gumbiner et al., 1991) and ZO-3 (130 kD; Balda et al., 1993) were identified by their co-immunoprecipitation with ZO-1. They both also possess three PDZ, a SH3 and a GK domain and associate with ZO-1 forming heterodimers although they do not appear to directly interact with

each other (Wittchen et al., 1999). Both are expressed in epithelial and endothelial cells. A splice variant of ZO-2 has been detected within pancreatic cells that may have a role in cell cycle progression as its expression is higher in pancreatic adenocarcinoma cells (Chlenski et al., 1999). There are currently no identified splice variants of ZO-3. Within cells lacking tight junctions such as fibroblasts and cardiac muscle cells, ZO-1 and –2 both associate with adherens junctions by binding of α-catenin (Itoh et al., 1997; Itoh et al., 1999a). In subconfluent cells and at the leading edge of a wounded monolayer the intracellular distribution of ZO-1 and –2 is a mix of junctional and nuclear suggesting that they may also have a role in the regulation of transcription and cell growth. ZO proteins are able to form a link similar to that of the catenins within adherens junctions between the actin cytoskeleton and the transmembrane adhesion proteins of tight junctions (Itoh et al., 1999b). The transmembrane proteins of tight junctions are occludin, claudins and the junctional cell adhesion molecules (JAMs) that are described individually in greater detail below. ZO-1, -2 and –3 are all capable of binding F-actin directly (Fanning et al., 1998; Wittchen et al., 1999) with ZO-1 also able to associate with the actin-binding proteins cortactin and 4.1 (Katsube et al., 1998). ZO-2 is able to bind 4.1 but not cortactin (Mattagajasingh et al., 1999). Other identified binding partners of ZO-1 include connexin 43 (Toyofuku et al., 1998), AF6 (also called afadin; Prasad et al., 1993), atypical protein kinase C isotype-specific interacting protein (ASIP), cingulin, ZO-1-associated nucleic acid binding protein (ZONAB) and ZO-1-associated kinase (ZAK). AF6 is a mammalian homologue of the *Drosophila* canoe protein and may only be expressed in epithelia. It shares some homology with the kinesin unc104 and with the myosin V family of proteins although it lacks a motor domain (Ponting, 1995; Yamamoto et al., 1997). ASIP is a PDZ-containing protein that is a mammalian homologue of the *C.elegans* partitioning defective protein-3 (PAR-3) that is involved in cell polarity determination during development. ASIP contains a binding site for atypical protein kinase C (aPKC) and co-localises with PKCλ at tight junctions (Izumi et al., 1998). Cingulin is another myosin-like molecule that binds ZO proteins at its globular head terminus and other cingulin molecules at its globular tail in

addition to interacting with myosin itself (Cordenonsi et al., 1999). Cingulin is reportedly expressed only within epithelial cells. ZONAB is a Y-box transciption factor believed to influence the cell cycle (Balda and Matter, 2000) and ZAK is the serine kinase described above that phosphorylates ZO-1, the significance of which is uncertain (Balda et al., 1996).

The first transmembrane protein of tight junctions to be identified was occludin, a 65 kD protein first isolated from chick (Furuse et al., 1993) and later from mammalian cells (Ando-Akatsuka et al., 1996). The structure of occludin is similar to that of connexins and claudins with four transmembrane domains, a short intracellular N-terminus, a large intracellular C-terminus, an intracellular turn and two extracellular loops. Despite their topological similarity, occludin shares no sequence homology with claudin proteins. Occludin and its role within tight junction strands are described in greater detail in chapter 3.

Five years after the discovery of occludin, two members of a gene family termed claudins were identified as transmembrane proteins that localise exclusively to tight junctions (Furuse et al., 1998a). Over 20 claudins have now currently been identified with the expression of each being limited to specific cell types, most of which express at least two different types within the same tight junction strand (Tsukita et al., 2001). Brain ECs, for example, are known to express claudin-5 and -12 and perhaps also claudin-1 and –3 (Morita et al., 1999; Nitta et al., 2003; Matter and Balda, 2003). Claudins have a predicted topology similar to that of occludin with four transmembrane domains, two extracellular loops, an intracellular turn and both N- and C-termini localised intracellularly. They are smaller than occludin at approximately 25 kD with comparatively shorter extracellular loops and C-termini. There is accumulating evidence that claudins form the structural backbone of tight junction strands and are largely responsible for their barrier function (Furuse et al., 2002). Upon transfection into fibroblasts that lack tight junctions, claudins confer greater adhesion to the cells than occludin and both claudin-1 and -2 (and possibly others) are capable of generating structures that resemble complete, endogenous tight junction strands (Furuse et al., 1998b). Occludin transfection, however, does not lead to such tight

junction strand formation and epithelial cells derived from occludin-deficient stem cells are still able to form tight junction strands (Saitou et al., 1998). Overexpression of claudin-1 in Madin Darby canine kidney (MDCK) epithelial cells leads to an increase in TER and decreased paracellular permeability to molecular tracers (Inai et al., 1999) whereas occludin transfection increases TER but also increases paracellular permeability (Balda et al., 1996). Further evidence for the central role of claudins in determining the permeability of tight junctions has been demonstrated by studies selectively removing claudins from tight junction strands. Claudin-3 and -4 are both receptors for an enterotoxin derived from the bacterium *Clostridium perfringens* that binds and disassociates them from tight junctions (Sonada et al., 1999). Treatment of MDCK monolayers, the high-resistance strain of which expresses claudin-1 and -4 and the low-resistance strain that additionally expresses claudin-2, with this toxin causes disintegration of tight junction strands and a decrease in TER even though claudin-1 and occludin remain at the junctions. Also, claudin-11 is known to be the only claudin present in the tight junctions of myelin sheaths and in Sertoli cells of the blood-testes barrier. Claudin-11 knockout mice show a complete lack of tight junction strands at both sites and exhibit both neurological defects and male sterility demonstrating that claudin-11 is crucially responsible for the formation and function of tight junction strands in these tissues (Gow et al., 1999). Each claudin type expressed influences the integrity and selectivity of the barrier formed by the tight junction strands they produce. Expression of claudin-2 in high-resistance MDCK cells causes their TER to drop to that of low-resistance MDCK cells whereas claudin-3 transfection has no effect suggesting that claudin-2 expression creates channels or pores that allow the greater paracellular flux of ions (Furuse et al., 2001). Inter-claudin interactions both in *cis* and in *trans* may be important regulators of the permeability properties of such pores as claudins show discrimination in their binding to other claudins across the paracellular cleft. This has been shown using fibroblasts transfected with either claudin-1, -2 or –3 (Furuse et al., 1999). Both claudin-1 and –2 transfectants were able to bind claudin-3 transfectants but could not adhere to each other. The manner of *cis* interactions

between claudin molecules or between claudins and occludin are unknown. The concept that claudins form paracellular pores of a certain selectivity within tight junction strands is further suggested by an understanding of the first known inherited disease of tight junctions. Hereditary renal hypomagnesaemia caused by a defective claudin-16 (originally termed paracellin-1) gene is characterised by massive loss of magnesium and calcium in the urine leading to hypomagnesaemia and seizures (Simon et al., 1999). Magnesium is usually resorbed within the kidney from the glomerular filtrate via a paracellular route in the thick ascending limb of Henle. Claudin-16 expression is also restricted to this anatomical location and so the simplest explanation is that claudin-16 (perhaps in combination with other elements) forms selective aqueous channels or pores that allow the paracellular passage of divalent cations such as Mg^{2+} and Ca^{2+}. Further evidence for the structural importance of claudins and the existence of paracellular pores of certain selectivity comes from studies with knockout mice. Knockout of the claudin-1 gene leads to death one day after birth following extreme dehydration caused by transepidermal water loss (Furuse et al., 2002). The tight junctions (that within the epidermis of these animals are based on claudin-4 only) also show increased permeability to a very small (0.6 kD) tracer molecule suggesting that claudin-1 directly contributes to the barrier function of this tissue. Knockout of claudin-5 did not alter either the morphology of cerebral blood vessels or the ultrastructural appearance of tight junctions between brain endothelial cells (Nitta et al., 2003). The permeability of the BBB, however, did show increased selective permeability to molecular tracers with a molecular mass smaller than 0.8 kD. These claudin-5 knockout mice died approximately 10 hours following birth yet no significant histological anomalies were found, again highlighting the central importance of claudin molecules in determining tissue barrier function. It would appear, therefore, that claudins are necessary for the formation of tight junction strands and that by varying the claudin expression profile and their mixing ratios, as well as through inclusion of occludin, cells are able to generate cell-type specific selective barriers that allow the cells to fulfil their physiological role in diverse tissues (Van Itallie et al., 2001; Tsukita and Furuse., 2001). The

molecular complexity of adherens and tight junctions and other junctional complexes is represented schematically in Fig 1.2.

Intermingled with occludin and claudins within tight junction strands of epithelial and endothelial cells are another group of proteins termed JAMs of which four have currently been identified (Martin-Padura et al., 1998; Cunningham et al., 2000; Aurrand-Lions et al., 2001; Hirabayashi et al., 2003). JAMs (~40-50 kD) are transmembrane proteins of the immunoglobulin (Ig) superfamily that associate in *trans* across the paracellular cleft (Bazzoni et al., 2000a). They contain two Ig-like domains in their extracellular portion, a transmembrane domain and a short cytoplasmic tail containing a PDZ domain; through which JAMs interact with ZO-1, cingulin, AF-6 and Cas kinase (Bazzoni et al., 2000b; Martinez-Estrada et al., 2001). Both JAM-1 and –2 when transfected into Chinese hamster ovary (CHO) cells establish adhesive cell contacts and reduce paracellular permeability although this may be due to increased organisation of other junctional elements rather than any direct contribution of JAMs to junctional integrity. This contribution is believed to be minor as treatment of endothelial monolayers with blocking, anti-JAM antibodies did not increase permeability (Martin-Padura et al., 1998). Whilst JAMs are located at cell junctions their main function may be in the regulation of leucocyte diapedesis rather than adhesive integrity. Indeed, treatment of endothelial monolayers with the blocking, anti-JAM antibody inhibited transendothelial migration of both monocytes and neutrophils (Martin-Padura et al., 1998; Del Maschio et al., 1999). In addition, JAM-1 has been identified as a ligand for the integrin lymphocyte function antigen (LFA-1) expressed on many circulating leucocytes including lymphocytes (Ostermann et al., 2002). JAM-2 has been demonstrated to be an endothelial receptor for JAM-3 present on the cell surface of circulating dendritic, natural killer (NK) and $CD8^+$ T cells (Liang et al., 2002). Many types of leucocyte express different JAMs as well as other junctional molecules and the possible implication of this is described in greater detail below. JAMs may therefore, in addition to their ability to interact with and organise tight junction elements, function as junctional cell adhesion molecules that 'guide' and facilitate the migration of firmly-adhered leucocytes through a paracellular pathway.

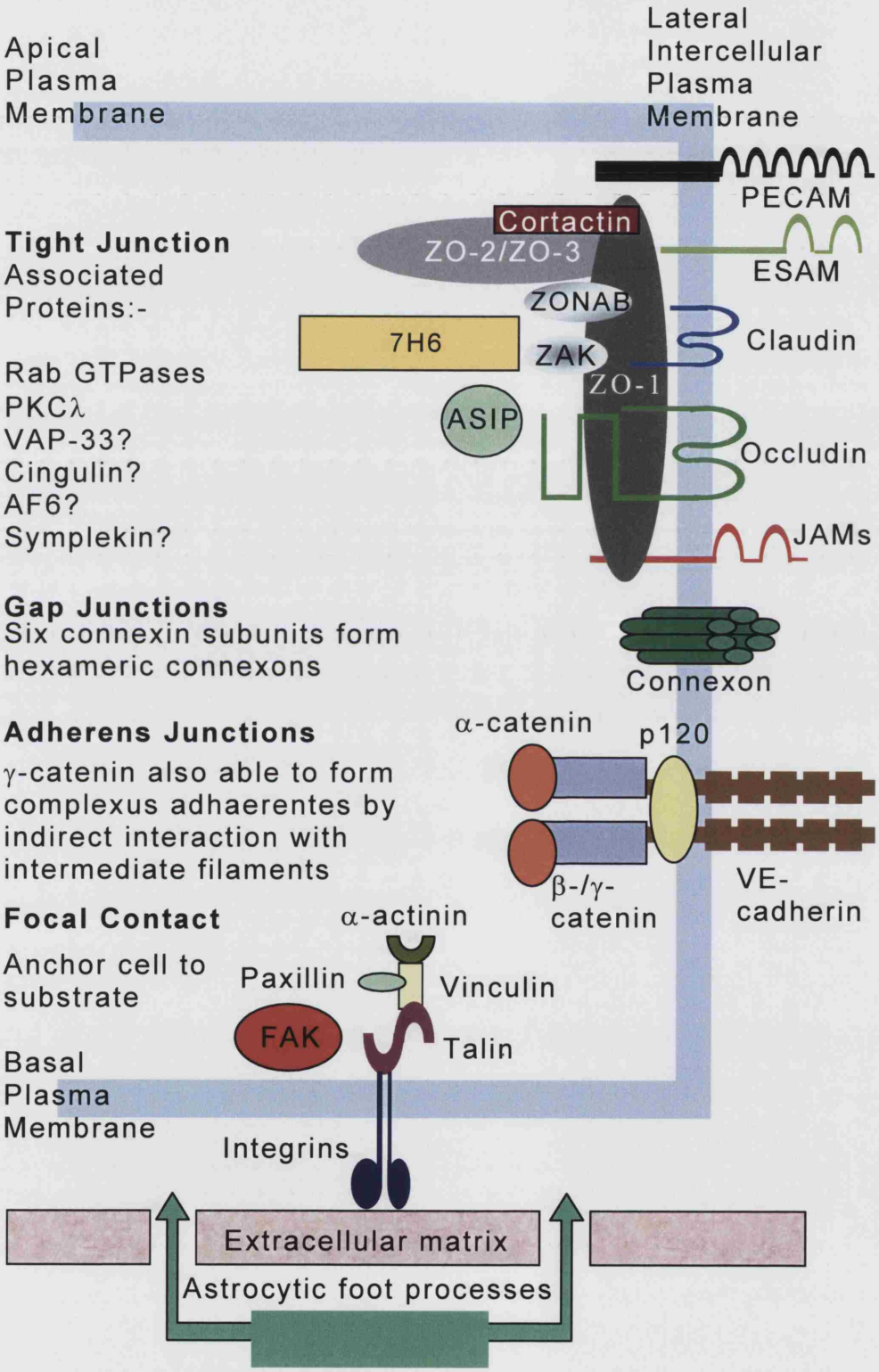
Apical
Plasma
Membrane
Lateral
Intercellular
Plasma
Membrane
PECAM
Cortactin
ZO-2/ZO-3
ESAM
Tight Junction
Associated
Proteins:-
ZONAB
7H6
ZAK
Claudin
ZO-1
ASIP
Occludin
JAMs
Rab GTPases
PKCλ
VAP-33?
Cingulin?
AF6?
Symplekin?
Gap Junctions
Six connexin subunits form
hexameric connexons
Connexon
Adherens Junctions
α-catenin
p120
γ-catenin also able to form
complexus adhaerentes by
indirect interaction with
intermediate filaments
β-/γ-
catenin
VE-
cadherin
Focal Contact
α-actinin
Anchor cell to
substrate
Paxillin
Vinculin
FAK
Talin
Basal
Plasma
Membrane
Integrins
Extracellular matrix
Astrocytic foot processes

Fig. 1.2 Schematic representation of the various molecular complexes present at endothelial cell-cell and cell-substrate interfaces

The molecular architecture of cell junctions has been revealed to be increasingly complex with many other cytoplasmic proteins also localising to this region. Only the most well characterised structural and scaffolding molecules of junctions and focal adhesions have been included. Overlap of protein symbols indicates demonstrated interaction. Question marks denote proteins identified within epithelial tight junctions only. For definition of abbreviations and greater desciption of each junctional component see section 1.2.1-3

Other tight junction-associated proteins include symplekin (127 kD; Keon et al., 1996), 7H6 (155kD; Zhong et al., 1993) and endothelial cell-selective adhesion molecule (ESAM, 55 kD; Nasdala et al., 2002). Symplekin has only been described in epithelial tight junctions but is present in all other cells where it localises to the nucleus and is believed to have a role in the polyadenylation of mRNA (Tagayaki and Manley, 2000). The 7H6 antigen is only expressed in fully polarised cells where it becomes phosphorylated when localised to junctions and may regulate barrier function (Zhong et al., 1994; Satoh et al., 1996). ESAM is a member of the Ig superfamily with a similar structure to JAMs except with a larger cytoplasmic domain and is capable of supporting homophilic cell-cell adhesion in transfected CHO cells (Nasdala et al., 2002). Conventional G proteins and many small GTPases such as rho, rac and cdc42 are also known to localise to and modulate the functions of tight junctions (Hopkins et al., 2000; Nusrat et al., 2000b; Wojciak-Stothard et al., 2001; Walsh et al., 2001; Adamson et al., 2002).

There is evidence to suggest that tight junctions may also have a role in the regulation of vesicle trafficking. Antibodies to the mammalian homologue of the sec6/8 complex, that localises to tight junctions and that in yeast is a component of the exocyst and required for vesicle targeting to the bud tip, inhibits delivery of vesicles containing low-density lipoprotein to the basolateral membrane while not affecting apical targeting of another protein in permeabilised MDCK cells (Grindstaff et al., 1998). The C-terminus of occludin has also been shown to bind vesicle-associated membrane protein (VAMP)-associated protein-33 (VAP-33) that is also involved in vesicle trafficking, as are members of the Rab family of small GTPases; several of which localise to tight junctions (Lapierre et al., 1999). Whether this function of tight junctions is limited to epithelia is currently unknown.

Circulating leucocytes and in situ immune cells have also been shown to express junctional proteins. Dendritic cells from lymph nodes and within the skin (Langerhans cells) express E-cadherin and this is required for their interaction with keratinocytes and retention in the dermis (Cumberbatch et al., 1996). Downregulation of E-cadherin in these cells promotes their displacment from the skin and entry into

the lymphatic system. Expression of E-cadherin has also been reported in thymocytes (Munro et al., 1996) and epithelia/mucosa-associated γ/δ T cells (Aiba et al., 1995). Transformed Jurkat T cells and those activated with mitogen for 12 days have also been found to express cadherins although the in vivo relevance of this is not known (Cepek et al., 1996; Kawamura-Konada et al., 1999). Both $CD4^+$ and $CD8^+$ T cells activated in vitro express occludin (Alexander et al., 1998) and a range of leucocytes including lymphocytes, monocytes and neutrophils are known to express platelet-endothelial cell adhesion molecule (PECAM) and the JAMs (Alexander et al., 2001). Expression of these molecules by circulating cells is believed to facilitate their passage through the lateral junctions of cell sheets. Their homophilic interaction brings the cell membranes into close proximity allowing further signalling and preserving the barrier function of the cell sheet. In addition to the role of adhesive cell-cell interactions in the migration of interdigitating leucocytes, these may also contribute to immunological synapse formation between lymphocytes and antigen presenting cells. Some junctional molecules are themselves also capable of transducing signals following ligation, as they do within endothelial and epithelial cells, although the pathways activated may differ between cell types.

1.2.3 Other Molecular Interactions at Cell-cell Junctions

In addition to any adherens and tight junction expression, most cells connect with those adjacent to them through small intercellular channels called gap junctions. Gap junctions are formed by the association across the paracellular cleft of two connexon units, one contributed from each cell, that form channels approximately 10 nm in diameter and that allow the passage of small (<1 kD) molecules between the cytosol of neighbouring cells (Lampe and Lau, 2000). Each connexon unit is an oligomer composed of six members of the connexin protein family of which there are more than 12 known members. Connexins are structurally similar to occludin and claudins with their molecular size varying by type but are approximately 25-45 kD. Ions are free to pass through gap junctions and so they are able to support conduction of electrical impulses in excitable cells. Other

substances believed to be able to cross junctions are metabolites and secondary messenger molecules. Deficiency or targeted disruption of a single connexin gene leads to a variety of serious pathologies ranging from deafness to fatality during development, demonstrating the essential role of gap junctions in many different biological processes (Lampe and Lau, 2000). The establishment of gap junctions is facilitated by the stable formation of adherens and tight junctions and the reported association of ZO-1 with connexins 43 and 45 as well as occludin with connexin 26 suggest gap junctions are intimately, although perhaps not functionally, linked with tight and/or adherens junctions. Indeed, the frequency of gap junctions observed in vivo correlates with that of tight junctions and the two structures are usually intercalated (Lampe and Lau, 2000). The structural similarity between connexins and the tight junction transmembrane proteins, in addition to the observation of tight junction strands having a similar diameter to gap junctions when viewed by electron microscopy, has led to the speculation that tight junction strands are composed of polymerised oligomeric subunits. The composition and interactions of these may be complex with differing patterns of claudin and occludin expression being one manner by which the necessary variation in the properties of tight junctions within different tissues are achieved. The possible composition and interactions within and between tight junction strands are depicted in Fig. 1.3.

In addition to adherens, tight and gap junctions, ECs also possess another transmembrane protein-based cell-cell adhesion system mediated by the homophilic interactions of PECAM. PECAM is described in greater detail in chapter 5.

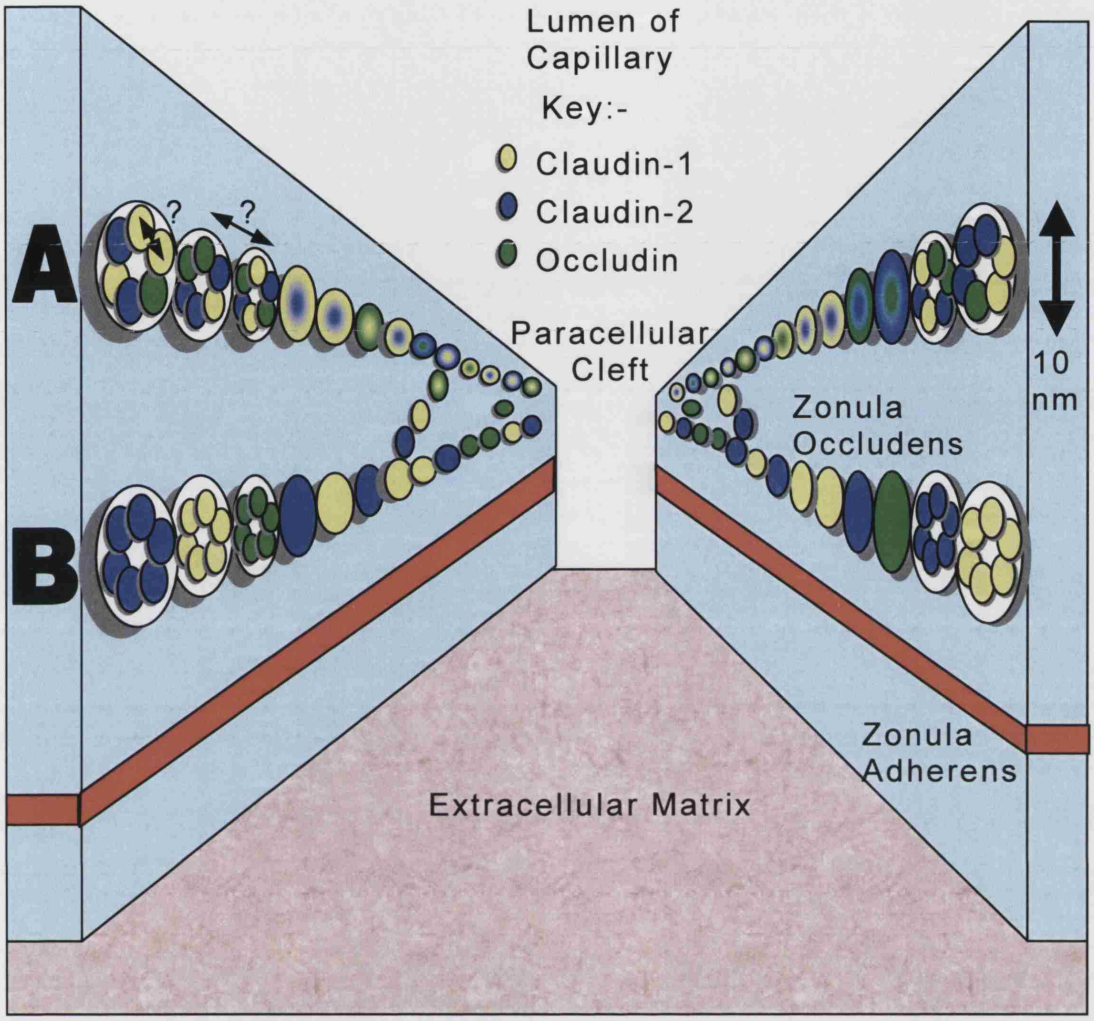

Fig. 1.3 Diagramatic representation of potential interactions within and between anastomosing tight junction strands in brain endothelial cells

The proposed structure of tight junction strands is based on the topological homology of the components (claudins and occludin) to connexins and the similar appearance of tight junction strands to gap junctions. The paracellular cleft is depicted as a wide channel, however, this space is reduced to such an extent as to give the appearance of apparent membrane fusion between adjacent cells. Theoretical T.J. 'subunits' are either heteromeric (**A**) (i.e claudins and occludins in either random or regulated ratios) or homomeric (**B**) (i.e. only a single claudin or occludin species within a subunit). Six monomers are depicted in each subunit but the actual numbers are unknown. The nature of the interactions between monomers within subunits and between subunits is also unknown. *Trans* interactions between strands may be homophilic (demonstrated by occludin interacting with occludin but not claudin-1 in transfected fibroblasts) or heterophilic as with claudin-1 and -3 and claudin-2 and –3 binding although some pairs such as claudin-1 and -2 do not adhere.

The mechanical integrity of epithelial monolayers is increased by linkage of the intermediate filament networks of adjacent cells via another cadherin-based adhesion plaque termed desmosomes. These are joined across the paracellular cleft by members of the desmocollin and desmoglein cadherin subgroups that bind γ-catenin that in turn binds desmoplakin or plakophilin that are both able to associate with intermediate filaments (Kowalczyk et al., 1998). Endothelial cells lack desmosomes but neighbouring cells intermediate filament networks are coupled through desmosome-like networks termed complexus adhaerentes (Schmelz et al., 1994) formed by way of the ability of γ-catenin to link VE-cadherin with desmoplakin or plakophilins and thus intermediate filaments.

Brain ECs lining the lumen of the capillaries are surrounded by a basal lamina and embedded within this are pericytes and astrocytic foot processes. The attachment of the endothelial cells to the extracellular matrix of the basal lamina is mediated through the interaction of specific integrin receptors on the cells' basolateral membrane with structural proteins such as collagen, fibrinogen, fibronectin, vitronectin and laminin. This adherence is strengthened and partly regulated by the formation of multi-protein complexes termed focal contacts (also called focal adhesions) (Sastry and Burridge, 2000). Proteins identified as being part of the focal adhesion complex include talin, vinculin, paxillin and α-actinin that serve to link focal contacts to the actin cytoskeleton. Many other signalling molecules including Src and focal adhesion kinase (FAK) also localise to focal contacts where they modulate focal contact interactions during a wide range of biological processes that may potentially affect the integrity of the endothelial barrier and/or leucocyte diapedesis.

1.3 Lymphocyte Trafficking

1.3.1 Process and Regulation of Lymphocyte Transendothelial Migration Across the Blood-brain Barrier

In order for leucocytes to be able to exit the circulation and enter into the tissues, whether during homeostatic immune surveillance or an ongoing immune response, they must be able to interact with and cross the single layer of ECs that line the microvessels. By regulating these interactions, the endothelium has a central role in the initiation and progression of the immune response. The interaction of leucocytes with the endothelium is mediated by several groups of cell adhesion molecules, some that are constitutively expressed and others whose expression is induced or upregulated following pro-inflammatory stimulation. Due to the extremely low number of leucocytes that can be found in healthy CNS tissue and the low basal expression of cell adhesion molecules on brain ECs, the CNS has been considered, along with the retina and the testes, as an immunologically privileged site (Antel and Owens, 1999; Hickey, 2001; Pachter et al., 2003). As greater understanding of immune responses within the CNS has accumulated, however, it now seems more appropriate to describe it as an environment of selective and modified immune reactivity (Ransohoff et al., 2003). The molecular interactions involved in lymphocyte trafficking (and that of other leucocyte subsets) has been extensively studied and the adhesive-rolling model of association is universally accepted as a working model (Springer, 1994). This process has been divided into a multi-step series of overlapping events during which lymphocytes are slowed in the circulation by rolling across the endothelial surface before signalling within both cell types induces the activation of receptors that promote firmer adhesion of the T cell and its arrest before diapedesis through the endothelial lateral cell junctions (Edens et al., 2002). This mechanism is believed to be that by which lymphocytes are recruited into the CNS although it should be noted that due to the low levels of trafficking into this tissue most of the work has been confined to disease and injury models. It should also

be noted that lymphocyte migration into the CNS is not a single process occurring at a single site and the cells that have managed to infiltrate the BBB may have gained acces via different routes involving differing migratory processes (Ransohoff et al., 2003). Migration into the spinal cord is little understood whereas migration into the brain has been suggested to occur by three potential pathways. These are migration from the blood into the CSF through the choroid plexuses, from the blood into the subarachnoid space and Virchow-Robin perivascular spaces or from the blood directly into the brain parenchyma. This caveat aside, the general process of lymphocyte extravasation is believed to be very similar to that described in peripheral high endothelial venules. There is some evidence however that migration of T cells into the CNS does not involve the rolling stage but rather that the intial interactions are those mediating firm adhesion (Engelhardt et al., 1997). Some of the adhesion and effector molecules involved also vary in a tissue-specific manner as they do between other peripheral tissue types. The sequence of overlapping events comprising the current working model of lymphocyte transendothelial migration into the CNS is shown diagramatically in Fig. 1.4.

The initial interaction of a lymphocyte with the endothelium is referred to as tethering and the subsequent interactions as rolling with both of these being mediated by members of the selectin family of proteins binding specific carbohydrate moieties present on the interacting cell (Lasky, 1995). Selectins are single chain transmembrane proteins containing a lectin domain in their extracellular portion and a short cytoplasmic tail that is capable of signal transduction upon ligation (Kansas, 1996, Hu et al., 2001). The three identified selectins are leucocyte (L)-selectin that is found on all leucocytes except a subpopulation of memory T cells, platelet (P)-selectin and endothelial (E)-selectin; both of which are expressed by vascular endothelium. The expression of L-selectin is regulated by both cytokines and the activation of the lymphocyte that induces an increase in expression followed by its shedding from the cell membrane, the biological significance of which is not clear (Brown, 2001). The ligands of L-selectin include the carbohydrate moiety sialyl Lewis-X present on mucosal addressin cell adhesion molecule

(MAdCAM) with other ligands including glycosylation-dependent cell adhesion molecule (GlyCAM), CD34 and podocalyxin (Rosen and Bertozzi, 1994). All of these molecules are constitutively expressed and so during inflammation are modulated in some way to induce binding or as yet unidentified ligands become available to increase the amount of initial tethering that occurs. P- and E-selectin are both greatly upregulated on the endothelial cell surface following activation by cytokines or pro-inflammatory mediators. P-selectin is stored intracellularly within vesicles (Weibel-Palade bodies) and is translocated to the membrane within minutes of an inflammatory signal (Hattori et al., 1989; McEver et al., 1989) whereas E-selectin appears after approximately 2 hours following de novo protein synthesis (Wellicome et al., 1990). The ligand present on leucocytes for P- and E-selectin is P-selectin glycoprotein ligand-1 (PSGL-1; Piccio et al., 2002). L-selectin and the counter-receptors for endothelial selectins (mainly PSGL-1) are concentrated on the microvilli of leucocytes and it is these that initially contact the ECs (Picker et al., 1991; Moore et al., 1995). Selectin-ligand interactions tether the lymphocyte to the endothelium, allowing them to roll along the surface in the direction of blood flow and from where they receive and send additional signals to the endothelium. In the absence of subsequent adhesive interactions, lymphocytes return to the circulation as the relatively weak and transitory selectin interactions are broken under conditions of flow.

During their rolling phase across the endothelial surface, lymphocytes receive signals mainly in the form of chemokines but also from other factors such as platelet-activating factor (PAF) and the complement split product C5a (Brown, 2001). These factors may act in a paracrine manner or be immobilised on the endothelial glycocalyx until they bind to their complementary G-protein-linked 7-transmembrane spanning receptors on the lymphocyte cell surface (Baggiolini, 1998). Approximately 50 chemokines have been identified to date in humans and their selective expression and recognition contribute to the specificity of leucocyte recruitment to particular tissues. The shear flow of the circulation also facilitates the migration of T cells across endothelial monolayers following interactions with chemokines (Cinamon et al., 2001; Luscinskas et al., 2001). This

phenomenon has been termed chemorheotaxis although whether the force of flow modulates the T cell or endothelial cell in some way or whether it helps to physically 'push' the migrating cell through the monolayer is unclear.

Signals transduced through chemokine binding lead to conformational changes in integrin receptors on the lymphocyte cell surface from a low-affinity to a high-affinity state as well as their clustering on the cell surface and increased association with the cytoskeleton (Takagi and Springer, 2002). Integrins are heterodimeric cell adhesion molecules composed of non-covalently associated α and β subunits. Various combinations of the 16 different α chains with the 8 different β chains gives rise to the 20 identified molecules that are subdivided based on their β chain usage (Shimizu et al., 1999). The β_1 and β_2 subgroups are especially relevant to lymphocyte migration (Wong et al., 1999; Laschinger and Engelhardt, 2000; Faveeuw et al., 2000; Laschinger et al., 2002; Alter et al., 2003) with the β_1 group mediating adhesion to extracellular matrix proteins except in the case of $\alpha_4\beta_1$ (very late antigen-4, VLA-4) that is a receptor for vascular cell adhesion molecule (VCAM), an Ig superfamily cell adhesion molecule on the EC surface. The β_2 integrins such as $\alpha_L\beta_2$ (LFA-1) and $\alpha_M\beta_2$ (Mac-1) are expressed on circulating leucocytes and recognise the Ig superfamily cell adhesion molecule intercellular adhesion molecule-1 (ICAM-1). These interactions are divalent cation-dependent and are responsible for the firm adhesion of lymphocytes to ECs and their arrest within the bloodstream. In addition to the chemokine-mediated activation mentioned above, integrins are also upregulated and rendered more adhesive by signalling that occurs through selectin ligation (Dransfield and Hogg, 1989; Hwang et al., 1996). As stated above, the ligands for integrins are cell adhesion molecules of the Ig superfamily (Holness and Simmons, 1994) that themselves are upregulated by a range of pro-inflammatory stimuli including lipopolysaccharide (LPS), tumour necrosis factor-α (TNF-α), interferon-γ (IFNγ), interleukin-1 (IL-1) and cell stress (Hordijk, 2003). It has been demonstrated within the previous 12 years that these molecules are also capable of signal transduction upon aggregation (signalling cascades initiated through ICAM-1 ligation are described in

greater detail in chapter 4). Following the interaction of these receptor-ligand pairs, the lymphocyte assumes a flattened morphology prior to diapedesis (Johnson-Leger et al., 2000; Edens et al., 2002).

The migration of firmly-adhered lymphocytes through the endothelial lateral cell junctions is the least well understood stage of extravasation but must involve modulation of junctions and/or their proteolytic degradation to allow the migrating cell passage. Diapedesis via a paracellular pathway may not be the only mechanism by which leucocytes cross the endothelial barrier. There is evidence, at least in the case of neutrophil migration, for a transcytotic pathway (Feng et al., 1998) as well as indication that these cells may frequently migrate at tricellular corners of cells within an endothelial sheet (Burns et al., 2000). Tight junctions here are discontinuous and such migration does not appear to cause significant disruption to the junctional barriers. Chemokines also act as factors controlling lymphocyte chemotaxis and the movement of cells along such a chemotactic gradient presumably stimulates their migration through the endothelium as well as their passage through the tissues (Baggiolini, 1998; Brown, 2001). After passing through the paracellular cleft of brain ECs, infiltrating lymphocytes must cross the basement membrane that surrounds the blood vessels and this is achieved by the elaboration of proteases termed matrix metalloproteinases (MMPs) that are capable of degrading its constituents. There are at least 20 different MMPs that may be produced by leucocytes or by CNS-resident cells and their excessive accumulation is an additional mechanism leading to CNS pathology and damage to the BBB (Brown, 2001).

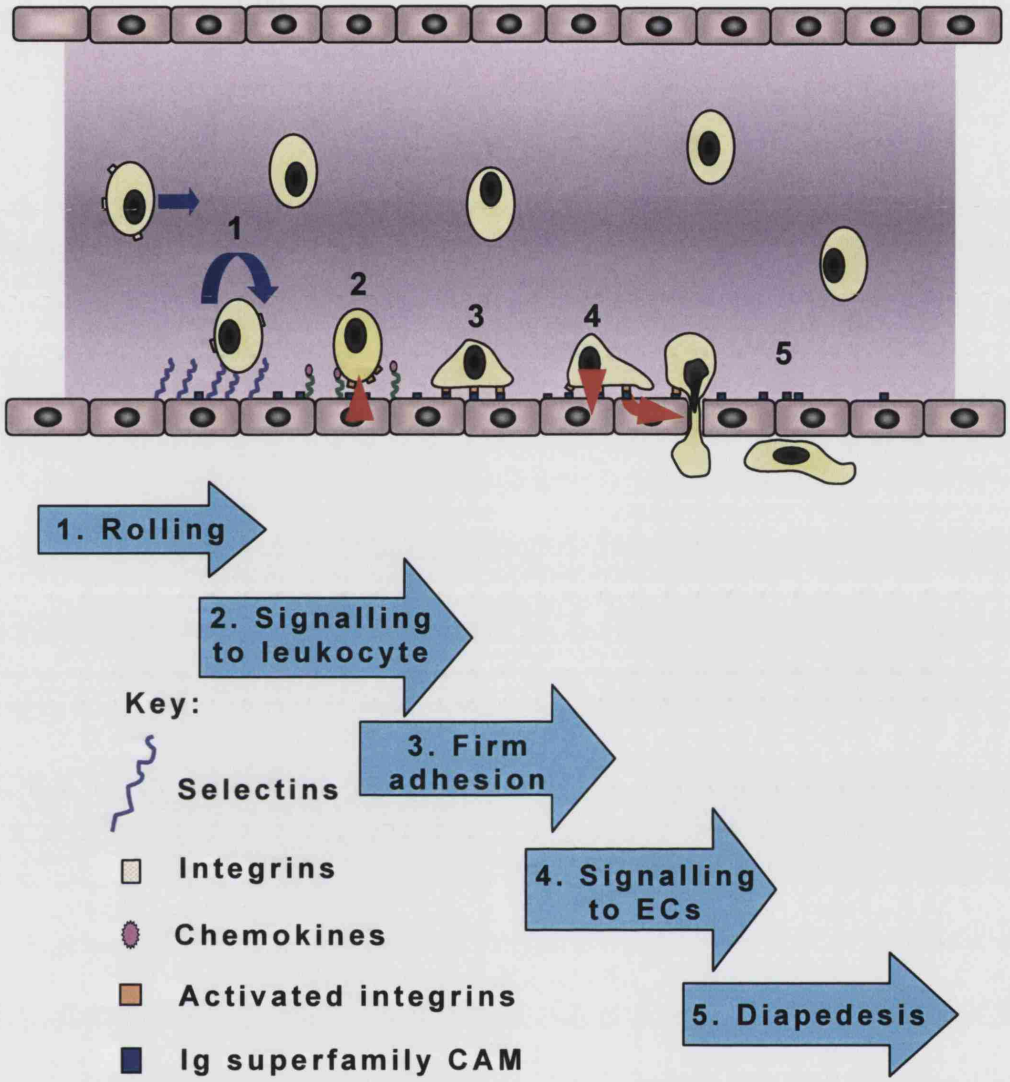

Fig. 1.4 Lymphocyte extavasation
The current process of lymphocyte extravasation into the central nervous system can be considered in terms of 5 sequential, overlapping steps. Initially, low affinity interactions between selectins and their ligands tether the circulating lymphocyte to the vessel wall (1). Signalling to the lymphocyte through selectin aggregation and chemokines immobilised on the endothelial glycocalyx induces activation of integrin high affinity receptors (2), causing firm adhesion of the lymphocyte to the vessel wall (3). Reciprocal signalling to the endothelial cell through immunoglobulin (Ig) superfamily cell adhesion molecules such as ICAM (4) then allow the lymphocyte to extravasate through the endothelial wall in a process termed diapedesis (5).

1.3.2 The Role of Lymphocytes in Chronic and Acute Neuroinflammatory Disease

Greatly increased lymphocyte and monocyte infiltration into the CNS is a hallmark of multiple sclerosis (MS) and other neuroinflammatory diseases. The pathology associated with these disorders is caused by an inflammatory cascade that is initiated by the diverse influences of many predisposing factors. MS is the most common autoimmune disease of the nervous system and affects approximately one million people worldwide with a female to male ratio of 2:1 and a predominance in temperate climates (Steinman, 1996). Despite vast amounts of research, the cause of MS remains unknown although perhaps this is likely due to MS representing a heterogenous collection of disorders with similar aetiology and pathology. Genetic factors are known to be important with a concordance rate in monozygotic twins of 30% and the possession of certain human leucocyte antigen (HLA) haplotypes predisposing to disease perhaps due to influences on the T cell repertoire of an individual (Ebers et al., 1995). Environmental and developmental factors are also known to be of importance with an individuals' geographic predisposition being determined by the location in which they spent the first 15 years of life (Steinman, 1996). Autoreactive T cells recognising neuronal antigens are present in the blood of 'normal' individuals and the cross-reactivity of these with microbial-derived epitopes may be one mechanism by which an autoimmune attack is initiated following infection (Steinman et al., 2002). The accumulation of predominantly activated $CD4^+$ T cells and macrophages but also of $CD8^+$ cytotoxic T lymphocytes (CTLs) and B cells at inflammatory foci leads to an autoimmune attack directed against myelinated neurones and often their irreversible damage. This neuronal loss leads to an inhibition and loss of signal transduction that can lead to ataxia, sensory disturbances, incontinence, visual impairment leading to blindness, spasticity and paralysis although cognitive function is unaffected. The phagocytic, CNS-resident microglial cells are believed to be the main cell type involved in antigen presentation to infiltrating lymphocytes and the activation of autoreactive T cell clones (Antel and Owens, 1999) that begin to produce IL-2, stimulating their own proliferation, and IFNγ. The increasing concentration of IFNγ activates microglia

and infiltrating macrophages causing their increased production of reactive oxygen and nitrogen intermediates (ROS and NOS respectively) and nitric oxide (NO) via a respiratory burst in addition to increasing their rate of phagocytosis, expression of major histocompatability (MHC) class II and co-stimulatory molecules and secretion of the pro-inflammatory cytokines TNF-α, IL-1, IL-6 and IL-12. IL-12 and IFNγ both act as polarogens by promoting the differentiation of $CD4^+$ T cells into a Th_1-like phenotype that drive a classical 'cell-mediated response'. The TNF-α, ROS, NOS, NO and defensins released by macrophages and microglia, in addition to the TNF-β, perforins, granzymes and MMPs released by CTLs and Th cells, generates an extremely proteolytic and degradative milieu that leads to neurologic damage. This is enhanced by autoantibodies from B cells and complement split products opsinising tissue autoantigens leading to their degradation by frustrated phagocytosis and antibody-dependent cellular cytotoxicity reactions.

1.4 Regulation of Junctional Integrity and Leucocyte Diapedesis by Modulation of Junctional Proteins

1.4.1 Modulation of Junctional Proteins by Metabolic Inhibitors, Pro-inflammatory Mediators and Cytokines

The literature describing modulation of junctional proteins in the establishment and regulation of both tight and adherens junction complexes is vast. Such modulation is frequently reported to affect the functional properties of the lateral cell junctions by influencing their adhesiveness and thus their barrier function. A diverse range of physiological and pathological stimuli including pro-inflammatory mediators, metabolic inhibitors, cytokines and growth factors have been shown to affect specific junctional components or complexes by a range of mechanisms such as post-translational modification, changes in expression levels and redistribution. Understanding of the pathways leading to such modifications is limited and fragmentary

therefore only the most well characterised and most relevant to brain EC junctional integrity will be described in detail here. The use of in vitro cell cultures and recombinant proteins has allowed the systematic study of the effects of individual factors on various cell types. The extrapolation of these data to the in vivo situation requires caution however as there is also extensive evidence for the pleiotropic, synergistic, redundant and inhibitory nature of the factors present within the chemical milieu to which cells are exposed in situ. Given their importance in diverse processes, these effector networks are necessarily complex and the response of different target cells may also vary. As an ever-increasing number of factors are shown to exert an influence on junctional integrity the physiological relevance of these in vitro observations remain to be proven.

Protein phosphorylation on tyrosine residues is a hallmark event of intracellular signal transduction and is a common mechanism regulating the activity of many proteins. Tyrosine phosphorylation has been demonstrated to be of key importance in both the (re)establishment of tight junctions and in the regulation of their functions. Treatment of brain endothelial and epithelial cell monolayers with protein tyrosine phosphatase inhibitors leads to increased tyrosine phosphorylation of components of both tight and adherens junctions (as well as other proteins) and a decrease in TER suggesting a reduction in their adhesiveness (Staddon et al., 1995). Several studies have demonstrated the dependence of tight junction (re)establishment on the activity of tyrosine kinases (Adamson et al., 1998; Gomez, 1999) as their inhibition with genistein prevents the reformation of a high-resistance barrier (Tsukamoto and Nigam, 1999; Atkinson and Rao, 2001; Meyer et al., 2001).

Histamine is a potent pro-inflammatory mediator that increases the permeability of post-capillary venules following its release by degranulation of mast cells following either lysis or antigen-mediated crosslinking of their cell-surface-bound IgE receptors. Histamine treatment of HUVEC monolayers induces increased tyrosine phosphorylation of the adherens junction components VE-cadherin, β- and γ-catenin as well as the dephosphorylation of p120 on serine/threonine residues (Andriopoulou et al., 1999; Ratcliffe et al., 1999). VE-cadherin reportedly also increasingly partitions into a

detergent-soluble cell fraction; interpreted as a decrease in association with the actin cytoskeleton. VE-cadherin may also increase in its association with the intermediate filament protein vimentin (Shasby et al., 2002). Within epithelial-derived ECV304 cells, histamine treatment induces serine/threonine phosphorylation of occludin via a rho/rho kinase (ROCK)-independent pathway (Hirase et al., 2001). Histamine treatment in both these systems increased paracellular permeability to the flux of molecular tracers suggesting that such modulation of junctional proteins affects their adhesiveness and the integrity of junctions.

Lysophosphatidic acid (LPA) has also been shown to increase the permeability of endothelial and epithelial monolayers, induce the dephosphorylation of p120 in HUVEC and the phosphorylation of occludin on serine/threonine residues in ECV304 cells although conversely through a rho/ROCK-dependent pathway (Ratcliffe et al., 1999; Hirase et al., 2001). This demonstrates that different mediators can produce a similar effect and have a common molecular end-point yet act through distinctly different signalling pathways.

Thrombin is another potent pro-inflammatory mediator known to increase the permeability of endothelial monolayers (Konstantoulaki et al., 2003). Downstream effects on junctional proteins following thrombin treatment include increased tyrosine phosphorylation of VE-cadherin-associated β- and γ-catenin as well as alterations in the composition of VE-cadherin complexes (Ukropec et al., 2000). In a similar manner to histamine and LPA, thrombin has also been shown to induce a dephosphorylation of p120 (Ratcliffe et al., 1999) whilst also being reported separately to induce tyrosine phosphorylation of this protein (Ukropec et al., 2000). Other factors and mediators shown to modulate endothelial permeability include shear stress, bradykinin and arachidonic acid (Abbott, 2000).

Many cytokines have been demonstrated to cause a decrease in the barrier function of epithelial and/or endothelial cell monolayers including IL-1, IL-4, IL-13, Transforming growth factor (TGF)-α and insulin-like growth factors (IGF)-I and –II. The mechanisms by which they exert their effects, however, are poorly understood although in many cases modulation of either the actin cytoskeleton or tight junction proteins has been observed (Walsh et al., 2000).

IFNγ is a 20-25 kD glycoprotein produced by activated T cells and NK cells that exhibits pleiotropic immunoregulatory effects during immune responses as well as decreasing the TER of microvascular ECs in vitro (Blum et al., 1997, Oshima et al., 2001). This may be due to changes in F-actin organisation and disassociation of tight junctions as there is evidence of redistribution of ZO-1 in microvascular ECs and of JAM in HUVECs when combined with TNF-α (Ozaki et al., 1999). Similar effects on epithelial cells have been reported with a gradual decrease in TER and a decrease in the total cellular level of ZO-1 that was commensurate with a redistribution of occludin, ZO-1 and ZO-2 away from tight junctions (Youakim and Ahdieh, 1999; Tedelind et al., 2003). There are no reports of IFNγ-induced alterations in the phosphorylation state of any juctional proteins. TNF-α is a 17 kD protein predominantly expressed by cells of the mononuclear lineage that is known to decrease the barrier function of endothelial and epithelial monolayer junctions via a pathway that activates rho, rac and cdc42 (Wojciak-Stothard et al., 1998). The molecular mechanisms involved are again poorly understood although induction of actin stress fibres and intercellular gaps has been described in HUVECs (Wojciak-Stothard et al., 1998). When used either alone or in combination with IFNγ, TNF-α treatment also causes a redistribution of VE-cadherin (Wong et al., 1999). The response of epithelial cells to TNF-α appears to vary depending on the tissue from which the cells are derived although in general TER is reduced (Walsh et al., 2000).

Vascular endothelial growth factor (VEGF, also known as vascular permeability factor) is a 45 kD homodimeric glycoprotein that stimulates endothelial growth and differentiation in addition to increasing the permeability of blood vessels. Treatment of HUVEC with VEGF has been shown to induce tyrosine phosphorylation of VE-cadherin, β-catenin, γ-catenin, p120 and PECAM although this was not associated with any apparent redistribution (Esser et al., 1998). VEGF also influences tight junctions by decreasing the amount of occludin and ZO-1 at junctions and causing F-actin rearrangement (Wang et al., 2001). The breakdown of cell junctions caused by these

cytokines may facilitate the transendothelial passage of leucocytes into the peripheral tissues.

Examples of cytokines that increase the barrier function of cell monolayers are scarce but has been observed following treatment of endothelial and epithelial monolayers with TGF-β1, a 25 kD protein that is also capable of negating the permeability effect of IFNγ and IL-4 (Planchon et al., 1999). The vascular bed from which ECs are derived may influence their response to TGF-β1 as three-dimensional microvascular cells displayed increased localisation of ZO-1 at junctions (Merwin et al., 1990) whereas pulmonary macrovascular cells responded by disorganisation of adherens junctions and a decrease in TER (Hurst et al., 1999).

1.4.2 Modulation of Junctional Proteins by Cell-cell Interactions

The transendothelial migration of leucocytes via a paracellular pathway must involve modulation of the EC lateral junctions to physically allow the migrating cell passage through the monolayer. During either immune surveillance or a normal immune response this occurs rapidly and without apparent damage to the ECs (Edens and Parkos, 2000). During migration, there is close association between the membranes of the leucocyte and the EC and this may serve to 'plug' the paracellular pathway and help maintain the solute barrier function (Huang et al, 1988). It has been known for over a decade that adhesion of polymorphonuclear cells (PMNs) to HUVEC monolayers does not affect their barrier function when the number of migratory cells is low whereas with a high number of migratory cells the permeability of the monolayer increases suggesting a more profound 'loosening' of the junctions during acute inflammatory reactions (Huang et al., 1993). The junctional proteins that are the downstream targets of leucocyte adhesion-mediated signalling cascades remain to be identified although in the last few years the first descriptions of such modulation have been reported.

Initially it had been reported that adhesion of PMNs to endothelial monolayers caused a rapid disorganisation of VE-cadherin accompanied by a loss in association with β- and γ-catenin and an

increase in endothelial permeability (Del Maschio et al., 1996). These observations, and the demonstration that neutrophil membrane preparations were able to induce the degradation of EC junctional components during co-culture (Allport et al., 1997), led to the suggestion that the increased calcium signalling observed following PMN adhesion (Huang et al., 1988) may activate the protease calpain that is capable of degrading cadherin-catenin complexes thus facilitating leucocyte migration. Subsequent studies have, however, indicated that these observations may be artefactual due to the activity of a neutrophil-derived protease called elastase released during processing of samples (Moll et al., 1998). This is indicated by the prevention of VE-cadherin degradation during co-culture with activated PMNs by the presence of specific inhibitors of elatase (Carden et al., 1998, Ionescu et al., 2003). Although artefactual with respect to the publication this is a mechanism likely employed by PMNs (and perhaps other leucocytes) to aid their migration. Indeed, it has been demonstrated that elastase is present on the leading edge of PAF-activated PMNs and that pre-treatment of these cells with an anti-elastase monoclonal antibody significantly inhibited their migration (Cepinskas et al., 1999). Such elastase-mediated degradation is probably not the sole mechanism that alters junctional integrity during leucocyte interactions and modulation involving post-translational modification and redistribution of junctional proteins have recently also been reported (Allport et al., 2002; Hermandt et al., 2003). Immunohistochemical studies of brain tissue following induction of an IL-1β inflammatory response show increased phosphotyrosine labelling of leucocytes and ECs in areas of extensive recruitment as well as focal disorganisation of occludin, ZO-1 and vinculin (Bolton et al., 1998). The permeability of HUVEC monolayers and isolated coronary microvessels has been demonstrated to increase following co-culture with activated PMNs and this was negated by treatment with either tyrosine or serine kinase inhibitors (Tinsley et al., 1999). This study also found increased actin stress fibre formation and disorganisation of VE-cadherin and β-catenin, both of which also exhibited increased tyrosine phosphorylation. A subsequent investigation by this group identified the tyrosine kinase

Src as responsible for the modification of β-catenin (Tinsley et al., 2002).

Despite large advances in the understanding of the molecular interactions involved in regulating the different stages of leucocyte adhesion to endothelial and epithelial cells, the modulation of cell junctions associated with leucocyte migration is still poorly understood. It is generally accepted however that the permeability increases observed during co-culture experiments relate to signals affecting the endothelial junctional proteins. Due to the myriad of possible molecular interactions between the surfaces of leucocytes and endothelial cells, as well as their release of cytokines and other factors that may themselves influence junctional proteins, delineating individual signal-response pathways may prove slow and difficult but their central importance in regulating immune responses and disease progression fully justifies such efforts.

Aim of the Thesis:

The experiments described in this thesis have attempted to further characterise the role of occludin in regulating brain endothelial cell-cell junctions and to attempt to identify novel signalling cascades modulating cell junctions following ligation of the cell adhesion molecule ICAM-1. The hypothesis to be tested in this study is that mimicking the interaction of antigen-activated T cells with brain ECs by antibody-mediated crosslinking of ICAM-1 on the surface of the endothelium will lead to alteration in components of adherens and/or tight junctions. Both aims of the thesis are directed towards providing greater understanding of the process and regulation of lymphocyte migration across brain ECs.

Chapter 2:

Materials and Methods

2.1 Reagents

All reagents used throughout were purchased from Sigma-Aldrich Company Ltd. (Poole, Dorset, UK) with the exception of those below.

Cell Culture

Hanks' buffered salt solution (HBSS) with and without Ca^{2+} and Mg^{2+}, Hams' F-10 medium with glutamax, minimal essential medium α with glutamax (MEMα), Dulbeccos' minimal essential medium with glutamax (DMEM), RPMI-1640 medium with L-glutamine, essential amino acids, sodium pyruvate, human endothelial basal growth medium with L-glutamine (hereafter serum-free medium, SFM), penicillin-streptomycin, heat-inactivated European foetal calf serum (FCS), all tissue culture plasticware and cryovials were purchased from Gibco Life Technologies Ltd (Paisley, UK). Untreated, 0.4 μm pore size, polycarbonate Transwell™ filters of 6.5 mm and 10 mm diameter were obtained from Corning Costar Corporation (Corning, NY, USA).

Cell and Molecular Biology

PCR buffer, deoxynucleotide triphosphates (dNTPs), 25 mmol dm^{-3} $MgCl_2$, *Thermus aquaticus* (Taq) DNA polymerase and the restriction enzymes *Kpn I*, *Sal I*, *EcoR I*, *Xba I*, *Bam H I*, *Sac II* and *Apa I* with buffers were purchased from Promega (Southampton, UK). Qiagen Ltd (Crowley, UK) supplied the Qiagen Plasmid Maxi- and mini-prep kits and the primers used in polymerase chain reaction (PCR) were obtained from Genosys (Sigma-Aldrich, UK). Methanol and ethanol were purchased from BDH Laboratory Supplies (Poole, UK) and the sterile distilled water (dH_2O) used in molecular biology reactions was obtained from Braun (Melsungen, Germany). Lipofectamine™ 2000, 1 kB DNA Standards ladder and DNA ligase with buffer were obtained from Gibco Life Technologies Ltd. Bio-Rad Laboratories Ltd (Hemel Hempstead, Herts, UK) supplied molecular biology grade agarose and Bradford reagent. 30% weight per volume (w/v) acrylamide, 0.8% w/v bisacrylamide stock solution and 10x sodium dodecylsulphate polyacrylamide gel electrophoresis (SDS-PAGE) running buffer were

both purchased from National Diagnostics (Atlanta, Georgia, USA). Molecular weight rainbow markers, protein G-sepharose, enhanced chemiluminescence (ECL) hyperfilm™, One-Phor-All (OPA) digest buffer and calf intestinal alkaline phosphatase with buffer were purchased from Amersham Pharmacia Biotech International (Little Chalfont, UK). Protran® nitrocellulose membrane was obtained from Schleicher and Schuell (Dassel, Germany) and blotting paper was from Whatman International Ltd (Maidstone, UK). Skimmed milk powder and 150 kD fluorescein isothiocyanate (FITC)-dextran were from Fluka (Sigma-Aldrich, UK). Protein A/G peroxidase and the bovine serum albumin (BSA) used for Bradford assays were obtained from Pierce (Chester, UK). ECL lumi-light™ reagents were from Roche (Mannheim, Germany). Calcein-AM, Oregon green-phalloidin and the anti-mouse Zenon 546 immunolabelling kit were purchased from Molecular Probes (Eugene, OR, USA) and Vectashield™ mounting medium was purchased from Vecta Laboratories (Peterborough, UK). BD Biosciences (Oxford, UK) supplied 26G syringes. Mutant chicken occludin cDNA sequences in the vector plasmid pCB6 and empty pCB6 were generous gifts from Dr Karl Matter (Institute of Ophthalmology, UK) and the pbabe hygro plasmid was a generous gift from Dr Michael Cheetham (Institute of Ophthalmology, UK).

Cell Lines

The GPNT 24.6 cell line (Regina et al., 1999) is a re-immortalised subclone of the Lewis rat brain endothelial cell line GP8 (Greenwood et al., 1996) that was derived from a primary cell culture and immortalised by expression of transfected SV40 large T antigen. The RBE4 cell line (Roux et al., 1994) is also derived from a primary Lewis rat brain endothelial cell culture but was immortalised by expression of the E1A antigen from herpes simplex virus. The rat retinal endothelial cell line JG2 (Greenwood et al., 1996) is also derived from a primary culture that was immortalised by expression of the SV40 large T antigen.

The Madin-Darby canine kidney (MDCK), human adult retinal pigment epithelium 19 (ARPE-19) and monkey kidney COS7 cell lines

are extensively characterised, commercially available epithelial cell lines.

Myelin basic protein (MBP)-specific T cells were a generous gift from Dr. Evelyn Beraud (Faculty of Medicine, University de la Mediteranee, France).

Antibodies

Antibodies were supplied and used as follows:

Antigen	Host Species	Clone	Use & Dilution	Source
α-catenin	Mouse	Not Specified	I.P 2 μg	Transduction Laboratories (Lexington, KY, USA)
α-catenin	Rabbit	Polyclonal	I.B 1/4000	Sigma-Aldrich
β-catenin	Mouse	Clone 14	I.P. 2 μg I.B. 1/500 I.F 1/1000	Transduction Laboratories
γ-catenin	Mouse	Not Specified	I.B 1/1000	Transduction Laboratories
ICAM-1	Mouse	1A29	Crosslinking 10 μg/ml	Serotec (Oxford, UK)
Mouse IgG (GAM)	Goat	Polyclonal	Crosslinking 10 μg/ml	Sigma-Aldrich
Occludin	Rabbit	Polyclonal	I.B. 1/1000	Zymed (San Francisco, CA, USA)
Chicken Occludin intracellular N-terminus	Rabbit	Polyclonal '626'	I.B 1/1000 I.F 1/100	See Below
Chicken Occludin intracellular C-terminus	Rabbit	Polyclonal 'Chocolate'	I.B 1/4000 I.F 1/500	See Below

P100/120	Mouse	Not Specified	I.P I.B	2 μg 1/1000	Transduction Laboratories
PECAM	Mouse	4E8	I.P I.F	1.5 μg 1 μg	Purified from hybridoma supernatant
PECAM	Goat	Polyclonal	I.B	1/200	Santa Cruz (Santa Cruz, CA, USA)
Phospho-tyrosine	Mouse	4G10	I.B	1/1000	Upstate Biotechnology (Lake Placid, NY, USA)
Phospho-Tyrosine	Mouse	P-Tyr-100	I.F	1 μg	Cell Signalling Technology (Beverly, MA,USA)
VCAM	Mouse	5F10	Crosslinking	10 μg/ml	See Below
VE-cadherin	Goat	Polyclonal	I.P I.B	1 μg 1/400	Research Diagnostics
ZO-1	Rabbit	Polyclonal	I.P I.B I.F	2 μg 1/2000 1/100	Zymed
Mouse, Rabbit & Goat IgGs	Goat & Donkey	Polyclonal	FITC-conjugated secondary antibodies for I.F and FACS I.F FACS	 1/50 1/50	Jackson (West Grove, PA, USA)

Table 2.1 The specificity, source and use of antibodies used during this study

Abbreviations: I.P, immunoprecipitation; I.B, immunoblot; I.F immunofluoresence; FACS, fluoresence-activated cell sorting (flow cytometry) Antibodies raised against VCAM and the N- and C-termini of chicken occludin were generous gifts from Dr Roy Lobb (Biogen, USA) and Dr Maria Balda (Institute of Ophthalmology, UK) respectively.

2.2 Cell Culture

The immortalised Lewis rat brain EC line GPNT 24.6 was cultured in a 1:1 mix of αMEM:Hams F10 supplemented with 10% v/v FCS, 5 μg/ml puromycin, 100 U/ml penicillin and 100 μg/ml streptomycin on rat tail type I collagen-coated plastic at 37°C under 5% humidified CO_2. To collagen-coat plasticware, the surfaces were immersed in 5% collagen (dissolved in 0.5 mol dm^{-3} ethanoic acid)/HBSS solution for at least 1 hour at room temperature before the solution was removed and the collagen crosslinked by placing the plasticware in an ammonia vapour-filled box for 20 minutes. Following fixation the plasticware was washed extensively with HBSS to neutralise the pH. For permeability experiments using Transwell™ filters fibronectin was used as a substrate as collagen did not attach evenly to the filters and consequently cells did not form confluent monolayers. Filters were coated by adding HBSS to the apical and basolateral chambers with the apical chamber being supplemented with 7 μg/ml human fibronectin. The plates were then incubated at 37°C under 5% humidified CO_2 for 1 hour. The apical and basolateral chambers were then washed three times with HBSS and kept in HBSS until cells were plated. Upon reaching confluence during routine culture, cells were passaged into new tissue culture flasks. Cells were split by washing three times with HBSS without Ca^{2+} and Mg^{2+} to remove divalent cations thereby reducing adhesive interactions between cells, followed by the addition of 0.25% trypsin so as to just cover the monolayer and the flask was placed in the incubator for 5 minutes to disassociate the cells from each other and the substrate. Cells were then collected in medium, centrifuged to remove the trypsin and resuspended in medium before replating. The immortalised Lewis rat brain EC lines GP8 3.4 and RBE4 were maintained in the same manner with the substitution of 5 μg/ml puromycin with 150 μg/ml G418 (geneticin sulphate) in the culture medium.

Epithelial cell lines were maintained in DMEM supplemented with 10% v/v FCS, 100 U/ml penicillin and 100 μg/ml streptomycin on untreated plastic at 37°C under 5% humidified CO_2.

For long-term storage of cells, following trypsinisation and centrifugation, cells were resuspended in 5% v/v dimethyl sulphoxide

(DMSO)/FCS and aliquoted into polypropylene cryovials and these immediately placed in a –80°C freezer. Within 1 week cells were then transferred to liquid nitrogen storage.

2.3 Morphology of Cell Monolayers

Confluent monolayers were trypsinised from flasks and cells counted using a haemocytometer. Cells were then plated at 1 x 10^5 /cm^2 on collagen-coated 35 mm^2 Petri dishes. 24 hours after plating cells were washed with HBSS and placed in fresh medium. Subconfluent images of each clone were then captured using a digital camera (Hamamatsu, Japan) connected to an inverted phase contrast microscope (Zeiss). Following a further 72 hours of culture cells formed nascent monolayers and images were captured following washing and changing of medium as before. Each clone was then cultured for a further 72 hours, washed, fresh medium added and images of long-confluent monolayers captured.

2.4 Fluorescence Microscopy

To investigate distribution of proteins within the monolayer, cells were fixed and indirectly immunolabelled with specific antibodies (see Table 2.1) followed by fluorophore-conjugated secondary antibodies before being viewed with a confocal laser scanning microscope. To generate images, specimens were scanned with an epifluorescent Zeiss LSM 510 scan head fitted to a Zeiss Axioplan 2 upright microscope operating in multitrack mode to prevent bleed-through between DAPI (364 nm) and FITC (488 nm) channels. Software-controlled adjustments were made to optimise pinhole diameters to 1 Airy unit for each channel. These were then further adjusted to give a fixed section thickness of 0.9 μm at x40 with objectives used being oil immersion apochromats. The signal output was then adjusted using acousto-optical filters to eliminate saturation and set the black level of the 8-bit detectors (8 bit = 256 shades of gray between white (255) and black (0)). The stage was then moved whilst scanning the specimen to set the upper and lower levels of a Z-stack, and the 'optimise slice' function utilised to ensure that each slice overlapped

its successor by 50%. Finally, the Z-stack was recorded using 4-fold frame averaging to suppress noise. Galleries were saved to disc and 3-dimensional projections produced from sequential sections (typically representing approximately 3 μm in thickness) using the Zeiss 2.8 Image Browser freeware programme. For the fixation of specimens a variety of methods were used depending on the antigen.

Methanol Fixation:-

Cells were grown to confluence in 35 mm^2 Petri dishes and fixed by removing the culture medium and replacing it immediately with -20°C methanol and incubating at -20°C for 5 minutes. All subsequent incubations were at room temperature. The methanol was diluted out and the dishes rinsed three times with phosphate-buffered saline (PBS). The dishes were then blocked with 50 μg/ml goat serum/PBS for 30 minutes before incubation with the manufacturer's recommended concentration of primary antibodies diluted in 10 μg/ml goat serum/PBS for 90 minutes. Dishes were then rinsed thoroughly with PBS and incubated with fluorophore-conjugated anti-isotype specific pre-adsorbed secondary antibodies diluted in 10 μg/ml goat serum/PBS for 45 minutes in the dark. To remove particulates from the secondary antibody, slight excess was taken from the stock vial and centrifuged at top speed for 2 minutes. Nuclei of cells were visualised by addition into the secondary antibody incubation buffer of Hoescht stain (bis-benzamidine) that binds double-stranded DNA. Dishes were then rinsed extensively with PBS and mounted under Vectashield™ with glass coverslips (grade 0) and viewed using a Zeiss confocal microscope.

Methanal (formaldehyde/formalin) Fixation:-

Following removal of cell medium cells were fixed with freshly prepared 3.7% methanal (formaldehyde, formalin)/PBS for 20 minutes at room temperature. This was then rapidly replaced with PBS and washed twice more. Samples were then permeabilised by adding ice-cold propanone (acetone) to the dish containing a residual amount of PBS for 30 seconds. This was then rapidly diluted out with 0.1% w/v BSA/PBS. This solution was used to block the dishes for 30 minutes

and as a diluent for subsequent antibody incubations that were performed as described above.

Ethanol Fixation:-

To visualise occludin, cells were fixed after removing the medium with ice-cold absolute ethanol on ice for 30 minutes. Dishes were then rehydrated with PBS and permeabilised with propanone before immunolabelling as described above.

Staining Following Crosslinking:-

Primary antibodies were labelled prior to addition to samples using an anti-mouse Zenon 546 kit according to manufacturers' instructions in order to minimise cross-reactivity of labelling antibodies with those bound on the cell surface following crosslinking. Briefly, 1μg/sample of primary antibody was reacted with 10 μl reagent A (fluorophore-conjugated F(ab) fragments) for 10 minutes and then excess reagent A was neutralised by 10 minutes incubation with reagent B (non-specific IgG) prior to addition to samples and processing as described above.

2.5 Cell Lysis

Dishes of cells to be lysed were placed on ice and rapidly rinsed twice with ice-cold HBSS containing 1 mmol dm^{-3} sodium orthovanadate (Na_3VO_4). After washing, cells were immediately lysed for 10 minutes with agitation at 4°C in 500 μl ice-cold lysis buffer (10 mmol dm^{-3} N-[2-hydroxyethyl]piperazine-N'-[2-ethanesulphonic acid] (HEPES) pH 7.5, 100 mmol dm^{-3} NaCl, 2 mmol dm^{-3} $MgCl_2$, 5 mmol dm^{-3} ethylenediaminetetraacetic acid (EDTA), 1% v/v NP-40 and a mixture of protease and phosphatase inhibitors: 10 μg/ml aprotinin, 10 μg/ml leupeptin, 50 mmol dm^{-3} β-glycerophosphate, 1 mmol dm^{-3} NaF, 500 μmol dm^{-3} phenylmethylsulphonylfluoride (PMSF) and 1 mmol dm^{-3} Na_3VO_4). On ice, cells were then scraped off with a rubber cell scraper and nuclei removed by centrifugation at 13,000 r.p.m for 10 minutes at 4°C. Following centrifugation the supernatant was retained as the cell extract.

In experiments investigating the interactions of occludin some dishes were lysed by denaturing lysis. Denaturing lysis was achieved following addition of 500 μl of boiling lysis buffer (Tris-buffered saline (TBS) containing 1% w/v SDS and 1 mmol dm^{-3} Na_3VO_4). Lysates were then immediately scraped off and collected into a microfuge tube that was then heated for 10 minutes at 90°C. The extract was then passed through a 26G syringe 10 times to shear the DNA before centrifugation at 13,000 r.p.m for 10 minutes at 4°C and the supernatant retained as the cell extract. Before cell extracts prepared like this could be subject to immunoprecipitation they were adjusted to 1x RIPA buffer (TBS containing 1% v/v NP-40, 0.5% w/v deoxycholate, 1 mmol dm^{-3} EDTA and phosphatase and protease inhibitors as before: 10 μg/ml aprotinin, 10 μg/ml leupeptin, 50 mmol dm^{-3} β-glycerophosphate, 1 mmol dm^{-3} NaF, 500 μmol dm^{-3} phenylmethylsulphonylfluoride (PMSF) and 1 mmol dm^{-3} Na_3VO_4) by adding 100 μl cell extract to 900 μl of 1.1x RIPA buffer.

2.6 Protein Concentration Determination (Bradford Assay)

Protein concentration of cell extracts were determined by the method of Bradford (Bradford, 1976). Duplicate 5 μl aliquots were taken from each sample and each added to 995 μl of Bradford reagent. These were mixed thoroughly and 200 μl from each was transferred to a 96-well plate and read at 570 nm in a spectrophotometer. A range of concentrations (2.5-25 μg/ml) of BSA was used to generate a standard curve and linear regression analysis using Prism© software was used to interpolate sample concentration from plate readings. There was no cross-reaction of Bradford reagent with the lysis buffer used in preparation of samples.

2.7 Immunoprecipitation

Cell extracts were placed into fresh microfuge tubes and immunoprecipitation was performed with specific antibodies for 3 hours at 4°C with end-over-end rotation. Immune complexes were then harvested by further incubation with 25 μl /sample protein G-

sepharose slurry (that had been equilibriated in lysis buffer prior to addition) for 1 hour with rotation at 4°C. Immune complexes were pelleted and washed three times with lysis buffer. Proteins were then eluted into 5x Laemmli sample buffer (250 mmol dm^{-3} Tris/ HCL pH 6.8, 50% glycerol, 500 mmol dm^{-3} dithiothreitol (DTT), bromophenol blue), heated for 5 minutes at 90°C, vortexed and centrifuged before samples were loaded onto tris-glycine slab gels and fractionated by SDS-PAGE.

2.8 Sodium Dodecylsulphate Polyacrylamide Gel Electrophoresis (SDS-PAGE)

Tris-glycine slab gels were cast using the Biorad Mini-protean II™ system. All apparatus was thoroughly washed and rinsed before use. SDS-PAGE running buffer was 25 mmol dm^{-3} Tris, 192 mmol dm^{-3} glycine, 0.1% w/v SDS. To visualise the migration of proteins and give an indication of the molecular weight of proteins detected by immunoblot, 8 μl of rainbow standard molecular weight markers (220, 97.4, 66, 46, 30, 21.5 and 14.3 kD) were loaded onto each gel alongside samples. Gels were typically run at 100 V for approximately 2 hours.

2.9 Electrotransfer, Immunoblotting and Densitometry

A Biorad wet-transfer gel tank was used to electrotransfer proteins to nitrocellulose membranes by overnight wetblotting (35 V for ~16 hours at 4°C). The nitrocelluose membrane, gel electrotransfer pads and blotting paper were equilibriated in transfer buffer (SDS-PAGE running buffer supplemented with 20% v/v methanol) before being arranged into 'sandwiches' composed of (from cathode to anode) a pad, 2 pieces of blotting paper, gel, membrane, 2 pieces of blotting paper and another pad. As each layer was added, the stack was compressed to remove air bubbles. After transfer the positions of rainbow standard molecular weight markers were marked on the blot and then the membrane blocked by a 1 hour incubation in 5% w/v milk/0.1% v/v Tween/Tris-buffered saline (TBS) (TBSTM). Membranes

were then hybridised with primary antibodies, diluted at the manufacturers recommended concentration in TBSTM overnight at 4°C or 2 hours at room temperature. After extensive washing with 0.1% Tween/TBS (TBST), horse radish peroxidase (HRP)-conjugated Protein A/G was diluted 1 /10,000 in TBSTM and this incubated with the blot for 45 minutes at room temperature and the membrane was again extensively washed with TBST. To visualise immunoreactive bands the membrane was then immersed in ECL Lumi-light™ reagent for 2 minutes, wrapped in transparent film and exposed to light-sensitive film in a darkroom. To strip membranes of bound antibodies before reprobing the membrane was incubated in stripping buffer (200 mmol dm^{-3} glycine/HCL pH 2.1, 1% v/v NP-40, 500 mmol dm^{-3} NaCl) for 20 minutes at room temperature. Membranes were then washed three times with TBST before being blocked and immunoblotted as before.

Semi-quantitative densitometric ratios for bands in immunoblots were obtained by firstly expressing scanned intensity values as a percentage of the value of control (untreated) samples. Densitometric intensity was then calculated by expressing the value obtained in phosphotyrosine blots as a ratio of the value obtained in the control (protein loading) blot for the corresponding sample. Mean densitometric intensity values were then calculated by pooling densitometric intensites for equivalent time-points from different experiments and expressing as mean ± SEM.

2.10 Molecular Biology

2.10.1 Bacterial Transformation

A 50 μl aliquot of competent *E.Coli* DH5α bacteria was thawed and incubated with 0.5 μg of plasmid DNA for 30 minutes on ice. The bacteria were then heat shocked for 90 seconds at 42°C, cooled on ice for 1 minute and then 200 μl of Lennox broth (L broth) added and the culture incubated at 37°C with shaking for 1 hour. 100 μl of the culture was then taken and spread onto an agar plate (containing 100 μg/ml ampicillin) using a sterile spreader and incubated overnight at

37°C. The next day a single colony was picked and streaked onto a fresh agar plate and this incubated overnight at 37°C as before. A colony was then picked from this streak plate and used to inoculate 5 mls of fresh L broth to make a starter culture for a glycerol stock and for use in mini- and maxi-DNA preps. Glycerol stocks of transformed bacteria were made by mixing 500 µl of bacterial culture with 500 µl of sterile 30% glycerol in a microfuge tube and stored at -80°C.

2.10.2 Preparation of Plasmid DNA

Starter cultures of single clones transformed with each construct were diluted 1/1000 into 500 ml L broth containing 100 µg/ml ampicillin and incubated overnight at 37 °C with shaking. The plasmid DNA was then harvested and purified using a Qiagen Plasmid Maxi Prep kit according to manufacturer's instructions. The bacterial cells were pelleted by centrifugation at 6000 x g for 15 min at 4°C. The pellet was then resuspended in 10 mls Buffer P1 (50 mmol dm^{-3} Tris/HCl pH 8, 10 mmol dm^{-3} EDTA, 100 µg/ml RNAse A) and lysed with 10 mls of Buffer P2 (200 mmol dm^{-3} NaOH, 1% w/v SDS) for 5 min at room temperature. Genomic DNA, proteins, cell debris and SDS was precipitated by adding 10 mls of ice-cold Buffer P3 (3 mol dm^{-3} potassium acetate pH 5.5) and incubating on ice for 20 min. The solution was then centrifuged at 20,000 x g for 30 min at 4°C and then the supernatant re-centrifuged for a further 15 min at 20,000 x g at 4°C. A QIAGEN-tip 500 column was pre-equibrilated by allowing 10 mls Buffer QBT (50 mmol dm^{-3} 3-[N-morpholino] propanesulphonic acid (MOPS) pH 7.0, 750 mmol dm^{-3} NaCl, 15% v/v isopropanol, 0.15% v/v Triton X-100) to flow through under gravity. The bacterial supernatant was then added and allowed to flow through the column under gravity. The column was washed twice with 30 mls of Buffer QC (50 mmol dm^{-3} MOPS pH 7, 1 mol dm^{-3} NaCl, 15% v/v isopropanol) by gravity flow and then the DNA was eluted into clean polypropylene tubes with 15 mls Buffer QF (50 mmol dm^{-3} Tris/HCl pH 8.5, 1.25 mol dm^{-3} NaCl, 15% v/v isopropanol). The DNA was then precipitated with 0.7 volumes (10.5 mls) of isopropanol at room temperature and immediately centrifuged at 15,000 x g for 30 minutes at 4°C. The supernatant was then carefully discarded to leave the precipitated

DNA and this was then washed by adding 5 mls of 70% ethanol. The DNA was then centrifuged at 15,000 x g at 4°C for a further 10 minutes. The supernatant was then discarded and the pellet air-dried before being redissolved in 500 µl of TE buffer (10 mmol dm^{-3} Tris/HCl pH 8, 1 mmol dm^{-3} EDTA), and the DNA yield determined using a spectrophotometer with ultraviolet absorbance at 260 nm.

2.10.3 Restriction Digests

DNA from PCR and maxi preps was digested with restiction enzymes to allow cloning procedures and as analytical assessment of DNA constructs. 20 µl reaction volumes were used for restriction enzyme digests. All digests were performed in 1x OPA buffer (100 mmol dm^{-3} Tris-Acetate pH 7.5, 500 mmol dm^{-3} potassium acetate, 100 mmol dm^{-3} magnesium acetate) except those involving *Bam H I* and *Sal I* for which OPA was used at 2x and digests using *EcoR I* were performed in buffer 'H' (50 mmol dm^{-3} Tris/HCL pH 7.5, 100 mmol dm^{-3} NaCl, 10 mmol dm^{-3} $MgCl_2$, 1 mmol dm^{-3} DTT). Digests were incubated at 37°C except those of *Apa I* for which 25°C was used. Typically in each digest 1-10 µg of DNA was digested with 10 U of each restriction enzyme and the volume was made up with dH_2O. Digests were incubated for 4 hours at the required temperature with the restriction enzyme being added in two aliquots, one at the start and another after 2 hours incubation.

2.10.4 Dephosphorylation of Digested DNA

Immediately following digestion plasmid DNA was dephosphorylated at the 3' and 5' ends to prevent plasmid recombination without inclusion of a DNA insert during ligation reactions. Digested plasmid DNA was adjusted with the supplied buffer (500 mmol dm^{-3} Tris/HCL pH 9, 10 mmol dm^{-3} $MgCl_2$) in a 100 µl reaction volume and incubated with 50 units of calf intestinal alkaline phosphatase for 1 hour at 37°C.

2.10.5 DNA Ligation

To ligate the digested DNA insert encoding the N-terminal truncated occludin sequence (approximate size 1.5 kb) into the digested and dephosphorylated pbabe hygro plasmid (approximate size 5 kb) 0.2 μg of plasmid DNA was added to 0.6 μg of insert DNA. The incubation buffer was adjusted with the supplied buffer (50 mmol dm^{-3} Tris/HCL pH 7.6, 10 mmol dm^{-3} $MgCl_2$, 1mmol dm^{-3} ATP, 1 mmol dm^{-3} DTT, 5% w/v polyethylene glycol-8000) and to this 5 units of T4 DNA ligase was added and the reaction volume made up to 20 μl with dH_2O. The reaction was incubated overnight at room temperature. Aliquots of reaction products were then digested and fractionated on agarose gels to check DNA recombination prior to transformation into competent *E.Coli*.

2.10.6 Purification of Plasmid DNA

Following digestion or dephosphorylation, DNA was purified by removal of proteins using phenol:chloroform extraction and resuspension in dH_2O. The volume of DNA solution was increased to 200 μl with TE buffer and 1 volume (200 μl) of chloroform/phenol added. The solution was vortexed briefly, centrifuged for 10 minutes at 10,000 r.p.m and the uppermost aqueous layer retained. Phenol was then precipitated by addition of 1 volume chloroform/isoamyl alcohol. The solution was vortexed and centrifuged as before and the uppermost aqueous layer retained. DNA was then precipitated by the addition of 2 volumes of absolute ethanol and 0.1 volume 3 mol dm^{-3} sodium acetate (pH 5.2), this was then vortexed and left at -20°C overnight. The precipitated DNA was pelleted by centrifugation for 20 minutes at 10,000 r.p.m at room temperature. The supernatant was then aspirated, 1 ml of 70% ethanol was added and the pellet resuspended before being pelleted by centrifugation again for 20 minutes at 10,000 r.p.m. The supernatant was removed and the pellet left to air-dry prior to the DNA being dissolved in sterile dH_2O.

2.10.7 Agarose Gels

To visualise DNA that had been prepared and to ensure reactions were successful, DNA was fractionated on agarose gels by

electrophoresis. These were prepared by dissolving 1% w/v agarose in TAE buffer (40 mmol dm^{-3} Tris acetate pH 8, 1 mmol dm^{-3} EDTA) by heating in a microwave on full power for approximately 1 minute. Once the agarose was fully dissolved the solution was allowed to cool slightly and 0.2 μg/ml ethidium bromide was added and gently mixed. Gels were cast using a BioRad Sub-Cell® GT tank that was then filled with TAE buffer once the gel had set. DNA samples including a DNA standards ladder were diluted with dH_2O and Ficoll orange loading buffer added as a loading dye to give a loading volume of 20 μl/sample. Gels were run for approximately 1 hour at 50 V. DNA bands were then visualised by placing the gel on an ultraviolet transilluminator.

2.10.8 Production of Competent Prokaryotic Cells

To produce a starter culture in the stationary phase of the growth cycle, 10 mls of L broth was inoculated with E. Coli DH5α cells and cultured overnight at 37°C with shaking. The starter culture was then diluted 1/100 into fresh L broth and shaken at 37°C until the optical density at 550 nm was between 0.45-0.55 indicating that the culture was in the log phase of proliferation. The culture was placed on ice for 10 minutes before centrifugation at 1700 x g for 10 minutes at 4°C to pellet the cells. The supernatant was then removed and the pellet resuspended in 20 mls of cold, filter sterilised buffer 1 (30 mmol dm^{-3} potassium acetate, 100 mmol dm^{-3} RbCl, 10 mmol dm^{-3} $CaCl_2$, 50 mmol dm^{-3} $MnCl_2.4H_2O$, 15% v/v glycerol) and placed on ice for 5 minutes. The cells were then pelleted by centrifugation as before except with the centrifuge brake switched off to prevent disruption of competent bacterial cells. The supernatant was then removed, the pellet resuspended in 2 mls of cold, filter sterilised buffer 2 (10 mmol dm^{-3} MOPS, 75 mmol dm^{-3} $CaCl_2$, 10 mmol dm^{-3} RbCl, 15% v/v glycerol) and incubated on ice for 10 minutes before aliquoting into pre-chilled microfuge tubes and storage at -80°C.

2.11 Construction of Occludin Mutants

Plasmid (pCB6) DNA containing chicken occludin cDNA sequences for co-transfection and 'empty' pCB6 and pbabe hygro plasmid DNA was recovered from lysates of transformed bacterial clones by maxi-DNA preps. To produce cDNA encoding chicken occludin with a truncated N-terminus, polymerase chain reaction (PCR) using wild type chicken occludin cDNA as a template was used to delete this domain and amplify the truncated sequence. To amplify the wild-type sequence, a sense primer complementary to the pCB6 plasmid upstream of the start of the occludin sequence and an antisense primer complementary to the pCB6 sequence downstream of the occludin sequence were used in PCR reactions. To allow cloning into the expression vector pbabe hygro *EcoR I* restriction sites were added to both primers and a *Sal I* site added only to the antisense primer (upstream of the *EcoR I* site). The oligonucleotide sequences were: sense primer 5'-AGAATGAATTCAGATCTGGTA-3'; antisense primer 5'-CTCGATGAATTCGTCGACGGCAACTTCCAAGGCCAG-3'. PCR was performed in 25 μl reaction volumes using a Genius thermal cycler (Techne, Cambridge, UK). Reactions were performed in PCR buffer (10 mmol dm^{-3} Tris/HCl pH 9, 50 mmol dm^{-3} KCl, 0.1% v/v Triton X-100, 1.5 mmol dm^{-3} $MgCl_2$) with 1 μg DNA, 100 pmol of each primer (primers reconstituted at 100 μmol dm^{-3} in sterile TE buffer), 10 mmol of each dNTP (in a total volume of 1 μl), 1 U Taq polymerase and then made up to 25 μl with dH_2O. The conditions of the PCR cycle were: denaturation 94°C/ 30 s; annealing 55°C/ 30 s and extension 72°C/ 3 minutes for 35 cycles with a final extension of 5 minutes and then held at 4°C. The PCR product from this reaction was then cleaned and purified and used in another PCR reaction using the same antisense primer with a different sense primer to truncate the N-terminus. This sense primer substituted $Ala^{55}\rightarrow$ Start/Met^{1} and left a predicted intracellular N-teminus of only 7 amino acids. An *EcoR I* restriction site was added to the primer immediately upstream of the new start codon. The oligonucleotide sequence of this sense primer was 5'-ATAGAATTCATGGTGCGGGGGCTGCAGGCG-3'. The conditions of the PCR cycle were: denaturation 94°C/ 30 s; annealing 58°C/ 30 s and extension 72°C/ 3 minutes for 35 cycles with a final

extension of 5 minutes and then held at 4°C. Following amplification the truncated occludin fragment was purified, sequentially digested with *Sal* I and *EcoR* I, repurified and ligated into the expression vector pbabe hygro that had also been digested with *EcoR I* and *Sal I*, dephosphorylated and purified. The truncated occludin PCR product migrated as a band approximately 150 base-pairs smaller than the wild-type sequence. This would be consistent with the removal of a sequence encoding the initial 54 amino acids of the protein. Competent DH5α bacterial cells were then transformed with the DNA ligation reaction product, spread onto agar-ampicillin plates and cultured overnight at 37°C. Colonies were then picked and restreaked onto fresh plates. Colonies from these plates were then used to make starter cultures for DNA mini-preps to produce enough DNA to check by restriction digest whether the truncated sequence had been incorporated into the plasmid.

2.12 Transfection of Brain Endothelial Cells

24 hours prior to transfection confluent monolayers of GPNT cells were split and replated at approximately 75% confluence in six wells of a six-well plate per construct to be transfected. On the day of transfection, cells were rinsed with HBSS and 2 mls of fresh medium (including antibiotics) was added to each well as recommended by the manufacturer as the ideal plating volume. DNA for co-transfection (co-transfection was used as the GPNT cells already possess resistance against puromycin that is conferred by the pCB6 plasmid) was diluted in opti-MEM® with a 1:10 ratio of pbabe hygro: PCB6-occludin construct. For each well 5 μg of DNA (0.5 μg pbabe hygro, 4.5 μg PCB6-occludin) was diluted into 250 μl opti-MEM as recommended and 10 μl of Lipofectamine™ 2000 (L2000) was diluted into 250 μl of opti-MEM per well and this incubated at room temperature for 5 minutes. The DNA and L2000 solutions were then mixed and DNA-lipid complexes allowed to form for 20 minutes at room temperature. Both DNA and L2000 were prepared as bulk solutions so for each six-well plate (one plate for each construct) there was 3 mls of DNA-L2000 mixture, 500 μl per well containing 5 μg of DNA complexed with L2000 at a ratio of 1 μg/2 μl w/v. 500 μl was added direct to the

culture medium and dispersed over the cells by gently rocking the plate. The plates were then placed in the incubator for 16 hours. Each well was then washed three times with HBSS and incubated in fresh medium without selective antibiotics for a further 24 hours. Each well was then trypsinised and passed into a separate 10 cm dish and cultured in the presence of 100 μg/ml hygromycin B (this concentration having previously been determined as causing 100% wild-type cell death after 7 days of culture). Colonies of antibiotic-resistant cells were of sufficient size to isolate 4 weeks following transfection. The colonies were isolated and passed into wells of a 24-well plate using cloning rings and cultured until confluent. Each well (representing a single clone) was then expanded and assayed for expression by immunoblot of cell lysates. Clones positive for transgene expression were then expanded and further characterised.

2.13 COS Cell Transfection

24 hours prior to transfection confluent COS7 cells were split and plated in 35 mm dishes at approximately 75% confluence. Before transfection, 100 mmol dm^{-3} chloroquine phosphate was diluted 1/1000 in 2% v/v FCS/DMEM (solution A). Half of solution A was then taken and 100 mg/ml diethylaminoethyl (DEAE)-dextran was diluted at 1/125 (solution B). 1 μg of DNA was then dissolved in 375 μl of solution A and this mixed with 375 μl of solution B. A control transfection with no DNA was performed in parallel. The cells were then rinsed with HBSS and the mixture added to the cells and placed in the incubator for 4 hours. Subsequently, the solution was removed and the cells washed three times with HBSS, fresh medium added and the cells cultured for 72 hours. The cells were then fixed and assayed for expression of occludin protein by direct immunofluorescence.

2.14 Permeability Assay

Brain endothelial cell permeability assays were performed as previously described by Andriopoulou (Andriopolou et al., 1999). Cells were plated at 1 x $10^5/cm^2$ on fibronectin-coated Transwell filters (6.5 mm diameter, 0.4 μm pore size) and cultured until confluent. If the cells were cultured in selective antibiotic this was now removed by

rinsing with HBSS and replacing with fresh medium without selection and cultured for a further 24 hours before being used in experiments. The volumes of medium in the apical and basal chamber were 100 μl and 600 μl respectively. The start of the experiment (time=0) was taken as the point when the medium in the apical chamber was changed to serum free medium (SFM) containing 1 mg/ml FITC-dextran and placed back in the incubator. At pre-determined time points 50 μl samples were removed from the basal chamber and diluted into separate microfuge tubes containing 950 μl sterile PBS. 50 μl of SFM was immediately added to the basal chamber following removal of samples to maintain hydrostatic pressure during the experiment. The fluorescence of samples was then measured using black 96-well plates and a fluorimeter set with excitation and emission at 494 nm and 517 nm respectively. In crosslinking experiments monolayers were cultured, quiesced and crosslinked as described in Chapter 4 with 1 mg/ml FITC-dextran being included with the secondary crosslinking goat anti-mouse (GAM) antibody and this was taken as time=0.

2.15 T Cell Transendothelial Migration Assay

Brain ECs were plated at 1 x 10^5/well in flat-bottomed 96 well plates and cultured until confluent. When using clones grown in selective antibiotic, on the day of reaching confluence the monolayers were washed with HBSS and fresh medium without selective antibiotic was added for a further 24 hours prior to the experiment.

MBP-specific T cells were cultured for 1-2 days prior to use in RPMI-1640 medium containing 2 mmol dm^{-3} L-glutamine supplemented with 10% v/v FCS, 100 U/ml penicillin, 100 μg/ml streptomycin, 1 mmol dm^{-3} sodium pyruvate and 25 μmol dm^{-3} 2-mercaptoethanol at 37°C under 5% CO_2. T cell culture medium was also supplemented with 10% v/v conditioned medium from a Swiss 3T3 fibroblast cell line expressing recombinant mouse IL-2 (a kind gift from Dr. H Karasuyama and Dr. F Melchers, Basel Institute for Immunology, Switzerland; Karasuyama and Melchers, 1988). The conditioned medium was evaluated for the presence of IL-2 by

bioassay (not described) and filtered through a 0.2 μm filter prior to use.

MBP-specific T cells were added to confluent endothelial monolayers in 96 well plates at a density of 2 x 10^4/well and then incubated for 4 hours, a time during which migration is linear as previously determined (Pryce et al, 1997), at 37°C under 5% CO_2. A field (200 x 200 μm) from each well was then randomly chosen and recorded for 3 minutes using a digital camera (Hamamatsu, Japan) connected to an inverted phase contrast microscope (Zeiss) with a temperature and atmosphere-controlled chamber connected to the stage. The addition of T cells was staggered to keep the time of incubation constant. The video was then played back at 160x normal speed to allow visualisation and counting of migrated and non-migrated T cells. Migrated and non-migrated T cells were differentiated respectively by their distinctive phase-dark and phase-bright appearance. A minimum of 6 wells were recorded for each cell line in each experiment.

2.16 Peripheral Lymph Node Cell Adhesion Assay

Brain ECs were plated at 1 x 10^5/well in flat-bottomed 96 well plates and cultured until confluent. When using clones grown in selective antibiotic, on the day of reaching confluence the monolayers were washed with HBSS and fresh medium without selective antibiotic was added for a further 24 hours prior to the experiment.

Peripheral lymph node cells (PLNC) were obtained from cervical and mesenteric peripheral lymph nodes of Lewis rats 2-4 days prior to the adhesion assay. Rats were euthanised by terminal anaesthesia using CO_2, lymph nodes were removed and placed into RPMI-1640 medium containing L-glutamine, 10% v/v FCS, 100 U/ml penicillin and 100 μg/ml streptomycin on ice. The suspension was then passed through a sterile metal sieve and the barrel of a syringe used to disrupt the lymph node capsules. The wash through was collected and the residual tissue was flushed with medium 3 times with the flow through being collected each time. PLNC were washed three times with medium and the final pellet was resuspended in 10 mls of medium. The PLNC were then counted using a haemocytometer and

suspended at a final concentration of 1 x 10^6 cells/ml and left at 37°C under 5% CO_2. PLNC were mitogen-activated by the addition of 5 μg/ml conconavalin A for at least 24 hours prior to being used in experiments.

A sufficient number of PLNC were removed from the culture flask (1 x 10^5/well X 1.5) and resuspended at 5 x 10^6/ml in fresh medium containing 1 μmol dm^{-3} calcein-AM and incubated at 37°C for 30 minutes. The PLNC were then resuspended at 1 x 10^6/ml and the number of labelled cells counted using an epifluorescent microscope. The cell suspension was then adjusted to 1 x 10^6 labelled PLNC/ml. Immediately following labelling of PLNC the medium from the 96-well plates was removed and 1 x 10^5 PLNC (100 μl of cell suspension) added to each well and then placed back in the incubator for 90 minutes. In addition to the endothelial monolayers PLNC were added to empty wells on a separate plate to measure the total amount of fluorescence added to each well and fresh PLNC medium was added to another set of empty wells to give a measure of background fluorescence. After 90 minutes the lymphocytes were removed (except from the totals plate) by gently shaking the plates and non-adherent PLNC removed by washing the wells 4 times from different poles of the well with warm HBSS. Each well was then left in 100 μl of fresh PLNC medium and the plates centrifuged for 5 minutes at 200 x g at room temperature. The fluorescence in the wells was then measured by a fluorimeter set with excitation and emission at 494 nm and 517 nm respectively with the same gain value used for each of the different plates. To get the percentage of PLNC adhesion, measurements were expressed as a fraction of the fluorescence of the totals plate from which the measurement of background fluorescence was deducted. PLNC adhesion was typically around 15%. A minimum of 12 wells for each cell line was used in each experiment.

2.17 Transendothelial Electrical Resistance

Brain ECs were plated at 1 x $10^5/cm^2$ on fibronectin-coated Transwell filters (10 mm diameter, 0.4 μm pore size) and cultured until confluent. If the cells were cultured in selective antibiotic this was

now removed by rinsing with HBSS and replacing with fresh medium without selection and cultured for a further 24 hours. TER was then determined as described previously by Balda (Balda et al., 1993). Briefly, an AC square wave current of ± 20 μA at 12.5 Hz was applied to the cell culture medium with a silver electrode and any voltage change measured using a silver/silver chloride electrode connected to an EVOM. The electrical resistance of fibronectin-coated filters in medium without cells was also tested to measure background resistance. Subsequently, the tissue culture medium was replaced and monolayers cultured for a further 24 hours before another set of TER measurements taken. Each cell line was tested on triplicate filters.

2.18 Cell Adhesion Molecule Crosslinking

Brain ECs were cultured on collagen-coated plastic until confluent. On the day of attaining confluence, cells were quiesced by changing the medium for 24 hours (without washing of monolayers) to serum-free medium (SFM) supplemented with antibiotics (100 U/ml penicillin and 100 μg/ml streptomycin) and 100 U/ml interferon-γ to upregulate expression of cell adhesion molecules. To crosslink ICAM-1, dishes were rinsed with warm HBSS before incubation with 10 μg/ml monoclonal mouse anti-rat ICAM-1 (clone 1A29, with SFM as diluent) for 30 minutes in the incubator. Following this monolayers were rapidly rinsed twice with warm HBSS to remove excess primary antibody and were incubated with 10 μg/ml goat anti-mouse IgG (GAM, with SFM as diluent) for varying times. To crosslink VCAM the monolayers were incubated with monoclonal mouse anti-rat VCAM antibody 5F10 instead of 1A29 and then treated with GAM as with ICAM crosslinking.

2.19 Pervanadate Preparation and Treatment

Brain ECs were treated with pervanadate, a cell-permeant inhibitor of protein tyrosine phosphatases, as a positive control in experiments investigating tyrosine phosphorylation. Pervanadate at 100 μmol dm^{-3} was prepared by incubating equal volumes of 100 mmol dm^{-3} Na_3VO_4

(pH 10) and fresh 30% v/v H_2O_2 solution for 15 minutes at room temperature before being diluted 1/500 in HBSS. This was used immediately to replace the cell culture medium and the dish placed in the incubator for 15 minutes before rinsing and preparation of cell extract as described in section 2.5.

2.20 Detergent Solubility of Junctional Proteins

Triton solubility of junctional proteins was determined as previously described by Esser et al. (1998). Following ICAM-1 crosslinking, cells were rinsed twice with ice-cold HBSS and solubilised with ice-cold 0.5% v/v Triton X-100/TBS for 3 minutes at 4°C. This buffer was collected from the dish, centrifuged at 4°C for 10 minutes at 13,000 r.p.m and defined as the Triton-soluble fraction. The dishes were then washed twice with TBS containing protease and phosphatase inhibitors (identical to those used in lysis buffer described above in Cell Lysis) and then further extracted with this buffer supplemented with 0.5% w/v SDS and 1% v/v NP-40 for 20 minutes at 4°C. Dishes were then scraped and the extract passed through a 26G syringe ten times before centrifugation and the supernatant defined as the triton-insoluble fraction. Proteins from equal volumes of each fraction were then fractionated by SDS-PAGE, transferred to nitrocellulose and proteins detected by immunoblotting.

2.21 Extraction of Proteins From Insoluble Pellets

Cells were grown to confluence and quiesced, ICAM-1 crosslinked and cells lysed as described in section 2.20. Following centrifugation and removal of the supernatant as the normal cell extract, 500 µl of fresh lysis buffer containing 600 mmol dm^{-3} NaCl was added, vigourously pipetted and incubated on ice for 30 minutes. Samples were then centrifuged as before and the supernatant removed and kept before 500 µl of fresh lysis buffer containing 1.2 mol dm^{-3} NaCl was added to each sample, followed by further vigourous pipetting and incubation on ice for 30 minutes. Samples were then centrifuged and the supernatant removed and kept. The protein concentration of each sample was then determined by Bradford assay to ensure that samples from the same stage of extraction were at the same

concentration and equal volumes loaded onto slab gels and fractionated by SDS-PAGE before transfer to nitrocellulose and immunoblotting.

Chapter 3:

Occludin Regulates T Cell Transendothelial Migration and Junctional Integrity of Brain Endothelial Cells

3.1 Introduction

Occludin is a 65 kD protein first isolated from chick (Furuse et al., 1993) and later from mammalian cells (Ando-Akatsuka et al., 1996) and was the first transmembrane tight junction protein identified. The molecular weight of intracellular occludin shows some degree of variation due predominantly to differential serine and, to a lesser extent, threonine phosphorylation. Using phospho-occludin-specific antibodies this differential phosphorylation of occludin has been shown to be related to its localisation within the cell (Sakakibara et al., 1997; Farshori and Kachar, 1999). Thus, within epithelial cells, poorly or non-phosphorylated occludin is predominantly distributed at the basolateral membrane and within the cytoplasm whereas with increasing phosphorylation, occludin localises to apical tight junctions and becomes increasingly detergent-insoluble. In addition, tyrosine phosphorylation of occludin via a genistein-sensitive pathway has been shown to play a role in the (re)formation of tight junctions and the barrier function in MDCK and Caco-2 cells (Tsukamoto and Nigam, 1999; Atkinson and Rao, 2001; Meyer et al., 2001). The serine/threonine phosphorylation status of occludin has also been reported to be affected by different inflammatory signalling cascades initiated by VEGF (Antonetti et al., 1999, Wang et al., 2001), histamine and LPA (Hirase et al., 2001). Taken together, these data demonstrate that the phosphorylation state of occludin alters both its cellular localisation and the functional properties of cell-cell tight junctions.

The structure of occludin is similar to that of connexins and claudins with four transmembrane domains, a short intracellular N-terminus, a large intracellular C-terminus, an intracellular turn and two extracellular loops. Schematic representations of wild-type and experimental mutants of occludin are shown in Fig. 3.1. The C-terminal domain of occludin binds to the PDZ domain of the cytoplasmic scaffold protein ZO-1 by way of its terminal YV amino acid motif (Furuse et al., 1994; Fanning et al., 1998). The C-terminus has also been shown to bind several other proteins in vitro including ZO-2 (Itoh et al., 1999), PKC-ζ, the regulatory subunit of phosphatidylinositol-3-kinase (PI3K), c-Yes and connexin 26 that

suggests a potential interaction, at least within epithelial cells, of tight and gap junctions (Nusrat et al., 2000a). Although the C-terminus appears to be primarily responsible for interactions with other intracellular proteins, the N-terminus has been shown to interact with the E3 ubiquitin-protein ligase Itch (Traweger et al., 2002). Via these interactions occludin not only functions as a structural molecule but is also capable of recruiting and acting as a scaffold for signalling molecules. Until recently, only a single form of occludin had been described but this has changed with the identification in MDCK cells of a cDNA splice variant from the single occludin gene that encodes an occludin with an altered, larger N-terminal domain (Muresan et al., 2000). In this splice variant, the first 17 amino acids of occludin are replaced by a 56 amino acid sequence with the remaining amino acid sequence being otherwise identical. This isoform has been designated occludin 1B and, as with occludin, localises to tight junctions but is expressed at a much lower level. In addition, the expression of three other occludin variants, termed occludin II, III and IV, and the existence of an alternative 1st coding exon within the occludin gene has been reported in the human colon epithelial cell line HT-29/B6 (Mankertz et al., 2002). Occludin II and III both lack the fourth transmembrane domain and, although localising at cell borders, do not co-localise with ZO-1 and so are presumably not incorporated into tight junctions. The C-terminal domain of these variants is not intracellular but extends into the extracellular space. Occludin IV has a short deletion (18 amino acids) in the membrane proximal region of the C-terminal domain and appears to have an identical distribution to occludin. The expression of variably spliced occludin cDNA from the single occludin gene leads to a variation in protein expression that may influence the biological properties and thus function of occludin within the cell, although how these molecules differ functionally (if at all) is not currently known. Occludin molecules associate homotypically in trans configuration across the paracellular cleft whereas cis interactions, either homotypic or with claudin proteins, have not been described. Although transfection of occludin into occludin-null fibroblasts increased cell-cell adhesion (Van Itallie and Anderson, 1997) and produced tight junction strands, as observed by electron microscopy, these strands were neither continuous nor

branching as with those resulting from claudin-1 transfection (Furuse et al., 1998b). This implies that occludin is not the principle transmembrane molecule involved in tight junction formation or that it requires association with other tight junction proteins to correctly localise and function. Further evidence that occludin is not essential for the formation of tight junction strands can be seen by targeted disruption of occludin expression in knockout mice. Such disruption is not lethal and mice exhibit a normal phenotype at birth but during post-partum development exhibit retarded growth and display abnormal reproductive behaviour. Knockout males do not reproduce with wild-type females whereas knockout females produce offspring with wild-type males but are unable to suckle them. Knockout adult mice also exhibit a diverse range of histopathologies including gastric hyperplasia, calcification of the brain and abnormalities of the salivary glands, testes and bones demonstrating the range of functions that tight junctions regulate in vivo (Saitou et al., 2000).

The level of expression of occludin also increases differentially during development as occludin has been shown to become more highly transcriptionally regulated and expressed in brain ECs compared to those from peripheral tissues (Hirase et al., 1997). It is tempting given this data and observations of alteration in occludin expression affecting junctional permeability (Wachtel et al., 1999; Simonovic et al., 2000; DeMaio et al., 2001; Huber et al., 2001; Antonetti et al., 2002) to speculate that occludin has a significant role in the generation of high-resistance junctions that contribute to the maintainance of the BBB. It increasingly appears that the N-terminus, C-terminus and two extracellular loop domains of occludin have distinct roles at the cell-cell junction and their mutation selectively modulates different junctional characteristics such as paracellular permeability, electrical resistance, leucocyte transmigration and tight junction organisation (Balda et al., 1996; Chen et al., 1997; Matter and Balda, 1998; Lacaz-Vieira et al., 1999; Bamforth et al., 1999; Mitic et al., 1999; Huber et al., 2000; Balda et al., 2000; Vietor et al., 2001). In several studies, Balda and colleagues demonstrated that expression of mutant forms of occludin in epithelial cells (MDCK) affects various functional properties of the epithelial cell sheet (Balda et al., 1996; Balda et al., 2000a; Huber et al., 2000). Expression of

ectopic wild-type chick occludin doubled the TER of the monolayer and at high levels of expression also, somewhat counterintuitively, also increased the paracellular permeability of the monolayer to molecular tracers. The ability of the epithelial monolayer to support neutrophil transmigration was unaffected. The expression of a modified occludin with a haemagglutinin epitope at the beginning of the N-terminal domain (termed HAocc) led to the same effects on TER and permeability but additionally led to a 4-fold increase in the amount of neutrophil migration across monolayers suggesting a role for the N-terminus in regulating this process. The further deletion of the C-terminus (a construct termed HAoccCT3) led to barrier properties similar to that of cells expressing HAocc although they were slightly more permeable to the flux of molecular tracers. This suggests that the C-terminus may have a role in regulating the permeability of the lateral cell junctions to the diffusion of molecules through a paracellular pathway rather than the regulation of neutrophil migration. In contrast to these constructs, the expression of an occludin mutant with a 13 amino acid deletion within the first extracellular loop domain (termed OccL1D) caused a decrease in both the paracellular permeability and amount of neutrophil migration across monolayers but did not raise the TER of the monolayer. The 13 amino acid deletion removed the central part of the first loop domain that contains a striking sequence of alternating glycine and tyrosine residues that possibly regulates the homo/heterotypic association of occludin molecules across the paracellular cleft. Using the same genetic constructs, we thus investigated whether the specific domains of occludin also influence transendothelial lymphocyte migration and other barrier properties of brain EC lines in a similar manner to those of epithelial cells. Schematic representations of the four occludin constructs expressed are shown in Fig. 3.1 and nucleotide and amino acid sequences of the four constructs and another construct encoding an N-terminal-truncated occludin (termed ΔNocc) are described in Appendix.

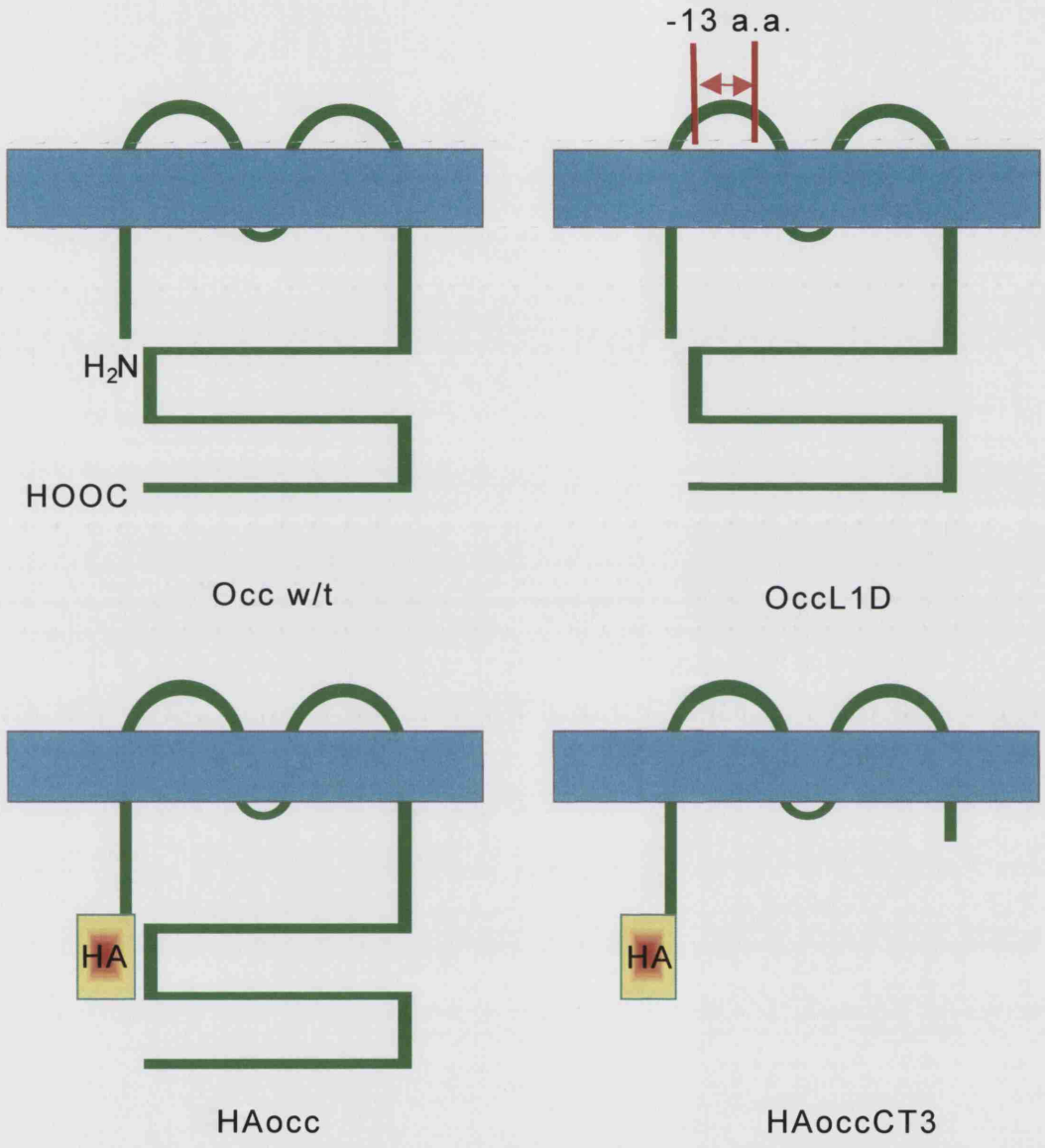

Fig. 3.1 Schematic representation of wild-type and mutant occludin proteins
Predicted topology of wild-type and mutant occludin proteins expressed in rat brain endothelial cells. Deleted amino acids within the first extracellular loop are indicated by a bar. Abbreviations: a.a, amino acids; HA, haemagglutinin epitope

3.2 Results

3.2.1 Endogenous occludin expression in epithelial and endothelial cell lines

The endogenous level of occludin expression in GPNT monolayers (Regina et al., 1999) was determined to assist the interpretation of any effects of occludin transfection. GPNT and another immortalised rat brain EC line, GP8, as well as the immortalised rat retinal EC line JG2 were compared with the epithelial cell lines MDCK and ARPE19 by immunoblot of whole cell extracts (Fig. 3.2). Both epithelial cell lines expressed high levels of occludin that migrated as a band of approximately 65 kD whereas occludin was undetectable in lysates from JG2 and GPNT EC lines. GP8 cells did express some occludin although at a much lower level than epithelial cells. The extent of tight junction formation in the GPNT cell line is unknown but may be highly compromised as they also fail to express endothelial-specific claudin-5 (unpublished observations).

3.2.2 Generation and expansion of clones expressing ectopic occludin

Many clones were generated following liposomal transfection of GPNT cells with occludin constructs (described in greater detail in section 2.12). These were expanded and cell extracts analysed by immunoblot to positively identify clones that highly express the ectopic occludin protein (Fig. 3.3). Several clones expressing the transgene very highly were generated for each construct except that of wild-type occludin where only a single highly expressing clone and a clone with negligible expression were generated. Some clones exhibited retarded growth or altered gross morphology and these were not expanded any further. There was no association with these changes with the transfection of a particular construct. The highly expressing clones were then analysed by immunofluorescence to ensure that expression of the ectopic occludin was homogeneous throughout the monolayers formed by each clone. Those that displayed heterogeneous expression were not expanded any further.

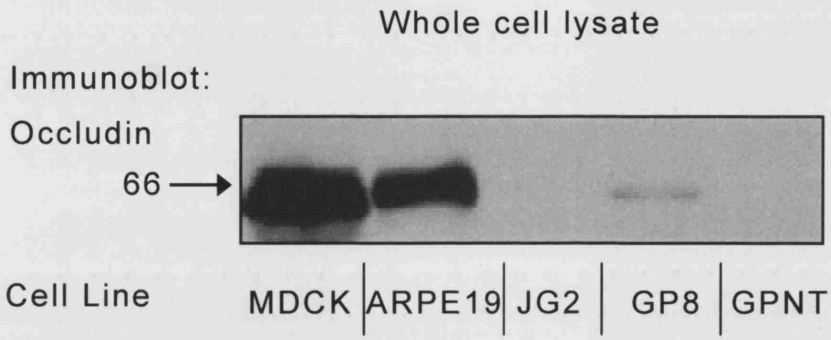

Fig. 3.2 Endogenous occludin expression in epithelial and endothelial cell lines
Equal amounts of protein from whole cell extracts of canine kidney epithelial (MDCK), human retinal pigment epithelial (ARPE19), immortalised rat retinal endothelial (JG2) and immortalised rat brain endothelial (GP8 and GPNT) cell lines were fractionated and immunoblotted with a commercial anti-occludin antibody from Zymed. Both epithelial cell lines express high levels of occludin whereas expression in the endothelial cell lines was either very low or undetectable. GP8 was the only immortalised endothelial cell line to express occludin. The position of molecular standards with known molecular mass (kD) is indicated by an arrow. Data shown are representative of 3 independent experiments.

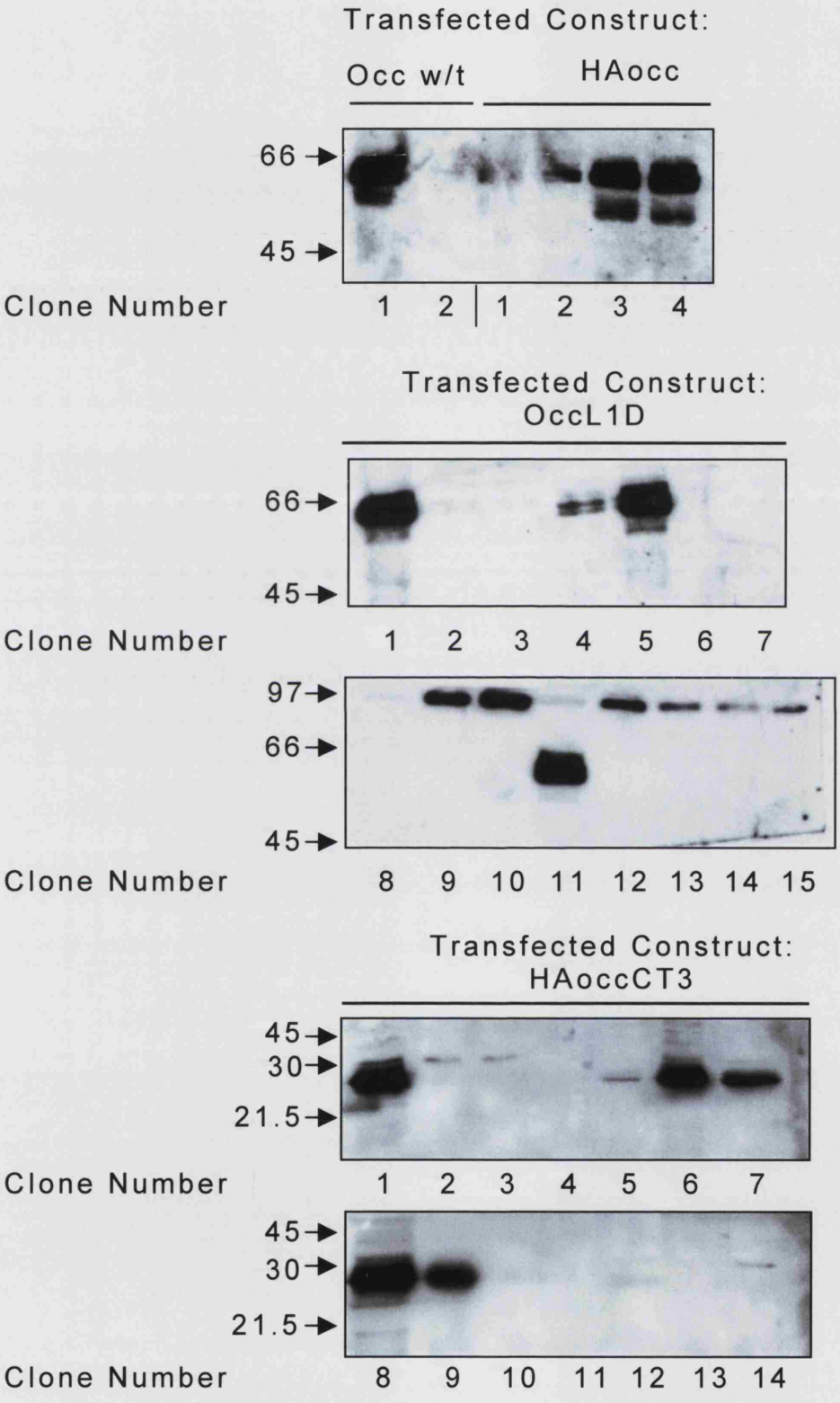
Transfected Construct:
Occ w/t
HAocc
66
45
Clone Number
1 2 1 2 3 4
Transfected Construct:
OccL1D
66
45
Clone Number
1 2 3 4 5 6 7
97
66
45
Clone Number
8 9 10 11 12 13 14 15
Transfected Construct:
HAoccCT3
45
30
21.5
Clone Number
1 2 3 4 5 6 7
45
30
21.5
Clone Number
8 9 10 11 12 13 14

Fig. 3.3 Immunoblot analysis of clones expressing ectopic occludin

Protein from whole cell extracts of clones isolated and expanded following occludin construct transfection was fractionated and immunoblotted with anti-ectopic occludin antibodies. Clones expressing HAoccCT3 were detected with an antibody specific to the N-terminus (626, not the HA tag) and all others with an antibody specific to the C-terminus (chocolate). Several clones with high expression of the ectopic occludin were generated for each construct with few clones representing 'false positives' that lack expression. Some clones expressed the ectopic occludin at a level low enough only to be detectable following long exposures of the immunoblot. The position of molecular standards with known molecular mass (kD) is indicated by arrows.

3.2.3 Truncated-N-terminus-occludin expression in COS cells

Two rounds of multiple transfections of GPNT cells with the N-terminal-deleted occludin construct (ΔNocc, see section 2.11) using an identical protocol to that used previously failed to produce a single viable clone. The monkey kidney epithelial cell line COS7 was transfected to determine if this construct could be expressed transiently within mammalian cells. Occludin was visualised in COS cells transfected with the construct using an anti-chicken occludin C-terminus antibody. COS cells transfected with unmodified pbabe hygro failed to show any expression of occludin whereas there were high levels of expression in many cells transfected with the occludin construct (Fig. 3.4). The protein did not appear to localise to any particular intracellular compartment but was present throughout the cell and was particularly concentrated within vesicles.

3.2.4 Ectopic expression of occludin in brain endothelial cells

After expansion and freezing of all highly expressing clones, single, representative clones of each construct that were homogeneously expressing the ectopic occludin constructs were selected for use in functional assays. Equal amounts of protein from cell extracts were immunoblotted with an antibody specific to the ectopic occludin to compare the level of transgene expression (Fig. 3.5). Each of the clones tested expressed ectopic occludin at a similar level. Wild-type occludin migrated as a 64 kD band as did HAocc with OccL1D slightly smaller. The much smaller HAoccCT3 had a relative molecular mass of approximately 26 kD. The same membrane was then stripped and re-probed using an anti-HA antibody to confirm the identity of the protein expressed by each clone. All clones were assayed at the third passage following transfection and the same clones used for immunoblot analysis were used between passage numbers 6-10 for all subsequent functional assays. Expression levels of the transgenic occludin were checked at alternate passages by immunofluorescence and did not show noticeable change up to passage 10.

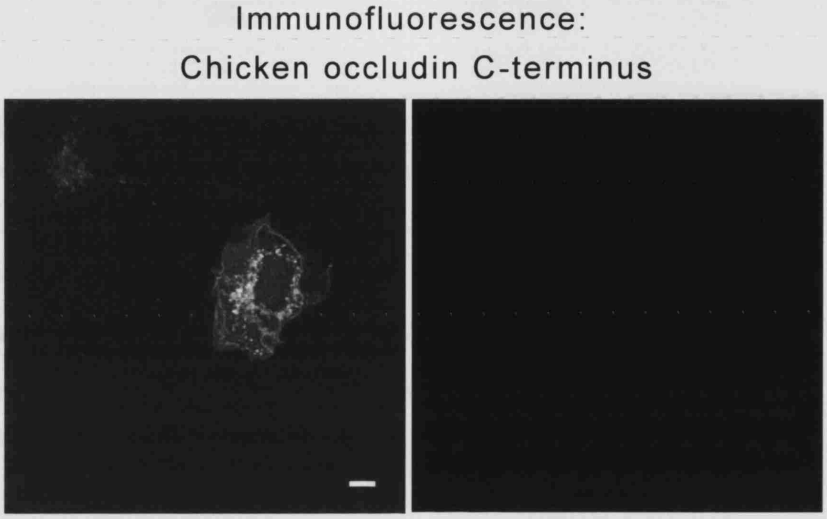

Fig. 3.4 Truncated-N-terminus-occludin expression in COS cells
COS7 cells were transfected with the truncated N-terminal occludin construct or with unmanipulated (empty) plasmid DNA. Following transfection, the cells were fixed with ethanol and processed for immunofluorescence using the anti-occludin C-terminus antibody. Numerous cells transfected with the truncated occludin construct expressed the mutant protein that was distributed throughout the cells and that appeared to accumulate particularly within intracellular vesicles. Images are projections of 4 sequential optical sections. Scale bar = 10 μm

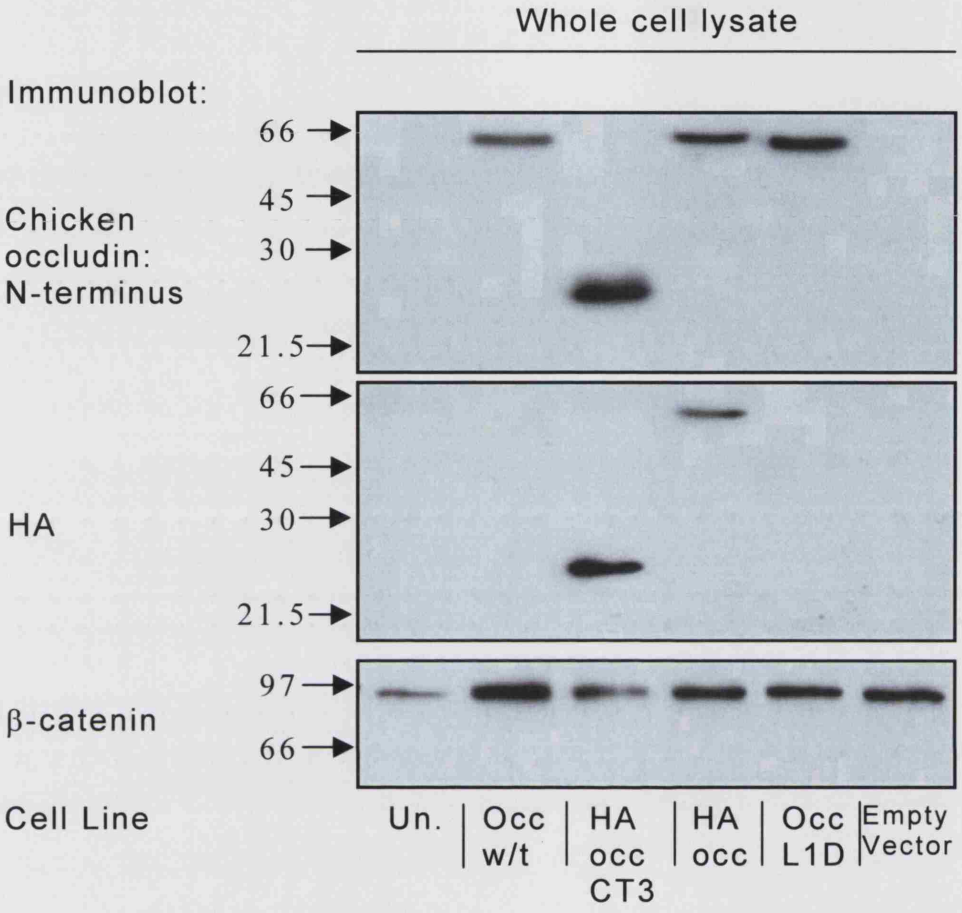

Fig. 3.5 Expression of ectopic occludin in GPNT brain endothelial cell lines

Equal amounts of protein from cell extracts of each clone or untransfected (Un.) cells were fractionated by SDS-PAGE and immunoblotted with an anti-chicken occludin N-terminus antibody. Membranes were then stripped and reprobed with an anti-HA antibody to ensure the correct identification of each construct and the membrane stripped and immunoblotted for β-catenin as an indication of protein loading. Expression of transfected occludin protein was high for all the constructs and approximately equal between each of the clones. The position of molecular standards with known molecular mass (kD) is indicated by arrows.

3.2.5 Morphology of occludin-transfected brain endothelial cell monolayers

Occludin is a tight junction protein localising at cell-cell contacts and so the possibility that the expression of the wild-type or mutant protein could influence cell and monolayer morphology was investigated (Fig. 3.6). Following plating at the same density, all clones exhibited similar fusiform morphology characteristic of microvascular brain ECs and all clones reached confluence on the same day. Both nascent (newly confluent) and long-confluent monolayers from all clones were identical in appearance with the cells gradually assuming a more rounded appearance over time.

Fig. 3.6 Morphology of occludin-transfected brain endothelial cell monolayers
Untransfected and transfected GPNT cells were seeded at equal density and images were then acquired using a digital camera connected to an inverted phase contrast microscope following defined periods of culture. Images were acquired 24 hours (subconfluent), 4 days (nascent monolayer) and 7 days (long confluent) after plating. All clones exhibited the same fusiform morphology characteristic of cultured endothelial cells and assumed a more rounded appearance with increasing confluence. Scale bar = 100 μm

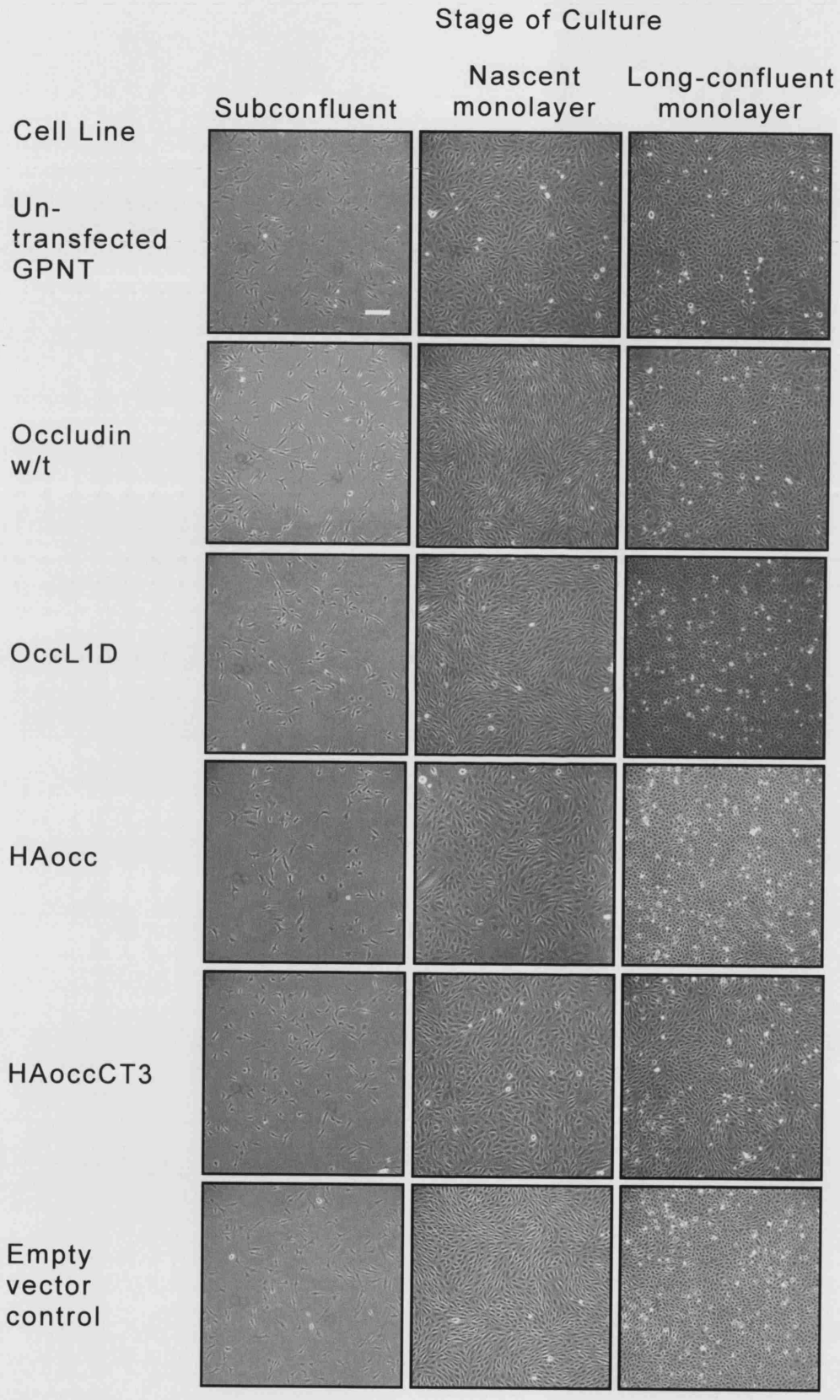
Stage of Culture
Subconfluent
Nascent monolayer
Long-confluent monolayer
Cell Line
Un-transfected GPNT
Occludin w/t
OccL1D
HAocc
HAoccCT3
Empty vector control

3.2.6 Localisation of junctional proteins and the actin cytoskeleton in brain endothelial cells expressing transgenic occludin

The intracellular distribution of various junctional proteins and the actin cytoskeleton within monolayers of each clone were analysed by immunocytochemistry and confocal microscopy (Fig. 3.7 panel A). Transgenic wild-type occludin localised to cell junctions with some located in the perinuclear Golgi apparatus. The occludin mutants HAocc and OccL1D also localised to cell junctions with some present in the cytoplasm although this was not as pronounced as with wild-type occludin. The distribution of HAoccCT3 was markedly different from the other constructs with none of the transfected occludin localising to cell junctions but appearing to concentrate only in the perinuclear Golgi apparatus. Cell lines were also stained for ZO-1 expression to indicate tight junctions. In the parent cell line, ZO-1 was almost entirely localised in a continuous configuration at cell borders. All other clones, except HAoccCT3, also exhibited a junctional distribution of ZO-1. The distribution of ZO-1 within cells expressing HAoccCT3, that itself was only present in the cytoplasm, was entirely cytoplasmic with no junctional staining. As an indicator of the organisation of adherens junctions, cells were stained for the adherens junction protein β-catenin. Within all cell lines, β-catenin was almost entirely localised to the cell junctions with the exception of the HAoccCT3 cell line where the junctional distribution was more discontinuous. The interactions and dynamic rearrangement of the actin cytoskeleton are known to be important for regulating the structure and function of cell-cell junctions (Adamson et al., 2002; Hordijk et al., 1999) and in the support of leucocyte transendothelial migration (Adamson et al., 1999). Therefore the arrangement of actin within the cell lines was of particular interest. The parent cell line contained mainly cortical actin bundles around the edge of each cell. The distribution within the other cell lines was also largely cortical but with an increased level of stress fibres, particularly in those expressing HAoccCT3. The presence of these stress fibres within the cells transfected with the empty vector control suggest that this is a result of the transfection and selection process and not due to

occludin expression. The exceptionally high level of stress fibres and decreased cortical actin observed in cells expressing HAoccCT3 may, however, be related to the disorganisation of both tight (ZO-1) and adherens (β-catenin) junctions although it is not possible to determine the interrelationship between such effects from these studies.

To ensure that the junctional disorganisation observed in cells expressing HAoccCT3 was not a peculiarity of this particular clone, a different clone expressing this construct and others expressing HAocc and OccL1D (also differing from those tested previously) were cultured and processed for immunofluorescence as before (Fig. 3.7 panel B). The occludin distributions within these clones were identical to those tested previously in that OccL1D and HAocc proteins both localised to cell junctions whereas HAoccCT3 was concentrated within perinuclear vesicles. There was also disorganisation of ZO-1 within this clone and large amounts of stress fibres. The β-catenin distribution, however, was more continuously distributed along cell borders compared to the other clone expressing this construct. The distribution of both ZO-1 and β-catenin within the clones expressing OccL1D and HAocc were both junctional without any apparent disorganisation.

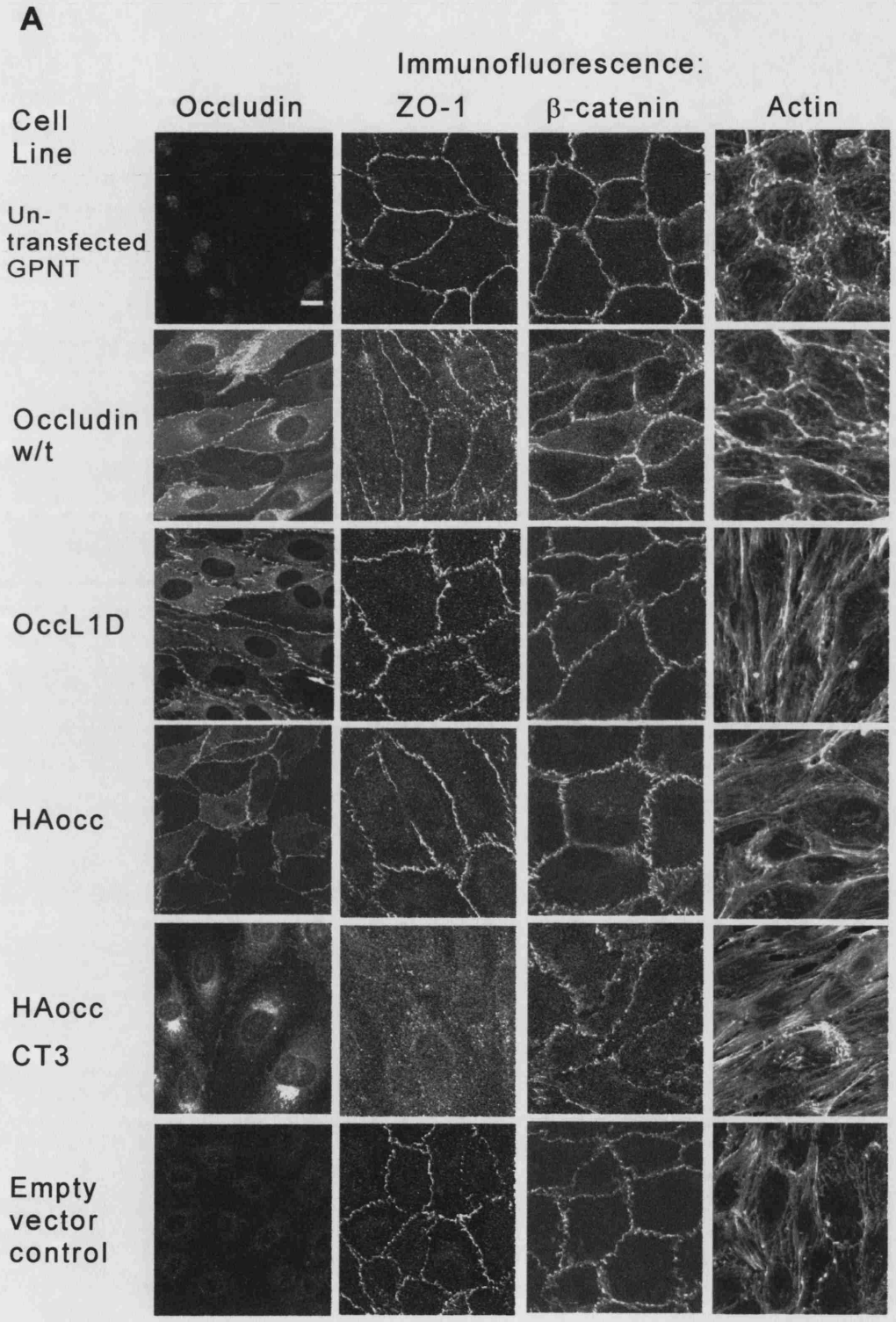
A
Immunofluorescence:
Occludin
ZO-1
β-catenin
Actin
Cell Line
Un-transfected GPNT
Occludin w/t
OccL1D
HAocc
HAocc CT3
Empty vector control

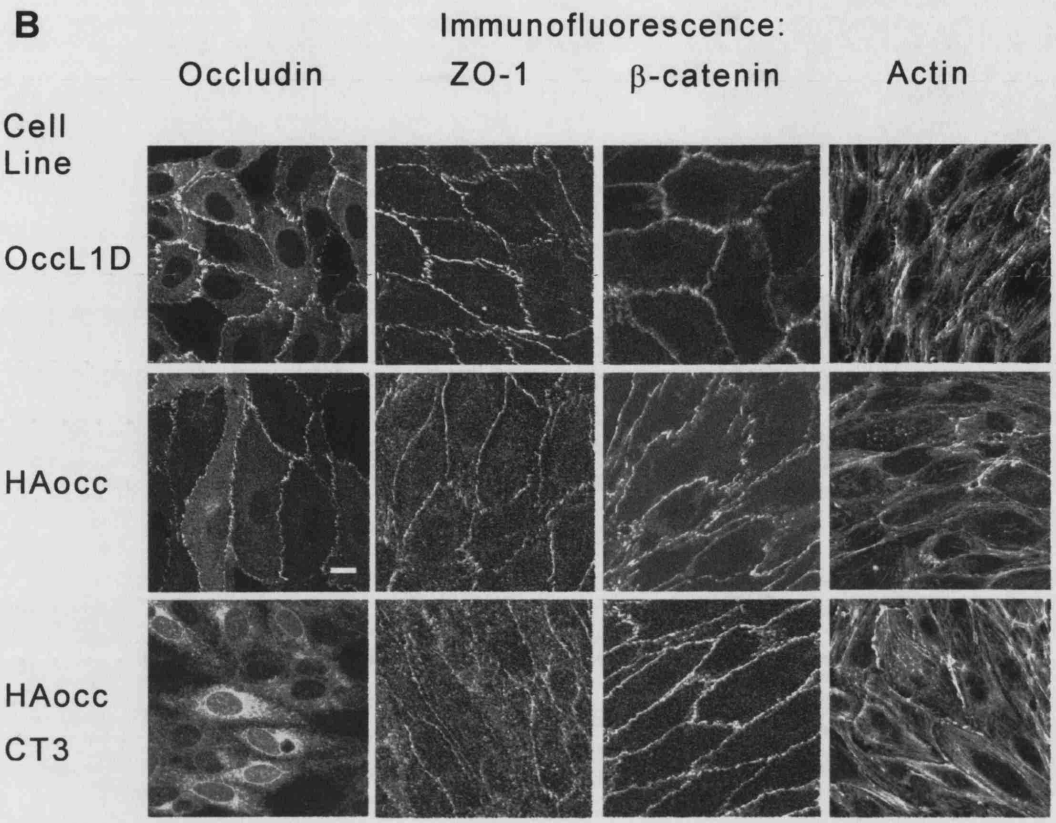

Fig. 3.7 Localisation of junctional proteins and the actin cytoskeleton in brain endothelial cells expressing transgenic occludin

Panel A, Untransfected and transfected GPNT cell lines were grown to confluence and fixed by different methods depending on the antigen. Methanol was used for ZO-1 and β-catenin staining, ethanol for occludin and methanal (formaldehyde) for actin. Ectopic occludin was visualised using the antibody specific for the N-terminus. Wild-type occludin, HAocc and OccL1D constructs localised to cell borders. The ZO-1 and β-catenin distributions within these cell lines were also predominantly at cell borders. Cells expressing the construct HAoccCT3, however showed disorganised ZO-1 and large numbers of actin stress fibres. This occludin construct also failed to localise to cell-cell junctions and was present only within cytoplasmic vesicles. Images are projections of 4 sequential optical sections through the whole cell except those of the actin cytoskeleton that are images of a single optical section from the apical aspect.

Panel B, Different clones expressing HAocc, HAoccCT3 and OccL1D than those used in previous immunofluoresence experiments were grown to confluence, fixed and processed for immunofluorescence. The only apparent difference between these clones and those used previously was that the distribution of β-catenin in the cells expressing HAoccCT3 appeared more continuously distributed at junctions. Scale bar in both panels = 10 μm

3.2.7 Occludin expression inhibits T cell transendothelial migration without affecting adhesion

The influence of occludin expression on the transendothelial migration of antigen-activated MBP-specific T cells was determined using a well-established assay (see section 2.15; Greenwood and Calder, 1993; Greenwood et al., 1996; Pryce et al., 1997; Fig. 3.8 Panel A). Transfection with the empty vector did not significantly alter T cell migration compared with the original parent cell line. Expression of wild-type occludin, however, resulted in a significant reduction of T cell migration by 27% ± 3% (mean ± SEM) when compared to the parent cell line and this was significantly lower ($p<0.05$) than cells transfected with the empty vector. The inhibition of T cell migration by wild-type occludin was not observed however in cells expressing HAocc suggesting a key role for the N-terminus of occludin in this process. OccL1D expression inhibited migration compared to the untransfected, parental cells to an almost identical extent as wild-type occludin (30% ± 5%) and this was also significantly lower than vector transfected controls ($p<0.05$), suggesting that the deleted amino acids within the first extracellular loop domain have little influence on migration. Cells expressing HAoccCT3 showed a profound decrease of approximately 50% ± 4% ($p<0.001$) in T cell migration compared to the parent cell line. To ensure the observed differences were due only to differences in the process of T cell diapedesis and not in the ability of T cells to adhere to the monolayer, a well-established adhesion assay was performed (see section 2.16, Male et al., 1990). No differences were observed in adhesion of fluorescently-labelled mitogen-activated peripheral lymph node cells (PLNC, that comprise almost entirely T cells) to monolayers of the different clones with the exception of that expressing HAoccCT3 (Fig. 3.8 Panel B). This clone exhibited a significantly higher (50% ± 14%, $p<0.01$) level of PLNC adhesion compared to the other cell lines.

Fig. 3.8 Occludin expression inhibits T cell transendothelial migration without affecting adhesion
Panel A,
Migration of antigen-activated MBP-specific T cells across confluent monolayers of GPNT cells expressing wild-type occludin and the mutant occludin protein OccL1D was significantly reduced compared to untransfected (Un.) and empty vector (Vect.) transfected cell lines. Migration across cells expressing the epitope-tagged HAocc construct was equal to that of untransfected cells. Migration across cells expressing HAoccCT3 was also significantly reduced compared to empty vector transfected cells. The mean percentage of T cell migration across each cell line is expressed as a percentage of the mean of migration across wild-type (untransfected) cells ± SEM. Data was pooled from 3 independent experiments each with a minimum of 6 wells recorded for each cell line in each experiment. An analysis of variance was performed on migration data and a significant difference was observed ($F=13.278$, $df = 5,94$, $p<.0001$). Post-hoc analysis by Fishers PLSD (5%) was performed to identify which of the groups was significantly different against control (Vect.). *, $p<0.05$; **, $p<0.001$.
Panel B,
Adhesion of fluorescently-labelled mitogen-activated PLNC to monolayers of untransfected (Un.) and transfected cell lines expressing each occludin construct was not significantly different except for cells expressing HAoccCT3 that exhibited greater levels of adhesion. Data was pooled from 3 independent experiments each with a minimum of 12 wells for each cell line. The mean percentage of PLNC adhesion to each cell line is expressed as a percentage of the mean of adhesion to wild-type (untransfected) cells ± SEM. The observed difference between control (Vect.) and the HAoccCT3 cell line was determined by Student's *t* test. *, $p<0.05$.

A

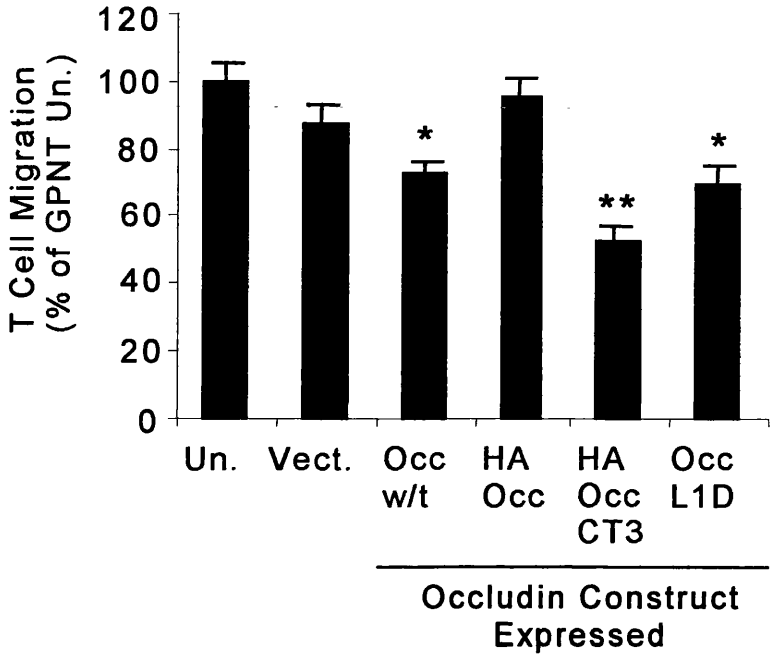
T Cell Migration
(% of GPNT Un.)
120
100
80
60
40
20
0
*
**
*
Un.
Vect.
Occ w/t
HA Occ
HA Occ CT3
Occ L1D
Occludin Construct Expressed

B

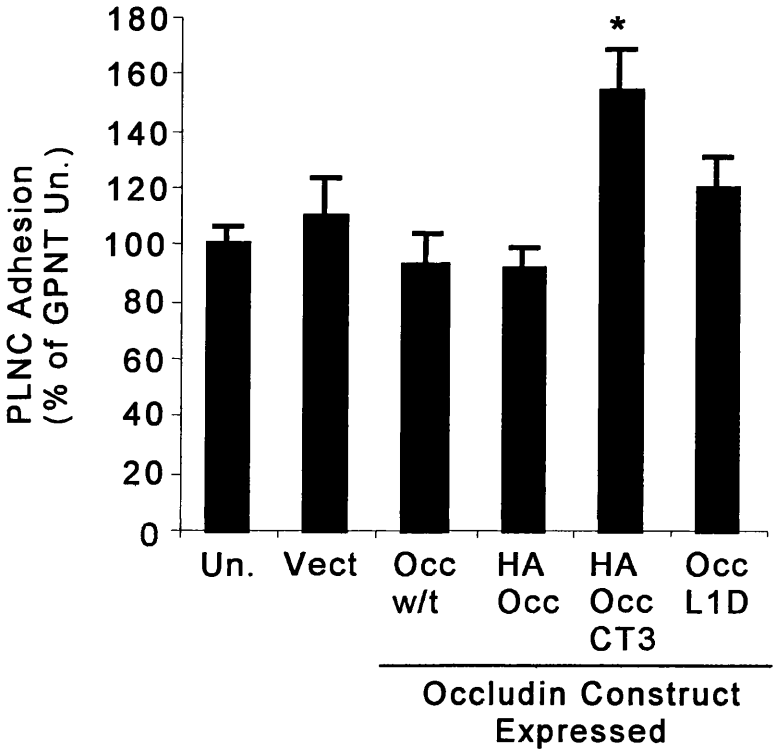
PLNC Adhesion
(% of GPNT Un.)
180
160
140
120
100
80
60
40
20
0
*
Un.
Vect
Occ w/t
HA Occ
HA Occ CT3
Occ L1D
Occludin Construct Expressed

3.2.8 Occludin expression does not produce 'electrically tight' monolayers

Resistance to the paracellular flux of ionic solutes caused by the sealing of the paracellular cleft between cells by lateral junctions is commonly used as a sensitive measure of junction 'tightness'. The electrical resistance of monolayers from each clone cultured on permeable filters was measured (Fig. 3.9). The untransfected parent GPNT cells did not generate an electrical resistance much greater than background (blank fibronectin-coated filters alone) showing that this phenotypic characteristic of brain ECs is not preserved in this cell line. The value obtained for blank filters was 85% ± 2.6% (mean ± SEM) of that obtained for filters with a monolayer showing the small contribution of the cells. The possibility that the loss of expression of occludin may account, at least in part, for these low-resistance junctions was not supported by the observation that none of the transfected occludin forms were able to confer high electrical resistance to cell junctions or indeed any measurable difference compared to the occludin deficient parental cell line. This demonstrates that occludin expression is not responsible for the establishment of high resistance brain endothelial cell junctions in vitro.

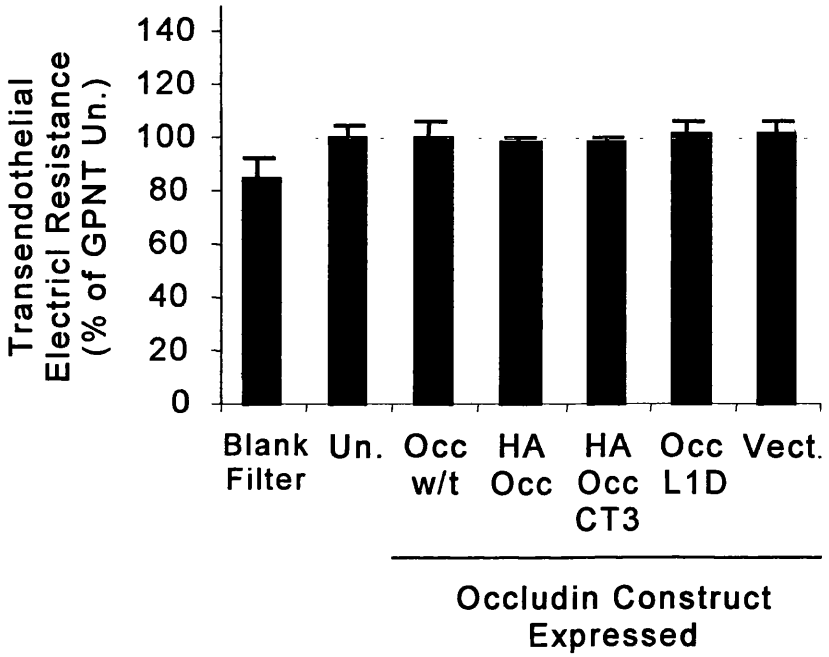

Fig. 3.9 Occludin expression does not produce 'electrically tight' monolayers

The transendothelial electrical resistance (TER) of monolayers of untransfected (Un.) and transfected GPNT cell lines (and fibronectin-coated blank filters) was measured in triplicate on 2 consecutive days. None of the cell lines were able to form monolayers that exhibited TER values significantly different from blank fibronectin-coated filters. Data from each cell line were pooled and the mean value for each cell line expressed as a percentage ± SEM of the mean obtained for wild type cells. The mean value for blank filters and untransfected cells (± SEM) were 85 ± 8 $\Omega.cm^2$ and 107 ± 5.5 $\Omega.cm^2$ respectively.

3.2.9 Occludin expression increases paracellular permeability

The permeability of monolayers to a 40 kD FITC-dextran tracer was investigated to determine whether the expression of occludin increased the integrity of the lateral cell-cell junctions resulting in a more restrictive paracellular barrier than those not expressing occludin (Fig. 3.10). Clones transfected with empty vector showed an overall increase in permeability compared to the parent cell line ECs although this difference did not reach statistical significance. The permeability of cells expressing wild-type occludin was significantly greater than that of untransfected cells but not from that of control-transfected cells suggesting that the transfection process or, more likely, the cloning process affected the barrier properties of the cells or that expression of wild-type occludin does not significantly influence the permeability properties of these cells' junctions. Other clones expressing mutant occludin proteins were significantly more permeable than clones transfected with empty vector control or wild-type occludin suggesting that each of the mutated domains may be important in maintaining junctional integrity ($p<0.05$).

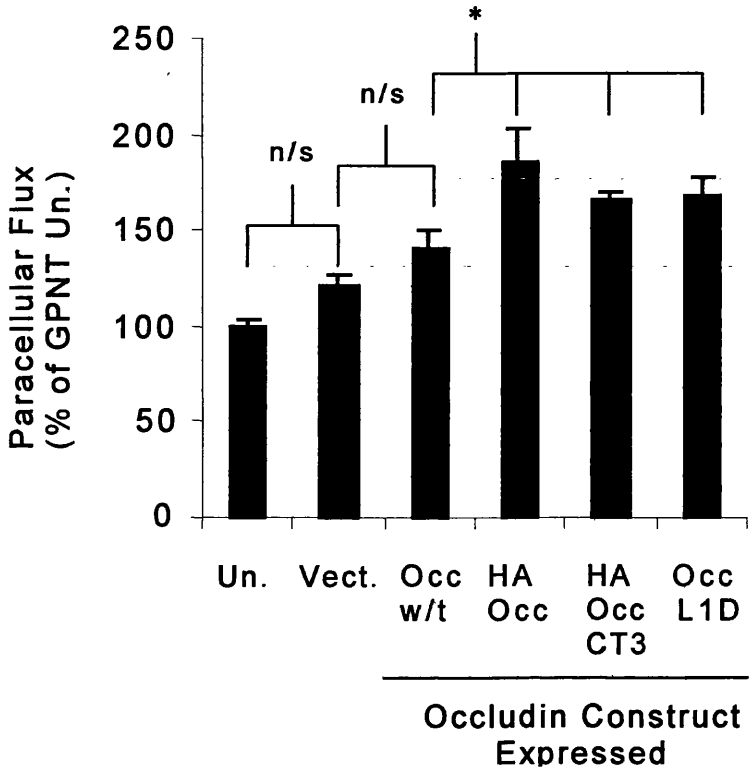

Fig. 3.10 Occludin expression increases paracellular permeability

Paracellular flux of a 40 kDa molecular tracer in the apical to basolateral direction was measured across untransfected (Un.) and transfected GPNT cell lines. Transfected cell lines displayed increased permeability compared to the untransfected cells. Cell lines expressing the mutant occludin constructs were significantly more permeable than the cells expressing wild-type occludin although these cells were themselves not significantly different from empty vector-transfected cells (Vect.). Data from 3 independent experiments with each cell line in duplicate were pooled and the mean value for each cell line expressed as a percentage ± SEM of the mean obtained for wild type cells. Data shown is from samples collected after 60 minutes and samples collected after 5, 15, 30 and 120 minutes (data not shown) give the same values. An analysis of variance was performed on the permeability data between the various groups and a significant difference was observed ($F = 10.776$, $df = 5,30$, $p<0.0001$). Post-hoc analysis by Fishers PLSD (5%) was performed to identify which of the groups was significantly different against control. n/s, not significant ($p>0.05$); *, $p<0.05$.

3.3 Discussion

From the data described above, we have observed that occludin expression is lost following immortalisation of brain ECs under these growth conditions. The culture conditions used in our study may therefore lack a stimulus or stimuli that are present in vivo. This downregulation of occludin does not prevent these cells from forming morphologically and functionally similar monolayers to primary cultures or from expressing other junctional molecules that localise to cell borders. Unlike the endothelial cell lines used here, the MDCK and ARPE-19 epithelial cell lines assayed for occludin expression both expressed high levels. This observation probably reflects the greater ease by which tight epithelial cells are able to retain their junctional integrity in vitro. Brain endothelial cells, on the other hand, are known to require specific, and as yet undefined, factors to maintain tight junctions. It is clear that the cell lines used in this study (as with other brain endothelial cell lines) do not possess bona fide tight junctions and hence do not fully retain their in vivo BBB characteristics. Monolayers of GPNT cells are less permeable to molecular tracers than monolayers of peripheral ECs such as HUVECs (Romero et al., 2003) and when viewed by transmission electron microscopy adjacent cells contain regions of apparent membrane fusion that would be expected to limit paracellular diffusion. Tight junctions between brain endothelial cells are based on polymerised fibrils composed of occludin and claudin species, in particular claudin-5 and claudin-12. By lacking endogenous expression of both claudin-5 and occludin, GPNT cells present a system within which to investigate the effects of not only the (re)introduction of wild-type protein but of mutants having specific domains of the protein modified or deleted. In this study we have investigated the relative importance of occludin in junction structure and function. Similar levels of expression of the transgene following transfection facilitated the interpretation and comparison of data between clones expressing different occludin constructs.

The introduction of wild-type occludin into our cell system led to an inhibition of transendothelial T cell migration. This reduced migration may be due to occludin-containing junctions presenting an

increased physical barrier to the paracellular passage of the T cells. Alternatively, introduction of occludin into the junctional complex may alter the signalling responses that regulate the disengagement of the junction that is necessary to allow the transmonolayer passage of T cells. This decrease in migration was not observed in studies of neutrophil migration across MDCK epithelial monolayers using the same constructs, presumably because the high level of endogenous occludin expression, and/or co-expression of claudins, provides this barrier already (Huber et al., 2000). Unlike cells expressing wild-type occludin, the modification of the cytoplasmic N-terminus with an HA epitope did not result in inhibition of T cell migration when compared with the parental GPNT cell line. As with wild-type occludin, the HA-tagged occludin is expressed correctly at the junction, and presumably forms normal homotypic interactions with adjacent cells. The difference in T cell migration between these two cell lines may therefore be due to properties inherent in the N-terminus that are altered by the presence of the HA tag. In MDCK cells expressing the same HA-tagged occludin construct, neutrophil migration was greatly enhanced suggesting that the barrier provided by the endogenous protein was compromised by incorporation of the mutant form (Huber et al., 2000). Our data would have been more compelling if we had been able to generate a cell line expressing occludin with a truncated N-terminus but attempts to express this construct were unsuccessful. The successful transient expression of this construct in COS7 cells may suggest that high expression levels of this protein may be deleterious to the cells in long-term culture. Occludin not only plays a role in cell-cell junctions but also in preserving the paracellular seal of the monolayer during cytokinesis (Kojima et al., 2001). Deletion of the N-terminal domain may cause occludin, or an interacting protein, to fail in fulfilling its role during cell division or junction formation. Presumably the modification of the N-terminus with the HA epitope affects a crucial part of the protein. However, untransfected cells that do not express occludin still proliferate normally.

The occludin mutant HAoccCT3 caused a profound decrease in T cell transmonolayer migration even though this construct is not incorporated into cell junctions. This observation is even more counterintuitive as this clone also exhibited highly disorganised ZO-1

and partially disorganised β-catenin expression suggesting that the junctions of this cell line are more disorganised. Thus, if T cells migrate through the paracellular route it would be expected that migration through monolayers of this clone would be enhanced. Whether this reduced T cell migration is due to the large amounts of stress fibres and an inability to remodel the actin cytoskeleton necessary for facilitating T cell migration or to a disruption of the signalling cascade at the junction remains to be evaluated. Contrary to these findings, expression of HAoccCT3 in MDCK cells led to increased neutrophil migration (Huber et al., 2000). This could be explained by the incorporation of HAoccCT3 into the cell-cell junctions of MDCK cells where, unlike GPNT cells, it could influence migration in a similar manner to the HAocc-expressing cells. In MDCK cells, the endogenous and transfected, mutant occludin are likely to interact and both be transported to the junction by virtue of the sorting signals contained within the wild-type protein.

Our observation that wild-type occludin expression in GPNT cells results in increased paracellular permeability has also been reported in MDCK cells (Huber et al., 2000). This is particularly surprising as occludin expression inhibits T cell transmonolayer migration. The process of transfection, or the additional number of cell doublings that the transfected cell lines have undergone, clearly resulted in these cells expressing greater permeability.

There is one caveat that must be considered when drawing conclusions from the data presented here. This is that the data from the functional assays are derived from experiments upon single, representative clones expressing each construct. The same clones were used throughout the experiments but due to their scale it was not possible within the time frame of this study to repeat the functional assays on multiple clones expressing the same construct. The clones used in this study all expressed the transgene at a similar level, behaved identically in culture and, by fluoresence microscopy, exhibited the same intracellular distribution of junctional proteins as other clones expressing the same construct. Although these observations suggest there was nothing exceptional about each of the clones used, the data would perhaps be more compelling if multiple clones expressing each construct were tested in functional assays.

This investigation shows that occludin expression restricts the transendothelial migration of T cells and so is likely to contribute to the restriction of lymphocyte migration through the BBB. Given the elevated levels of expression of occludin within BBB ECs in vivo compared to those from peripheral tissues it is tempting to speculate that this is one molecular aspect contributing to the phenomenon of the BBB and the low levels of lymphocyte trafficking through this particular vascular bed. We also provide evidence that in these brain-derived endothelial cells the occludin N-terminus may play a role in regulating barrier function in relation to leucocyte migration. As occludin has now been implicated in regulating both lymphocyte and neutrophil migration across brain endothelial and MDCK cell monolayers respectively, it may represent part of a common mechanism regulating the paracellular migration of leucocytes across tissue barrier sites. We also demonstrate that some BBB characteristics such as high electrical resistance are not restored by occludin expression alone. Whilst acknowledging their limitations, these cell lines still represent a robust and flexible model for studying BBB cell biology with assays that require significant amounts of material. The enigma of BBB ECs losing their in vivo characteristics when placed in culture is the focus of much current research. The generation of truly representative BBB cell lines is of tremendous interest and potential for vascular cell biologists and pharmacologists yet at present much further work is required as this goal has only been partially achieved.

Chapter 4:

Crosslinking of ICAM-1 Induces Increased Permeability and Tyrosine Phosphorylation of VE-cadherin in Brain Endothelial Cells

4.1 Introduction

ICAM-1 is a 76-115 kDa transmembrane glycoprotein that belongs to a subset of the immunoglobulin (Ig) superfamily of proteins that are specialised for binding to integrins (Wang and Springer, 1998). Other members of this subset, that share greater sequence homology to each other compared to other Ig superfamily proteins, include ICAM-2, -3, -4, -5, VCAM-1 and MAdCAM. ICAM-1 is expressed by epithelial and endothelial cells, fibroblasts, monocytes, macrophages as well as T and B lymphocytes. The basal level of ICAM-1 expression in most cell types is low but can be upregulated by a wide variety of stimuli including pro-inflammatory cytokines such as TNF-α, IL-1β and IFN-γ, LPS, the phorbol ester phorbol-12-myristate-13-acetate, IGF-1, viral and intracellular bacterial infection and cell stress (Dietrich, 2002). ICAM-1 is composed of five extracellular Ig-like domains at the N-terminal end, a transmembrane domain and a very short (28 amino acids in humans) cytoplasmic tail at the C-terminal end. Schematic representations of ICAM-1 and other cell adhesion molecules of the immunoglobulin superfamily are shown in Fig. 4.1. It is able to bind many ligands including β_2 integrins such as LFA-1 (CD11a/CD18) and Mac-1 (CD11b/CD18) on leucocytes as well as fibrinogen, hyaluronan, CD43, p150/95, coxsackie A13 rhinovirus and *Plasmodium Falciparum*-infected erythrocytes. LFA-1 binds to the first and second Ig-like domains and Mac-1 to the third, these interactions being largely responsible for the firm adhesion of circulating leucocytes to the endothelial surface of post-capillary venule walls (Girard and Springer, 1995). LFA-1 is believed to be normally responsible for mediating binding of migrating T cells whereas Mac-1 appears to regulate adhesion and subsequent migration of monocytes. The process of (patho)physiologic lymphocyte transendothelial migration and the role of ICAM-1 as an adhesion molecule are discussed in greater detail in section 1.3. On the cell surface, ICAM-1 is present as a dimer that, in leucocytes, is believed to orientate the molecule in a way both favourable for trans interactions and inhibitory to cis interactions with LFA-1 (Wang and Springer, 1998).

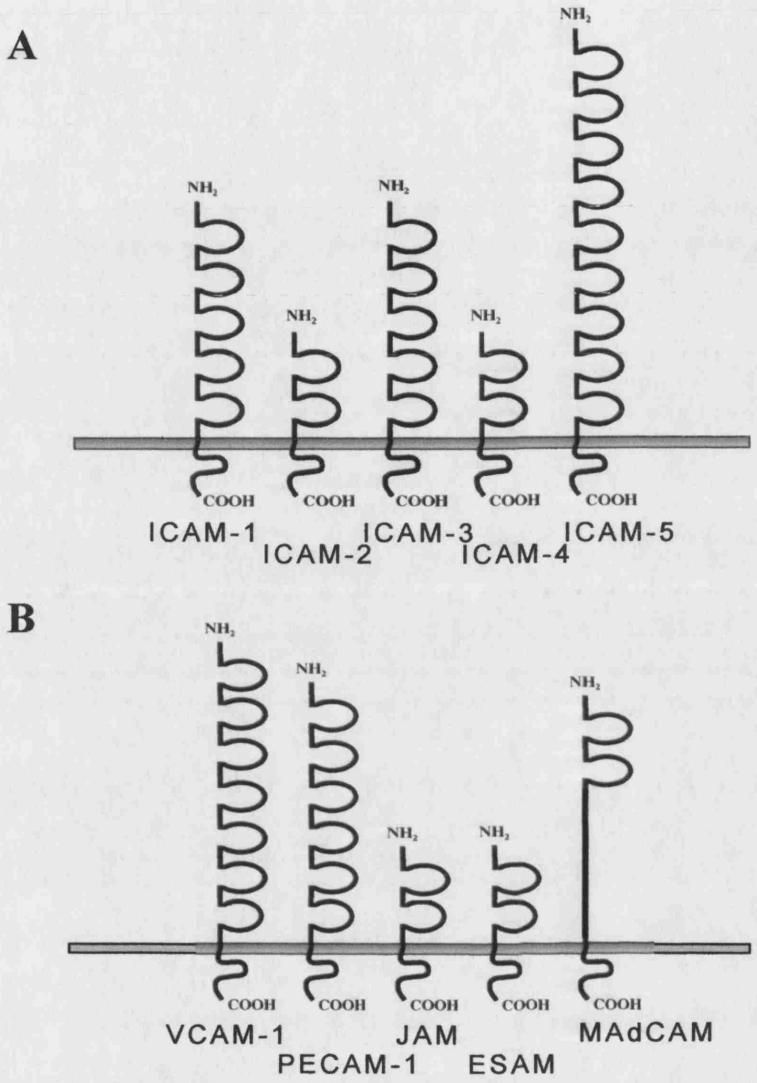

Fig. 4.1 Schematic representation of cell adhesion molecules of the immunoglobulin superfamily
The immunoglobulin fold domains within the extracellular portion of each protein are depicted diagrammatically for comparison. The intracellular domains of each protein are depicted as identical but may vary significantly in size. The structure and function of these proteins are described in greater detail within sections 1.2 and 1.3. Abbreviations: ICAM, intercellular adhesion molecule; VCAM, vascular cell adhesion molecule; PECAM, platelet endothelial cell adhesion molecule; JAM, junctional cell adhesion molecule; ESAM, endothelial cell-specific adhesion molecule; MAdCAM, mucosal addressin cell adhesion molecule

Although ICAM-1 functions as a mechanical anchoring molecule, upon clustering on the cell surface it is also capable of transducing intracellular signals (Greenwood et al., 2002) in a similar manner described for other Ig superfamily cell adhesion molecules such as ICAM-2 (Perez et al., 2002), VCAM-1 (Ricard et al., 1997; Lorenzon et al., 1998), PECAM (Pellegata et al., 1998), MHC class II (Truman et al., 1996; Greer et al., 1998; Etienne et al., 1999) and carcinoembryonic antigen-related cell adhesion molecule-1 (CEACAM-1, Budt et al., 2002). Activation of ICAM-1 signalling has been investigated experimentally for a decade mainly by the use of anti-ICAM-1 antibodies followed by secondary anti-isotype antibodies to aggregate (crosslink) surface ICAM-1 (Durieu-Trautman et al., 1994; see Fig. 4.2). Alternatively, fibrinogen has also been used as an activating ligand (Tsakadze et al., 2002). Interestingly, the signalling elicited by these two distinct stimuli exhibit differences. Moreover, the downstream signalling pathways activated by ICAM-1 signalling vary between cell types as well as within a single cell type such as endothelia derived from different vascular beds.

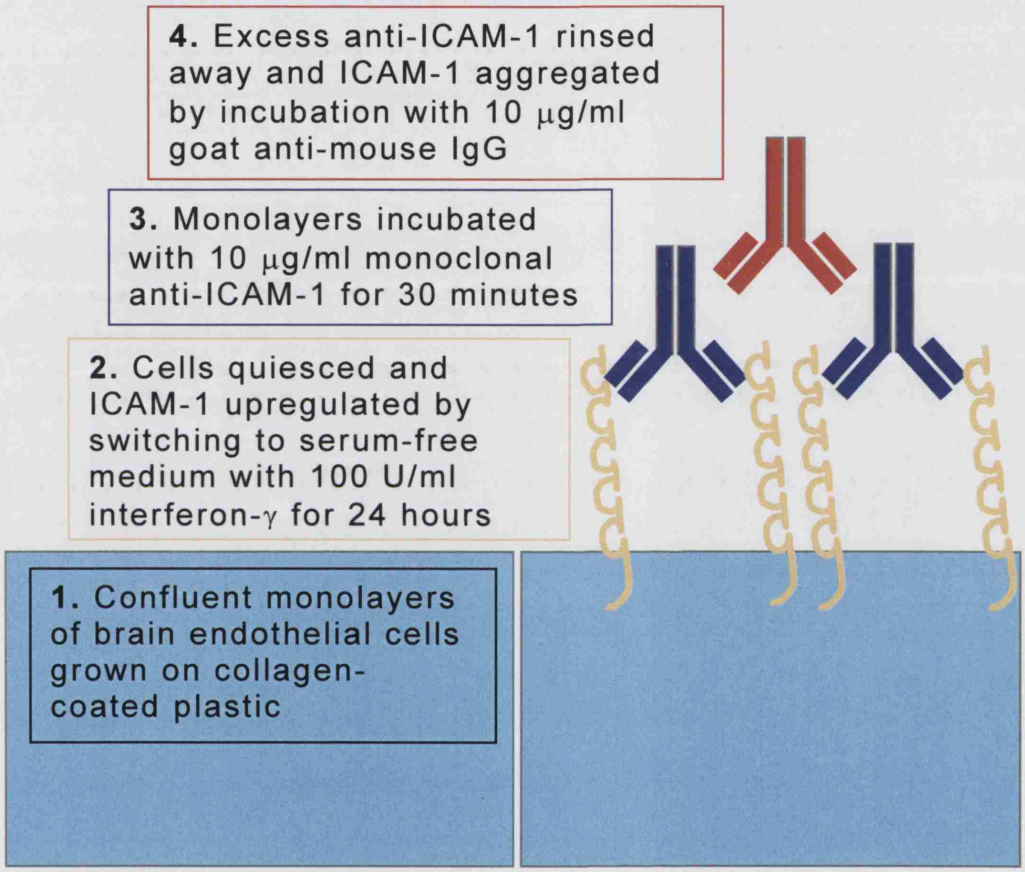

Fig. 4.2 Schematic representation and step-wise description of ICAM-1 crosslinking protocol
All crosslinking experiments described were performed using this prototcol.

Early studies on endothelial signalling during leucocyte transmigration identified that migration of PMNs across an endothelial monolayer induced by a chemoattractant caused a transient increase in endothelial intracellular free calcium levels that was not induced following adhesion alone in the absence of a chemotactic gradient (Huang et al., 1993). Elevation of intracellular calcium has also been described following ICAM-1 crosslinking in a variety of cell types including fibroblasts (Clayton et al., 1998), HUVECs and brain ECs (Etienne-Manneville et al., 2000). In brain ECs, crosslinking ICAM-1 results in the tyrosine phosphorylation of phospholipase Cγ (PLCγ), inositol phosphate production and increased intracellular calcium that was detectable after 2 minutes of crosslinking (Etienne-Manneville et al., 2000). It has been proposed that such signalling leads, via a PKC-dependent pathway, to the activation of the tyrosine kinase Src and phosphorylation of cortactin, a protein involved in the regulation of cortical actin. Following ICAM-1 crosslinking, PKC activation was also found to be required for the subsequent induction of actin stress fibres, tyrosine phosphorylation of FAK and paxillin and the activation of c-Jun N-terminal kinase (JNK) but not for the tyrosine phosphorylation of p130-Crk-associated substrate (CAS) or its association with the adaptor protein Crk (these downstream signals are discussed in greater detail below). These PKC-dependent pathways were themselves dependent on actin cytoskeletal rearrangement as they all could be inhibited by pre-treatment of the endothelial cells with cytochalasin D (an inhibitor of F-actin polymerisation) whereas the PKC-independent phosphorylation of CAS was unaffected. Crosslinking of VCAM-1 has also been reported to lead to elevated intracellular calcium levels (van Wetering et al., 2002) and treatment of ECs with intracellular calcium chelators significantly reduces lymphocyte transendothelial migration demonstrating the importance of such calcium signalling to the migration event (Huang et al., 1993). The importance of heterotrimeric G protein-mediated pathways to T cell migration across brain endothelial monolayers has also been recently shown (Adamson et al., 2002a). Inhibition of such signalling drastically reduced T cell transendothelial migration across monolayers of brain ECs whereas

migration of T cells across monolayers of peripheral high endothelial venule ECs was only partially inhibited.

Remodelling of the endothelial cytoskeleton is intimately involved in supporting the transmigration of leucocytes from the circulation into the tissue parenchyma. Following the capture and firm adhesion of the leucocyte, the EC can be seen to partially envelop the leucocyte in a cup-like membrane structure that contains large amounts of luminal cell adhesion molecules, submembranous actin and the ezrin/radixin/moesin (ERM) proteins that link transmembrane receptors to the actin cytoskeleton (Barreiro et al., 2002; Carmen et al., 2003). ICAM-1 is able to interact with the cytoskeleton both directly and indirectly and, following crosslinking, has been demonstrated to partition into a detergent-insoluble cell fraction. This observation has been interpreted as either an increase in association with the cytoskeleton (Amos et al., 2001) or with lipid-raft domains (Tilghman and Hoover, 2002a) although both possibilities may occur and indeed may describe the same intracellular compartment/structure. The cytoplasmic tail of ICAM-1 is able to bind several cytoskeletal-associated proteins including the actin bundling protein α-actinin (Carpen et al., 1992), the ERM proteins ezrin and moesin (Thompson et al., 2002) that serve to organise cortical actin and glyceraldehyde-3-phosphate dehydrogenase (GAPDH) that is involved in bundling of microtubules as well as β-tubulin itself (Federici et al., 1996). The tyrosine kinase Src and its phosphorylated substrate cortactin have also been detected in ICAM-1 immunoprecipitates (IPs) from crosslinked EC extracts (Tilghman and Hoover, 2002b).

Many proteins interacting with ICAM-1 in vitro and within ICAM-1 IPs have yet to be identified and these will surely lead to a more complete understanding of both how ICAM-1 associates with the cytoskeleton and how after crosslinking the cytoskeleton is remodelled to provide and sustain the endothelial 'docking structure' that facilitates efficient leucocyte diapedesis. The Src-homology-2 protein tyrosine phosphatase (shp2) has also been detected in ICAM-1 IPs following ligation with fibrinogen that also induces tyrosine phosphorylation of ICAM-1 itself although the phosphorylated tyrosine residue(s) are not within the cytoplasmic tail (Tsakadze et al., 2002).

More recent evidence, however, suggests that ICAM-1 does not become phosphorylated following either crosslinking or T lymphocyte adhesion (Greenwood et al., 2003a) and the ICAM-1-shp2 interaction has not been described following these stimuli suggesting this may be a specific effect of the interaction of fibrinogen with ICAM-1. As briefly stated earlier, in addition to the cellular docking structure, crosslinking of ICAM-1 and co-culture with activated T cells induces actin stress fibre formation in brain ECs via a PKC- and rho-dependent pathway (Adamson et al., 1999). The full physiological relevance of this observation is not clear but is believed to be an important component of the signalling pathway responsible for facilitating lymphocyte migration, possibly through mediating the disassembly of lateral cell-cell junctions.

The formation of actin stress fibres following ICAM-1 crosslinking is a similar response to that observed initially in fibroblasts following activation of the rho GTPase proteins of the ras superfamily. Indeed, treatment of brain endothelial monolayers prior to ICAM-1 crosslinking with the bacterial exoenzyme C3 transferase, that specifically inhibits rho proteins by ADP-ribosylation, prevents not only stress fibre formation but also the downstream phosphorylation of FAK, CAS, paxillin and JNK (Etienne et al., 1998). The activation of rho by ICAM-1 crosslinking can be detected directly by measuring the amount of GTP-loaded rho within cell extracts. Treatment with C3 transferase prevents such GTP-loading (hence activation) that occurs following ICAM-1 crosslinking in untreated monolayers. Functional rho is also critical for lymphocyte migration as pre-treatment of brain endothelial monolayers with C3 transferase greatly reduces (by approximately 80%) T cell migration in vitro (Adamson et al, 1999). It is not currently known how rho proteins are activated following ICAM-1 crosslinking. It is possible that cytoskeletal rearrangements mediated by PKC may lead, via activation of Src (Brandt et al., 2002), to rho activation or alternatively ERM proteins, whose activity at the cell membrane itself requires activated rho, may promote rho activation by sequestration of GTP/GDP exchange inhibitors that prevent inhibition of rho activation.

As mentioned earlier, the downstream effect of signalling cascades initiated through ICAM-1 appear to differ between cell

types. Within brain ECs there is, as stated previously, induced tyrosine phosphorylation of the cytoskeleton-associated proteins FAK, CAS and paxillin that localise mainly to focal adhesions and are usually activated by interactions of the cell with integrins of the basal lamina (Etienne et al., 1998). There is also much evidence of signalling to the nucleus via activation of extracellular signal regulated kinase (ERK) cascades. Within brain ECs, there is activation of JNK (Etienne-Manneville et al., 2000) whereas activation of p38 is reported in macrovascular pulmonary ECs (Wang and Doerschuk, 2001) with activation of ERKs following ICAM-1 crosslinking also reported in HUVECs and non-endothelial cells (Lawson et al., 1999). In HUVECs, crosslinking of ICAM-1 has been shown to induce expression of VCAM-1 and the chemokines IL-8 and RANTES (Lawson et al., 1999) whilst in astrocytes identical treatment leads to the elaboration of the pro-inflammatory cytokines TNF-α, IL-1α, IL-1β and IL-6 (Etienne-Manneville et al., 1999, Lee et al., 2000). In mononuclear cells a respiratory burst is initiated in the presence of the bacterial-derived peptide N-formyl-met-leu-phe (Rothlein et al., 1994). These differential effects clearly demonstrate that the outcome of ICAM-1-mediated signalling is cell-type dependent and raises the possibility for pharmacological targeting of specific intracellular signalling cascades. In the context of neuroinflammation, brain endothelial cell-specific pathways may thus be targetted as a means of controlling neuroinflammation. A summary of signalling pathways activated following crosslinking of ICAM-1 identified in brain endothelial cells is shown in Fig. 4.3.

The data presented in this chapter is the first evidence that signalling induced by ligation of an EC surface adhesion molecule (ICAM-1) modulates the phosphorylation of a junctional protein (VE-cadherin, described in greater detail in section 1.2.1) and that this is commensurate with an increase in endothelial monolayer permeability suggesting that this is one mechanism that facilitates the paracellular migration of leucocytes from the circulation into the CNS.

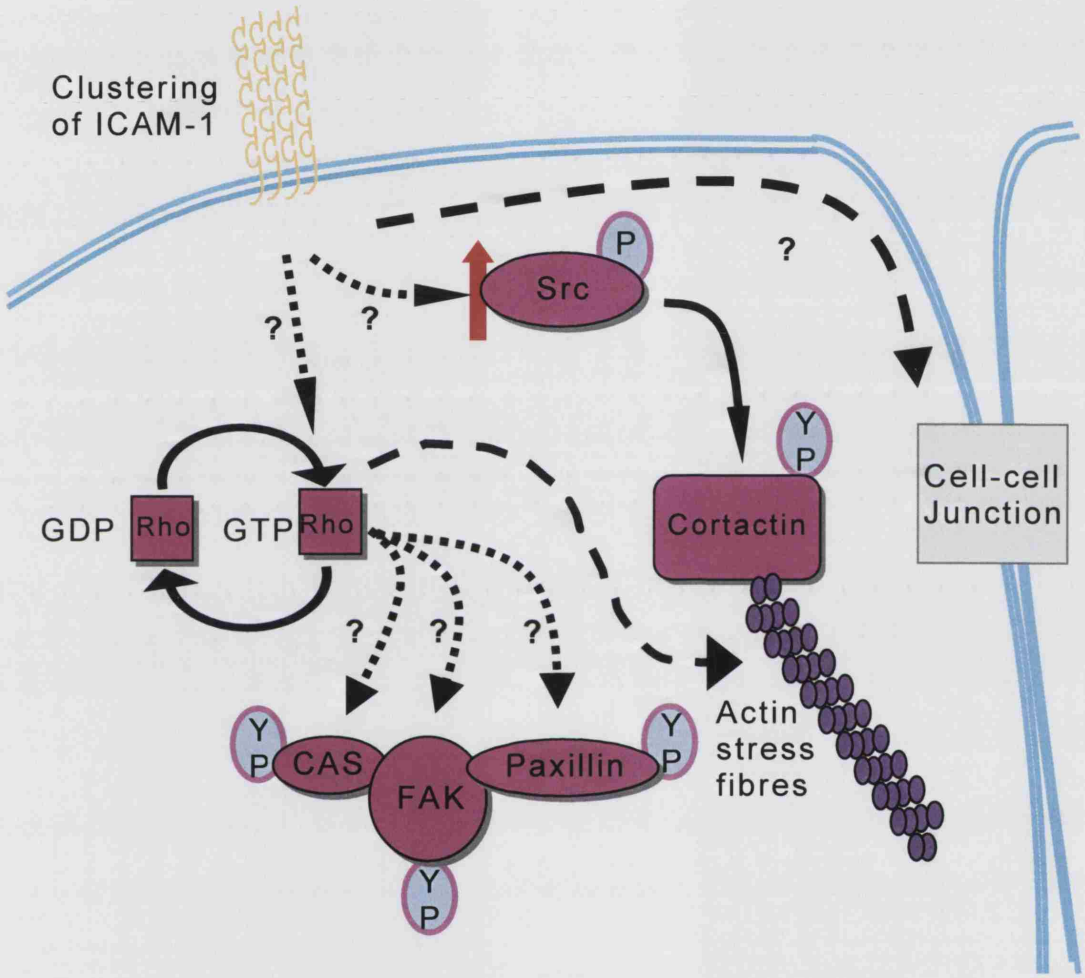

Fig. 4.3 Previously identified signalling pathways in brain endothelial cells initiated by ICAM-1 crosslinking
Dashed lines and question marks indicate unknown signalling pathways. No pathway leading from ICAM-1 clustering to cell-cell junctions has been described. Abbreviations: P, phosphoamino acid group; YP, phosphotyrosine; GD(T)P, guanine nucleotide di(tri)phosphate; CAS, p130-Crk-associated substrate; FAK, focal adhesion kinase

4.2 Results

4.2.1 ICAM-1 crosslinking induces F-actin bundling and increased phosphotyrosine labelling at cell borders

Crosslinking of ICAM-1 has previously been shown to transduce intracellular signals that induce actin stress fibres and tyrosine phosphorylation of several proteins within the brain EC lines RBE4 and GP8 (Durieu-Trautman et al., 1994; Adamson et al., 1999). To ensure that GPNT cells are capable of supporting ICAM-mediated signalling, monolayers were ICAM-1 crosslinked and labelled with fluorophore-conjugated phalloidin. We also investigated whether any increase in tyrosyl-phosphorylated proteins within the cells following ICAM-1 crosslinking are associated with a particular cellular compartment and when any such changes occur relative to F-actin rearrangement (Fig. 4.4). The distribution of F-actin changed from that of loosely organised fibres present throughout the cell to being, in addition to throughout the cell, almost continous at cell-cell borders 5 minutes following ICAM-1 crosslinking. With increasing time of ICAM-1 crosslinking, the actin fibres around cell borders became increasingly organised into large bundles and after 30 minutes these had formed into well-organised cortical rings of F-actin immediately underneath the cell-cell junctions. The amount of phosphotyrosine labelling increased markedly following ICAM-1 crosslinking. This increased labelling was diffusely distributed throughout the cells but was especially evident at cell-cell junctions where the labelling often formed a continuous delineation between neighbouring cells. The increased tyrosine phosphorylation was evident 5 minutes following crosslinking, appeared to peak around 15 minutes and after 30 minutes of crosslinking the distribution was similar to that observed in uncrosslinked cells. The increased tyrosine phosphorylation at cell borders was commensurate with the appearance of the continuous distribution of F-actin at the borders but the phosphotyrosine labelling had decreased at the time when there was strong induction of cortical F-actin bundles.

Fig. 4.4 ICAM-1 crosslinking induces F-actin bundling and increased phosphotyrosine labelling at cell borders

ICAM-1 was crosslinked for varying times and cells were fixed with methanal and processed for immunofluorescence. Phosphotyrosyl-containing proteins were labelled using the P-Tyr-100 antibody. After 30 minutes of ICAM-1 crosslinking, fully developed rings of bundled F-actin were visible at cell borders. There was also increased tyrosyl-phosphorylated protein labelling throughout the cell and this was especially evident at cell-cell junctions. The increased phosphotyrosine labelling appeared to peak prior to the development of cortical actin bundles and had decreased to near baseline levels after 30 minutes. Scale bar = 10 μm

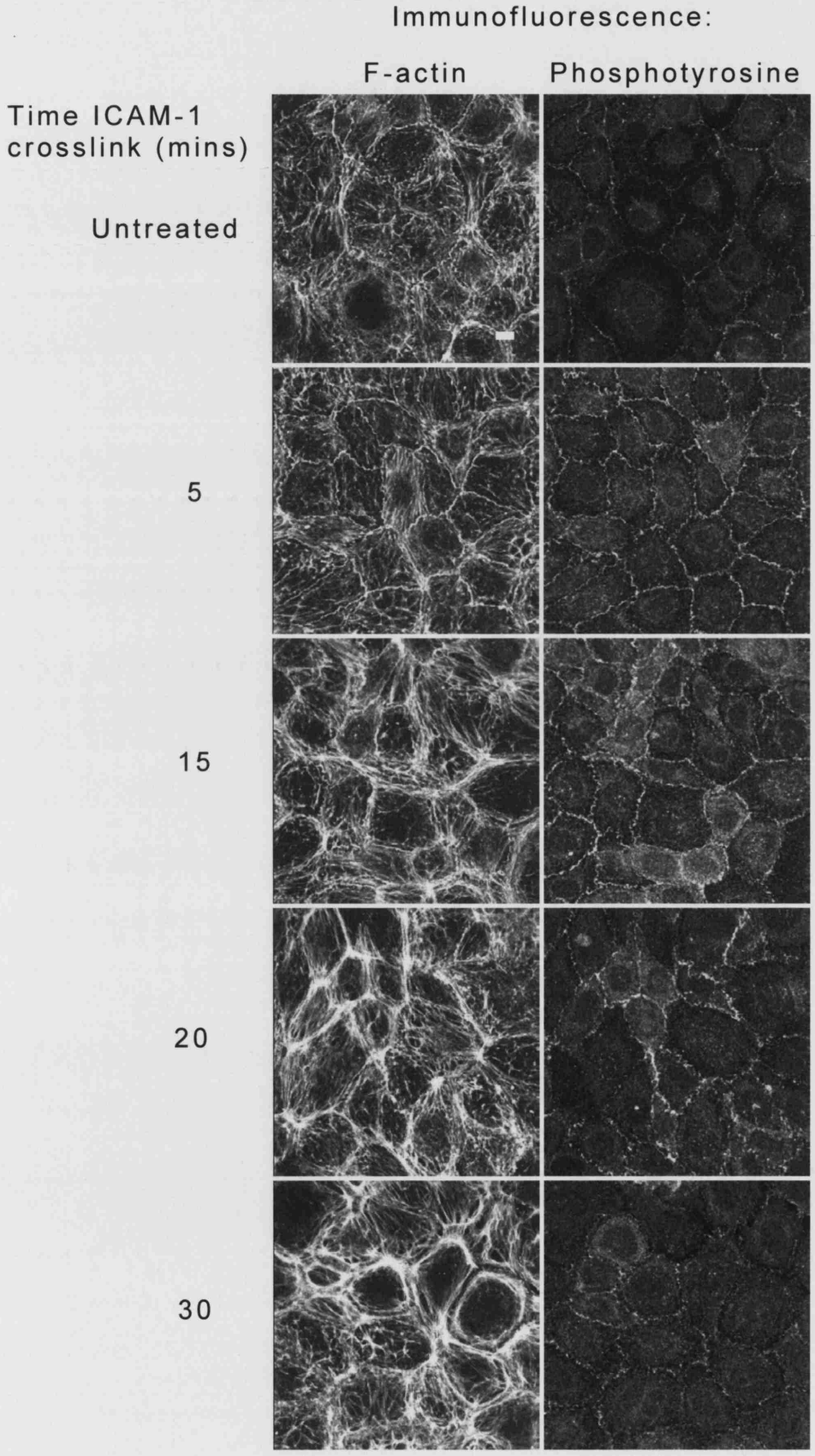
Immunofluorescence:
F-actin
Phosphotyrosine
Time ICAM-1 crosslink (mins)
Untreated
5
15
20
30

4.2.2 VE-cadherin and co-immunoprecipitated proteins are highly tyrosine phosphorylated during culture in growth medium

Tyrosine phosphorylation has been reported to modulate the adhesive function of many junctional proteins (described in greater detail in section 1.4), therefore the possibility that components of cell-cell junctions are downstream targets of ICAM-1-mediated intracellular signalling cascades was investigated by isolating individual junctional proteins from cell extracts following ICAM-1 crosslinking. It is possible that factors within the serum present in the growth medium used to culture the cells may induce tyrosine phosphorylation of junctional proteins and thus inhibit the formation of stable junctions. This may occur through modulating the junctional proteins directly or by providing a constant stimulus for the cells to proliferate; a process that would not promote stable junction assembly (Lampugnani et al., 1997). If under these in vitro culture conditions the junctional proteins are in a state of hyper-tyrosine phosphorylation then this may mask potential changes induced by other signalling pathways. In the first instance we thus investigated whether, following ICAM-1 crosslinking, we could identify alterations in tyrosine phosphorylation of junctional proteins in complete growth medium.

The adherens junction protein VE-cadherin, that is believed to be the central structural molecule of adherens junctions (Dejana et al., 1999; Hordijk et al., 1999), was immunoprecipitated from control and ICAM-1-crosslinked brain endothelial cell monolayers grown in complete culture medium. Under these conditions, VE-cadherin (130 kD) in addition to several co-immunoprecipitating proteins at approximately 102, 98 and 84 kD, possibly representing α-, β- and γ-catenin respectively, were all constitutively and highly tyrosine phosphorylated (Fig. 4.5). It was therefore decided to quiesce the endothelial cells by serum-starvation for 24 hours prior to ICAM-1 crosslinking. The process of serum starvation has been used previously within our and other laboratories for investigating other signalling cascades that may be sensitive to serum-derived growth/trophic factors. All other experiments within the crosslinking

studies described in this thesis were therefore performed following 24 hours serum starvation of confluent monolayers.

4.2.3 Both β- and γ-catenin co-immunoprecipitate with VE-cadherin from brain endothelial cells

To positively identify some of the proteins present in the VE-cadherin immunoprecipitates as other constituents of the adherens junction complex, VE-cadherin was immunoprecipitated from both untreated and ICAM-1-crosslinked GPNT cell extracts and samples immunoblotted for both of the catenins known to directly associate with its intracellular domain. Both β- and γ-catenin co-immunoprecipitated with VE-cadherin and this association was unaffected by ICAM-1 crosslinking (Fig. 4.6).

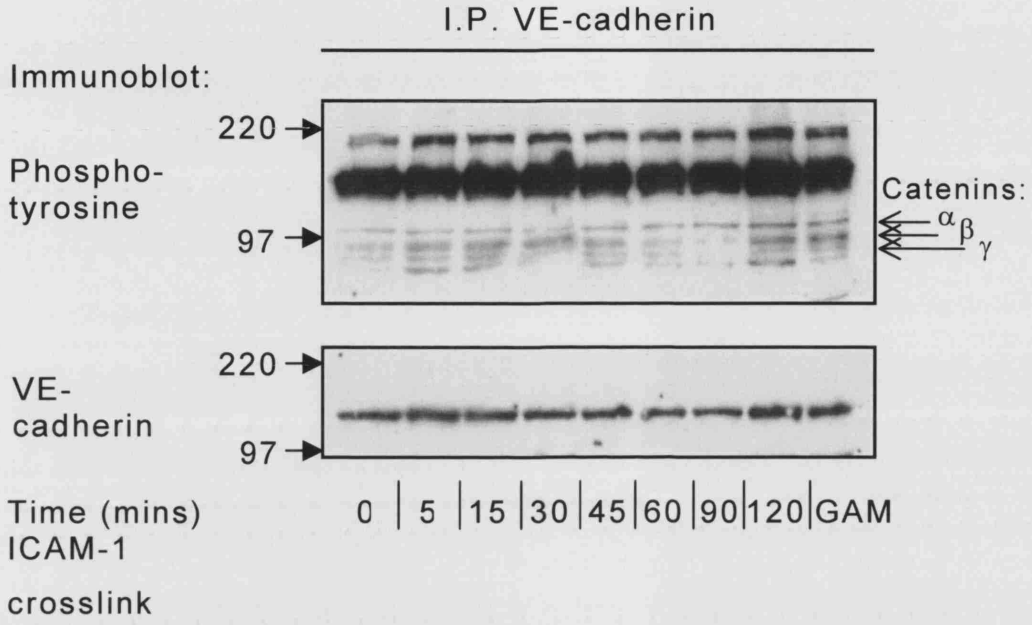

Fig. 4.5 VE-cadherin and co-immunoprecipitated proteins are highly tyrosine phosphorylated during culture in complete growth medium
GPNT ICAM-1 was crosslinked for varying times, VE-cadherin immunoprecipitated from cell extracts and samples fractionated by SDS-PAGE prior to immunoblotting for phosphotyrosine (4G10). Membranes were then stripped and reprobed for VE-cadherin as an indication of protein loading. VE-cadherin (130 kD) was extremely highly tyrosine phosphorylated in these culture conditions and this did not change following ICAM-1 crosslinking. Several other co-immunoprecipitating proteins were also highly tyrosine phosphorylated. GAM denotes samples not crosslinked but treated with GAM alone for 15 minutes. The position of molecular standards with known molecular mass (kD) is indicated by arrows.

Fig. 4.6 Both β- and γ-catenin co-immunoprecipitate with VE-cadherin from brain endothelial cells
GPNT cell monolayers were either ICAM-1 crosslinked (XL) for 30 minutes or untreated (-) before being lysed and VE-cadherin immunoprecipitated. Samples were then fractionated by SDS-PAGE and immunoblotted for VE-cadherin with a polyclonal antibody. Membranes were then successively stripped and re-probed for β- and γ-catenin. Both catenins co-immunoprecipitate with VE-cadherin and this does appear to be affected by ICAM-1 crosslinking. The position of molecular standards with known molecular mass (kD) is indicated by arrows. Data shown are representative of 3 independent experiments

4.2.4 Tyrosine phosphorylation of VE-cadherin increases following ICAM-1 crosslinking in brain endothelial cells

Following ICAM-1 crosslinking, junctional proteins were isolated by immunoprecipitation (IP) from crosslinked whole cell extracts and samples immunoblotted for phosphotyrosine. VE-cadherin IPs revealed a single tyrosine phosphorylated band of approximately 130 kD whose phosphotyrosine status increased with time of ICAM-1 crosslinking (Fig. 4.7). The increase in phosphorylation was evident after 15 minutes and by 30 minutes had increased to double that exhibited by uncrosslinked samples. This induced phosphorylation increased further still and was approximately three times that of control samples after 90 minutes of ICAM-1 crosslinking. The scale of this observed effect is reminiscent of the tyrosine phosphorylation changes of VE-cadherin observed following neutrophil co-culture with coronary venular ECs (Tinsley et al., 1999), exposure of dermal microvascular ECs to histamine (Andriopoulou et al., 1999) and HUVEC exposure to VEGF (Esser et al., 1998). In each case it has been reported that the observed changes in phosphotyrosine are not a strictly 'on-off' mechanism but an overall increase in phosphotyrosine content from a low basal level in unstimulated cells to a significantly enhanced level in treated cells. There were no other phosphotyrosine containing bands in VE-cadherin immunoprecipitates suggesting that associated catenins do not alter in their tyrosine phosphorylation status. To ensure that the observed increase in tyrosine phosphorylation of VE-cadherin is not an indirect effect of aggregating cell-surface molecules, cell-surface major histocompatability complex (MHC) class I molecules (Greenwood et al., 1996) were crosslinked using an identical protocol to that used for crosslinking ICAM-1. There was no evidence of tyrosine phosphorylation of immunoprecipitated VE-cadherin in samples treated with the anti-MHC antibody alone or those having this molecule crosslinked. There was a partial response to the addition of the anti-ICAM-1 antibody possibly due to the dimerisation of ICAM-1 upon the cell surface being capable of transducing signals sufficient to elicit limited signalling.

Fig. 4.7 Tyrosine phosphorylation of VE-cadherin increases following ICAM-1 crosslinking in brain endothelial cells

Panel A, VE-cadherin was immunoprecipitated from ICAM-1 crosslinked GPNT cell extracts, samples fractionated by SDS-PAGE and immunoblotted for phosphotyrosine (4G10). Membranes were then stripped and reprobed for VE-cadherin as an indication of protein loading. The tyrosine phosphorylation of VE-cadherin (130 kD) increased steadily following ICAM-1 crosslinking up to the final time point. There was no evidence of tyrosine phosphorylation of co-immunoprecipitated β- and γ-catenin. GAM denotes samples not crosslinked but treated with GAM alone for 15 minutes. The position of molecular standards with known molecular mass (kD) is indicated by arrows. Data shown are representative of 4 independent experiments.

Panel B, Densitometric analysis of VE-cadherin tyrosine phosphorylation. The densitometric intensities (see section 2.9) expressed as a percentage of control (uncrosslinked) intensity from 4 independent experiments were pooled and plotted as mean (±SEM) values. Mean values for each time point were compared with control by Students t-test. *, $P<0.05$; **, $P<0.01$

Panel C, Tyrosine phosphorylation of VE-cadherin does not increase following MHC class I crosslinking in brain endothelial cells. GPNT cells were either untreated (-) or treated with anti-ICAM-1 antibody (1A29) alone for 30 minutes (1°) or ICAM-1 crosslinked for 30 minutes (XL). Alternatively, GPNT cells were treated with anti-MHC class I (DAKO) antibody alone for 30 minutes (MHC 1°) or had MHC class I crosslinked for 30 minutes using the anti-MHC class I antibody followed by GAM (MHC XL).

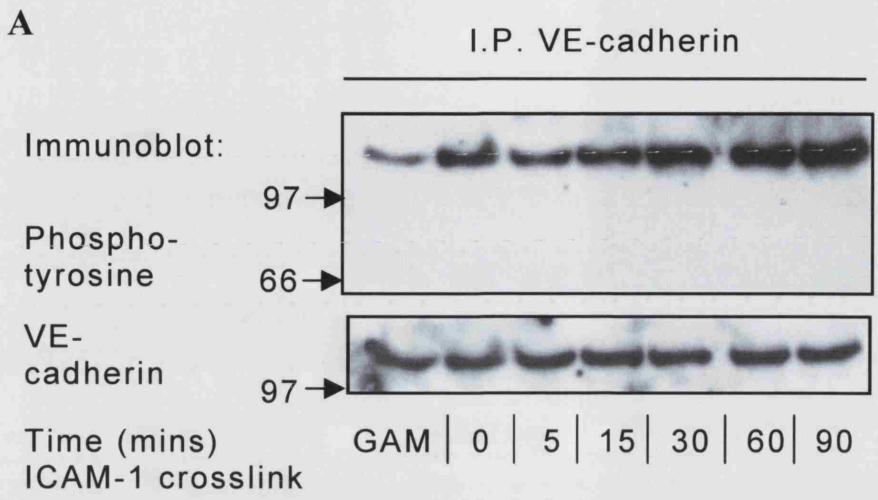
A
I.P. VE-cadherin
Immunoblot:
97
Phospho-
tyrosine
66
VE-
cadherin
97
Time (mins)
ICAM-1 crosslink
GAM | 0 | 5 | 15 | 30 | 60 | 90

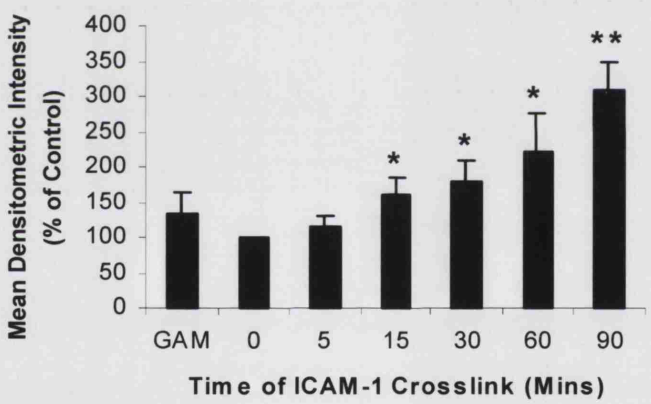
B
Mean Densitometric Intensity
(% of Control)
400
350
300
250
200
150
100
50
0
*
*
*
**
GAM
0
5
15
30
60
90
Time of ICAM-1 Crosslink (Mins)

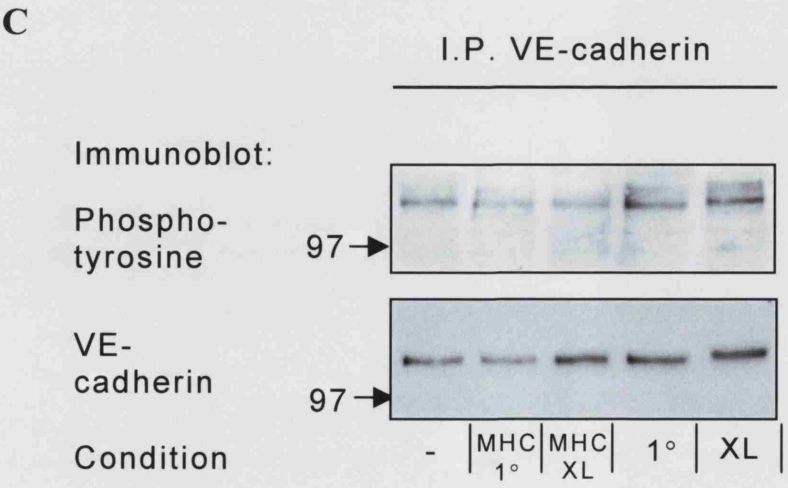
C
I.P. VE-cadherin
Immunoblot:
Phospho-
tyrosine
97
VE-
cadherin
97
Condition
-
MHC
1°
MHC
XL
1°
XL

4.2.5 ICAM-1 crosslinking induces tyrosine phosphorylation of VE-cadherin in the brain endothelial cell line RBE4

To confirm that ICAM-1 crosslinking in brain endothelial cells results in increased tyrosine phosphorylation of VE-cadherin, an alternative rat brain endothelial cell line, RBE4, was used. VE-cadherin was immunoprecipitated from RBE4 cells following ICAM-1 crosslinking under identical experimental conditions to those described for GPNT cells (Fig. 4.8). As in GPNT cells, VE-cadherin tyrosine phosphorylation increased steadily over time up to 90 minutes following crosslinking in RBE4 cells. Also as with GPNT cells, there were no indications that any other tyrosine phosphorylated proteins were present in VE-cadherin immunoprecipitates.

4.2.6 VE-cadherin is present in detergent-insoluble and detergent-soluble fractions of cell extracts and the distribution is not affected by ICAM-1 crosslinking

VE-cadherin is known to interact directly with vimentin and indirectly with the actin cytoskeleton through α-catenin (described in greater detail in Chapter 1). This interaction provides a connection linking the cytoskeletons of neighbouring cells through the lateral cell-cell junctions. Via these interactions it is possible that the cytoskeleton is able to regulate cell junctions and vice versa. We therefore investigated whether ICAM-1 crosslinking alters the association of VE-cadherin with the cytoskeleton by investigating its detergent solubility. An increase in the detergent-solubility of VE-cadherin, suggestive of a decreased association with cytoskeletal elements, has been previously described following treatment with histamine; a stimulus that also induced tyrosine phosphorylation of VE-cadherin (Andriopoulou et al., 1999). Following ICAM-1 crosslinking, however, no alteration in the distribution of VE-cadherin between the detergent-soluble and –insoluble fraction was observed with VE-cadherin being partitioned equally between the two fractions (Fig. 4.9 Panel A). To ensure that VE-cadherin partitioning is not being distorted by indirect binding to other proteins, the insoluble cell fraction was washed with

a range of high salt-containing buffers. Following recovery of the cell extract by the normal protocol (described in section 2.5), the insoluble pellet was resuspended in fresh buffer with greatly elevated concentrations of NaCl (0.6 or 1.2 mol dm^{-3}). These samples were subsequently immunoblotted for VE-cadherin (Fig. 4.9 Panel B). The exposure of the Triton X-100 insoluble cell fractions to high NaCl-containing buffers, both in resting cells and following ICAM-1 crosslinking, did not result in any further extraction of VE-cadherin from the insoluble pellet. These studies suggest that the presence of VE-cadherin in the Triton X-100 insoluble fraction is unlikely to be due to indirect binding to other proteins contained within the insoluble pellets.

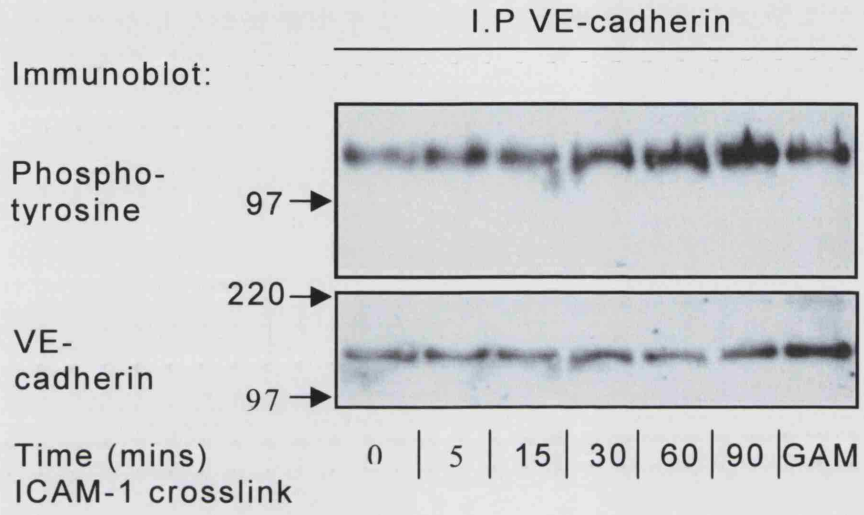

Fig. 4.8 ICAM-1 crosslinking induces tyrosine phosphorylation of VE-cadherin in the brain endothelial cell line RBE4

RBE4 cell surface ICAM-1 was crosslinked for varying times and VE-cadherin immunoprecipitated from cell extracts. Samples were fractionated by SDS-PAGE and immunoblotted for phosphotyrosine (4G10). Membranes were then stripped and reprobed for VE-cadherin as an indication of protein loading. As in GPNT cells, the tyrosine phosphorylation induced by ICAM-1 crosslinking increased up to the final time point. GAM denotes samples not crosslinked but treated with GAM alone for 15 minutes. The position of molecular standards with known molecular mass (kD) is indicated by arrows. Data shown are representative of 2 independent experiments.

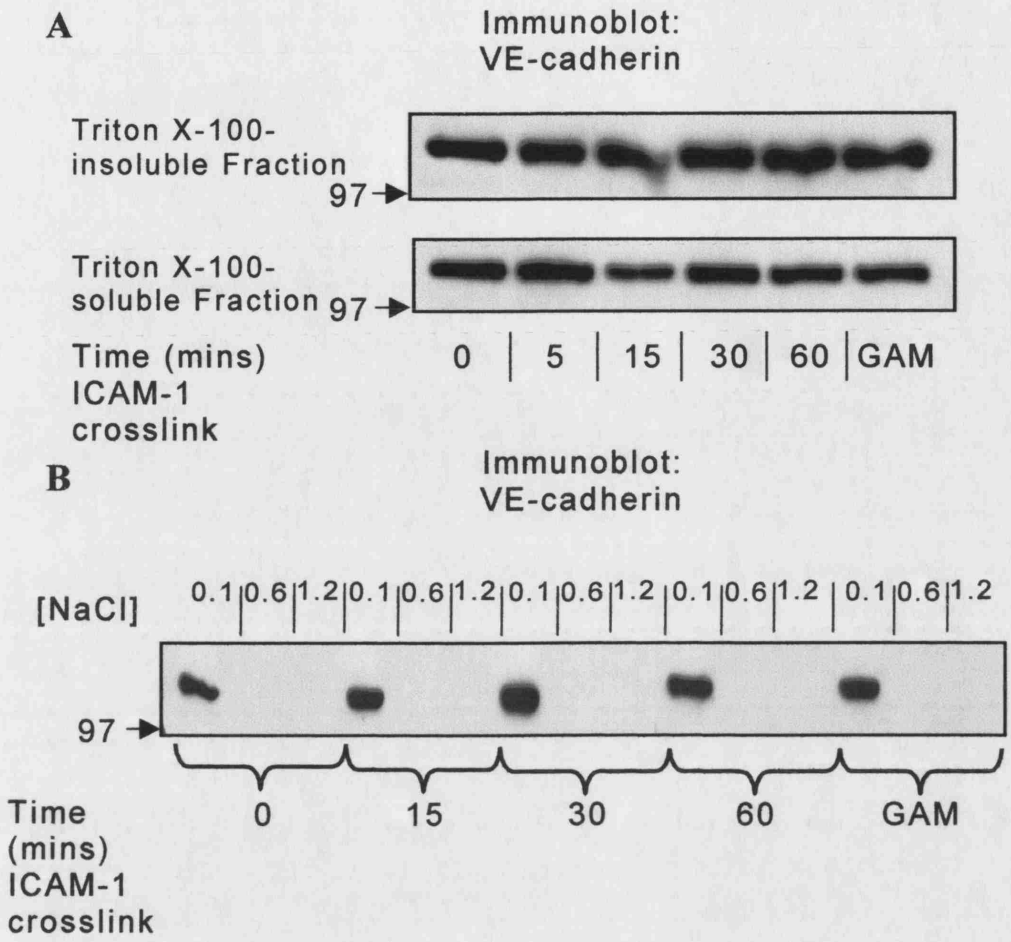

Fig. 4.9 VE-cadherin is equally distributed between detergent-insoluble and detergent-soluble fractions of cell extracts and this is not affected by ICAM-1 crosslinking

Panel A, GPNT monolayers were ICAM-1 crosslinked for varying times and cells fractionated into Triton-soluble and Triton-insoluble fractions (see section 2.22). Samples were fractionated by SDS-PAGE and immunoblotted for VE-cadherin. VE-cadherin was equally distributed between the triton-soluble and –insoluble cell fractions and this did not change following ICAM-1 crosslinking. Data are representative of 2 independent experiments.

Panel B, GPNT monolayers were ICAM-1 crosslinked for varying times, monolayers lysed and the insoluble pellet extracted with increasing concentrations of NaCl (see section 2.23). Equal volumes of samples were then fractionated by SDS-PAGE and immunoblotted for VE-cadherin. The extraction of VE-cadherin by the protocol used is efficient and increasing the concentration of sodium chloride does not increase the amount of VE-cadherin recovered from the insoluble pellet following lysis in either untreated cells or following ICAM-1 crosslinking.

4.2.7 ICAM-1 crosslinking does not alter tyrosine phosphorylation of γ-catenin but does increase tyrosine phosphorylation of co-immunoprecipitated VE-cadherin

As demonstrated above, immunoprecipitation of VE-cadherin from brain endotheial cells results in the co-immunoprecipitation of γ-catenin. Moreover, this data showed that the co-immunoprecipitated γ-catenin was not tyrosine phosphorylated under either non-crosslinked or ICAM-1 crosslinked conditions. However, as not all cellular γ-catenin is associated with VE-cadherin, γ-catenin was immunoprecipitated directly from cell extracts of ICAM-1 crosslinked monolayers and phosphotyrosine immunoblots generated that demonstrated that γ-catenin was not tyrosine phosphorylated throughout the time course of the experiment (Fig. 4.10). However, a very prominent phosphotyrosine labelled band of approximately 130 kD whose phosphotyrosine increased over the time of ICAM-1 crosslinking was detected in anti-γ-catenin immune complexes. The molecular size of this band and the kinetics of the phosphorylation suggested that this band represented co-immunoprecipitated VE-cadherin. Following stripping and re-probing of the membrane with an anti-VE-cadherin antibody the identity of this band was confirmed as VE-cadherin. This increase in phosphotyrosine was not due to an increase in protein as the amount of VE-cadherin present in all γ-catenin IPs remained constant throughout the time course. This demonstrates that these two molecules remain associated following the tyrosine phosphorylation of VE-cadherin induced following ICAM-1 crosslinking.

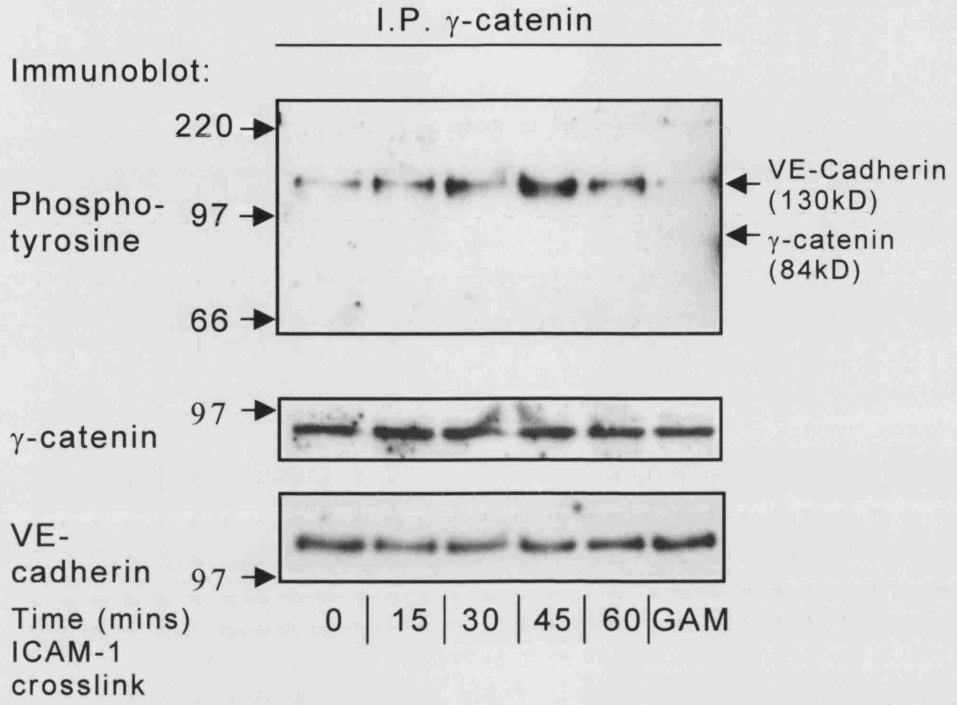

Fig. 4.10 Tyrosine phosphorylation of γ-catenin is unaltered following ICAM-1 crosslinking whereas co-immunoprecipitated VE-cadherin becomes tyrosine phosphorylated without change in association to γ-catenin in brain endothelial cells

ICAM-1 was crosslinked for a time course and γ-catenin immunoprecipitated from GPNT cell extracts. Samples were fractionated by SDS-PAGE and immunoblotted for phosphotyrosine (4G10) before membranes were stripped and reprobed for γ-catenin as an indication of protein loading and then stripped and reprobed for VE-cadherin. There was no evidence of tyrosine phosphorylation of γ-catenin (84 kD) but co-immunoprecipitating VE-cadherin was increasingly tyrosine phosphorylated following ICAM-1 crosslinking. The approximate position of γ-catenin is indicated by its position within a pervanadate-treated positive control lane (omitted for clarity). GAM denotes samples not crosslinked but treated with GAM alone for 15 minutes. The position of molecular standards with known molecular mass (kD) is indicated by arrows. Data shown are representative of 3 independent experiments.

4.2.8 ICAM-1 crosslinking does not alter tyrosine phosphorylation of β-catenin but does increase tyrosine phosphorylation of co-immunoprecipitated VE-cadherin

To establish whether β-catenin becomes tyrosine phosphorylated following ICAM-1 crosslinking, brain endothelial cell extracts were prepared and β-catenin was immunoprecipitated. Samples were then immunoblotted to detect phosphotyrosine-containing proteins (Fig. 4.11). As with γ-catenin, ICAM-1 crosslinking did not lead to tyrosine phosphorylation of β-catenin at any time point during the experiment. In a similar manner to that observed for γ-catenin, a tyrosine phosphorylated band of 130 kD appeared that showed increased phosphotyrosine intensity following crosslinking. Stripping and reprobing of the membrane confirmed that this band was VE-cadherin. There was no change in the relative association between these two molecules following ICAM-1 crosslinking.

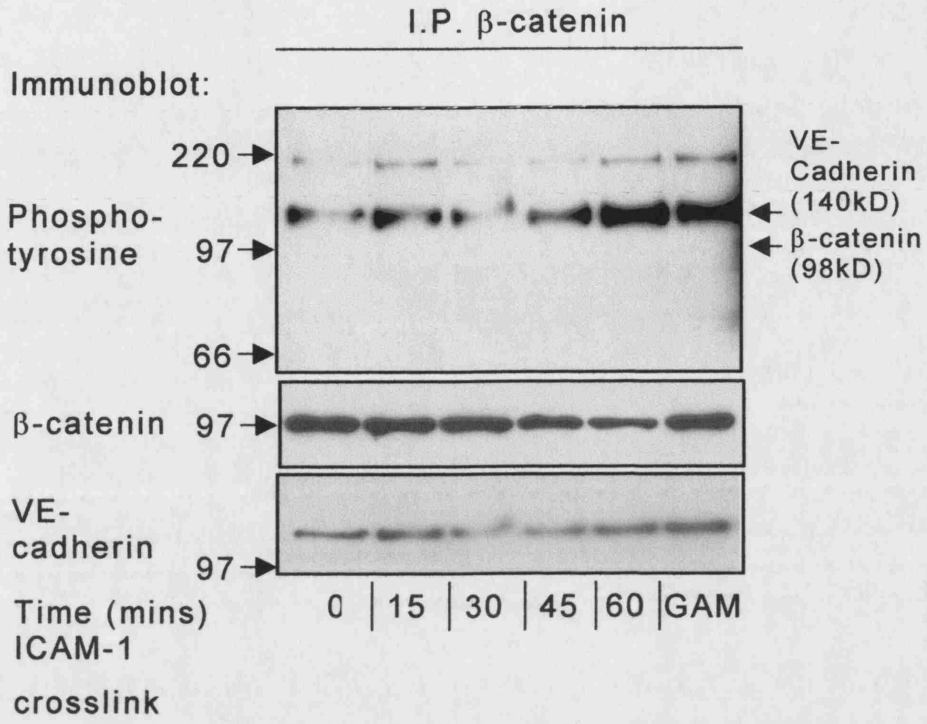

Fig. 4.11 Tyrosine phosphorylation of β-catenin is unaltered following ICAM-1 crosslinking whereas co-immunoprecipitated VE-cadherin becomes tyrosine phosphorylated without change in association to β-catenin in brain endothelial cells

ICAM-1 was crosslinked and β-catenin immunoprecipitated from GPNT cell extracts. Samples were then fractionated by SDS-PAGE and immunoblotted for phosphotyrosine (4G10). Membranes were then stripped and reprobed for β-catenin as an indication of protein loading and then stripped and immunoblotted for VE-cadherin. As with γ-catenin, there was no evidence of tyrosine phosphorylation of β-catenin (98 kD) but co-immunoprecipitated VE-cadherin became increasingly tyrosine phosphorylated following ICAM-1 crosslinking. The position of β-catenin is indicated by its position within a pervanadate-treated positive control lane (omitted for clarity). GAM denotes samples not crosslinked but treated with GAM alone for 15 minutes. The position of molecular standards with known molecular mass (kD) is indicated by arrows. Data shown are representative of 3 independent experiments.

4.2.9 Tyrosine phosphorylation of α-catenin is unaltered following ICAM-1 crosslinking

As with γ- and β-catenin, the potential for α-catenin to be tyrosine phosphorylated following ICAM-1 crosslinking was assayed. α-catenin was immunoprecipitated as with the other catenins and immune complexes immunoblotted for phosphotyrosine (Fig. 4.12). α-catenin was not tyrosine phosphorylated throughout the time course of crosslinking studied. The appearance of a tyrosine phosphorylated band of approximately 130 kD was once again present that was more intense at the 60 minute time point. Re-probing of this blot with the VE-cadherin antibody did not detect VE-cadherin which may be due to the very low levels of co-immunoprecipitated VE-cadherin within the α-catenin IPs. This likely resulted in a below-threshold signal following successive stripping of the membrane. It is known that the association of α-catenin with VE-cadherin is indirect, being mediated via either β- or γ-catenin and hence co-immunoprecipitation with either anti-α-catenin or anti-VE-cadherin monoclonal antibodies is inefficient (Lampugnani et al., 1995). As the 130 kD band was detected with an anti-phosphotyrosine monoclonal antibody but not the VE-cadherin antibody this suggests that the co-immunoprecipitated form of VE-cadherin, if this is the true identity of the band, may be highly phosphorylated.

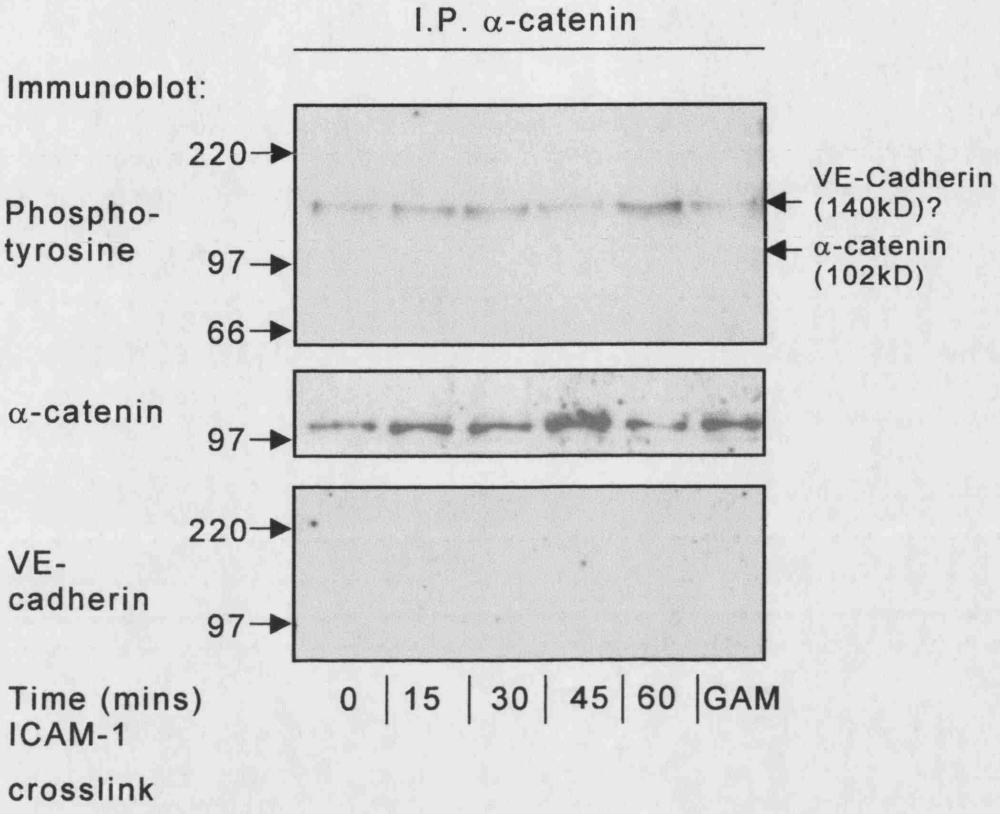

Fig. 4.12 Tyrosine phosphorylation of α-catenin is unaltered following ICAM-1 crosslinking

ICAM-1 was crosslinked and α-catenin immunoprecipitated from GPNT cell extracts using an antibody generated in mice. Samples were fractionated by SDS-PAGE and immunoblotted for phosphotyrosine (4G10). Membranes were then stripped and reprobed with a rabbit polyclonal antibody to α-catenin as an indication of protein loading and then stripped and immunoblotted for VE-cadherin. As with β- and γ-catenin, there was no evidence of tyrosine phosphorylation of α-catenin but a co-immunoprecipitating protein of approximately 130 kD increased in tyrosine phosphorylation following ICAM-1 crosslinking but a similar band was not detected following re-probing with the anti-VE-cadherin antibody. The position of α-catenin is indicated by a pervanadate-treated positive control lane (omitted for clarity). GAM denotes samples not crosslinked but treated with GAM alone for 15 minutes. The position of molecular standards with known molecular mass (kD) is indicated by arrows. Data shown are representative of 3 independent experiments.

4.2.10 Tyrosine phosphorylation of p120 is unaltered following ICAM-1 crosslinking

The VE-cadherin-associated catenin p120 was also immunoprecipitated from crosslinked brain endothelial cell extracts and analysed by phosphotyrosine immunoblotting. Unlike VE-cadherin, but similar to α-, β and γ-catenin, p120 was not detectably tyrosine phosphorylated throughout the duration of the crosslinking experiment (Fig. 4.13). However, unlike the other catenins studied there was no trace of a tyrosine phosphorylated protein around 130 kD. The lack of co-immunoprecipitated VE-cadherin was confirmed by the absence of immunoreactivity following reprobing with a VE-cadherin antibody. This finding suggests that in confluent monolayers of brain ECs there is no, or very weak, interaction between these two molecules as has been demonstrated previously in HUVECs (Lampugnani et al., 1997). In contrast to the other catenins, it has also been reported that pro-inflammatory mediators such as VEGF do not induce tyrosine phosphorylation of p120 but rather a dephosphorylation on serine and threonine residues as indicated by a shift in electrophoretic mobility of the protein (Ratcliffe et al., 1997; Ratcliffe et al., 1999; Wong et al., 2000). In our study, however, we were unable to observe a change in molecular size following ICAM-1 crosslinking although a clear shift towards a higher molecular weight was visible following pervanadate-induced hyperphosphorylation.

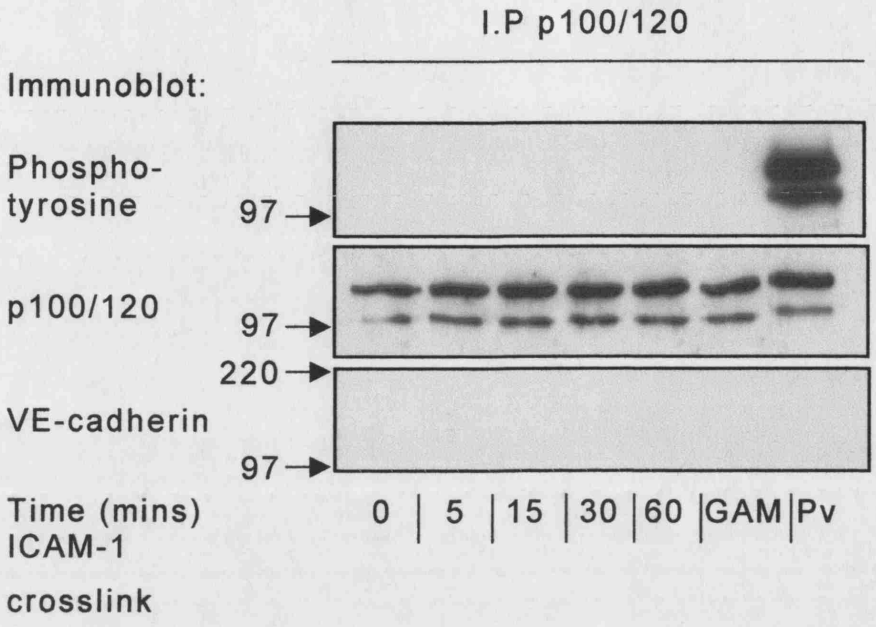

Fig. 4.13 Tyrosine phosphorylation of p120 is unaltered following ICAM-1 crosslinking
ICAM-1 was crosslinked and p120 immunoprecipitated from GPNT cell extracts. Samples were then fractionated by SDS-PAGE and immunoblotted for phosphotyrosine (4G10). Membranes were then stripped and reprobed for p120 as an indication of protein loading and then stripped and immunoblotted for VE-cadherin. There was no evidence of tyrosine phosphorylation of p120 in either untreated or ICAM-1 crosslinked cells. There was no detectable phosphotyrosine bands at the position of VE-cadherin and re-probing with the anti-VE-cadherin antibody failed to detect a signal. There was also no change in the electrophoretic mobility of p120 following ICAM-1 crosslinking as occurs following stimulation of endothelial cell with a range of pro-inflammatory mediators. GAM denotes samples not crosslinked but treated with GAM alone for 15 minutes. Pv denotes samples treated with pervanadate. The position of molecular standards with known molecular mass (kD) is indicated by arrows. Data shown are representative of 3 independent experiments.

4.2.11 Tyrosine phosphorylation of ZO-1 is unaltered following ICAM-1 crosslinking

In addition to components of adherens junctions, the potential for crosslinking of ICAM-1 to induce changes in tyrosine phosphorylation of tight junction components, previously suggested as a potential mechanism regulating vascular and endothelial permeability, was also assertained. Due to the lack of expression of endogenous claudin-5 (unpublished observations), only ZO-1 and occludin (using the cell line expressing wild-type chick occludin described in chapter 3) were assayed. Following crosslinking of ICAM-1 there was no tyrosine phosphorylation of ZO-1 throughout the duration of the experiment (Fig. 4.14 Panel A) or any noticeable change in electrophoretic mobility. A reduction in electrophoretic mobility was evident following treatment of ECs with pervanadate, a strong inducer of tyrosine phosphorylation (Fig. 4.14 Panel B).

4.2.12 Tyrosine phosphorylation of occludin is unaltered following ICAM-1 crosslinking

The possibility that occludin is modulated by intracellular signalling pathways elicited following ICAM-1 crosslinking was investigated by repeating the protocol described above using the cell line expressing wild-type chick occludin (described in chapter 3). Following crosslinking of ICAM-1 there was no indication of induced tyrosine phosphorylation of the ectopic occludin (Fig. 4.15).

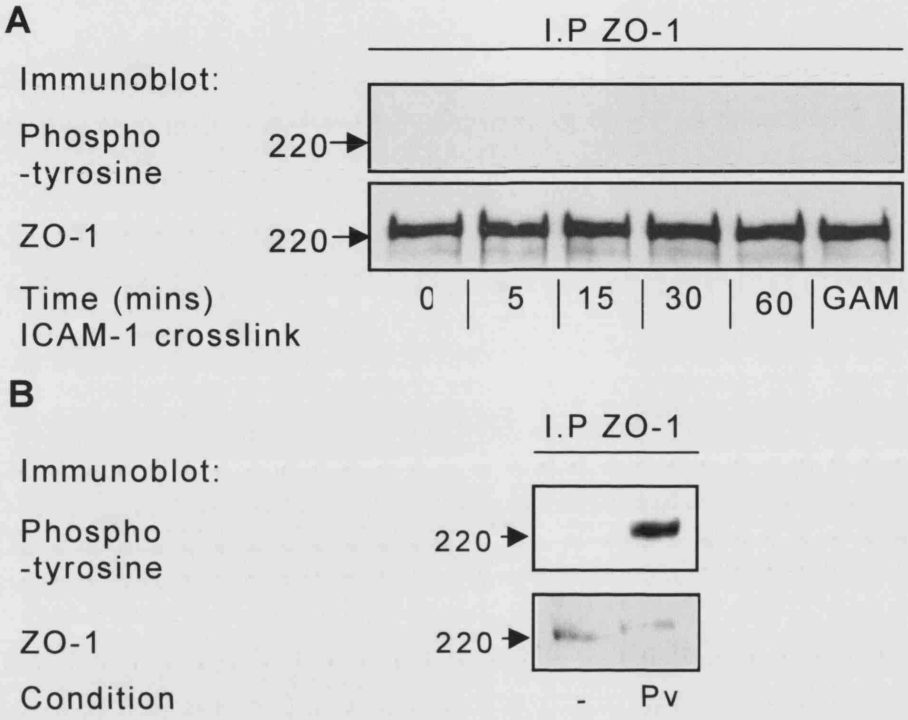

Fig. 4.14 Tyrosine phosphorylation of ZO-1 is unaltered following ICAM-1 crosslinking

Panel A, ICAM-1 was crosslinked for varying times and ZO-1 immunoprecipitated from GPNT cell extracts. Samples were then fractionated by SDS-PAGE and immunoblotted for phosphotyrosine (4G10). Membranes were then stripped and reprobed for ZO-1 as an indication of protein loading. There was no evidence of tyrosine phosphorylation of ZO-1 in either untreated or ICAM-1 crosslinked monolayers. GAM denotes samples not crosslinked but treated with GAM alone for 15 minutes. The position of molecular standards with known molecular mass (kD) is indicated by arrows. Data shown are representative of 3 independent experiments.

Panel B, GPNT monolayers were either untreated (-) or treated with pervanadate (Pv). Cells were then lysed, and processed for immunoprecipitation and immunoblotting of ZO-1 as above. ZO-1 is capable of becoming tyrosine phosphorylated and under these conditions its electrophoretic mobility is reduced.

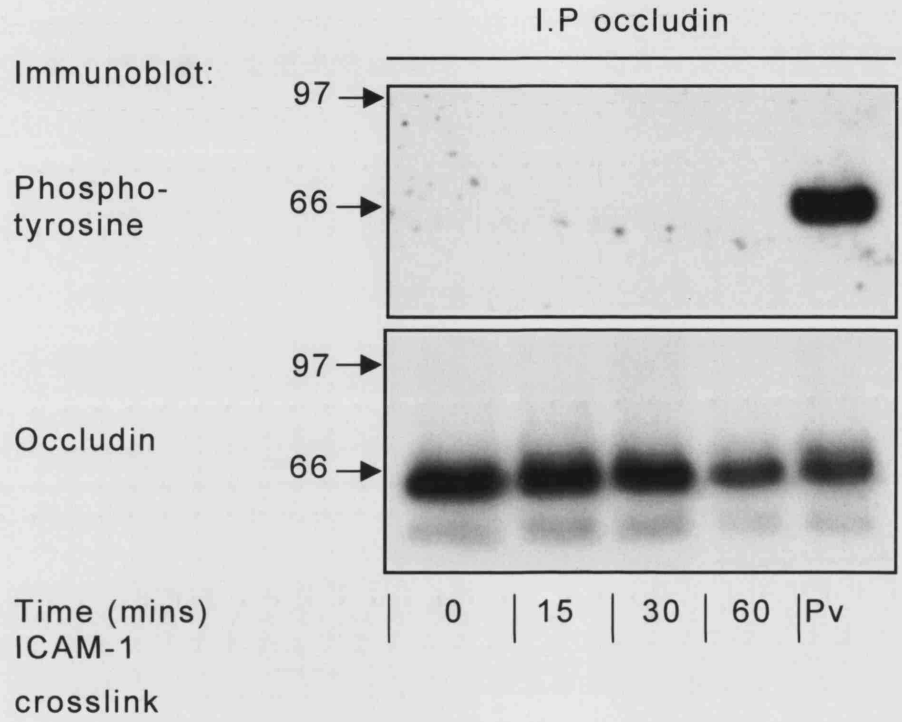

Fig. 4.15 Tyrosine phosphorylation of occludin is unaltered following ICAM-1 crosslinking
ICAM-1 was crosslinked on occludin-transfected GPNT cells for varying times and occludin immunoprecipitated from cell extracts. Samples were then fractionated by SDS-PAGE and immunoblotted for phosphotyrosine (4G10). Membranes were then stripped and reprobed for occludin as an indication of protein loading. There was no evidence of tyrosine phosphorylation of ectopic occludin in either untreated or ICAM-1 crosslinked cells. GAM denotes samples not crosslinked but treated with GAM alone for 15 minutes. The position of molecular standards with known molecular mass (kD) is indicated by arrows. Data shown are representative of 3 independent experiments.

4.2.13 The permeability of brain endothelial cell monolayers is increased following ICAM-1 crosslinking

As ICAM-1 crosslinking results in F-actin rearrangement and tyrosine phosphorylation of junctional proteins, we next investigated whether there was any alteration in the functional integrity of the EC monolayer following crosslinking of ICAM-1. The permeability of GPNT monolayers grown on semi-permeable filters to fluorophore-conjugated dextrans (FITC-dextran) of 4, 40 and 140 kD was assayed. Permeability to the 40 and 140 kD tracers was found to be significantly increased following crosslinking of ICAM-1 when compared to control monolayers treated with the secondary antibody (GAM) alone (Fig. 4.16) suggesting a reduction in the integrity of cell-cell junctions. The observed difference in permeability between the two groups became more pronounced with increasing molecular size of the tracer. There was no difference between groups in the diffusion of a 4 kD FITC-dextran tracer across the monolayers (Panel A) but significant differences were observed when the tracer was 40 kD in size ($P < 0.05$, Panel B) becoming more significant with 140 kD FITC-dextran ($P < 0.001$, Panel C). The different results obtained with tracers of different size suggests that there is a size limit to molecules that the junctions of these cells are able to provide a diffusion barrier against. Thus, molecules of around 4 kD are too small to be inhibited in their diffusion across the monolayer by lateral cell-cell junctions in this model. The permeability differences between the two groups were evident from 10 minutes following crosslinking to the end of the experiment after 50 minutes.

Fig. 4.16 The permeability of brain endothelial cell monolayers is increased following ICAM-1 crosslinking
Permeability assays were performed following ICAM-1 crosslinking using 4 kD (panel A), 40 kD (panel B) or 140 kD FITC-dextran (panel C) as a molecular tracer. Control filters were not incubated with the anti-ICAM-1 antibody but treated with SFM containing GAM and FITC-dextran alone. There were no significant differences in permeability between the crosslinked and control monolayers with the 4 kD tracer but the ICAM-1 crosslinked monolayers were more permeable to the two larger tracers than the control monolayers. This permeability difference was evident after 10 minutes of crosslinking with both 40 kD and 140 kD tracers and when using the 140 kD tracer the relative difference between the ICAM-1 crosslinked and control monolayers increased over time. Data from 3 independent experiments, each performed in triplicate, were pooled and expressed as the mean ± SEM for each time point for both crosslinked and control samples. Significant differences between crosslinked and control values were determined by Student's *t* test for each time point. *, $p<.05$. **, $p<.01$. ***, $p<.001$.

A

4 kDa FITC-dextran

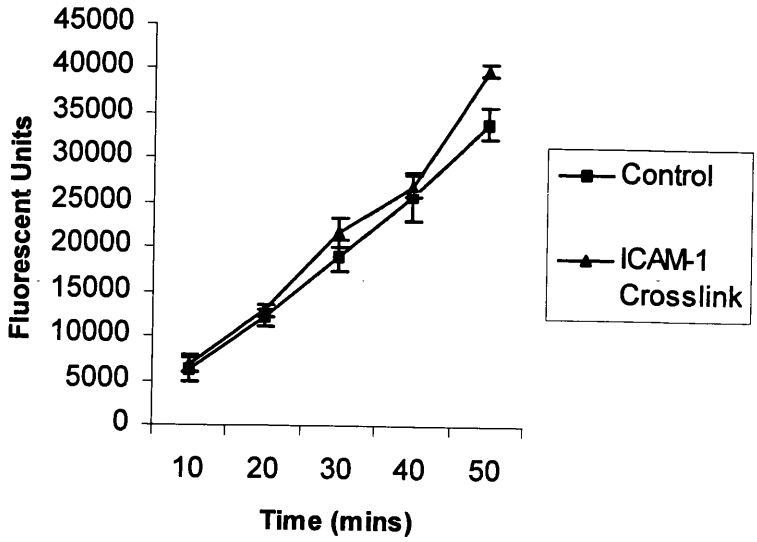

B

40 kDa FITC-dextran

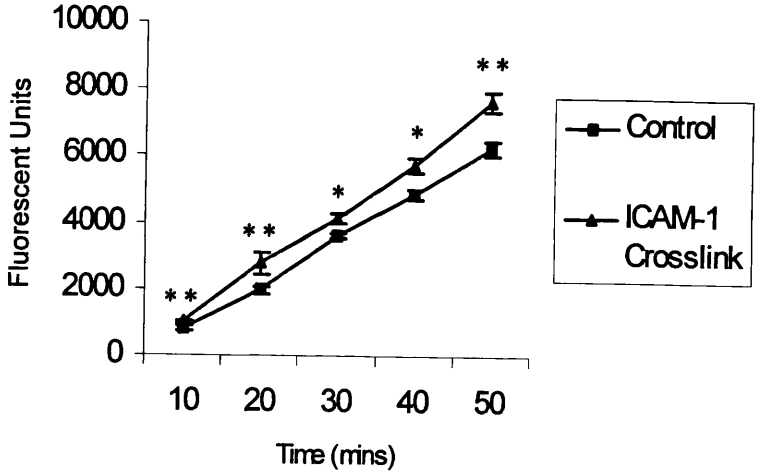

C

140 kDa FITC-dextran

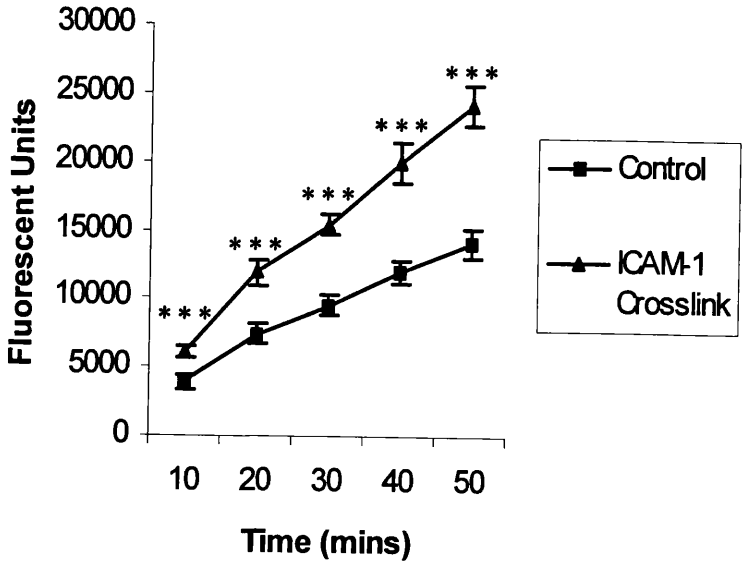

4.3 Discussion

It has been demonstrated in the past decade that ECs are actively involved in leucocyte recruitment following signalling cascades initiated through cell surface adhesion molecules such as ICAM-1 (Greenwood et al., 2002; Hordijk, 2003). These presumably 'prepare' the EC to support the migration of an interacting immune cell. A link between cell adhesion molecule signalling and modulation of cell junctions has been suggested in presentations and publications ever since the first paper describing ICAM-1 signalling (Durieu-Trautman et al., 1994). The data presented in this chapter identifies the first downstream effect of such signalling on a junctional protein. Not only did we observe induction of tyrosine phosphorylation of VE-cadherin but also an increase in monolayer permeability suggesting that this pathway has functional relevance. Indeed, evidence from studies using blocking antibodies and calcium chelators demonstrate VE-cadherin to be of central importance in regulating endothelial permeability (Corada et al., 1999; Hordijk et al., 1999; Gao et al., 2000).

Increased tyrosine phosphorylation of VE-cadherin and catenins has previously been described in response to both co-culture with activated neutrophils (Tinsley et al., 1999; Tinsley et al., 2002) and to pro-inflammatory mediators such as VEGF (Esser et al., 1998; Nawroth et al., 2002), histamine (Andriopoulou et al., 1999; Shasby et al., 2002) and thrombin (Ukropec et al., 2000). In each case, tyrosine phosphorylation was also associated with an increase in endothelial permeability. In the studies presented here with brain endothelial cells there was no tyrosine phosphorylation of either α-, β-, γ- or p120-catenin and no change in the association of β- or γ-catenin with tyrosyl-phosphorylated VE-cadherin. It remains to be elucidated whether the lack of phosphotyrosine signalling to catenins following ICAM-1 crosslinking represents a more discrete mechanism of junctional disengagement than that elicited through pro-inflammatory mediators, where sustained hyperpermeability and junctional 'leakiness' is observed. In coronary venular endothelial cells, co-culture with activated neutrophils results in both β-catenin and VE-cadherin becoming tyrosine phosphorylated (Tinsley et al., 1999).

Whilst this may be particular to signals induced by neutrophils or to this vascular endothelium, it is possible that the multitude of ICAM-1-independent interactions that occur during leucocyte migration are necessary to trigger the requisite signalling cascades required for tyrosine phosphorylation of catenins. Thus, activation of ICAM-1 mediated signalling pathways may only be one component of a complex array of activation pathways that lead to full junctional disengagement. The nature of the signalling pathway that leads to tyrosine phosphorylation of VE-cadherin is currently unknown and is the subject of an on-going investigation within this lab. Nonetheless, data from several sources make it apparent that the function of cadherins and the actin cytoskeleton are intimately connected (Braga et al., 1997; Takaishi et al., 1997; Hordijk et al., 1999, Adamson et al., 2002; Lampugnani et al., 2002; van Wetering et al., 2002). As demonstrated by Hordijk and colleagues (Hordijk et al., 1999), the distribution of VE-cadherin within both immortalised cell lines and freshly-isolated endothelium is regulated by factors affecting the actin cytoskeleton. Treatment of HUVEC cultures with the β_2 adrenergic receptor agonist isoproterenol, that increases intracellular levels of cAMP, reduced the amount of stress fibres and increased cortical actin. Concomitant with these changes was an alteration in the spatial distribution of VE-cadherin at cell borders, where it was found to become linear and continuous, and a decrease in transmonolayer permeability that was associated with the cells assuming a more flattened morphology. From these data the authors conclude that β_2 adrenergic stimulation alters the 'normal' phenotype of these cells. Interestingly, this altered phenotype is reminiscent of the brain EC phenotype. It could be argued, therefore, that the increase in cortical F-actin stress fibres and the increased permeability in brain ECs following crosslinking of ICAM-1 is the converse of this phenomena and that actin reorganisation, VE-cadherin modulation and increased permeability are part of a mechanism through which 'tight' brain ECs transiently assume the phenotype of more 'leaky' peripheral endothelia such as HUVECs. As has been highlighted in the introduction, actin stress fibre formation is dependent on signalling through the small GTPase rho and this has also been shown to be involved in the regulation of adherens junction integrity. Moreover, in

brain endothelial cells the intimate involvement of the actin cytoskeleton and rho proteins has previously been demonstrated in mediating ICAM-1-induced signalling and subsequent leucocyte transendothelial migration (Etienne et al., 1998; Adamson et al., 1999; Sans et al., 2001; van Buul et al., 2002). Pharmacological inhibitors of rho activation may therefore have potential as inhibitors of leucocyte recruitment at the BBB although it is likely that specificity may be difficult to achieve resulting in possibly toxic side-effects.

Except for the large submembranous scaffold protein ZO-1 and ectopic occludin, this investigation only considered adherens junction proteins. The transmembrane protein constituents of tight junctions are occludin and the claudin proteins. The lack of endogenous claudin-5 expression and the paucity of reliable anti-claudin antibodies prevented investigation into signalling to these proteins. It is possible that the phosphorylation of VE-cadherin following ICAM-1 crosslinking and the disassociation of adherens junctions may in turn destabilise tight junctions. Alternatively, the signalling pathway from ICAM-1 may diverge to modulate both adherens and tight junction components in parallel. Interestingly, recent reports describe the regulation of occludin by both PKC (Andreeva et al., 2001) and rho-mediated signalling (Hirase et al., 2001), both of which are activated following ICAM-1 crosslinking in brain endothelial cells (Etienne et al., 1998; Adamson et al., 1999).

The demonstration that junctional proteins can be modulated by cell adhesion molecule-mediated signalling represents a step forward in unravelling the highly complex process of leucocyte migration across the BBB. Whether the pathways described here are true for all vascular beds, or whether this is a brain endothelial-specific mechanism requires further investigation. Greater understanding of these pathways will undoubtedly reveal molecular targets for the rational development of treatments for (neuro)inflammatory disease. The results presented here do not attempt to understate the importance of other adhesion molecules such as VCAM-1, PECAM and the JAMs whose biology and roles in inflammation represent equally valid targets for anti-inflammatory research and therapy.

Chapter 5:

Crosslinking of ICAM-1 Modulates PECAM in Brain Endothelial Cells

5.1 Introduction

Both epithelial and ECs possess adherens and tight junctions that provide and regulate their lateral cell-cell adhesion (described in greater detail in Chapter 1). ECs lack desmosomes, hemidesmosomes and desmosomal cadherins that connect adjacent epithelial cells and that internally interact with the intermediate filament network. They do however possess an additional cell-cell adhesive interaction that is mediated by the homophilic interaction of PECAM-1 (hereafter PECAM) across the paracellular cleft (Newman, 1997). PECAM is a 120 kD glycoprotein belonging to the Ig superfamily of cell adhesion molecules and is frequently used as an endothelial-specific marker. In addition to ECs, PECAM is also expressed by platelets, monocytes, neutrophils, NK and T cells (Alexander et al., 2001). Within confluent monolayers of ECs, PECAM localises to the region of cell-cell contact and to the apical lumen-facing aspect of blood vessels whereas within migratory ECs and in subconfluent endothelial cultures it is diffusely distributed on the cell surface (Schimmenti et al., 1992). The importance of PECAM to leucocyte adhesion and transendothelial migration has been demonstrated by in vitro and in vivo studies using pre-treatment of either the ECs or neutrophils/monocytes with anti-PECAM antibodies. Leucocyte transmigration is significantly inhibited in both cases in vitro and in vivo suggesting that both are important for efficient cell-cell interactions (Muller et al., 1993; Vaporciyan et al., 1993; Wakelin et al., 1996; Thompson et al., 2000; Mamdouh et al., 2002; Cao et al., 2002). Leucocytes in PECAM gene knockout mice show a transient arrest between the vascular endothelium and the basal lamina during transmigration at inflammatory foci (Duncan et al., 1999; Thompson et al., 2001). These knockout mice also suffer from prolonged bleeding times due to the inefficient EC-platelet interaction. Transvascular migration of leucocytes is thought to occur predominantly at post-capillary venules during homeostatic conditions and, as the distribution of PECAM is throughout the vascular system, it suggests that PECAM may serve other regulatory and signalling functions. Indeed, as with ICAM-1, PECAM is more than a mechanical, anchoring cell adhesion molecule and is capable of transducing signals upon oligomerisation following either homophilic

interactions or antibody-mediated PECAM crosslinking (Piali et al., 1993; Berman and Muller, 1995; Pellegatta et al., 1998). Engagement of cell-surface PECAM in platelets, neutrophils, NK and T cells leads to an upregulation of integrin function by the induction of high avidity sites and cytoskeletal association of β_2 and β_1 integrins (Piali et al., 1993; Berman and Muller, 1995) possibly through signalling by the small GTPase Rap (Bos et al., 2003). These changes regulate leucocyte adhesion and migration across ECs as well as the subendothelial extracellular matrix (Buckley, 2001). Following both biochemical and mechanical stimulation of ECs, PECAM has been demonstrated to undergo phosphorylation of specific tyrosine residues within an immunoreceptor tyrosine-based activation motif (ITAM) spanning residues 663 to 686 within the cytoplasmic tail (Lu et al., 1997). This has been shown to mediate selective recruitment of several signalling molecules including Shp-1 (Hua et al., 1998) and –2 (Jackson et al., 1997), SHIP, PLC-γ (Pumphrey et al., 1999) and PI3K (Pellegatta et al., 1998). Both β- and γ-catenin are also able to associate with PECAM and it has been suggested that via association with γ-catenin, PECAM may be a constituent and regulator of the complexus adhaerentes adhesion system within ECs (Ilan et al., 1999; Ilan et al., 2000).

The data presented in this chapter demonstrates that the junctional cell adhesion molecule PECAM, in addition to VE-cadherin as described in Chapter 4, is a downstream target of intracellular signalling induced by ICAM-1 crosslinking in GPNT brain ECs.

5.2 Results

5.2.1 PECAM becomes tyrosine phosphorylated following ICAM-1 crosslinking

PECAM immunoprecipitates from brain endothelial lysates using the monoclonal antibody 4E8 revealed a band of 120 kD whose phosphotyrosine content increased following ICAM-1 crosslinking (Fig. 5.1). Stripping and reprobing of the blot with a polyclonal anti-PECAM antibody confirmed the identity of the band to be PECAM and that protein loading was equal. The increased tyrosine

phosphorylation of PECAM was evident after 15 minutes of addition of the crosslinking secondary antibody and was maximal after approximately 30 minutes. The phosphorylation at 60 minutes had decreased to a level similar to that observed after 15 minutes and remained at this level until the final time point of 90 minutes. As with VE-cadherin, it was investigated whether crosslinking of MHC class I could induce the tyrosine phosphorylation of PECAM in the same manner as ICAM-1. There was no evidence of tyrosine phosphorylation of immunoprecipitated PECAM in all samples except that which had been ICAM-1 crosslinked suggesting that this induced tyrosine phosphorylation is not a result of non-specific aggregation of cell-surface molecules.

5.2.2 PECAM association with β- and γ-catenin is increased following ICAM-1 crosslinking

We next investigated whether β- and γ-catenin are associated with PECAM in GPNT cells and whether such an association alters following ICAM-1 crosslinking. The amount of β- and γ-catenin that was co-immunoprecipitated within PECAM IPs was greatly increased following ICAM-1 crosslinking and this correlated with the increased tyrosine phosphorylation of PECAM (Fig. 5.2). There was no evidence of tyrosine phosphorylation of the co-immunoprecipitated catenins. The increase in γ-catenin was less pronounced that that of β-catenin but showed similar kinetics. An increase in association of both catenins to PECAM was also observed in cells treated with the secondary antibody (GAM) alone and this was much more apparent with β-catenin.

Fig. 5.1 PECAM becomes tyrosine phosphorylated following ICAM-1 crosslinking

Panel A, ICAM-1 was crosslinked for varying times and PECAM immunoprecipitated from cell extracts using the monoclonal antibody 4E8. Samples were then fractionated by SDS-PAGE and immunoblotted for phosphotyrosine (4G10). Membranes were then stripped and reprobed using a polyclonal antibody to PECAM as an indication of protein loading. Tyrosine phosphorylation of PECAM (120 kD) was increased after 15 minutes of ICAM-1 crosslinking and was maximal at 30 minutes after which it decreased slightly until the final time point of 90 minutes. GAM denotes samples not crosslinked but treated with GAM alone for 15 minutes. The position of molecular standards with known molecular mass (kD) is indicated by arrows. Data shown are representative of 3 independent experiments.

Panel B, Densitometric analysis of PECAM tyrosine phosphorylation. The densitometric intensities expressed as a percentage of control (uncrosslinked) intensity from 3 independent experiments were pooled and plotted as mean(±SEM) values.

Panel C, Tyrosine phosphorylation of PECAM does not increase following MHC class I crosslinking in brain endothelial cells. GPNT cells were either untreated (-) or treated with anti-ICAM-1 antibody (1A29) alone for 30 minutes (1°) or ICAM-1 crosslinked for 30 minutes (XL). Alternatively, GPNT cells were treated with anti-MHC class I antibody (DAKO) alone for 30 minutes (MHC 1°) or had MHC class I molecules crosslinked for 30 minutes using the anti-MHC class I antibody followed by GAM (MHC XL).

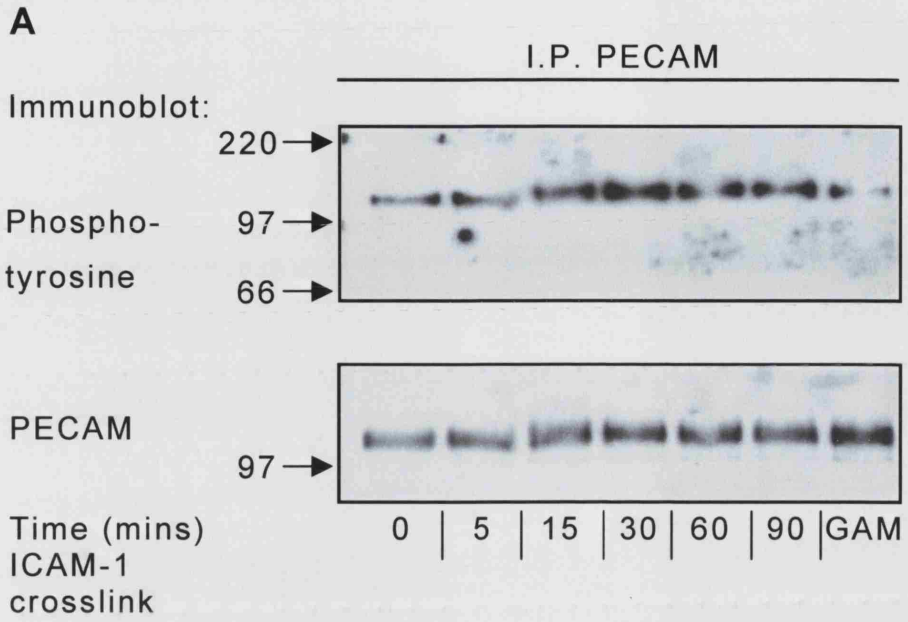
A
I.P. PECAM
Immunoblot:
220
Phospho-
97
tyrosine
66
PECAM
97
Time (mins)
0
5
15
30
60
90
GAM
ICAM-1
crosslink

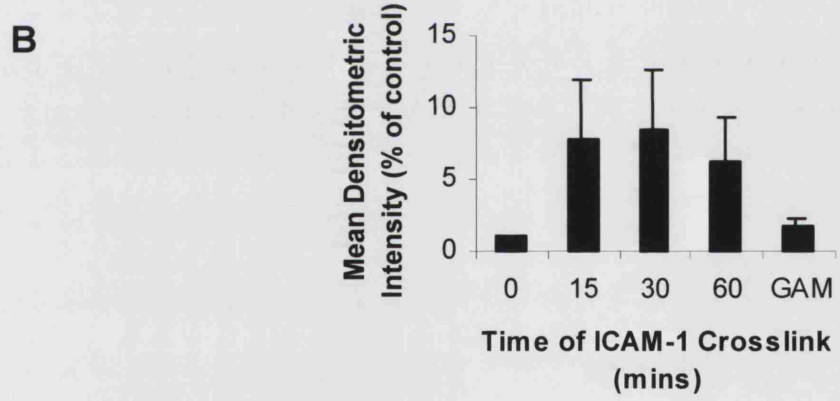
B
Mean Densitometric Intensity (% of control)
15
10
5
0
0
15
30
60
GAM
Time of ICAM-1 Crosslink (mins)

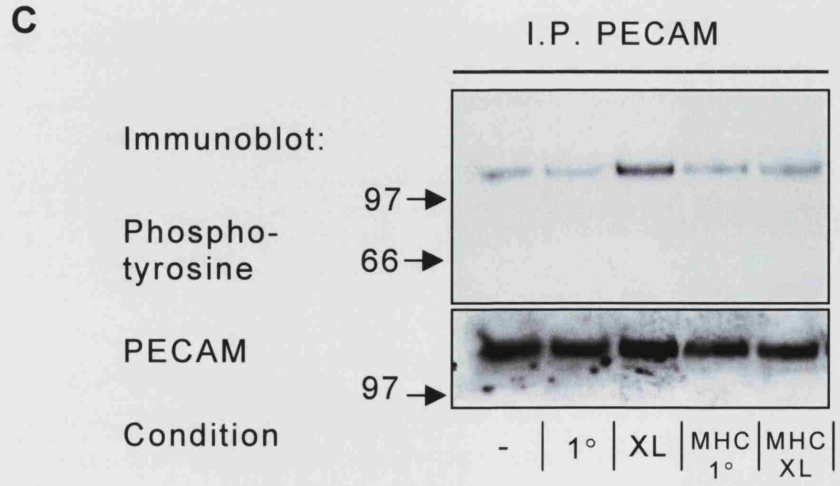
C
I.P. PECAM
Immunoblot:
97
Phospho-
66
tyrosine
PECAM
97
Condition
-
1°
XL
MHC 1°
MHC XL

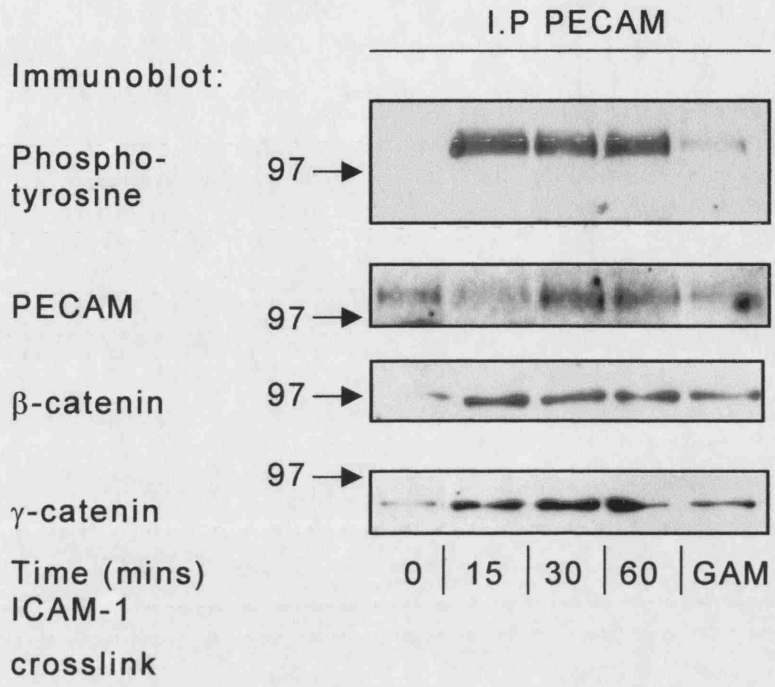

Fig. 5.2 PECAM association with β- and γ-catenin is increased following ICAM-1 crosslinking
ICAM-1 was crosslinked for varying times and PECAM immunoprecipitated from cell extracts using the monoclonal antibody 4E8. Samples were then fractionated by SDS-PAGE and immunoblotted for phosphotyrosine (4G10). Membranes were then stripped and reprobed using a polyclonal antibody to PECAM as an indication of protein loading and then succesively stripped and immunoblotted for β-catenin and γ-catenin. The amount of both β- and γ-catenin within PECAM IPs increased following ICAM-1 crosslinking commensurate with the increased tyrosine phosphorylation of PECAM. There was no evidence of tyrosine phosphorylation of co-immunoprecipitated catenins in the phosphotyrosine immunoblots (see also Fig. 5.1). GAM denotes samples not crosslinked but treated with GAM alone for 15 minutes. The position of molecular standards with known molecular mass (kD) is indicated by arrows. Data shown is representative of 3 independent experiments.

5.2.3 The distribution of PECAM within the brain endothelial monolayer becomes less junctional following ICAM-1 crosslinking

To see if the increased tyrosine phosphorylation of PECAM was also associated with a change in its subcellular localisation, we next investigated the distribution of PECAM following ICAM-1 crosslinking by immunofluoresence (Fig. 5.3). The distribution of PECAM in untreated, control monolayers was almost entirely junctional. Following crosslinking of ICAM-1, however, this distribution became increasingly homogenous and after 30 minutes large areas of the monolayer had a diffuse distribution of PECAM over the cell surface. The change in localisation was observed to occur slightly later than the increase in tyrosine phosphorylation with little redistribution after 10-20 minutes of ICAM-1 crosslinking.

5.2.4 PECAM remains within the detergent-soluble fraction of brain endothelial cells following ICAM-1 crosslinking

It has been demonstrated that in migrating and 3-dimensional HUVEC cultures as well as in PECAM-transfected HEK 293 cells that increased association of PECAM with γ-catenin correlates with an increase in the amount of PECAM within a Triton X-100 detergent-insoluble fraction of the cell. This is also associated with PECAM partially co-localising with vimentin that suggests an increase in the association with the cytoskeleton (Ilan et al., 2000). Due to the perceived importance of the cytoskeleton in regulating transendothelial migration, we investigated whether PECAM alters in its Triton X-100 detergent solubility following ICAM-1 crosslinking (Fig. 5.4). PECAM was exclusively located within the triton X-100-soluble fraction of control brain endothelial cells and remained in this fraction following ICAM-1 crosslinking. These data clearly demonstrate that PECAM does not associate with the detergent-insoluble cell fraction under control or crosslinked conditions. Moreover, it demonstrates that association with catenins is not the basis for associating with the insoluble fraction and, by implication, the cytoskeleton.

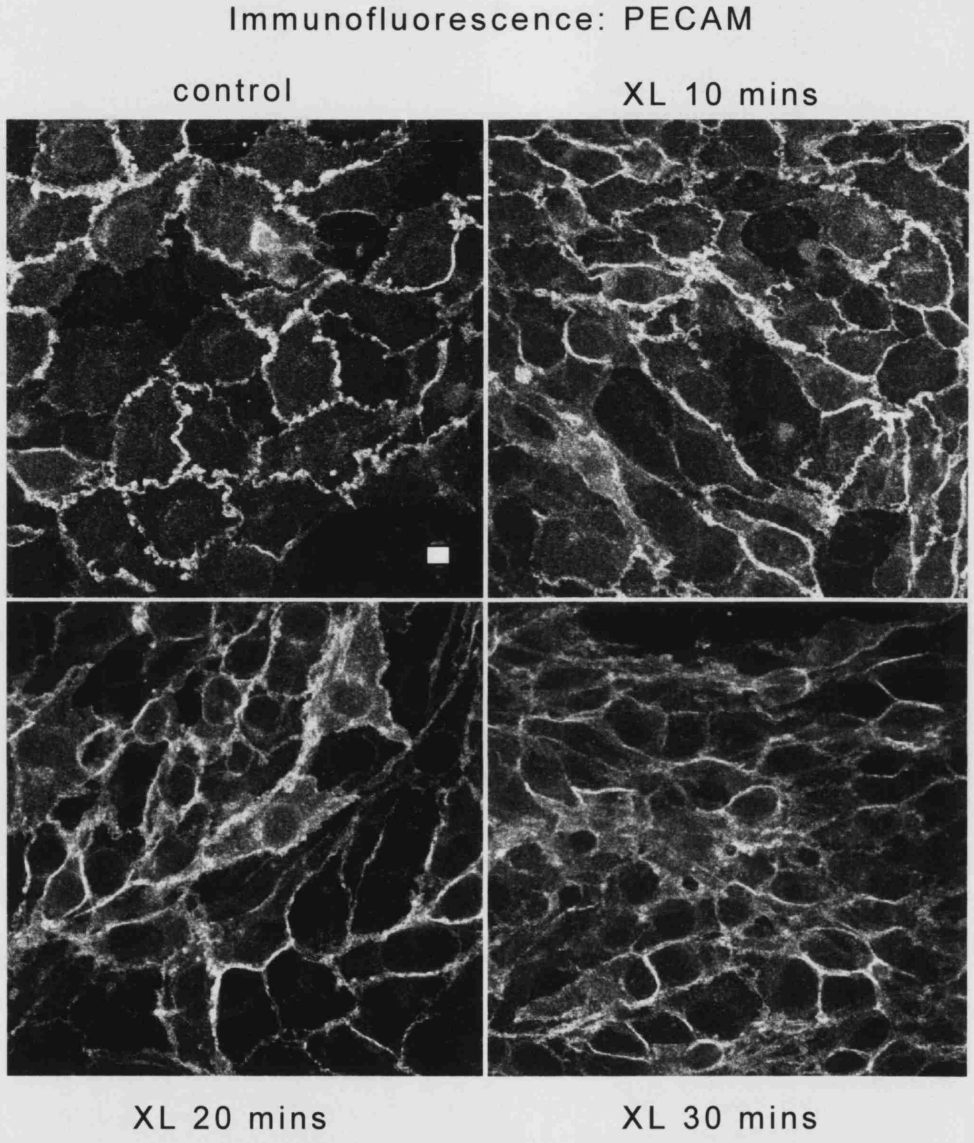

Fig. 5.3 The distribution of PECAM within the brain endothelial monolayer becomes less junctional following ICAM-1 crosslinking
ICAM-1 was crosslinked (XL) for varying times and GPNT cells were fixed with methanal and processed for immunofluorescence using the monoclonal antibody 4E8. PECAM was almost exclusively localised to cell-cell junctions in control (untreated) GPNT monolayers but became diffusely distributed upon the cell surface follwing ICAM-1 crosslinking. Scale bar = 10 μm

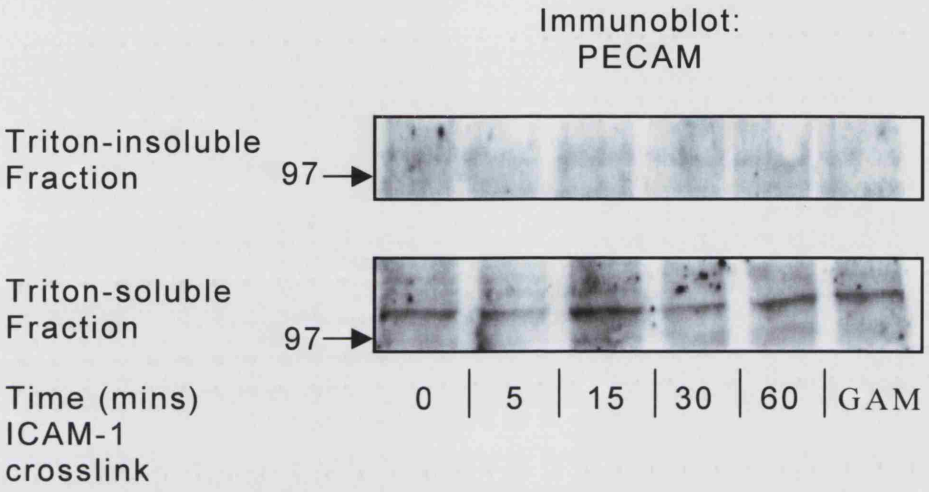

Fig. 5.4 PECAM is within the detergent-soluble fraction of cell extracts from brain endothelial cells and this is unaltered following ICAM-1 crosslinking
ICAM-1 was crosslinked for varying times, cells fractionated into Triton X-100-soluble and –insoluble fractions, samples resolved by SDS-PAGE and immunoblotted for PECAM using a polyclonal antibody. PECAM was only detectable within the detergent-soluble fraction of the cells and this did not alter following ICAM-1 crosslinking. GAM denotes samples not crosslinked but treated with GAM alone for 15 minutes. The position of molecular standards with known molecular mass (kD) is indicated by arrows. Data shown are representative of 2 independent experiments.

5.2.5 Tyrosine phosphorylation of PECAM induced by ICAM-1 crosslinking is unaffected by inhibitors of the rho signalling pathway whereas the recruitment of catenins is inhibited by pre-treatment with the rho-GTPase inhibitor C3 transferase

Pre-treatment of cell monolayers with various metabolic inhibitors to help identify important signalling pathways failed to inhibit the tyrosine phosphorylation of PECAM following ICAM-1 crosslinking. However, when membranes were stripped and reprobed for β-catenin, the samples treated with C3 transferase did not show the ICAM-1-induced increase in PECAM/β-catenin association suggesting that inhibition of rho-family small GTPases inhibits this association (Fig. 5.5 panel A). Treatment of the cells with Y27632, an inhibitor of rho-kinase (ROCK) that is a downstream effector of activated rho, did not inhibit this association. Similar to the effect of inhibitors on the PECAM/β-catenin association, the increased association of γ-catenin was also unaffected by the inhibitors except for C3 transferase. This suggests that there may be a common rho-sensitive/ROCK-independent mechanism by which these two catenins associate with PECAM (Fig. 5.5 panel B). To determine whether any of the inhibitor treatments were affecting the organisation of cell junctions, monolayers were treated with inhibitors or vehicle in an identical manner to that carried out for the immunoblot analysis. Following treatment, and without ICAM-1 crosslinking, cell monolayers were then stained with anti-ZO-1 as a marker of cell junctions (Fig. 5.5 panel C). None of the treatments induced noticeable change in the distribution of ZO-1.

Fig. 5.5 Tyrosine phosphorylation of PECAM induced by ICAM-1 crosslinking is unaffected by inhibitors of rho signalling whereas the recruitment of catenins is inhibited by pre-treatment with the rho-GTPase inhibitor C3 transferase

Panel A and B,

Prior to crosslinking of ICAM-1, GPNT cells were treated with either 10 μmol dm^{-3} cytochalasin D (CytoD) for 30 minutes; 10 μg/ml C3 transferase (C3) for 16 hours or 10 μmol dm^{-3} Y27632 for 30 minutes. Alternatively cells received no inhibitor treatment (-). ICAM-1 was then crosslinked for varying times or cells received GAM only (GAM) and PECAM IPs were prepared from cell extracts as before. Samples were then fractionated by SDS-PAGE and immunoblotted for phosphotyrosine (4G10). Membranes were then stripped and reprobed for PECAM as an indication of protein loading and then succesively stripped and immunoblotted for β-catenin (panel A) and γ-catenin (panel B). None of the inhibitors had an effect on the induced tyrosine phosphorylation of PECAM. The association of both catenins, however, was inhibited by pretreatment with C3-transferase. Data shown are representative of 2 independent experiments in each case.

Panel C,

Confluent monolayers of GPNT cells were treated with a range of inhibitors as described above. SFM indicates cells switched to serum-free medium containing interferon-γ for 24 hours without any inhibitor. Following treatments, cells were fixed with methanol and processed for immunofluorescence. None of the inhibitor treatments induced a disorganisation of ZO-1 suggestive of an effect on cell-cell junctions. None of these samples were ICAM-1 crosslinked. Images are projections of 5 sequential optical sections through the cell. Scale bar = 10 μm

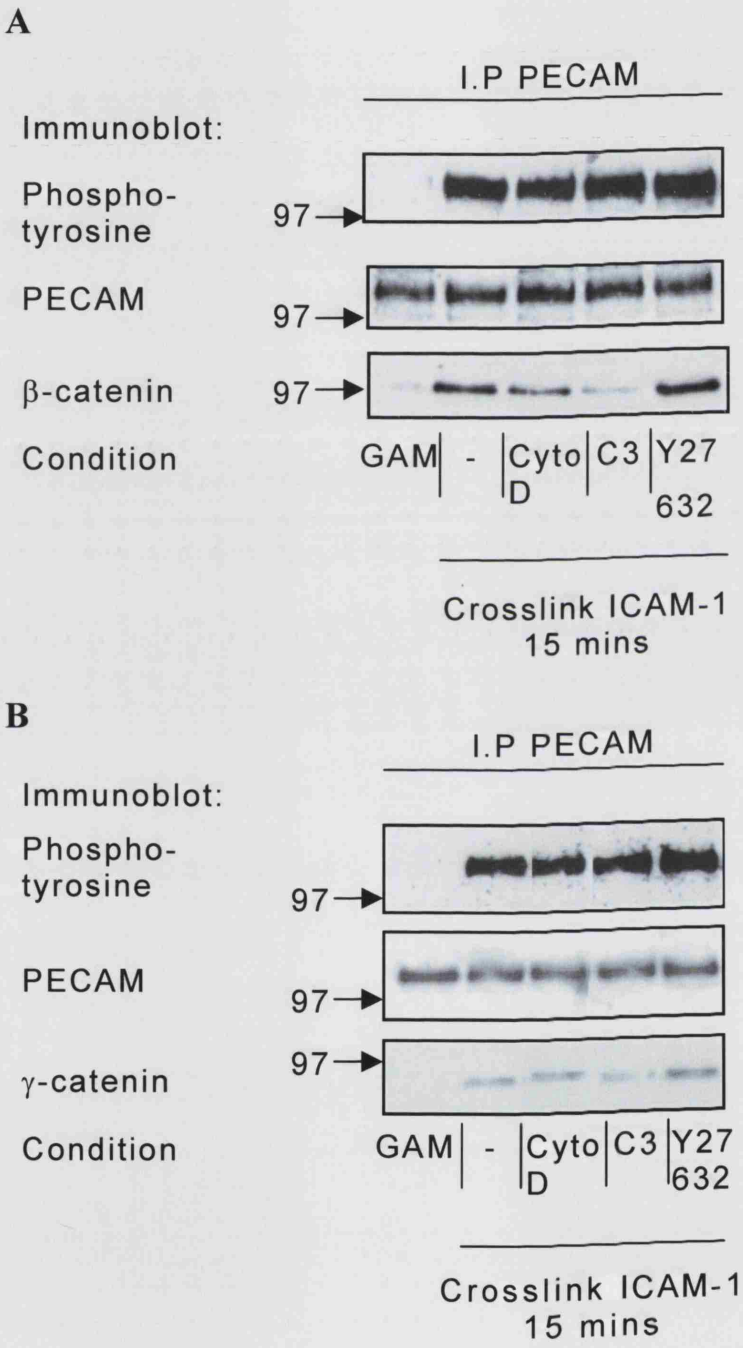
A
I.P PECAM
Immunoblot:
Phospho-tyrosine
97
PECAM
97
β-catenin
97
Condition
GAM
-
Cyto D
C3
Y27 632
Crosslink ICAM-1 15 mins
B
I.P PECAM
Immunoblot:
Phospho-tyrosine
97
PECAM
97
γ-catenin
97
Condition
GAM
-
Cyto D
C3
Y27 632
Crosslink ICAM-1 15 mins

C

Immunofluorescence: ZO-1

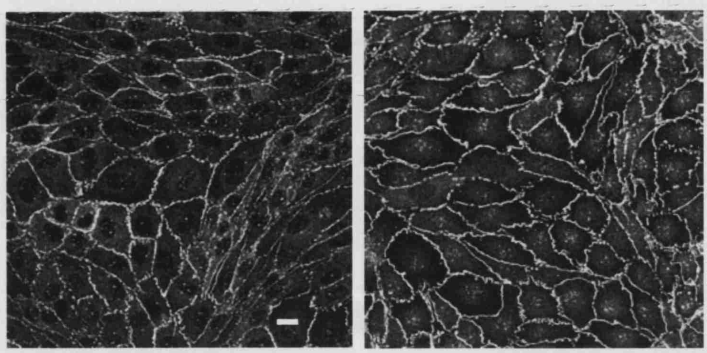

Untreated SFM

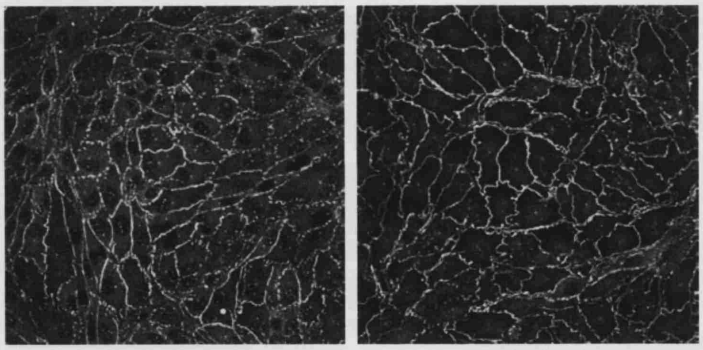

C3 Y27632

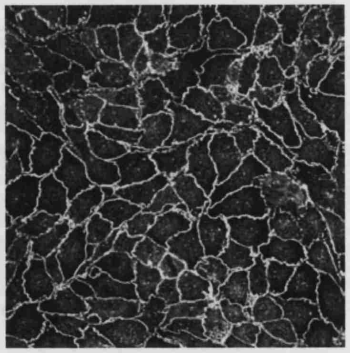

CytoD

5.3 Discussion

Here we provide evidence that crosslinking of ICAM-1 induces tyrosine phosphorylation of the cell adhesion molecule PECAM and this is commensurate with an increase in association with predominantly β-, but also γ-, catenin. Whether these observations are true for all ECs or are particular to brain ECs requires further investigation. The ICAM-1 induced tyrosine phosphorylation of PECAM showed similar kinetics to that observed for VE-cadherin phosphorylation but was perhaps evident slightly sooner. As with VE-cadherin, the level of tyrosine phosphorylation did not return to baseline levels after 90 minutes of crosslinking. This suggests that this is either a slow process or that additional signals are required to activate requisite phosphatases, such as through the ligation of another endothelial ligand that may even be PECAM itself. It must be noted however that the continual stimulation supplied by bound crosslinking antibodies is not necessarily physiological and this may explain the lack of downregulation.

The work of Ilan and colleagues (Ilan et al., 1999 and 2000) has led to the hypothesis that PECAM may function as a reservoir for cytoplasmic catenins as well as serving as a scaffold molecule for bringing phosphorylated catenins into close proximity with the phosphatase SHP-2. This phosphatase also interacts with the cytoplasmic tail of PECAM and catalyses the catenins dephosphorylation. This group also suggest that, in addition to its other roles, PECAM reduces the amount of catenins available and so may downregulate catenin-mediated signalling and transcriptional activity. Their studies on angiogenesis provide one example where such regulation would be desirable, or even necessary, in that ECs are continually exposed to VEGF that, amongst other proteins, activates β-catenin. The constant activation of β-catenin is associated with cell transformation (Zhurinsky et al., 2000) and thus PECAM-catenin interactions may be a mechanism ensuring stability during endothelial proliferation and morphogenesis. Previously published data, and that described in this chapter, suggest a hierarchy of binding interactions between PECAM, β-catenin and possibly γ-catenin that are mediated by the tyrosine phosphorylation of both

PECAM and catenins. It would appear that, under resting conditions, PECAM and β-catenin are not tyrosine phosphorylated and consequently little, if any, interaction between these two proteins occurs. Ilan and colleagues demonstrate that if β-catenin becomes tyrosine phosphorylated however, there is a dramatic increase in the amount of association with PECAM and this is independent of PECAM tyrosine phosphorylation. Data from our study, however, shows that if PECAM is tyrosine phosphorylated there is association with unphosphorylated β-catenin. Tyrosine-phosphorylated PECAM bound both β- and γ-catenin. None of the data described in this chapter conflict with the proposed hypothesis or previous data describing PECAM-catenin interactions. The studies of Ilan and colleagues highlight the importance of β-catenin tyrosine phosphorylation and γ-catenin serine/threonine phosphorylation in regulating these associations. In their system substitution of tyrosine residues in the cytoplasmic tail of PECAM to phenylalanine did not influence catenin association suggesting that tyrosine phosphorylation of PECAM is not important. Under their experimental conditions, however, there was no situation where PECAM was tyrosine phosphorylated and β-catenin was not.

In our studies there was a small but noticeable increase in the association of catenins with PECAM following treatment with the GAM antibody alone. The source of this effect is possibly due to addition of fresh undefined commercial serum-free medium used as diluent for the antibodies during crosslinking. This fresh medium added with the antibody treatments would, amongst other things, raise the concentration of glucose that has previously been shown to induce PECAM phosphorylation in cultured endothelial cells and hyperglycemic murine embryos (Ilan et al., 2000). In the latter case, these conditions led to a decreased association with γ-catenin. This shows that levels of glucose can influence PECAM-catenin associations and may at least partially explain the differences between the amount of recruitment of these two catenins and why an effect is observed in cells treated with GAM alone.

None of the inhibitors tested in our study were able to inhibit the phosphorylation of PECAM and so this pathway has yet to be

characterised. However, pre-treatment of the ECs with recombinant C3 transferase significantly inhibited the increased association of both γ- and β-catenin with PECAM. C3 inhibits small GTPases of the rho family that are involved in regulating many cell processes including cytoskeletal rearrangement, focal adhesions, cell junctions and transcriptional signalling. Previous work in our lab and others has identified the importance of functional rho in regulating transendothelial migration (Adamson et al., 1999). The current finding that rho is also involved in the association of PECAM with catenins is a novel finding and may be an important component of the endothelial rho-mediated mechanism controlling leucocyte migration. It is interesting that although C3 transferase significantly inhibits the association of PECAM with β- and γ-catenin, one of the major downstream effector pathways, rho kinase (ROCK), was without effect when inhibited by the ROCK inhibitor Y27632. ROCK is not the only effector mechanism utilised by the rho GTPase pathway and indeed there are suggestions that ROCK may not be the major pathway transducing rho-mediated signalling arising from ICAM-1 crosslinking. This suggestion is supported by the fact that T cell transendothelial migration in vitro is potently inhibited by C3 transferase (Adamson et al., 1999) but not by Y27632 (unpublished observations). Also, inhibition of leucocyte migration in EAE animals treated with protein prenyl transferase inhibitors (Walters et al., 2002) and statins (Greenwood et al, 2003) via a rho-dependent mechanism is not mimicked by Y27632 (unpublished observations). This suggests that other rho effector pathways may contribute to the signalling pathways elicited following ICAM-1 crosslinking.

In addition to its changes in phosphorylation status and binding partners, PECAM also redistributed itself on the cell surface which may allow it to facilitate the migration of an interacting leucocyte or subsequent cohorts of leucocytes. The redistribution of PECAM away from cell junctions may also weaken the barrier function of cell-cell junctions although the contribution across the paracellular cleft of homotypically-associated PECAM per se to junction integrity is not known. PECAM may provide little adhesive strength between cells but rather be incorporated proximal or intermixed with junctions until an appropriate signal causes it to redistribute thus making it available for

EC-leucocyte interactions (Mamdouh et al., 2003). In addition, although PECAM homotypic binding itself may not contribute significantly to the integrity of the junctional seal, its interaction with other junction-associated proteins may be critical for their correct function.

In summary, we demonstrate that crosslinking of brain endothelial surface ICAM-1 induces tyrosine phosphorylation of PECAM. Pecam also redistributes from an almost entirely junctional localisation to a more diffuse appearance. PECAM also becomes associated with both β-, and to a lesser extent, γ-catenin through a rho-sensitive/ROCK-independent pathway. The full physiological relevance of these observations and any potential implication in the process of leucocyte transendothelial migration is unclear but worthy of further investigation. It is hoped that in the future it will be possible to more fully define the molecular events regulating (patho)physiological leucocyte trafficking across different vascular beds.

Chapter 6:

Conclusion & Perspectives

Conclusion & Perspectives

The data presented here demonstrate that these immortalised brain (and retinal) ECs have negligible or undectable expression levels of the transmembrane protein occludin. The inability of occludin expression to decrease the permeability or to restore 'electrical-tightness' to the brain EC junctions (as well as the otherwise 'normal' appearance and behaviour of the untransfected cells that do not express occludin) suggests that occludin may have a minor structural role in tight junctions but its expression may act as a selective regulator of junctional properties. The (re)introduction of occludin into the cell junctions inhibited the transendothelial migration of T cells and this effect was dependent on an unmodified N-terminus in a similar manner to that previously described in a study of neutrophil transepithelial migration (Huber et al., 2000). This domain of occludin may therefore have an important role within a general mechanism regulating cell migration across a monolayer. The modulation of cell junctions by leucocytes has been demonstrated previously in experimental co-culture systems. The demonstration of downstream modulation of junctional integrity and the tyrosine phosphorylation of VE-cadherin by clustering of cell-surface ICAM-1 identifies for the first time a potential mechanism that may induce the localised disengagement of junctions and thus facilitation of paracellular migration following lymphocyte adhesion to ECs. The additional identification of the junction-associated cell adhesion molecule PECAM as another downstream target of phosphorylation cascades initiated through ICAM-1 suggests that this is another molecule involved in supporting junctional disassociation and/or pro-migratory adhesive interactions.

Further work is required not only to identify other downstream targets of ICAM-1-mediated signalling but also to elucidate the pathways involved. Hopefully this will reveal exquisite targets for the rational development of more effective pharmacotherapies. Several studies have targetted the signalling responses observed following leucocyte co-culture and adhesion molecule crosslinking as a means of inhibiting the migration event. Some of these approaches such as those inhibiting calcium signalling using chelators (Huang et al.,

1993) or phosphorylation cascades by using protein kinase inhibitors (Constantin et al., 1999) show profound abilities to reduce transendothelial migration and/or signalling cascades in vitro but their central role in the regulation of many cell processes in vivo severely limits their therapeutic potential. Likewise, pre-treatment of brain endothelial monolayers with cytochalasin D greatly reduced T cell migration in vitro (Adamson et al., 1999) but the therapeutic potential of such compounds is undermined by their high systemic toxicity in vivo. The importance of rho in ICAM-1-mediated signalling, leucocyte transmigration and the apparent specificity of this pathway to brain ECs has led to its pharmacological targeting as a means of regulating neuroinflammation in the context of experimental autoimmune encephalomyelitis (EAE), an animal model of MS (Walters et al., 2002). The biological activity of rho proteins is dependent on their localisation to the cytoplasmic leaflet of cell membranes that in turn is dependent on their C-terminal prenylation with either a geranylgeranyl or farnesyl moiety (Adamson et al., 1992a and b). These isoprenoids are metabolic products of cholesterol biosynthesis and are covalently attached to rho by prenyl transferases. Treatment of brain endothelial monolayers with prenyl transferase inhibitors significantly inhibits T cell migration in vitro and, when administered to disease-induced Biozzi ABH mice prior to disease onset, attenuates clinical signs of EAE, without an apparent reduction in peripheral inflammatory response (Walters et al., 2002). HMG-CoA reductase inhibitors (statins) have also been used to inhibit lymphocyte migration and attenuate EAE. Statins, that are widely used to treat atherosclerosis and hypercholesterolaemia, interfere with cholesterol biosynthesis and consequently the biosynthesis of isoprenoid pyrophosphates and thus subsequent prenylation of rho. As with prenyl transferase inhibitors, this results in a failure of rho prenylation and its localisation to the correct cellular compartment that results in an inhibition of the ICAM-1-induced rho-mediated signalling pathway, inhibition of T cell migration in vitro and attenuation of EAE (Greenwood et al., 2003b). In addition to their effect on rho inhibition, there is evidence that statins modulate immune responses in other ways beneficial in the treatment of neuroinflammatory disease (Youssef et al., 2002). Recently, cell-permeant peptides

corresponding to the cytoplasmic domain of ICAM-1 have been shown to act as inhibitors of ICAM-1-mediated signalling and to inhibit T cell transendothelial migration in vitro (Greenwood et al., 2003a). For this strategy to be successful as an in vivo therapy, however, the peptides must be able to persist within the proteolytic environment of the circulation long enough to exert an effect. It would also be hoped that this or any other potential therapy would not lead to a systemic suppression of leucocyte trafficking that may immunocompromise the patient. Even with such obvious gaps in our current knowledge of all the important processes in lymphocyte recruitment into the CNS, this should not detract from the huge amount of progress made in this and related fields in the last 20 years. It may be reasonably expected that following the next 20 years the pathogenesis of neuroinflammatory diseases such as MS would be sufficiently understood so as to allow almost complete therapeutic management.

Despite large amounts of investment and effort to understand and treat neuroinflammatory disease, current, predominantly pharmaceutical, approaches have only modest success in modifying the progression of these diseases. The sequelae of MS, and many other neuroinflammatory diseases, are entirely attributable to pathology within the CNS caused by a characteristic infiltration of a large number of leucocytes that initiate an autoimmune response against and cause damage to myelinated neuronal axons. If the entry of autoaggressive leucocytes into the CNS could be restricted, if not prevented, during inflammatory episodes then so also would the subsequent degree of pathology. It has been known for some time that T cells and macrophages accumulate within inflammatory MS plaques but the events that allow the integrity of the BBB, that usually restricts such access, to be compromised has revealed an increasingly complex set of mechanisms. The low-permeability, high electrical-resistance lateral cell-cell junctions of brain ECs are the major structural element in the functional BBB and it is these that must be modulated to allow the paracellular migration of leucocytes from the circulation into the brain parenchyma. During the last ten years the molecular architecture of these structures has been increasingly revealed with the continuing rapid discovery of novel junctional proteins and interactions adding to the level of structural

and regulatory complexity. Understanding the functions of the many different junctional components is however a much slower task and functional data on many junctional proteins is sparse. The power of modern biochemical analysis is the rate-limiting step in this progress. The establishment and regulation of brain EC junctions is dependent on the interaction and modulation of complex macromolecular assemblies and determining how these relate to each other during highly orchestrated cellular events is experimentally difficult. A lot of the work in this thesis, and in cell biology in general, is concerned with observing changes in a single component often isolated from cell homogenates and assayed for its biochemical characteristics. How any such observed changes relate to the initial stimulus or their downstream effects on the cell are difficult to both determine and interpret. Until the development of the ability to visualise in situ the interplay of interacting molecules and related events, the most effective method to identify signalling pathways is by a systematic, step-wise dissection of each potential component and to attempt to link these temporally into a series of events. The study of cell-cell junctions is further complicated by the different in vitro model systems used to investigate them and this is especially relevant with respect to brain ECs. Much of the work on junctions is performed on epithelial cells but whilst the junctions of brain ECs are perhaps quite similar to epithelia in terms of their tight junction expression and functional characteristics, the extrapolation of data from epithelial systems is not ideal and differences in their composition are well documented. Endothelial-based research often utilises ECs derived from peripheral vascular beds and again there is evidence that the specialised nature of brain ECs requires that researchers should be mindful of any potential differences when extrapolating from data obtained using these cells. Due to the small amount of biological material that can be isolated from brain microvessels, there is a need for a truly representative BBB EC line. Identification of the requirements to retain the in vivo phenotype during in vitro culture is of enormous potential in all areas of neurobiology. The development and use of ever-more representative in vitro models of the BBB is obviously intimately connected with the study of processes in which it plays a role.

References

Abbott N.J. & Pichon Y. (1987) The Glial Blood-brain Barrier of Crustacea and Cephalopods: A Review. *J. Physiol. (Paris)* 82: 304-13

Abbott N.J. (2000) Inflammatory Mediators and Modulation of Blood-brain Barrier Permeability. *Cell Mol. Neurobiol.* 20: 131-47

Abbott N.J. (2002) Astrocyte-endothelial Interactions and Blood-brain Barrier Permeability. *J. Anat.* 200: 629-38

Aberle H., Schwartz H., Hoschuetzky H. & Kemler R. (1996) Single Amino Acid Substitutions in Proteins of the Armadillo Gene Family Abolish Their Binding to α-catenin. *J. Biol. Chem.* 271: 1520-6

Aberle H., Bauer A., Stappert J., Kispert A. & Kemler R. (1997) β-catenin is a Target for the Ubiquitin-proteasome Pathway. *EMBO J.* 16: 3797-3804

Adamson P., Paterson H.F. & Hall A. (1992a) Intracellular Localisation of the $p21^{rho}$ Proteins. J. Cell Biol. 119: 617-22

Adamson P., Marshall C.J., Hall A. & Tilbrook P.A. (1992b) Post-translational Modifications of $p21^{rho}$ Proteins. *J. Biol. Chem.* 267: 20033-8

Adamson P., Etienne S., Couraud P-O., Calder V. & Greenwood J. (1999) Lymphocyte Migration Through Brain Endothelial Cell Monolayers Involves Signalling Through Endothelial ICAM-1 Via a Rho-Dependant Pathway. *J. Immunol.* 162: 2964-73

Adamson P., Wilbourne B., Etienne-Manneville S., Calder V., Beraud E., Milligan G., Couraud P-O & Greenwood J. (2002a) Lymphocyte Trafficking Through the Blood-brain Barrier is Dependent on Endothelial Cell Heterotrimeric G-protein Signalling. *FASEB J.* 16: 1185-94

Adamson R.H., Liu B., Fry G.N., Rubin L.L. & Curry F.E. (1998) Microvascular Permeability and Number of Tight Junctions are Modulated by cAMP. *Am. J. Physiol. Heart Circ. Physiol.* 274: H1885-H1894

Adamson R.H, Curry F.E., Adamson G., Liu B., Jiang Y., Aktories K., Barth H., Daigeler A., Golenhofen N., Ness W. & Drenckhahn D. (2002b) Rho and Rho Kinase Modulation of Barrier Properties: Cultured Endothelial Cells and Intact Microvessels of Rats and Mice. *J. Physiol.* 539: 295-308

Ahrens T., Lambert M., Pertz O., Sasaki T., Schulthess T., Mege R.M., Timpl R. & Engel J. (2003) Homoassociation of VE-cadherin Follows a Mechanism Common to "Classical" Cadherins. *J. Mol. Biol.* 325: 733-42

Aiba S., Nakagawa S., Ozawa H. & Tagami H. (1995) Different Expression of E-cadherin by Two Cutaneous γ/δ TcR+ T-cell Subsets. *J. Invest. Dermatol.* 105: 379-82

Allport J.R., Ding H., Collins T., Gerritsen M.E. & Luscinskas F.W. (1997) Endothelial-dependent Mechanisms Regulate Leucocyte Transmigration: A Process Involving the Proteasome and Disruption of the Endothelial-cadherin Complex at Endothelial Cell-to-cell Junctions. *J. Exp. Med.* 186: 517-27

Allport J.R., Lim Y.C., Shipley J.M., Senior R.M., Shapiro S.D., Matsuyoshi N., Vestweber D. & Luscinskas F.W. (2002) Neutrophils From MMP-9 or Neutrophil Elastase-deficient Mice Show No Defect in Transendothelial Migration Under Flow in vitro. *J. Leukoc. Biol.* 71: 821-8

Allt G. & Lawrenson J.G. (2001) Pericytes: Cell Biology and Pathology. *Cells Tissues Organs* 169: 1-11

Alexander J.S., Dayton T., Davis C., Hill S., Jackson T.H., Blaschuk O., Symonds M., Okayama N., Kevil C.G., Laroux F.S., Berney S.M. & Kimpel D. (1998) Activated T-lymphocytes Express, Occludin, a Component of Tight Junctions. *Inflammation* 22: 573-82

Alexander J.S., Elrod J.W. & Park J.H. (2001) Roles of Leukocyte and Immune Cell Junctional Proteins. *Microcirculation* 8: 169-79

Alter A., Duddy M., Hebert S., Biernacki K., Prat A., Antel J.P., Yong V.W., Nuttall R.K., Pennington C.J., Edwards D.R. & Bar-Or A. (2003) Determinants of Human B Cell Migration Across Brain Endothelial Cells. *J. Immunol.* 170: 4497-4505

Amos C., Romero I.A., Schültze C., Roussell J., Pearson J.D., Greenwood J. & Adamson P. (2001) Cross-linking of Brain Endothelial Intercellular Adhesion Molecule (ICAM)-1 Induces Association of ICAM-1 with Detergent-insoluble Cytoskeletal Fraction. *Arterioscler. Thromb. Vasc. Biol.* 21: 810-16

Anastasiadis P.Z. & Reynolds A.B. (2000) The p120 Catenin Family: Complex Roles in Adhesion, Signaling and Cancer. *J. Cell Sci.* 113: 1319-34

Anastasiadis P.Z. & Reynolds A.B. (2001) Regulation of Rho GTPases by p120-catenin. *Curr. Opin. Cell Biol.* 13: 604-10

Ando-Akatsuka Y., Saitou M., Hirase T., Kishi M., Sakakibara AA., Itoh M., Yonemura S., Furuse M. & Tsukita S. (1996) Interspecies Diversity of the Occludin Sequence: cDNA Cloning of Human, Mouse, Dog and Rat-kangaroo Homologues. *J. Cell. Biol.* 133: 43-7

Andreeva A.Y., Krause E., Muller E-C., Blasig I.E. & Utepbergenov D.I. (2001) Protein Kinase C Regulates the Phosphorylation and Cellular Localization of Occludin. J. Biol. Chem. 276: 38480-38486

Andriopoulou P., Navarro P., Zanetti A., Lampugnani M.G. & Dejana E. (1999) Histamine Induces Tyrosine Phosphorylation of Endothelial Cell-to-Cell Adherens Junctions. *Arterio. Thromb. Vasc. Biol.* 19: 2286-97

Antel J.P. & Owens T. (1999) Immune Regulation and CNS Autoimmune Disease. *J. Neuroimmunol.* 100: 181-9

Antonetti D.A., Barber A.J., Hollinger L.A., Wolpert E.B. & Gardner T.W. (1999) Vascular Endothelial Growth Factor Induces Rapid Phosphorylation of Tight Junction Proteins Occludin and Zonula Occluden 1. *J. Biol. Chem.* 274: 23463-7

Antonetti D.A., Wolpert E.B., DeMaio L., Harhaj N.S. & Scaduto R.C. Jr (2002) Hydrocortisone Reduces Retinal Endothelial Cell Water and Solute Flux Coincident With Increased Content and Decreased Phosphorylation of Occludin. *J. Neurochem.* 80: 667-77

Atkinson K.J. & Rao R.K. (2001) Role of Protein Tyrosine Phosphorylation in Acetaldehyde-induced Disruption of Epithelial Tight Junctions. *Am. J. Physiol. Gastrointest. Liver Physiol.* 280: G1280-8

Baggiolini M. (1998) Chemokines and Leucocyte Traffic. *Nature* 392: 565-8

Balda M.S. & Anderson J.M. (1993) Two Classes of Tight Junctions Are Revealed by ZO-1 Isoforms. *Am. J. Physiol.* 264: C918-24

Balda M.S., González-Mariscal L., Matter K., Cereijido M. & Anderson J.M. (1993) Assembly of the Tight Junction: the Role of Diacylglycerol. *J. Cell Biol.* 123: 293-302

Balda M.S., Whitney J.A., Flores C., Gonzalez S., Cereijido M. & Matter K. (1996a) Functional Dissociation of Paracellular Permeability and Transepithelial Electrical Resistance and Disruption of the Apical-Basolateral Intramembrane Diffusion Barrier by Expression of a Mutant Tight Membrane Protein. *J. Cell Biol.* 134: 1031-49

Balda M.S., Anderson J.M. & Matter K. (1996b) The SH3 domain of the Tight Junction Protein ZO-1 Binds to a Serine Protein Kinase that Phosphorylates a Region C-terminal to this Domain. *FEBS Lett.* 399: 326-32

Balda M.S & Matter K. (1998) Tight Junctions. *J. Cell Sci.* 111: 541-7

Balda M.S., Flores-Maldonado C., Cereijido M. & Matter K. (2000) Multiple Domains of Occludin are Involved in the Regulation of Paracellular Permeability. *J. Cell. Biochem.* 78: 85-96

Balda M.S. & Matter K. (2000) The Tight Junction Protein ZO-1 and an Interacting Transcription Factor Regulate ErbB-2 Expression. *EMBO J.* 19: 2024-33

Bamforth S.D., Kniesel U., Wolburg H., Engelhardt B. & Risau W. (1999) A Dominant Mutant of Occludin Disrupts Tight Junction Structure and Function. *J Cell Sci.* 112: 1879-88

Banks W.A. (1999) Physiology and Pathology of the Blood-brain Barrier: Implications for Microbial Pathogenesis, Drug Delivery and Neurodegenerative Disorders. *J. Neurovirol.* 5: 538-55

Bär T. (1980) The Vascular System of the Cerebral Cortex. *Adv. Anat. Embryol. Cell Biol.* 59: 1-62

Barreiro O., Yanez-Mo M., Serrador J.M., Montoya M.C., Vicente-Manzanares M., Tejedor R., Furthmayr H. & Sanchez-Madrid F. (2002) Dynamic Interaction of VCAM-1 and ICAM-1 with Moesin and Ezrin in a Novel Endothelial Docking Structure For Adherent Leucocytes. *J. Cell Biol.* 157: 1233-45

Bauer H-C. & Bauer H. (2000) Neural Induction of the Blood-brain Barrier: Still and Enigma. *Cell Mol. Neurobiol.* 20: 13-28

Bazzoni G., Martinez-Estrada O.M., Mueller F., Nelboeck P., Schmid G., Bartfai T., Dejana E. & Brockhaus M. (2000a) Homophilic Interaction of Junctional Adhesion Molecule. *J. Biol. Chem.* 275: 30970-76

Bazzoni G., Martinez-Estrada O.M., Orsenigo F., Cordenonsi M., Citi S. & Dejana E. (2000b) Interaction of Junctional Adhesion Molecule with the Tight Junction Components Z0-1, Cingulin and Occludin. *J. Biol. Chem.* 275: 205020-26

Bek S. & Kemler R. (2002) Protein Kinase CKII Regulates the Interaction of β-catenin with α-catenin and its Protein Solubility. *J. Cell Sci.* 115: 4743-53

Ben Ze'ev, Shtutman M. & Zhurinsky J. (2000) The Integration of Cell Adhesion with Gene Expression: The Role of β-Catenin. *Exp. Cell Res.* 261: 75-82

Berman M.E. & Muller W.A. (1995) Ligation of Platelet/Endothelial Cell Adhesion Molecule 1 (PECAM-1/CD31) on Monocytes and Neutrophils Increases Binding Capacity of Leukocyte CR3 (CD11b/CD18). *J. Immunol.* 154: 299-307

Blum M.S., Toninelli E., Anderson J.M., Balda M.S., Zhou J.L.O.D., Pardi R. & Bender J.R. (1997) Cytoskeletal Rearrangement Mediates Human Microvascular Endothelial Tight Junction Modulation by Cytokines. *Am. J. Physiol.* 273: H286-94

Bolton S.J., Anthony D.C. & Perry V.H. (1998) Loss of the Tight Junction Proteins Occludin and Zonula Occludens-1 From Cerebral Vascular Endothelium During Neutrophil-induced Blood-brain Barrier Breakdown In Vivo. *Neuroscience* 86: 1245-57

Boulton M. et al. (1999) Contribution of Extracranial Lymphatics and Arachnoid Villi to the Clearance of a CSF Tracer in the Rat. *Am. J. Physiol.* 276: R818-23

Bos J.L., de Bruyn K., Enserink J., Kuiperij B., Rangarajan S., Rehmann H., Riedl J., de Rooij J., van Mansfeld F. & Zwartkruis F. (2003) The Role of Rap1 in Integrin-mediated Cell Adhesion. *Biochem. Soc. Trans.* 31:83-6

Bradford M.M. (1976) A Rapid and Sensitive Method for the quantitation of microgram quantities of Protein Using the Principle of Protein-dye Binding. *Anal. Biochem.* 72: 248-54

Braet F. & Wisse E. (2002) Structural and Functional Aspects of Liver Sinusoidal Endothelial Cell Fenestrae: A Review. *Comp. Hepatol.* 1:1

Braga V.M., Machesky L.M., Hall A. & Hotchin N.A. (1997) The Small GTPases Rho and Rac are Required for the Establishment of Cadherin-dependent Cell-cell Contacts. *J. Cell Biol.* 137: 1421-31

Brandt D., Gimono M., Hillman M., Haller H. & Mischak H. (2002) Protein Kinase C Induces Actin Reorganisation Via a Src- and Rho-dependent Pathway. *J. Biol. Chem.* 277: 20903-10

Brown K.A. (2001) Factors Modifying the Migration of Lymphocytes Across the Blood-brain Barrier. *Int. Immunopharmacol.* 1: 2043-62

Buckley C.D. (2001) PECAM-1/CD31: More Than Just Glue. *Transplantation* 71: 457-60

Budt M., Cichocka I., Reutter W. & Lucka L. (2002) Clustering-induced Signaling of CEACAM1 in PC12 Cells. *Biol. Chem.* 383: 803-12

Burns A.R., Bowden R.A., MacDonell S.D., Walker D.C., Odebunmi T.O., Donnachie E.M., Simon S.I., Entman M.L. & Smith C.W. (2000) Analysis of Tight Junctions During Neutrophil Transendothelial Migration. *J. Cell Sci.* 113: 45-57

Butt A.M., Jones H.C. & Abott N.J. (1990) Electrical Resistance Across the Blood-brain Barrier in Anaesthetised Rats: A Developmental Study. *J. Cell Physiol. (London)* 429: 47-62

Cao G., O'Brien C.D., Zhou Z., Sanders S.M., Greenbaum J.N., Makrigiannakis A. & DeLisser H.M. (2002) Involvement of Human PECAM-1 in Angiogenesis and in vitro Endothelial Cell Migration. *Am. J. Physiol. Cell Physiol.* 282: C1181-90

Cassella J.P., Lawrenson J.G. & Firth J.A. (1997) Development of Endothelial Paracellular Clefts and Their Tight Junctions in the Pial Microvessels of the Rat. *J. Neurocytol.* 26: 567-75

Carden D., Xiao F., Moak C., Willis B.H., Robinson-Jackson S. & Alexander S. (1998) Neutrophil Elastase Promotes Lung Microvascular Injury and Proteolysis of Endothelial Cadherins. *Am. J. Physiol.* 275: H385-92

Carmeliet P., Lampugnani M.G., Moons L., Breviario F., Bono F., Balconi G., Compernolle V., Spagnuolo R., Dewerchin M., Zanetti A., Oosthuyse B., Angelillo A., Nuyens D., Clotman F., de Ruiter M.C., Gittenberger-de Groot A., Herbert J.M., Lupu F., Collen D. & Dejana E. (1999) Targeted Deficiency or Cytosolic Truncation of the VE-cadherin Gene in Mice Impairs VEGF-mediated Endothelial Survival and Angiogenesis. *Cell* 98: 147-57

Carman C.V., Jun C.D., Salas A. & Springer T.A. (2003) Endothelial Cells Proactively Form Microvilli-like Membrane Projections Upon Intercellular Adhesion Molecule 1 Engagement of Leukocyte LFA-1. *J.Immunol.* 171: 6135-44

Carpen O., Pallai P., Staunton D.E. & Springer T.A. (1992) Association of Intercellular Cell Adhesion Molecule-1 (ICAM-1) With Actin-Containing Cytoskeleton and α-actinin. *J. Cell Biol.* 118: 1223-34

Cepek K.L., Rimm D.L. & Brenner M.B. (1996) Expression of a Candidate Cadherin in T Lymphocytes. *Proc. Natl. Acad. Sci. USA* 93: 6567-71

Cepinskas G., Sandig M. & Kvietys P.R. (1999) PAF-induced Elastase-dependent Transendothelial Migration is Associated with the Mobilisation of Elastase to the Neutrophil Surface and Localisation to the Migrating Front. *J. Cell Sci.* 112: 1937-45

Chen Y-H., Merzdorf C., Paul D.L. & Goodenough D.A. (1997) COOH Terminus of Occludin is Required for Tight Junction Barrier Function in Early *Xenopus* Embryos. *J. Cell Biol.* 138: 891-99

Chlenski A., Ketels K.V., Tsao M., Talamonti M.S., Tsao M., Koutnikova H., Oyasu R., Scarpelli D.G. (1999) Tight Junction Protein ZO-2 is Differentially Expressed in Normal Pancreatic Ducts Compared to Human Pancreatic Adenocarcinoma. *Int. J. Cancer* 82: 137-44

Cinamon G., Shinder V & Alon R. (2001) Shear Forces Promote Lymphocyte Migration Across Vascular Endothelium Bearing Apical Chemokines. *Nature Immunol.* 2: 515-22

Clayton A., Evans R.A., Pettit E., Hallett M., Williams J.D. & Steadman R. (1998) Cellular Activation Through the Ligation of Intercellular Adhesion Molecule-1. J. Cell. Sci. 111: 443-53

Cleaver O. & Melton D.A. (2003) Endothelial Signalling During Development. *Nat. Med.* 9: 661-8

Constantin G., Laudanna C., Brocke S. & Butcher E.C. (1999) Inhibition of Experimental Autoimmune Encephalomyeltis By a Tyrosine Kinase Inhibitor. *J. Immunol.* 162: 1144-49

Corada M., Mariotti M., Thurston G., Smith K., Kunkel R., Brockhaus M., Lampugnani M.G., Martin-Padura I., Stoppacciaro A., Ruco L., McDonald D.M., Ward P.A. & Dejana E. (1999) Vascular Endothelial-cadherin is an Important Determinant of Microvascular Integrity *in vivo*. *Proc. Natl. Acad. Sci. USA* 96: 9815-20

Cordenonsi M., D'Atri F., Hammar E., Parry D.A.D., Kendrick-Jones J., Shore D & Citi S. (1999) Cingulin Contains Globular and Coiled-coil Domains and Interacts with ZO-1, ZO-2, ZO-3 and Myosin. *J. Cell Biol.* 147: 1569-81

Cordon-Cardo C., O'Brian J.P., Casals D., Rittman-Grauer L., Biedler J.L., Melamed M.R. & Bertino J.R. (1989) Multidrug-resistance Gene (P-glycoprotein) is Expressed by Endothelial Cells at Blood-brain Barrier Sites. *Proc. Natl. Acad. Sci. USA* 86: 695-8

Couraud P-O., Greenwood J., Roux F. & Adamson P. (2003) Development and Characterisation of Immortalised Cerebral Endothelial Cell Lines. *Methods Mol. Med.* 89: 349-64

Cserr H.F., Cooper D.N. & Milhorat T.H. (1977) Flow of Cerebral Interstitial Fluid as Indicated by the Removal of Extracellular Markers from Rat Caudate Nucleus. *Exp. Eye Res.* 25: 461-73

Cserr H.F., Cooper D.N., Suri P.K. & Patlak C.S. (1981) Efflux of Radiolabelled Polyethylene Glycols and Albumin from Rat Brain. *Am. J. Physiol.* 240: F319-28

Cserr H.F. & Knopf P.M. (1992) Cervical Lymphatics, the Blood-brain Barrier and the Immunoreactivity of the Brain: A New View. *Immunol. Today* 13: 507-12

Cucullo L., McAllister M.S., Kight K., Krizanac-Bengez L., Marroni ., Mayberg M.R., Stanness K.A., & Janigro D. (2002) A New Dynamic in vitro Model for the Multidimensional Study of Astrocyte-endothelial Cell Interactions at the Blood-brain Barrier. *Brain Res.* 951: 243-54

Cumberbatch M., Deraman R.J. & Kimber I. (1996) Adhesion Molecule Expression by Epidermal Langerhans Cells and Lymph Node Dendritic Cells: A Comparison. *Arch. Dermatol. Res.* 288: 739-44

Cunningham S.A., Arrate M.P., Rodriguez J.M., Bjercke R.J., Vanderslice P., Morris A.P & Brock T.A. (2000) A Novel Protein with Homology to the Junctional Adhesion Molecule- Characterisation of Leukocyte Interactions. *J. Biol. Chem.* 275: 34750-56

Daniel J.M. & Reynolds A.B. (1995) The Tyrosine Kinase Substrate p120cas Binds Directly to E-cadherin But Not to the Adenomatous Polyposis Coli Protein Or α-catenin. *Mol. Cell Biol.* 15: 4819-24

Daniel J.M. & Reynolds A.B. (1999) The Catenin p120(ctn) Interacts With Kaiso, a Novel BTB/POZ Domain Zinc Finger Transcription Factor. *Mol. Cell Biol.* 19: 3614-23

de Boer A.G. & Breimer D.D. (1996) Reconstitution of the Blood-brain Barrier in Cell Culture for Studies of Drug Transport and Metabolism. *Adv. Drug Deliv. Rev.* 22: 251-64

de Boer A.G., Gaillard P.J. & Breimer D.D. (1999) The Transference of Results Between Blood-brain Barrier Cell Culture Systems. *Eur. J. Pharm. Sci.* 8: 1-4

Dejana E., Bazzoni G. & Lampugnani M.G. (1999) Vascular Endothelial (VE)-Cadherin: Only an Intercellular Glue? *Exp. Cell Res.* 252: 13-19

Dejana E., Spagnuolo R. & Bazzoni G. (2001) Interendothelial Junctions and Their Role in the Control of Angiogenesis, Vascular Permeabiliy and Leukocyte Transmigration. *Thromb. Haemost.* 86: 308-15

Dejana E. (2004) Endothelial Cell Junctions: Happy Together. *Nat. Rev. Mol. Cell Biol.* 5: 61-70

Del Maschio A., Zanetti A., Corada M., Rival Y., Ruco L., Lampugnani M.G., Dejana E. (1996) Polymorphonuclear Leucocyte Adhesion Triggers the Disorganization of Endothelial Cell-to-cell Adherens Junctions. *J. Cell Biol.* 135: 497-510

Del Maschio A., De Luigi A., Martin-Padura I., Brockhaus M., Bartfai T., Fruscella P., Adorini L., Martino G.V., Furlan R., De Simoni M.G. & Dejana E. (1999) Leucocyte Recruitment in the Cerebrospinal Fluid of Mice with Experimental Meningitis is Inhibited by an Antibody to Junctional Adhesion Molecule (JAM). *J. Exp. Med.* 190: 1351-6

DeMaio L., Chang Y.S., Dardner T.W., Tarbell J.M. & Antonetti D.A. (2001) Shear Sress Regulates Occludin Content and Phosphorylation. *Am. J. Physiol. Heart Circ. Physiol.* 281: H105-113

Demeule M., Regina A., Jodoin J., Laplante A., Dagenais C., Berthelet F., Moghrabi A. & Beliveau R. (2002) Drug Transport to the Brain: Key Roles for the Efflux Pump P-glycoprotein in the Blood-brain Barrier. *Vascul. Pharmacol.* 38: 339-48

De Vos A.F. et al. (2002) Transfer of Central Nervous System Autoantigens and Presentation in Secondary Lymphoid Organs. *J. Immunol.* 169: 5415-23

Dietrich J.B. (2002) The Adhesion Molecule ICAM-1 and its Regulation in Relation to the Blood-brain Barrier. *J. Neuroimmunol.* 128: 58-68

Domotor E., Sipos I., Kittel A., Abbott N.J. & Adam-Vizi V. (1999) Improved Growth of Cultured Brain Microvascular Endothelial Cells on Glass Coated with a Biological Matrix. *Neurochem. Int.* 33: 473-78

Dragsten P.R., Blumanthal R. & Handler J.S. (1981) Membrane Asymmetry in Epithelia: Is the Tight Junction a Barrier to Diffusion in the Plasma Membrane? *Nature* 294: 718-22

Dransfield I. & Hogg N. (1989) Regulated Expression of Mg^{2+} Binding Epitope on Leucocyte Integrin α Subunits. *EMBO J.* 8: 3759-65

Duncan G.S., Andrew D.P., Takimoto H., Kaufman S.A., Yoshida H., Spellberg J., Luis de la Pompa J., Elia A., Wakeham A., Karan-Tamir B., Muller W.A., Senaldi G., Zukowski M.M. & Mak T.W. (1999) Genetic Evidence for Functional Redundancy of Platelet/Endothelial Cell Adhesion Molecule-1 (PECAM-1): CD31-deficient Mice Reveal PECAM-1-dependent and PECAM-1-independent Functions. *J. Immunol.* 162: 3022-30

Durieu-Trautman O., Chaverot N., Cazaubon S., Strosberg A.D. & Couraud P-O. (1994) Intercellular Adhesion Molecule 1 Activation Induces Tyrosine Phosphorylation of the Cytoskeleton-associated Protein Cortactin in Brain Microvessel Endothelial Cell. *J. Biol. Chem.* 269: 12536-40

Ebers G.C., Sadovnick A.D. & Risch N.J. (1995) A Genetic Basis for Familial Aggregation in Multiple Sclerosis. Canadian Collaborative Study Group. *Nature* 377: 150-1

Edens H.A. & Parkos C.A. (2000) Modulation of Epithelial and Endothelial Paracellular Permeability by Leukocytes. *Adv. Drug Deliv. Rev.* 41: 315-28

Edens H.A., Levi B.P., Jaye D.L., Walsh S., Reaves T.A., Turner J.R., Nusrat A. & Parkos C.H. (2002) Neutrophil Transepithelial Migration: Evidence for Sequential, Contact-dependent Signaling Events and Enhanced Paracellular Permeability Independent of Transjunctional Migration. *J. Immunol.* 169: 476-86

Engelhardt B., Vestweber D., Hallman R. & Schulz M. (1997) E- and P-selectin are Not Involved in the Recruitment of Inflammatory Cells Across the Blood-brain Barrier in Experimental Autoimmune Encephalomyelitis. *Blood* 90: 4459-72

Esser S., Lampugnani M.G., Corada M., Dejana E. & Risau W. (1998) Vascular Endothelial Growth Factor Induces VE-cadherin Tyrosine Phosphorylation in Endothelial Cells. *J. Cell Sci.* 111: 1853-65

Etienne-Manneville S., Chaverot N., Strosberg A.D. & Couraud P-O. (1999) ICAM-1 coupled Signalling Pathways in Astrocytes Converge to Cyclic AMP Response Element-binding Protein Phosphorylation and TNF-α Secretion. *J. Immunol.* 163: 668-74

Etienne-Manneville S., Manneville J-B., Adamson P., Wilbourn B., Greenwood J. & Couraud P-O. (2000) ICAM-1-coupled Cytoskeletal Rearrangements and Transendothelial Lymphocyte Migration Involve Intracellular Calcium Signalling in Brain Endothelial Cell Lines. *J. Immunol.* 165: 3375-83

Etienne S., Adamson P., Greenwood J., Strosberg A.D., Cazaubon S. & Couraud P-O. (1998) ICAM-1 Signaling Pathways Associated with Rho Activation in Microvascular Brain Endothelial Cells. *J. Immunol.* 161: 5755-5761

Etienne S., Bourdoulous S., Strosberg A.D. & Couraud P-O. (1999) MHC Class II Engagement in Brain Endothelial Cells Induces PKA-dependent Interleukin-6

Secretion and Phosphorylation of cAMP-response Element Binding Protein. *J. Immunol.* 163: 3636-41

Fanning A.S., Jameson B.J., Jesaitis L.A. & Anderson J.M. (1998) The Tight Junction Protein ZO-1 Establishes a Link Between the Transmembrane Protein Occludin and the Actin Cytoskeleton. *J. Biol. Chem.* 273: 29745-53

Farshori P. & Kachar B. (1999) Redistribution and Phosphorylation of Occludin During Opening and Resealing of Tight Junctions in Cultured Epithelial Cells. *J Membrane Biol.* 170: 147-156

Faveeuw C., Di Mauro M.E., Price A.A. & Ager A. (2000) Roles of α_4 Integrins/VCAM-1 and LFA-1/ICAM-1 in the Binding and Transendothelial Migration of T Lymphocytes and T Lymphoblasts Across High Endothelial Venules. *Int. Immunol.* 12: 241-51

Federici C., Camoin L., Hattab M., Strosberg A.D. & Couraud P-O. (1996) Association of the Cytoplasmic Domain of Intercellular-adhesion Molecule-1 with Glyceraldehyde-3-phosphate Dehydrogenase and β-tubulin. *Eur. J. Biochem.* 238: 173-80

Fehling H-J., Lacaud G., Kubo A., Kennedy M., Robertson S., Keller G. & Kouskoff V. (2003) Tracking Mesoderm Induction and its Specification to the Hemangioblast During Embryonic Stem Cell Differentiation. *Development.* 130: 4217-27

Feng D., Nagy J.A., Pyne K., Dvorak H.F. & Dvorak A.M. (1998) Neutrophils Emigrate From Venules by a Transendothelial Cell Pathway in Response to fMLP. *J. Exp. Med.* 187: 903-15

Ferber A., Yaen C., Sarmiento E. & Martinez J. (2002) An Octapeptide in the Juxtamembrane Domain of VE-cadherin is Important for p120ctn Binding and Cell Proliferation. *Exp. Cell Res.* 274: 35-44

Ferruzza S., Scarino M-L., Rotilio G., Ciriolo M.R., Santoroni P. Muda A.O. & Sambuy Y. (1999) Copper Treatment Alters the Permeability of Tight Junctions in Cultured Human Intestinal Caco-2 Cells. *Am. J. Physiol.* 270 *(Gastrointest. Liver Physiol.* 40): G1138-48

Furuse M., Hirase T., Itoh M., Nagafuchi A., Yonemura S., Tsukita S. & Tsukita S. (1993) Occludin: a Novel Integral Membrane Protein Localising at Tight Junctions. J. Cell Biol. 123: 1777-88

Furuse M., Itoh M., Hirase T., Nagafuchi A., Yonemura S., Tsukita S. & Tsukita S. (1994) Direct Association of Occludin with ZO-1 and Its Possible Involvement in the Localisation of Occludin at Tight Junctions. *J. Cell Biol.* 127: 1617-26

Furuse M., Fujita K., Hiiragi T., Fujimoto K. & Tsukita S. (1998a) Claudin-1 and -2: Novel Integral Membrane Proteins Localising at Tight Junctions with No Sequence Similarity to Occludin. *J. Cell Biol.* 141: 1539-50

Furuse M., Sasaki H., Fujimoto K. & Tsukita S. (1998b) A Single Gene Product, Claudin-1 or -2, Reconstitutes Tight Junction Strands and Recruits Occludin in Fibroblasts. *J. Cell Biol.* 143: 391-401

Furuse M., Sasaki H. & Tsukita S. (1999) Manner of Interaction of Heterogenous Claudin Species Within and Between Tight Junction Strands. *J. Cell Biol.* 147: 891-903

Furuse M., Furuse K. Sasaki H. & Tsukita S. (2001) Conversion of *Zonulae Occludentes* from Tight to Leaky Strand Type by Inroducing Claudin-2 into Madin-Darby Canine Kidney I Cells. *J. Cell Biol.* 153: 263-72

Furuse M., Hata M., Furuse K., Yoshida Y., Haratake A., Sugitani Y., Noda T., Kubo A. & Tsukita S. (2002) Claudin-based Tight Junctions are Crucial for the Mammalian Epidermal Barrier: a Lesson from Claudin-1-deficient Mice. *J. Cell Biol.* 156: 1099-1111

Gao X., Kouklis P., Xu N., Minshall R.D., Sandoval R., Vogel S.M. & Malik A.B. (2000) Reversibility of Increased Microvessel Permeability in Response to VE-cadherin Disassembly. *Am. J. Physiol. Lung Cell Mol. Physiol.* 279: L1218-25

Girard J.P. & Springer T.A. (1995) High Endothelial Venules (HEVs): Specialised Endothelium for Lymphocyte Migration. *Immunol. Today* 16: 449-57

Golden P.L. & Pollack G.M. (2003) Blood-brain Barrier Efflux Transport. *J. Pharm. Sci.* 92: 1739-53

Gomez S., del Mont Llosas M., Verdu J., Roura S., Lloreta J., Fabre M. & Garcia de Herreros A. (1999) Independent Regulation of Adherens and Tight Junctions by Tyrosine Phosphorylation in Caco-2 Cells. *Biochim. Biophys. Acta* 1452: 121-32

González-Mariscal L., Betanzos A. & Ávila-Flores A. (2000) MAGUK Proteins: Structure and Role in the Tight Junction. *Sem. Cell Dev. Biol.* 11: 315-24

Gow A., Southwood C.M., Li J.S., Pariali M., Riordan G.P., Brodie S.E., Danias J., Bronstein J.M., Kachar B. & Lazzarini R.A. (1999) CNS Myelin and Sertoli Cell Tight Junction Strands are Absent in *Osp/Claudin-11* Null Mice. *Cell* 99:649-59

Grebenkämper K., Galla H-J. (1994) Translational Diffusion Measurements of a Fluorescent Phospholipid Between MDCK-1 Cells Support the Lipid Model of the Tight Junctions. *Chem. Phys. Lipids* 71: 133-43

Greenwood J. & Calder V. (1993) Lymphocyte Migration Through Cultured Endothelial Cell Monolayers Derived From the Blood-retinal Barrier. Immunology 80: 401-6

Greenwood J., Pryce G., Devine L., Male D.K., dos Santos W.L.C., Calder V.L. & Adamson P. (1996) SV40 Large T Immortalised Cell Lines of the Rat Blood-Brain and Blood-Retinal Barriers Retain Their Phenotypic and Immunologic Characteristics. *J. Neuroimmunol.* 71: 51-63

Greenwood J., Etienne-Manneville S., Adamson P. & Couraud P-O. (2002) Lymphocyte Migration into the Central Nervous System: Implication of ICAM-1 Signalling at the Blood-brain Barrier. *Vascul. Pharmacol.* 38: 315-22

Greenwood J., Amos C.L., Walters C.E., Couraud P-O., Lyck R., Engelhardt B. & Adamson P. (2003a) Intracellular Domain of Brain Intercellular Adhesion Molecule-1 is Essential for T Lymphocyte-mediated Signaling and Migration. *J. Immunol.* 171: 2099-108

Greenwood J., Walters C.E., Pryce G., Kanuga N., Beraud E., Baker D. & Adamson P. (2003b) Lovastatin Inhibits Brain Endothelial Cell Rho-mediated Lymphocyte migration and Attenuates Experimental Autoimmune Encephalomyelitis. *FASEB J.* 17: 905-7

Greer S.F., Lin J., Clarke C.H. & Justement L.B. (1998) Major Histocompatibility Class II-mediated Signal Transduction is Regulated by the Protein Tyrosine Phosphatase CD45. *J. Biol. Chem.* 273: 11970-79

Grindstaff K.K., Yeaman C., Anandasabapathy N., Hsu S.C., Rodriguez-Boulan E., Scheller R.H. & Nelson W.J. (1998) Sec6/8 Complex is Recruited to Cell-cell Contacts and Specifies Vesicle Delivery to the Basal-lateral Membrane in Epithelial Cells. *Cell* 93: 731-40

Gross P.M. amd Wiendl H. (1987) Peering Through the Windows of the Brain. *J. Cereb. Blood Flow Metab.* 7: 663-72

Gumbiner B., Lowenkopf T. & Apatira D (1991) Identification of a 160-Kda Polypeptide That Binds to the Tight Junction Protein ZO-1. *Proc. Natl. Acad. Sci. USA* 88: 3460-64

Gumbleton M. & Audus K.L. (2001) Progress and Limitations in the Use of in vitro Cell Cultures to Serve as a Permeability Screen for the Blood-brain Barrier. *J. Pharm. Sci.* 90: 1681-98

Haskins J., Gu L., Wittchen E.S., Hubbard J. & Stevenson B.R. (1998) ZO-3, a Novel Member of the MAGUK Protein Family Found at the Tight Junction, Interacts with ZO-1 and Occludin. *J. Cell Biol.* 141: 199-208

Hein M., Madefessel C., Haag B., Teichmann K., Post A. & Galla H. (1992) Reversible Modulation of Transepithelial Resistance in High and Low Resistance MDCK-cells by Basic Amino Acids, Ca^{2+}, Protamine and Protons. *Chem. Phys. Lipids* 63: 223-33

Hermant B., Bibert S., Concord E., Dublet B., Weidenhaupt M., Vernet T. & Gulino-Debrac D. (2003) Identification of Proteases Involved in the Proteolysis of Vascular Endothelium Cadherin During Neutrophil Transmigration. *J. Biol. Chem.* 278: 14002-12

Herrenknecht K. Ozawa M., Eckerskorn C., Lottspeich F., Lenter M. & Kemler R. (1991) The Uvomorulin-anchorage Protein Alpha Catenin is a Vinculin Homologue. *Proc. Natl. Acad. Sci. USA* 88: 9156-60

Hickey W.F. (2001) Basic Principles of Immunological Surveillance of the Central Nervous System. *Glia* 36: 118-24

Hirabayashi S., Tajima M., Yao I., Nishimura W., Mori H. & Hata Y. (2003) JAM4, a Junctional Cell Adhesion Molecule Interacting with a Tight Junction Protein, MAGI-1. *Mol. Cell Biol.* 23: 4267-82

Hirase T., Staddon J.M., Saitou M., Ando-Akatsuka Y., Itoh M., Furuse M., Fujimoto K., Tsukita S. & Rubin L.L. (1997) Occludin as a Possible Determinant of Tight Junction Permeability in Endothelial Cells. *J. Cell Sci.* 110: 1603-13

Hirase T., Kawashima S., Wong E.Y.M., Ueyama T., Rikitake Y., Tsukita S., Yokoyama M. & Staddon J.M. (2001) Regulation of Tight Junction Permeability and Occludin Phosphorylation by RhoA-p160ROCK-dependent and -independent Mechanisms. *J. Biol. Chem.* 276: 10423-31

Holness C.L. & Simmons D.L. (1994) Structural Motifs for Recognition and Adhesion in Members of the Immunoglobulin Superfamily. *J. Cell Sci.* 107: 2065-70

Hopkins A.M., Li D., Mrsny R.J, Walsh & Nusrat A. (2000) Modulation of Tight Junction Function by G Protein-coupled Events. *Adv. Drug Deliv. Rev.* 41: 329-40

Hordijk P.L., Anthony E., Mul F.P.J., Rientsma R., Oomen L.C.J.M. & Roos D. (1999) Vascular-endothelial-cadherin Modulates Endothelial Monolayer Permeability. *J. Cell Sci.* 112: 1915-23

Hordijk P.L. (2003) Endothelial Signaling in Leucocyte Transmigration. *Cell Biochem. Biophys.* 38: 305-22

Hu Y., Szente B., Kiely J-M. & Gimbrone jr. M.A. (2001) Molecular Events in Transmembrane Signalling via E-selectin. *J. Biol. Chem.* 276: 48549-48553

Hua C.T, Gamble J.R., Vadas M.A., & Jackson D.E. (1998) Recruitment and Activation of SHP-1 Protein-tyrosine Phosphatase by Human Platelet Endothelial Cell Adhesion Molecule-1 (PECAM-1). Identification of Immunoreceptor Tyrosine-based Inhibitory Motif-like Binding Motifs and Substrates. *J.Biol.Chem.* 273: 28332-40

Huang S-H. & Ambrose Y.J. (2001) Cellular Mechanisms of Microbial Proteins Contributing to Invasion of the Blood-brain Barrier. *Cell. Microbiol.* 3: 277-87

Huang A.J., Manning J.E., Bandak T.M., Ratau M.C., Hanser K.R. & Silverstein S.C. (1993) Endothelial Cell Cytosolic Free Calcium Regulates Neutrophil Migration Across Monolayers of Endothelial Cells. *J. Cell Biol.* 120: 1371-80

Huber D., Balda M.S. & Matter K. (2000) Occludin Mediates Transepithelial Migration of Neutrophils. *J. Biol. Chem.* 275: 5773-78

Huber J.D., Egleton R.D. & Davis T.P. (2001) Molecular Physiology and Pathophysiology of Tight Junctions in the Blood-brain Barrier. *Trends Neurosci.* 24: 719-25

Hurst R.D. & Fritz I.B. (1996) Properties of an Immortalised Vascular Endothelial/Glioma Cell Co-culture Model of the Blood-brain Barrier. *J. Cell Physiol.* 167: 81-8

Hurst V.I., Goldberg P.L., Minnear F.L., Heimark R.L. & Vincent P.A. (1999) Rearrangement of Adherens Junctions by Transforming Growth Factor-β1: Role of Contraction. *Am. J. Physiol.* 276: L582-95

Hwang S.T., Singer M.S., Giblin P.A., Yednock T.A., Bacon K.B., Simon S.I. & Rosen S.D. (1996) GlyCAM-1, a Physiologic Ligand for L-selectin, Activates β_2 Integrins on Naïve Peripheral Lymphocytes. *J. Exp. Med.* 184: 1343-8

Ilan N., Mahooti S., Rimm D.L. & Madri J.A. (1999) PECAM-1 (CD31) Functions As a Reservoir for and a Modulator of Tyrosine-Phosphorylated β-catenin. *J. Cell Sci.* 112: 3005-3014

Ilan N., Cheung L., Pinter E. & Madri J.A. (2000) Platelet-endothelial Cell Adhesion Molecule-1 (PECAM-1 (CD31), a Scaffolding Molecule for Selected Catenin Family Members Whose Binding is Mediated by Different Tyrosine and Serine/Threonine Phosphorylation. *J. Biol. Chem.* 275 : 21435-43

Inai T., Kobayashi J. & Shibata Y. (1999) Claudin-1 Contributes to the Epithelial Barrier Function in MDCK Cells. *Eur. J. Cell Biol.* 78: 849-55

Ionescu C.V., Cepinskas G., Savickiene J., Sandig M. & Kvietys P.R. (2003) Neutrophils Induce Sequential Focal Changes in Endothelial Adherens Junction Components: Role of Elastase. *Microcirculation* 10: 205-20

Itoh M., Yonemura S., Nagafuchi A., Tsukita S. & Tsukita S. (1991) A 220-kD Undercoat-constitutive Protein: Its Specific Localisation to Cadherin-based Cell-cell Adhesion Sites. *J. Cell Biol.* 115: 1449-62

Itoh M., Nagafuchi A., Yonemura S., Kitani-Yasuda T., Tsukita S. & Tsukita S. (1993) The 220-kD Protein Colocalising With Cadherin in Non-epithelial Cells is Identical to ZO-1, A Tight Junction-associated Protein in Epithelial Cells: cDNA Cloning and Immunoelectron Microscopy. *J. Cell Biol.* 121: 491-502

Itoh M., Nagafuchi A., Moroi S. & Tsukita S. (1997) Involvement of ZO-1 in Cadherin-based Cell Adhesion Through Its Direct Binding of α-catenin and Actin Filaments. *J. Cell Biol.* 138: 181-92

Itoh M., Morita K. & Tsukita S. (1999a) Characterisation of ZO-2 as a MAGUK Family Member Associated with Tight as Well as Adherens Junctions with a Binding Affinity to Occludin and α Catenin. *J. Biol. Chem.* 274: 5981-86

Itoh M., Furuse M., Morita K., Kubota K., Saitou M. & Tsukita S. (1999b) Direct Binding of Three Tight Junction-associated MAGUKs, ZO-1, ZO-2 and ZO-3 with the COOH Termini of Claudins. *J. Cell Biol.* 147: 1351-63

Izumi Y., Hirose T., Tamai Y., Hirai S., Nagashima Y., Fujimoto T., Tabuse Y., Kemphues K.J. & Ohno S. (1998) An Atypical PKC Directly Associates wih and Colocalises at the Epithelial Tight Junction with ASIP, a Mammalian Homologue of *Caenorhabditis elegans* Polarity Protein PAR-3. *J. Cell Biol.* 143: 95-106

Jackson D.E., Ward C.M., Wang R. & Newman P.J. (1997) The Protein –tyrosine Phosphatse SHP-2 Binds Platelet/Endothelial Cell Adhesion Molecule-1 (PECAM-1) and Forms a Distinct Signalling Complex During Platelet Aggregation. *J. Biol. Chem.* 272: 6986-93

Janzer R.C. & Raff M.C. (1987) Astrocytes Induce Blood-brain Barrier Properties in Endothelial Cells. *Nature* 325: 253-7

Johanson C.E. (1980) Permeability and Vascularity of the Developing Brain: Cerebellum vs. Cerebral Cortex. *Brain Res.* 190: 3-16

Johnson-Leger C., Aurrand-Lions M. & Imhof B.A. (2000) The Parting of the Endothelium: Miracle, or Simply a Junctional Affair? *J. Cell Sci.* 113: 921-33

Joo F. (1996) Endothelial Cells of the Brain and Other Organ Systems: Some Similarities and Differences. *Prog. Neurobiol.* 48: 255-73

Kachar B. & Reese T. (1982) Evidence for the Lipidic Nature of Tight Junction Strands. *Nature* 296: 464-6

Kansas G.S. (1996) Selectind and Their Ligands: Current Cocepts and Controversies. *Blood* 88: 3259-87

Kaplan D.D., Meigs T.E. & Casey P.J. (2001) Distinct Regions of the Cadherin Cytooplasmic Domain Are Essential for Functional Interaction with $G\alpha_{12}$ and β-catenin. *J. Biol. Chem.* 276: 44037-43

Karasuyama H. & Melchers F. (1988) Establishment of Mouse Cell Lines Which Constitutively Secrete Large Quantities of Interkeukin 2, 3, 4 or 5, Using Modified cDNA Expression Vectors. *Eur. J. Immunol.* 18: 97-104

Katsube T., Takahisa M., Ueda R., Hashimoto N., Kobayashi M. & Togashi S. (1998) Cortactin Associates with the Cell-cell Junction Protein ZO-1 in Both Drosophila and Mouse. *J. Biol. Chem.* 273: 29672-7

Kawamura-Kodama K., Tsutsui J., Suzuki S.T., Kanzaki T. & Ozawa M. (1999) N-cadherin Expressed on Malignant T cell Lymphoma Cells is Functional, and Promotes Heterotypic Adhesion Between the Lymphoma Cells and Mesanchymal Expressing N-cadherin. *J. Invest. Dermatol.* 112: 62-6

Keon B.H., Schafer S., Kuhn C., Grund C & Franke W.W. (1996) Symplekin, a Novel Type of Tight Junction Plaque Protein. *J. Cell Biol.* 134: 1003-18

Klingler C., Kneisel U., Bamforth S.D., Wolburg H., Engelhardt B. & Risau W. (2000) Disruption of Epithelial Tight Junctions is Prevented by Cyclic Nucleotide-dependent Protein Kinase Inhibitors. *Histochem. Cell Biol.* 113: 349-61

Kojima T., Kokai Y., Chiba H., Osanai M., Kuwahara K., Mori M., Mochizuki Y. & Sawada N. (2001) Occludin and Claudin-1 Concentrate in the Midbody of Immortalised Mouse Hepatocytes During Cell Division. *J. Histochem. Cytochem.* 49: 333-39

Konstantoulaki M., Kouklis P. & Malik A.B. (2003) Protein Kinase C Modifications of VE-cadherin, p120 and β-catenin Contribute to Endothelial Barrier Dysregulation Induced by Thrombin. *Am. J. Physiol. Lung Cell Mol. Physiol.* 285: L434-42

Kowalczyk A.P., Navarro P., Dejana E., Bornslaeger E.A., Green K.J., Kopp D.S. & Borgwardt J.E. (1998) VE-cadherin and Desmoplakin are Assembled into Dermal Microvascular Endothelial Intercellular Junctions: A Pivotal Role for Plakoglobin in the Recruitment of Desmplakin to Intercellular junctions. *J. Cell Sci.* 111: 3045-57.

Lacaud G., Gore L., Kennedy M., Kouskoff V., Kingsley P., Hogan C, Carlsson L., Speck N., Palis J. & Keller G. (2002) *Runx1* is Essential for Hematopoietic Commitment at the Hemangioblast Stage of Development In Vitro. *Blood.* 100: 458-66

Lacaz-Vieira F., Jaegar M.M.M., Farshori P. & Kachar B. (1999) Small Synthetic Peptides Homologous to Segments of the First External Loop of Occludin Impair Tight Junction Resealing. *J. Membrane Biol.* 168: 289-97

Lampe P.D. & Lau A.F. (2000) Regulation of Gap Junctions by Phosphorylation of Connexins. *Arch. Biochem. Biophys.* 384: 205-15

Lampugnani M.G., Corada M., Cavead L., Breviario F., Ayalon O., Geiger B. & Dejana E. (1995) The Molecular Organisation of Endothelial Cell to Cell Junctions: Differential Association of plakoglobin, β-catenin and α-catenin with vascular endothelial cadherin (VE-cadherin). *J. Cell Biol.* 129: 203-17

Lampugnani M.G., Corada M., Andriopoulou P., Esser S., Risau W. & Dejana E. (1997) Cell Confluence Regulates Tyrosine Phosphorylation of Adherens Junction Components in Endothelial Cells. *J. Cell Sci.* 110: 2065-77

Lampugnani M.G., Zanetti A., Breviario F., Balconi G., Orsenigo F., Corada M., Spagnuolo R., Betson M., Braga V. & Dejana E. (2002) VE-cadherin Regulates Endothelial Actin Activating Rac and Increasing Membrane Association of Tiam. *Mol. Biol. Cell* 13: 1175-89

Lapierre L.A., Tuma P.L., Goldenring J.R., Nararre J. & Anderson J.M. (1999) VAP-33 Localises with Occludin at the Intercellular Tight Junction and Also with Intracellular Vesicles. *J. Cell Sci.* 112: 3723-32

Lapierre L.A. (2000) The Molecular Structure of the Tight Junction. *Adv. Drug Deliv. Rev.* 41: 255-64

Laschinger M. & Engelhardt B. (2000) Interaction of α4-integrin with VCAM-1 is Involved in Adhesion of Encephalitogenic T Cell Blasts to Brain Endothelium But Not in Their Transendothelial Migration in vitro. *J. Neuroimmunol.* 102: 32-43

Laschinger M., Vajkoczy P. & Engelhardt B. (2002) Encephalitogenic T Cells Use LFA-1 for Transendothelial Migration But Not During Capture and Initial Adhesion Strengthening in Healthy Spinal Cord Microvessels in vivo. *Eur. J. Immunol.* 32: 3598-606

Lasky L.A. (1995) Selectin-carbohydrate Interactions and the Initiation of the Inflammatory Response. *Ann. Rev. Biochem.* 64: 113-39

Lawson C., Ainsworth M. Yacoub M. & Rose M. (1999) Ligation of ICAM-1 on Endothelial Cells Leads to Expression of VCAM-1 Via a Nuclear Factor-κB-independent Mechanism. *J. Immunol.* 162: 2990-96

Lee S.J., Drabik K., van Wagoner N.J., Lee S., Choi C., Dong Y. & Benveniste E.N. (2000) ICAM-1-induced Expression of Proinflammatory Cytokines in Astrocytes: Involvement of Extracellular Signal-regulated Kinase and p38 Mitogen-activated Protein Kinase Pathways. *J. Immunol.* 165: 4658-66

Leier I., Jedlitschky G., Buchholz U., Center M., Cole S.P.C., Deeley R.G. & Keppler D. (1996) ATP-dependent Glutathione Disulphide Transport Mediated by the MRP Gene-encoded Conjugate Export Pump. *Biochem J.* 314: 433-7

Liang T.W., Chiu H.H., Gurney A., Sidle A., Tumas D.B., Schow P., Foster J., Klassen T., Dennis K., Demarco R.A., Pham T., Frantz G. & Fong S. (2002) Vascular Endothelial-Junctional Adhesion Molecule (VE-JAM)/ JAM 2 Interacts with T, NK and Dendritic Cells through JAM 3. *J. Immunol.* 168: 1618-26

Lorenzon P., Vecile E., Nardon E., Ferrero E., Harlan J.M., Tedesco F. & Dobrina A. (1998) Endothelial Cell E- and P-selectin and Vascular Cell Adhesion Molecule-1 Function as Signalling Receptors. *J. Cell Biol.* 142: 1381-91

Lu T.T., Barreuther M., Davis S. & Madri J.A. (1997) Platelet Endothelial Cell Adhesion Molecule-1 is Phosphorylatable By c-Src, Binds Src-src Homology 2 Domain, and Exhibits Immunoreceptor Tyrosine-based Activation Motif-like Properties. *J. Biol. Chem.* 272: 14442-6

Luscinskas F.W., Lim Y-C. & Lichtman A.H. (2001) Wall Shear Stress: the Missing Step for T Cell Transmigration. *Nature Immunol.* 2: 478-80

Male D., Pryce G., Hughes C. & Lantos P.L. (1990) Lymphocyte Migration Into Brain Modelled in vitro: Control by Lymphocyte Activation, Cytokines and Antigen. *Cell. Immunol.* 127: 1-11

Mamdouh Z., Chen X., Pierini L.M., Maxfield F.R. & Muller W.A. (2003) Targeted Recycling of PECAM from Endothelial Surface-connected Compartments During Diapedesis. *Nature* 421: 748-53

Mankertz J., Waller J.S., Hillenbrand B., Tavalali S., Florian P., Schoneberg T., Fromm M. & Schulzke J.D. (2002) Gene Expression of the Tight Junction Protein Occludin Includes Differential Splicing and Alternative Promotor Usage. *Biochem. Biophys Res. Commun.* 298: 657-666

Martinez-Estrada M.O., Villa A., Breviario F., Orsenigro F., Dejana E. & Bazzoni G. (2001) Association of Junctional Adhesion Molecule with Calcium/Calmodulin-dependent Serine Protein Kinase (CASK/LIN-2) in Human Epithelial Caco-2 Cells. *J. Biol. Chem.* 276: 9291-6

Martin-Padura I., Lostaglio S., Schneemann M., Williams L., Romano M., Fruscell P., Panzeri C., Stoppacciaro A., Ruco L., Villa A., Simmons D. & Dejana E. (1998) Junctional Adhesion Molecule, a Novel Member of the Immunoglobulin Superfamily That Distributes at Intercellular Junctions and Modulates Monocyte Transmigration. *J. Cell Biol.* 142:117-27

Mattagajasingh S.N., Juang S.C., Hartenstein J.S., Benz E.J. (1999) Protein 4.1R Interacts with Zonula Occludens-2 (ZO-2) and Possibly Links the Tight Junction with the Actin Cytoskeleton. *Mol. Biol. Cell* 10: 2357

Matter K. & Balda M.S. (1998) Biogenesis of Tight Junctions: The C-Terminal Domain of Occludin Mediates Basolateral Targeting. *J. Cell Sci.* 111: 511-19

Matter K. & Balda M.S. (2003) Holey Barrier: Claudins and the Regulation of Brain Endothelial Permeability. *J. Cell Biol.* 161: 459-60

Merwin J.R., Anderson J.M., Kocher O. Van Itallie C.M. & Madri J.A. (1990) Transforming Growth Factor-β1 Modulates Extracellular Matrix Organisation and Cell-cell Junctional Complex Formation During In Vitro Angiogenesis. *J. Cell Physiol.* 142: 117-28

Meyer T.N., Schwesinger C., Ye J., Denker B.M. & Nigam S.K. (2001) Reassembly of the Tight Junction after Oxidative Stress Depends on Tyrosine Kinase Activity. *J. Biol. Chem.* 276: 22048-55

Miller D.W. (1999) Immunobiology of the Blood-brain Barrier. *J. Neurovirol.* 5: 570-8

Mitic L.L., Schneeberger E.E., Fanning A.S. & Anderson J.M. (1999) Connexin-Occludin Chimeras Containing the ZO-binding Domain of Occludin Localise at MDCK Tight Junctions and NRK Cell Contacts. *J. Cell Biol.* 146: 683-93

Mitic L.L., Van Itallie C.M. & Anderson J.M. (2000) Molecular Physiology and Pathophysiology of Tight Junctions I. Tight Junction Strucure and Function: Lessons from Mutant Animals and Proteins. *Am. J. Physiol. Gastrointest. Liver Physiol.* 279: G250-G254

Moll T., Dejana E. & Vestweber D. (1998) In Vitro Degradation of Endothelial Cadherins by a Neutrophil Protease. *J. Cell Biol.* 140: 403-7

Montesano R. & Orci L. (1988) Intracellular Diaphragmed Fenestrae in Cultured Capillary Endothelial Cells. *J. Cell Sci.* 89:441-7

Moore K.L., Patel K.D., Bruehl R.E., Li F., Johnson D.A., Lichenstein H.S., Cummings R.D., Bainton D.F. & MacEver R.P. (1995) P-selectin Glycoprotein Ligand-1 Mediates Rolling of Human Neutrophils on P-selectin. *J. Cell Biol.* 128: 661-71

Morita K., Sasaki H., Furuse M. & Tsukita S. (1999) Endothelial Claudin: Claudin 5/TMVCF Constitutes Tight Junction Strands in Endothelial Cells. *J. Cell. Biol.* 147: 185-94

Muller W.A., Weigel S.A., Deng X. & Petzelbauer P. (1993) PECAM-1 is Required for Transendothelial Migration of Leucocytes. *J. Exp. Med.* 178: 449-60

Munro S.B., Duclos A.J., Jackson A.R., Baines M.G. & Balschuk O.W. (1996) Characterisation of Cadherins Expressed by Murine Thymocytes. *Cell Immunol.* 169: 309-12

Muresan Z., Paul D.L., Goodenough D.A. (2000) Occludin 1B: a Variant of the Tight Junction Protein Occludin. *Mol. Biol. Cell* 11: 627-34

Nag S. (1995) Role of the Endothelial Cyoskeleton in Blood-brain Barrier Permeability to Protein. *Acta Neuropathol.* 90: 454-60

Nasdala I., Wolburg-Buchholz K., Wolburg H., Kuhn A., Ebnet K., Brachtendorf G., Samulowitz U., Kuster B., Engelhardt B., Vestweber D. & Butz S. (2002) A Transmembrane Protein Selectively Expressed on Endothelial Cells and Platelets. *J. Biol. Chem.* 277: 16294-303

Navarro P., Ruco L. & Dejana E. (1998) Differential Localisation of VE- and N-cadherin in Human Endothelial Cells. VE-cadherin Competes with N-cadherin for Junctional Localisation. *J. Cell Biol.* 140: 1475-84

Nawroth R., Poell G., Ranft A., Kloep S., Samulowitz U., Fachinger G., Golding M., Shima D.T., Deutsch U. & Vestweber D. (2002) VE-PTP and VE-cadherin Ectodomains Interact to Facilitate Regulation of Phosphorylation and Cell Contacts. *EMBO J.* 21: 4885-95

Nelson C.M. & Chen C.S. (2003) VE-cadherin Simultaneously Stimulates and Inhibits Cell Proliferation by Altering Cytoskeletal Structure and Tension. *J. Cell Sci.* 116: 3571-81

Newman P.J. (1997) The Biology of PECAM-1. *J. Clin. Invest.* 99: 3-8

Nitta T., Hata M., Gotoh S., Seo Y., Sasaki H., Hashimoto N., Furuse M. & Tsukita S. (2003) Size-selective Loosening of the Blood-brain Barrier in Claudin-5-deficient Mice. *J. Cell Biol.* 161: 653-60

Nusrat A., Chen J.A., Foley C.S., Liang T.W., Tom J., Cromwell M., Quan C. & Mrsny R.J. (2000a) The Coiled-coil Domain of Occludin Can Act to Organise Structural and Functional Elements of the Epithelial Tight Junction. *J. Biol. Chem.* 275: 29816-29822

Nusrat A., Turner J.R. & Madara J.L. (2000b) Molecular Physiology and Pathophysiology of Tight Junctions IV. Regulation of Tight Junctions by Extracellular

Stimuli: Nutrients, Cytokines and Immune Cells. *Am. J. Physiol. Gastrointest. Liver Physiol.* 279: G851-G857

Ohkubo T. & Ozawa M. (1999) p120(ctn) Binds to the Membrane-proximal Region od the E-cadherin Cytoplsamic Domain and is Involved in Modulation of Adhesion Activity. *J. Biol. Chem.* 274: 21409-15

Oshima T., Laroux F.S., Coe L.L., Morise Z., Kawachi S., Bauer P., Grisham M.B., Specian R.D., Carter P., Jennings S., Granger D.N., Joh T. & Alexander J.S. (2001) Interferon-γ and Interleukin-10 Reciprocally Regulate Endothelial Junction Integrity and Barrier Function. *Microvasc. Res.* 61:130-43

Ostermann G., Weber K.S.C., Zernecke A., Schroder A. & Weber C. (2002) JAM-1 is a Ligand of the β_2 Integrin LFA-1 Involved in Transendothelial Migration of Leukocytes. *Nat. Immunol.* 3: 151-8

Ozaki H., Ishii K., Horiuchi H., Arai H., Kawamoto T., Okawa K. Iwamatsu A. & Kita T. (1999) Cutting Edge: Combined Treatment of TNF-α and IFN-γ Causes Redistribution of Junctional Cell Adhesion Molecule in Human Endothelial Cells. *J. Immunol.* 163: 553-7

Öztas B. (1998) Sex and the Blood-brain Barrier. *Pharm. Res.* 37: 165-7

Pachter J.S., de Vries H.E. & Fabry Z. (2003) The Blood-brain Barrier and its Role in Immune Privilege in the Central Nervous System. *J. Neuropathol. Exp. Neurol.* 62: 593-604

Pardridge W.M. (1997) Drug Delivery to the Brain. *J. Cereb. Blood Flow Metab.* 17: 713-31

Pellegatta F., Chierchia S.L. & Zocci M.R. (1998) Functional Association of Platelet-endothelial Cell Adhsion Molecule-1 and Phosphoinositide 3-kinase in Human Neutrophils. *J. Biol. Chem.* 273: 27768-71

Perez O.D., Kinoshita S., Hitoshi Y., Payan D.G., Kitamura T., Nolan G.P. & Lorens J.B. (2002) Activation of the PKB/AKT Pathway by ICAM-2. *Immunity* 16: 51-65

Persidsky Y. (1999) Model Systems for Studies of Leukocyte Migration Across the Blood-brain Barrier. *J. Neurovirol.* 5: 579-90

Piali L., Albelda S.M., Baldwin H.S., Hammel P., Gisler R.H. & Imhof B.A. (1993) Murine Platelet Endothelial Cell Adhesion Molecule (PECAM-1)/CD31 Modulates Beta 2 Integrins on Lymphokine-activated Killer Cells. *Eur. J. Immunol.* 23: 2464-71

Piccio L., Rossi B., Scarpini E., Laudanna C., Giagulli C., Issekutz A.C, Vestweber D., Butcher E.C. & Constantin G. (2002) Molecular Mechanisms Involved in Lymphocyte Recruitment in Inflamed Brain Microvessels: Critical Roles for P-Selectin Glycoprotein Ligand-1 and Heterotrimeric G_i-Linked Receptors. *J. Immunol.* 168: 1940-9

Picker L.J., Warnock R.A., Burns A.R., Doerschuk C.M., Berg E.L. & Butcher E.C. (1991) The Neutrophil Selectin LECAM-1 Presents Carbohydrate Ligands to the Vascular Selectins ELAM-1 and GMP-140. *Cell* 66: 921-33

Planchon S., Fiocchi C., Takafuji V. & Roche J.K. (1999) Transforming Growth Factor-β1 Preserves Epithelial Barrier Function: Identification of Receptors, Biochemical Intermediates and Cytokine Antagonists. *J. Cell Physiol.* 181: 55-66

Ponting C.P. (1995) AF-6/cno: Neither a Kinesin nor a Myosin, But a Bit of Both. *Trends Biochem. Sci.* 20: 265-6

Ponting C.P. (1997) Evidence For PDZ DomainS IN Bacteria, Yeast and Plants. *Protein Sci.* 6: 464-8

Prasad R., Gu Y., Alder H., Nakamura T., Canaani O., Saito H., Huebner K., Gale R.P., Nowell P.C., Kuriyama K et al. (1993) Cloning of the ALL-1 Fusion Partner, the AF-6 Gene, Involved in Acute Myeloid Leukemias with the t(6;11) Chromosome Translocation. *Cancer Res.* 53: 5624-28

Prat A., Biernacki K., Wosik K. & Antel J.P. (2001) Glial Cell Influence on the Human Blood-brain Barrier. *Glia* 36: 145-55

Prescott L. & Brightman M.W. (1998) Circumventricular Organs of the Brain. In Pardridge, W.M. (ed.) *An Introduction to the Blood-brain Barrie: Methodology, Biology and Pathology*, Cambridge University Press, Cambridge. pp. 270-6

Pryce G., Male D., Campbell I. & Greenwood J. (1997) Factors Controlling T-Cell Migration Across Rat Cerebral Endothelium In Vitro. *J. Neuroimmunol.* 75: 84-94

Pumphrey N.J., Taylor V., Freeman S., Douglas M.R., Bradfield P.F., Young S.P., Lord J.M., Wakelam M.J., Bird I.N., Salmon M. & Buckley C.D. (1999) Differential Association of Cytoplasmic Signalling Molecules SHP-1, SHP-2, SHIP and Phospholipase C-gamma1 with PECAM-1/CD31. *FEBS Lett.* 450: 77-83

Qin Y. & Sato T.N. (1995) Mouse Multidrug Resistance 1a/3 Gene is the Earliest Known Endothelial Cell Differentiation Marker During Blood-brain Barrier Development. *Dev. Dyn.* 202: 172-80

Ransohoff R.M., Kivisakk P. & Kidd G. (2003) Three or More Routes For Leukocyte Migration Into the Central Nervous System. *Nature Rev. Immunol.* 3: 569-81

Ratcliffe M.J., Rubin L.L. & Staddon J.M. (1997) Dephosphorylation of the Cadherin-associated p100/p120 Proteins in Response to Activation of Protein Kinase C in Epithelial Cells. *J. Biol. Chem.* 272: 31894-31901

Ratcliffe M.J., Smales C. & Staddon J.M. (1999) Dephosphorylation of the Catenins p120 and p100 in Endothelial Cells in Response to Inflammatory Stimuli. *Biochem. J.* 338: 471-8

Reese T.S. & Karnovsky M.J. (1967) Fine Structural Localisation of a Blood-brain Barrier to Exogenous Peroxide. *J. Cell Biol.* 34: 207-17

Regina A., Romero I.A., Greenwood J., Adamson P., Bourre J.M., Couraud P-O. & Roux E. (1999) Dexamethasone Regulation of P-glycoprotein Activity in an Immortalised Rat Brain Endothelial Cell Line, GPNT. *J. Neurochem.* 73: 1954-63

Ricard I., Payet M.D. & Dupuis G. (1997) Clustering the Adhesion Molecules VLA-4 (CD49d/CD29) in Jurkat T Cells or VCAM-1 in Endothelial (ECV 304) Cells Activates

the Phosphoinositide Pathway and Triggers Ca^{2+} Mobilisation. *Eur. J. Immunol.* 27: 1530-1538

Risau W., Hallmann R. & Albrecht U. (1986) Differentiation-dependent Expression of Protein in Brain Endothelium During Development of the Blood-brain Barrier. *Dev. Biol.* 117: 537-45

Risau W. & Wolburg H. (1990) Development of the Blood-brain Barrier. *Trends Neurosci.* 13: 174-8

Robinson C & Baker S.F. (2001) Peptidase Allergens, Occludin and Claudins. Do Their Interactions Facilitate the Development of Hypersensitivity Reactions at Mucosal Surfaces? *Clin. Exp. Allergy* 31: 186-92

Romero I.A., Radewicz K., Jubin E., Michel C.C., Greenwood J., Couraud P-O. & Adamson P. (2003) Changes in Cyoskeletal and Tight Junctional Proteins Correlate with Decreased Permeability Induced by Dexamethasone in Cultured Rat Brain Endothelial Cells. *Neurosci. Lett.* 344: 112-6

Rosen S.D. and Bertozzi C.R. (1994) The Selectins and Their Ligands. *Curr. Opin. Cell Biol.* 6: 663-73

Rothlein R., Kishimoto T.K., & Mainolfi E. (1994) Crosslinking of ICAM-1 Induces Co-signalling of an Oxidative Burst From Mononuclear Leucocytes. *J. Immunol.* 152: 2488-95

Roux F., Durieu-Trautmann O., Chaverot N., Claire M., Mailly P., Bourne J.M., Strosberg A.D. & Couraud P-O. (1994) Regulation of γ-glutamyl Transpeptidase and Alkaline Phosphatase Activities in Immortalised Rat Brain Microvessel Endothelial Cells. *J. Cell Physiol.* 159: 101-13

Rubin L.L., Hall D.E., Porter S., Barbu K., Cannon C., Horner H.C., Janatpour M., Liaw C.W., Manning K. & Morales J. (1991) A Cell Culture Model of the Blood-brain Barrier. *J. Cell Biol.* 115: 1725-35

Rubin L.L. & Staddon J.M. (1999) The Cell Biology of the Blood-brain Barrier. *Ann. Rev. Neurosci.* 22: 11-28

Saitou M., Fujimoto K., Doi Y., Itoh M., Fujimoto T., Furuse M., Takano H., Noda T. & Tsukita S. (1998) Occludin-deficient Embryonic Stem Cells Can Differentiate Into Polarised Epithelial Cells Bearing Tight Junctions. *J. Cell Biol.* 141: 397-408

Saitou M., Furuse M., Sasaki H., Schulzke J-D., Fromm M., Takano H., Noda T. & Tsukita S. (2000) Complex Phenotype of Mice Lacking Occludin, a Component of Tight Junction Strands. *Mol. Biol. Cell* 11: 4131-42

Sakakibara A., Furuse M., Saitou M., Ando-Akatsuka Y. & Tsukita S. (1997) Possible Involvement of Phosphorylation of Occludin in Tight Junction Formation. *J. Cell Biol.* 137: 1393-1401

Saloman D., Sacco P., Roy S., Simcha I., Johnson K., Wheelock M. & Ben-Ze'ev A. (1997) Regulation of β-catenin Levels and Localisation By Overexpression of Plakoglobin and Inhibition of the Ubiquitin-proteasome System. *J. Cell Biol.* 139: 1325-35

Sans E., Delachlanal E. & Duperray A. (2001) Analysis of the Roles of ICAM-1 in Neutrophil Transmigration Using a Reconstituted Mammalian Cell Expression Model: Implication of ICAM-1 Cytoplasmic Domain and Rho-dependent Signaling Pathways. *J. Immunol.* 166: 544-51

Sastry S.K. & Burridge K. (2000) Focal Adhesions: A Nexus for Intracellular Signalling and Cytoskeletal Dynamics. *Exp. Cell Res.* 261: 25-36

Satoh H., Zhong Y., Isomura H., Saitoh M., Enomoto K., Sawada N. & Mori M. (1996) Localisation of 7H6 Tight Junction-associated Antigen Along the Cell Border of Vascular Endothelial Cells Correlates with Paracellular Barrier Function Against ions, Large Molecules and Cancer Cells. *Exp. Cell Res.* 222: 269-74

Schiera G., Bono E., Raffa M.P., Gallo A., Pitarresi G.L., Di Liegro I. & Savetierri G. (2003) Synergistic Effects of Neurons and Astrocytes on the Differentiation of Brain Capillary Endothelial Cells in Culture. *J. Cell Mol. Med.* 7: 165-70

Schimmenti L.A., Yan H.C., Madri J.A. & Albelda SM. (1992) Platelet Endothelial Cell Adhesion Molecule, PECAM-1, Modulates Cell Migration. *J. Cell Physiol.* 153: 417-28

Schinkel A.H., Smit J.J., van Tellingen O., Beijnen J.H., Wagenaar E., van Deemter L., Mol C.A.A.M., van der Valk M.A., Robanus-Maandag E.C., te Riele H.P. et al (1994) Disruption of the Mouse mdr1a P-glycoprotein Gene Leads to a Deficiency in the Blood-brain Barrier and to Increased Sensitivity to Drugs. *Cell* 77:491-502

Schinkel A.H., Wagenaar E., Mol C.A.A.M. & Deemter L. (1996) P-glycoprotein in the Blood-brain Barrier of Mice Influences the Brain Penetration and Pharmacological Activity of Many Drugs. *J. Clin. Invest.* 97: 2517-24

Schmelz M., Moll R., Kuhn C. & Franke W.W. (1994) Complexus Adhaerentes, a New Group of Desmoplakin-containing Junctions in Endothelial Cell: II Different Types of Lymphatic Vessels. *Differentiation* 57: 97-117

Schulze C. & Firth J.A. (1992) Interendothelial Junctions During Blood-brain Barrier Development in the Rat: Morphological Changes at the Level of Individual Tight Junctional Contacts. *Dev. Brain Res.* 69: 85-95

Schulze C. & Firth J.A. (1993) Immunohistochemical Localisation of Adherens Junction Components in Blood-brain Barrier Microvessels of the Rat. *J. Cell Sci.* 104: 773-82

Seelig A. (1998) A General Pattern for Substrate Recognition by P-glycoprotein. *Eur. J. Biochem.* 251: 252-61

Segal M.B. (2000) The Choroid Plexuses and the Barriers Between the Blood and Cerebrospinal Fluid. *Cell Mol. Neurobiol.* 20: 183-96

Shasby D.M., Ries D.R., Shasby S.S. & Winter M.C. (2002) Histamine Stimulates Phosphorylation of Adherens Junction Proteins and Alters Their Link to Vimentin. *Am. J. Physiol. Lung Cell. Mol. Physiol.* 282: L1330-38

Shima D.T. & Mailhos C. (2000) Vascular Developmental Biology: Getting Nervous. *Curr. Opin. Genet. Dev.* 10: 536-42

Shimizu Y., Rose D.M. & Ginsberg M.H. (1999) Integrins in the Immune System. *Advan. Immunol.* 72: 325-80

Simcha I., Shtutman M., Saloman D., Zhurinsky J., Sadot E., Geiger B. & Ben-Ze'ev A. (1998) Differential Nuclear Translocation and Transactivation Potential of β-Catenin and Plakoglobin. *J. Cell Biol.* 141: 1433-48

Simionescu M., Simionescu N. & Palade G.E. (1976) Segmental Differentiations of Cell Junctions in the Vascular Endothelium. Arteries and Veins. *J. Cell Biol.* 68: 705-28

Simon D.B., Lu Y., Choate K.A., Velazquez H., Al-Sabban E., Praga M., Casari G., Bettinelli A., Colussi G., Rodriguez-Soriano J., McCredie D., Milford D., Sanjad S. & Lifton R.P. (1999) Paracellin-1, a Renal Tight Junction Protein Required for Paracellular Mg2+ Resorption. *Science* 285: 103-6

Simonovic I., Rosenberg J., Koutsouris A. & Hecht G. (2000) Enteropathogenic *Escherichia Coli* Dephosphorylates and Dissociates Occludin from Intestinal Epithelial Tight Junctions. *Cell. Microbiol.* 2: 305-315

Sonada N., Furuse M., Sasaki H., Yonemura S., Katahira J., Horiguchi Y. & Tsukita S. (1999) Clostridium Perfringens Enterotoxin Fragment Removes Specific Claudins From Tight Junction Strands: Evidence for Direct Involvement of Claudins in Tight Junction Barrier. *J. Cell Biol.* 147: 195-204

Songyang Z., Fanning A.S., Fu C., Xu J., Marfatia S.M., Chishti A.H., Crompton A., Chan A.C., Anderson J.M. & Cantley LC. (1997) Recognition of Unique Carboxyl-terminal Motifs Distinct PDZ Domains. *Science* 275: 73-7

Springer T.A. (1994) Traffic Signals for Lymphocyte Recirculation and Leukocyte Emigration: The Multistep Paradigm. *Cell* 76:301-314.

Staddon J.M., Herrenknecht K., Smales C. & Rubin L.L. (1995) Evidence that Tyrosine Phosphorylation May Increase Tight Junction Permeability. *J. Cell Sci.* 108: 609-19

Stanness K.A., Guateo E. & Janigro D. (1996) A Dynamic Model of the Blood-brain Barrier 'In Vitro'. *Neurotoxicology.* 17: 481-96

Steinberg M.S. & McNutt P.M. (1999) Cadherins and Their Connections: Adhesion Junctions Have Broader Functions. *Curr. Opin. Cell Biol.* 11: 554-60

Steinman L. (1996) Multiple Sclerosis: A Coordinated Immunological Attack against Myelin in the Central Nervous System. *Cell* 85: 299-302

Steinman L., Martin R., Bernard C. Conlon P & Oksenberg J.R. (2002) Multiple Sclerosis: Deeper Understanding of Its Pathogenesis Reveals New Targets For Therapy. *Ann. Rev. Neurosci.* 25: 491-505

Stevenson B.R., Sciciliano J.D., Mooseker M.S., & Goodenough D.A. (1986) Identification of ZO-1: a High Molecular Weight Polypeptide Associated with the Tight Junction (Zonula Occludens) in a Variety of Epithelia. *J. Cell Biol.* 103: 755-66

Stewart P.A. (2000) Endothelial Vesicles in the Blood-brain Barrier: Are They Related to Permeability? *Cell Mol. Neurobiol.* 20: 149-63

Strazielle N. & Ghersi-Egea J-F. (2000) Choroid Plexus in the Nervous System: Biology and Pathophysiology. *J. Neuropathol. Exp. Neurol.* 59: 561-74

Takaishi K., Sasaki T., Kotani H., Nishioka H. & Takai Y. (1997) Regulation of Cell-cell Adhesion by Rac and Rho Small G Proteins in MDCK Cells. *J. Cell Biol.* 139: 1047

Takagi J. & Springer T.A. (2002) Integrin Activation and Structural Rearrangement. *Immunol. Rev.* 186: 141-63

Tagayaki Y. & Manley J.L. (2000) Complex Protein Interactions Within the Human Polyadenylation Machinery Identify a Novel Component. *Mol. Cell Biol.* 20: 1515-25

Tedelind S., Ericson L.E., Karlsson J.O. & Nilsson M. (2003) Interferon-γ Down-regulates Claudin-1 and Impairs the Epithelial Barrier Function in Primary Cultured Human Erythrocytes. *Eur. J. Endocrinol.* 149: 215-21

Telò P., Breviario F., Huber P., Panzeri C. & Dejana E. (1998) Identification of a Novel Cadherin (VE-cadherin-2) Located at Intercellular Junctions in Endothelial Cells. *J. Biol. Chem.* 273: 17565-72

Terasaki T. & Hosoya K. (1999) The Blood-brain Barrier Efflux Transporters as a Detoxifying System for the Brain. *Adv. Drug Deliv. Rev.* 36: 195-209

Thompson P.W., Randi A.M. & Ridley A.J. (2002) Intercellular Adhesion Molecule (ICAM)-1, But Not ICAM-2, Activates RhoA and Stimulates c-fos and rhoA Transcription in Endothelial Cells. *J Immunol.* 169: 1007-13

Thompson R.D., Wakelin M.W., Larbi K.Y., Dewar A., Asimakopoulos G., Horton M.A., Nakada M.T. & Nourshargh S. (2000) Divergent Effects of Platelet-endothelial Cell Adhesion Molecule-1 and beta 3 Integrin Blockade on Leukocyte Transmigration in vivo. *J. Immunol.* 165: 426-34

Thompson R.D., Noble K.E., Larbi K.Y., Dewar A., Duncan G.S., Mak T.W. & Nourshargh S. (2001) Platelet-endothelial Cell Adhesion Molecule-1 (PECAM-1)-deficient Mice Demonstrate a Transient and Cytokine-specific Role for PECAM-1 in Leukocyte Migration Through the Perivascular Basement Membrane. *Blood* 97: 1854-60

Thoresan M.A., Anastasiadis P.Z., Daniel J.M., Ireton R.C., Wheelock M.J., Johnson K.R., Hummingbird D.K. & Reynolds A.B. (2000) Selective Uncoupling of the p120ctn From E-cadherin Disrupts Strong Adhesion. *J. Cell Biol.* 148: 189-201

Tilghman R.W. & Hoover R.L. (2002a) E-selectin and ICAM-1 are Incorporated into Detergent-insoluble Membrane Domains Following Clustering in Endothelial Cells. *FEBS Letters.* 525: 83-7

Tilghman R.W & Hoover R.L. (2002b) The Src-cortactin Pathway is Required for Clustering of E-selectin and ICAM-1 in Endothelial Cells. *FASEB J.* 17: 1257-9

Tinsley J.H., Wu M.H., Ma W., Taulman A.C. & Yuan S.Y. (1999) Activated Neutrophils Induce Hyperpermeability and Phosphorylation of Adherens Junction Proteins in Coronary Venular Endothelial Cells. *J. Biol. Chem.* 274: 24930-4

Tinsley J.H., Ustinova E.E., Xu W. & Yuan S.Y. (2002) Src-dependent, Neutrophil-mediated Vascular Hyperpermeability and β-catenin Modification. *Am. J. Physiol. Cell Physiol.* 283: C1745-51

Toyofuku T., Yabuki M., Otsu K., Kuzuya T., Hori M. & Tada M. (1998) Direct Association of the Gap Junction Protein Connexin-43 with ZO-1 in Cardiac Myocytes. *J. Biol. Chem.* 273: 12725-31

Traweger A., Fang D., Liu Y-C., Stelzhammer W., Krizbai I.A., Fresser F., Bauer H-C. & Bauer H. (2002) The Tight Junction-specific Protein Occludin Is a Functional Target of the E3 Ubiquitin-protein Ligase Itch. *J. Biol. Chem.* 277: 10201-8

Truman J-P., Choqueux C., Charron D. & Mooney N (1996) HLA Class II Molecule Signal Transduction Leads to Either Apoptosis or Activation Via Two Different Pathways. *Cell. Immunol.* 172: 149-57

Tsakadze N.L., Zhao Z. & D'Souza S.E. (2002) Interactions of Intercellular Adhesion Molecule-1 with Fibrinogen. *Trends Cardiovasc. Med.* 12: 101-8

Tsukamoto T. & Nigam S.K. (1999) Role of Tyrosine Phosphorylation in the Reassembly of Occludin and Other Tight Junction Proteins. *Am. J. Physiol.* 276: F737-F750

Tsukita S., Nagafuchi A. & Yonemura S. (1992) Molecular Linkage Between Cadherins and Actin Filaments in Cell-cell Adherens Junctions. *Curr. Opin. Cell Biol.* 4: 834-9

Tsukita S. & Furuse M. (2000) Pores in the Wall: Claudins Constitute Tight Junction Strands Containing Aqueous Pores. *J. Cell Biol.* 149: 13-16

Tsukita S., Furuse M. & Itoh M. (2001) Multifunctional Strands in Tight Junctions. *Nature Rev. Mol. Cell Biol.* 2: 285-93

Ukropec J.A., Hollinger M.K., Salva S.M. & Woolkalis M.J. (2000) SHP2 Association with VE-cadherin Complexes in Human Endothelial Cells is Regulated by Thrombin. *J. Biol. Chem.* 275: 5983-86

van Buul J.D., Voermans C., van den Berg V., Anthony E.C., Mul F.P.J., van Wetering S., van der Schoot C.E. & Hordijk P.L. (2002) Migration of Human Hematopoietic Progenitor Cells Across Bone Marrow Endothelium is Regulated by Vascular Endothelial Cadherin. *J. Immunol.* 168: 588-96

van Hengel J., Vanhoenacker P., Staes K. & van Roy F. (1999) Nuclear Localisation of the p120(ctn) Armadillo-like Catenin is Counteracted by a Nuclear Export Signal and by E-cadherin Expression. *Proc. Natl. Acad. Sci. USA* 96: 7980-5

Van Itallie & Anderson J.M. (1997) Occludin Confers Adhesiveness When Expressed in Fibroblasts. *J. Cell Sci.* 110: 1113-21

Van Itallie C.M., Rahner C. & Anderson J.M. (2001) Regulated Expression of Claudin-4 Decreases Paracellular Conductance Through a Selective Decrease in Sodium Permeability. *J. Clin. Invest.* 107: 1319-27

van Meer G. & Simon K. (1986) The Function of Tight Junctions in Maintaining Differences in Lipid Composition Between Apical and Basolateral Cell Surface Domains of MDCK cells. *EMBO J.* 5: 1455-64

van Wetering S., van Buul J.D., Quik S., Mul F.P.J., Anthony E.C., ten Klooster J-P., Collard J.G. & Hordijk P.L. (2002) Reactive Oxygen Species Mediate Rac-induced Loss of Cell-cell Adhesion in Primary Human Endothelial Cells. *J. Cell Sci.* 115: 1837-46

Vaporciyan A.A., DeLisser H.M., Yan H., Mendiguren I.I., Thom S.R., Jones M.L., Ward P.A. & Albelda S.M. (1993) Involvement of the Platelet Endothelial Cell Adhesion Molecule-1 in Neutrohil Recruitment In Vivo. *Science* 262:1580-2

Vietor I., Bader T., Paiha K. & Huber L.A. (2001) Perturbation of the Tight Junction Permeability Barrier by Occludin Loop Peptides Activates β-catenin-TCF-LEF-mediated Transcription. *EMBO Reports* 2: 306-12

Wachtel M., Frei K., Ehler E., Fontana A., Winterhalter K. & Gloor S.M. (1999) Occludin Proteolysis and Increased Permeability in Endothelial Cells Through Tyrosine Phosphatase Inhibition. *J. Cell. Sci.* 112: 4347-4356

Wakelin M.W., Sanz M.J., Dewar A., Albelda S.M., Larkin S.W., Boughton-Smith N., Williams T.J. & Nourshargh S. (1996) An Anti-platelet-endothelial Cell Adhesion Molecule-1 Antibody Inhibits Leukocyte Extravasation From Mesenteric Microvessels in vivo by Blocking the Passage Through the Basement Membrane. *J. Exp. Med.* 184: 229-39

Walters C.E., Pryce G., Hankey D.J.R., Sebti S.M., Hamilton A.D., Baker D., Greenwood J. & Adamson P. (2002) Inhibition of Rho GTPases with Protein Prenyltransferase Inhibitors Prevents Leucocyte Recruitment to the Central Nervous System and Attenuates Clinical Signs of Disease in an Animal Model of Multiple Sclerosis. *J. Immunol.* 168: 4087-4094

Walsh S.V., Hopkins A.M., Chen J., Narumiya S., Parkos C.A. & Nusrat A. (2001) Rho Kinase Regulates Tight Junction Function and is Necessary for Tight Junction Assembly in Polarized Intestinal Epithelia. *Gastoenterology* 121: 566-79

Walsh S.V., Hopkins A.M. & Nusrat A. (2000) Modulation of Tight Junction Strucure and Function by Cytokines. *Adv. Drug Deliv. Rev.* 41: 303-313

Wang J-H. & Springer T.A. (1998) Structural Specialisations of Immunoglobulin Superfamily Members for Adhesion to Integrins and Viruses. *Immunol. Rev.* 163: 197-215

Wang Q. & Doerschuk C.M. (2001) The p38 Mitogen-activated Protein Kinase Mediates Cytoskeletal Remodeling in Pulmonary Microvascular Endothelial Cells Upon Intracellular Adhesion Molecule-1 Ligation. *J. Immunol.* 166: 6877-6884

Wang W., Dentler W.L. & Borchardt R.T. (2001) VEGF Increases BMEC Monolayer Permeability by Affecting Occludin Expression and Tight Junction Assembly. *Am. J. Physiol. Heart Circ. Physiol.* 280: H434-40

Weller R.O., Kida S. & Zhang E.T. (1992) Pathways of Fluid Drainage from the Brain: Morphological Aspects and Immunological Significance in Rats and Man. *Brain Pathol.* 2: 277-84

Widner H., Moller G. & Johansson B.B. (1988) Immune Response in Deep Cervical Lymph Nodes and Spleen in the Mouse After Antigen Deposition in Different Intracerebral Sites. *Scand. J. Immunol.* 28: 563-71

Williams K., Alvarez X. & Lackner A.A. (2001) Central Nervous System Perivascular Cells are Immunoregulatory Cells that Connect the CNS with the Peripheral Immune System. *Glia* 36: 156-64

Wójciak-Stothard B., Entwhistle A., Garg R. & Ridley A.J. (1998) Regulation of TNFαA-induced Reorganisation of the Actin Cytoskeleton and Cell-cell Junctions by Rho, Rac and Cdc42 in Human Endothelial Cells. *J. Cell Physiol.* 176: 150-65

Wójciak-Stothard B., Potempa S. Eichstoltz T. & Ridley A.J. (2001) Rho and Rac but not Cdc42 Regulate Endothelial Cell Permeability. *J. Cell Sci.* 114: 1343-1355

Wolburg H., Neuhaus J., Kniesel U., Krauss B., Scmid E-M., Öcalan M., Farrell C. & Risau W. (1994) Modulation of Tight Junction Structure in Blood-brain Barrier ECs. Effects of Tissue Culture, Second Messangers and Cocultured Astrocytes. *J. Cell Sci.* 107: 1347-57

Wolburg H. & Lippoldt A. (2002) Tight Junctions of the Blood-brain Barrier: Development, Composition and Regulation. *Vasc. Pharmacol.* 38: 323-37

Wong D. Prameya R & Dorovini-Zis K. (1999) In Vitro Adhesion and Migration of T Lymphocytes Across Monolayers of Human Brain Microvessel Endothelial Cells: Regulation by ICAM-1, VCAM-1, E-selectin and PECAM-1. *J. Neuropathol. Exp. Neurol.* 58: 138-52

Wong E.Y.M., Morgan L., Smales C., Lang P., Gubby S.E. & Staddon J.M. (2000) Vascular Endothelial Growth Factor Stimulates Dephosphorylation of the Catenins p120 and p100 in Endothelial Cells. *Biochem. J.* 346: 209-16

Wong R.K., Baldwin A.L. & Heimark R.L. (1999) Cadherin-5 Redistribution at Sites of TNF-α and IFN-γ-induced Permeability in Mesenteric Venules. *Am. J. Physiol.* 276: H736-48

Wu Z., Nybom P. & Magnusson K-E. (2000) Distinct Effects of *Vibrio Cholerae* Haemagglutinin Protease on the Structure and Localisation of the Tight Junction-associated Proteins Occludin and ZO-1. *Cell. Microbiol.* 2: 11-17

Yamamoto T., Harada N., Kano K., Taya S-I., Canaani E., Matsuura Y., Mizoguchi A., Ide C. & Kaibuchi K. (1997) The Ras Target AF-6 Interacts with ZO-1 and Serves as a Peripheral Component of Tight Junctions in Epithelial Cells. *J. Cell Biol.* 139: 785-95

Youakim A & Ahdieh M. (1999) Interferon-γ Decreases Barrier Function in T84 Cells by Reducing ZO-1 Levels and Disrupting Apical Actin. *Am. J. Physiol. Gastrointest. Liver Physiol.* 276: G1279-88

Youssef S., Stuve O., Patarroyo J.C., Ruiz P.J., Radosevich J.L., Hur E.M., Bravo M., Mitchell D.J., Sobel R.A., Steinman L. & Zamvil S.S. (2002) The HMG-CoA Reductase Inhibitor, Atorvastatin, Promotes a Th2 Bias and Reverses Paralysis in Central Nervous System Autoimmune Disease. *Nature* 420: 78-84

Zahraoui A., Louvard D. & Galli T. (2000) Tight Junction, a Platform for Trafficking and Signalling Protein Complexes. *J. Cell Biol.* 151: F31-F36

Zhadanov A.B., Provance Jr. D.W., Speer C.A., Coffin J.D., Goss D., Blixt J.A., Reichert C.M. & Mercer J.A. (1999) Absence of the Tight Junctional Protein AF6 Disrupts Epithelial Cell-cell Junctions and Cell Polarity During Mouse Development. *Curr. Biol.* 9: 880-8

Zhong Y., Saitoh T., Minase T., Sawada N., Enomoto K. & Mori M. (1993) Monoclonal Antibody 7H6 Reacts with a Novel Tight Junction-associated Protein Distinct From ZO-1, Cingulin and ZO-2. *J. Cell Biol.* 120: 477-83

Zhong Y., Enomoto K., Isomura H., Sawada N., Minase T., Oyamada M. & Konishi Y.M.M. (1994) Localisation of the 7H6 Antigen at Tight Junctions Correlates with the Paracellular Barrier Function of MDCK Cells. *Exp. Cell Res.* 214: 614-20

Zhurinsky J., Shtutman M. & Ben-Ze'ev A. (2000) Plakoglobin and β-Catenin: Protein Interactions, Regulation and Biological Roles. *J. Cell Sci.* 113: 3127-3139

Appendix

Nucleotide and amino acid sequence of occludin constructs used in brain endothelial cell transfections

Nucleotide sequence of wild type chick occludin cDNA
(size = 1.52Kb):-

```
1     atgttcagca agaagtccta cgacggcccc cccgcggggt acggcccccc cacggggtac
61    ggcgccccca cggctgatta cggctacggg tctccgccgc cgggctccta ctacgtggac
121   gacgctccgc agctcttcta caagtggacg tcgccgcccg gcgcggtgcg ggggctgcag
181   gcgggggtcc tcgtgctgtg catcgccatc ttcgcctgcg tcgcttccac gctcgcctgg
241   gattacggct acggcctggg gggggcgtac ggcaccgggc tgggggggtt ctacggctcc
301   aactactacg gcagcgggct gagctacagc tacggctacg ggggctacta cggaggggtg
361   aaccagcgca cggccaacgg cttcatgatc gccatggccg tgctgtgctt cctggcccag
421   ctggggctgc tggtggcggc gctcagcaaa tccggggcca cgcgctcgcg gcgcttctac
481   ctggccgtgc tggtgctgag cgccgtgctg gccttcgtca tgctcatcgc ctccatcgtc
541   tacatcatgg gcgtcaaccc gcaggcgcag atgtccagcg gttactacta cagccccttg
601   ttggccatgt gcagccaggc ctacggcagc acctacctca accagtacat ctaccactac
661   tgcaccgtgg acccccagga ggctgtggct gctgtctgtg ggttcctcat cgtcatcctg
721   ctctgcctca tctgcttctt cgcccagaag acgcgcagta agatctggcg ctacggcaaa
781   gccaacatct actgggaccg cgcgcccgtg gtgcaggagg ggcctgacgt ggaggagtgg
841   gtgaagaacg tggcggatgg ggccagcgtg caggacgaga cggccacgct tgcctactcg
901   gagaagccca ccagccctgt cgccgccccc ccctacagct acgtgccccc ccccagcgct
961   gggtactacc cctcgggcac ctacagcagc cggggcgacc agccggaccg ggccctcagt
1021  gccagccctg tgcatgggga ggaggaggag gagaagggga aggatcagcc cagcagaccg
1081  cccgcccgcc ggggccgccg ccgccgccgt aaccccgagt tggatgagtc ccagtatgag
1141  accgactaca ccacggccgt ggagtccagt gatgagcggg accaggagca gtgggccagt
1201  ctgtaccccc ccatcacgtc ggacggcgcc cgccagcgct acaagcagga gttcgacacc
1261  gacctgaagc gctacaagca gctctgtgct gagatggaca gcatcaacga ccgcctcaat
1321  cagctcagcc gacggctcga cagcatcacc gaggacagcc ctcaatacca ggatgtggca
1381  gaggagtaca atcagctcaa agacctgaag cggagcccag actaccaaag caagaagcag
1441  gagagcaaag tgctgcgcaa caagctcttc cacatcaagc gcatggtgag cgcctacgac
1501  aaggtgcggg ggtaa
```

HA (1) atgcaggacc tgccaggcaa cgacaacagc accgccggcc tt

Key:

- Nucleotide sequence substituted in epitope-tagged occludin (HAocc, size = 1.55 Kb) and carboxyl terminal-deleted epitope-tagged occludin (HAoccCT3).
- Codon sequence changed to atg (START/met) in ΔNocc and upstream sequence deleted (size = 1.36 Kb).
- Nucleotide sequence deleted in OccL1D (size = 1.48 Kb).
- Codon changed to att (STOP) in HAoccCT3 and downstrean sequence deleted (size = 0.8 Kb).

Wild-type Chicken Occludin Primary Sequence
($M_r \approx 64$ Kd)

1 MFSKKSYDGP PAGYGPPTGY GAPTADYGYG SPPPGSYYVD DAPQLFYKWT

51 SPPGAVRGLQ AGVLVLCIAI FACVASTLAW DYGYGLGGAY GTGLGGFYGS

101 NYYGSGLSYS YGYGGYYGGV NQRTANGFMI AMAVLCFLAQ LGLLVAALSK

151 SGATRSRRFY LAVLVLSAVL AFVMLIASIV YIMGVNPQAQ MSSGYYYSPL

201 LAMCSQAYGS TYLNQYIYHY CTVDPQEAVA AVCGGLIVIL LCLICFFAQK

251 TRSKIWRYGK ANIYWDRAPV VQEGPDVEEW VKNVADGASV QDETATLAYS

301 EKPTSPVAAP PYSYVPPPSA GYYPSGTYSS RGDQPDRALS ASPVHGEEEE

351 EKGKDQPSRP PARRGRRRRR NPELDESQYE TDYTTAVESS DERDQEQWAS

401 LYPPITSDGA RQRYKQEFDT DLKRYKQLCA EMDSINDRIN QLSRRLDSIT

451 EDSPQYQDVA EEYNQLKDLK RSPDYQSKKQ ESKVLRNKLF HIKRMVSAYD

501 KVRG

HA (1) MQDLPGNDNSTAGL

Key:

- Amino acid sequence substituted in epitope-tagged occludin (HAocc, $M_r \approx 65$ Kd) and carboxyl terminal-deleted epitope-tagged occludin (HAoccCT3),
- Alanine^{55} changed to START/methionine^{1} in ΔNocc and upstream sequence deleted (predicted $M_r \approx 57$ Kd).
- Amino acid sequence deleted in OccL1D ($M_r \approx 63$ Kd).
- Serine^{253} changed to STOP codon in HAoccCT3 and downstrean sequence deleted ($M_r \approx 26$ Kd).
- Transmembrane domain.